

Spring 2015

## Assessment of the Wear Effects of Alumina-Nanofluids on Heat-Exchanger Materials

FNU Aktaruzzaman

Follow this and additional works at: <https://digitalcommons.georgiasouthern.edu/etd>



Part of the [Tribology Commons](#)

---

### Recommended Citation

F. Aktaruzzaman, G.J. Molina, V. Soloiu, and M. Rahman, Assessment of the wear effects of alumina-nanofluids on heat-exchanger materials, MS thesis, Georgia Southern University, 2015.

This thesis (open access) is brought to you for free and open access by the Graduate Studies, Jack N. Averitt College of at Digital Commons@Georgia Southern. It has been accepted for inclusion in Electronic Theses and Dissertations by an authorized administrator of Digital Commons@Georgia Southern. For more information, please contact [digitalcommons@georgiasouthern.edu](mailto:digitalcommons@georgiasouthern.edu).

# ASSESSMENT OF THE WEAR EFFECTS OF ALUMINA-NANOFLUIDS ON HEAT-EXCHANGER MATERIALS

by

FNU AKTARUZZAMAN

(Under the Direction of Gustavo J. Molina)

## ABSTRACT

Nanofluids are nano-size-powder suspensions in liquids that are mainly studied for their abnormal thermal transport properties, and hence as enhanced alternatives to ordinary cooling fluids. The tribological effects of nanofluids are, however, largely unknown, in particular their likely wear and/or erosion effects, because of their interaction with cooling-system (heat-exchanger) materials. The thesis presents research to establish methodologies for testing and evaluating surface-change by nanofluid impact. The work is presented on development of novel test rigs and testing methodologies, and on the use of typical surface analysis tools for assessment of wear and erosion that may be produced by nanofluids; prediction of such effects in cooling systems is discussed.

Two new tests rigs were designed and developed: a multiple nozzle test rig and a parallel flow test rig. A main purpose of this research work was to assess the use of these new test rigs to evaluate nanofluid wear, and the ad-hoc newly proposed testing methodologies are discussed. Experimental results are presented on typical nanofluids (as 2%-volume of alumina nanopowders in 50/50 water/ethylene glycol solution, and in distilled water) which are jet-impinged (on aluminum and copper specimens) with 3.5 m/s to 15.5 m/s jet-speeds and in a 1 m/s parallel-flow (along the test specimen surface) during long test periods. The obtained

surface modifications were assessed by roughness measurements, by weighing of removed-material, and by optical-microscopy. The results are presented on the observed substantially different surface modifications when same tests are conducted in aluminum and copper, and by both the base fluids and its alumina-nanofluids. The likely mechanisms of early erosion and abrasion, and the possibility of extrapolating the test-rig results and methodologies to typical cooling systems are discussed.

**INDEX WORDS:** Nanofluid, Jet impingement, Surface roughness, Microscopy, Erosion.

ASSESSMENT OF THE WEAR EFFECTS OF ALUMINA-  
NANOFLUIDS ON HEAT-EXCHANGER MATERIALS

by

FNU AKTARUZZAMAN

B.Sc. (Eng.) in Mechanical Engineering, Bangladesh University of Engineering and  
Technology, Bangladesh 2009

A Thesis Submitted to the Graduate Faculty of the Georgia Southern University  
in Partial Fulfillment of the Requirement of the Degree

MASTERS OF SCIENCE IN APPLIED ENGINEERING

in

Energy Science Degree Concentration

Georgia Southern University

Statesboro, Georgia

© 2015

FNU AKTARUZZAMAN

All Rights Reserved

ASSESSMENT OF THE WEAR EFFECTS OF ALUMINA-  
NANOFLUIDS ON HEAT-EXCHANGER MATERIALS

by

FNU AKTARUZZAMAN

Major Professor:  
Committee:

Gustavo J. Molina  
Valentin Soloiu  
Mosfequr Rahman

Electronic Version Approved:  
May 2015

## **DEDICATION**

To my family who have been always  
beside me to work hard and pursue my goals.

## **ACKNOWLEDGEMENTS**

I wish to express my sincere gratitude to Dr. Gustavo Molina, chairman of my advisory committee, for his invaluable suggestions, guidance, continuous encouragement and help during the course of this research.

I would also like to thank Dr. Valentin Soloiu and Dr. Mosfequr Rahman for serving on my advisory committee. Their recommendations during this research work proved extremely useful. I am especially indebted to Dr. Brian L. Vlcek and Dr. Valentin Soloiu for their generous assistance, support and advice, which played a big role in the success of this study, and to Dr. Rahman, for his suggestions during numerous meetings we had.

I am very grateful to the Department of Mechanical Engineering for the financial support provided for this research and for my Graduate Assistantship. I would also like to express my gratefulness to the staff of the Department of Mechanical Engineering, and to the staffs of the Machine Shop and the Electronics Shop. I specially acknowledge the assistance Spencer Harp and Andrew Michaud for helping during the experimental setup development.

Finally, I wish to give special thanks to Faculty Research Committee, GSU, for the financial support for this research through a Faculty Research Seed Grant and Dr. Valentin Soloiu for the summer support through NSF funded REU tutor position.



## TABLE OF CONTENTS

	Page
<b>ABSTRACT.....</b>	<b>1</b>
<b>DEDICATION.....</b>	<b>6</b>
<b>ACKNOWLEDGEMENTS .....</b>	<b>7</b>
<b>LIST OF TABLES .....</b>	<b>11</b>
<b>LIST OF FIGURES .....</b>	<b>13</b>
<b>CHAPTER 1 .....</b>	<b>23</b>
1 INTRODUCTION .....	23
1.1 <i>Problem statement and rationale</i> .....	23
1.2 <i>The research questions of interest</i> .....	24
<b>CHAPTER 2 .....</b>	<b>26</b>
2 LITERATURE REVIEW.....	26
2.1 <i>Introduction</i> .....	26
2.2 <i>Literature review on nanofluids</i> .....	26
2.3 <i>Wear, corrosion and abrasion</i> .....	35
2.4 <i>Literature review on wear and erosion by nanofluids</i> .....	37
2.5 <i>Literature review on nanofluid test methodologies and used instruments</i> .....	44
<b>CHAPTER 3.....</b>	<b>499</b>
3 DESIGN, DEVELOPMENT AND CONSTRUCTION OF TEST INSTRUMENTS.....	499
3.1 <i>Motivation</i> .....	499
3.2 <i>Design and building process</i> .....	50

3.3	<i>Jet impingement test rigs</i> .....	51
3.4	<i>Parallel flow setup</i> .....	70
<b>CHAPTER 4</b>	.....	74
4	<b>TEST METHODOLOGIES AND TESTED FLUIDS AND MATERIALS</b> .....	74
4.1	<i>Test methodologies</i> .....	74
4.2	<i>Test specimen preparation techniques</i> .....	75
<b>CHAPTER 5</b>	.....	77
5	<b>EXPERIMENTAL</b> .....	77
5.2	<i>Test results for 10.7 m/s jet impingement treatments</i> .....	109
5.3	<i>Test results for 15.5 m/s jet impingement treatments</i> .....	137
5.4	<i>Test results for parallel flow treatments</i> .....	151
<b>CHAPTER 6</b>	.....	164
6	<b>DISCUSSION</b> .....	164
6.1	<i>Discussion of instrument development</i> .....	164
6.2	<i>Discussion of jet impingement instrument design and development</i> .....	164
6.3	<i>Discussion of wear and erosion data for jet impingement tests</i> .....	167
6.4	<i>Discussion of surface roughness, weight measurement data and image analysis of parallel flow tests</i> .....	178
<b>CHAPTER 7</b>	.....	180
7	<b>CONCLUSIONS</b> .....	180
7.1	<i>Conclusions</i> .....	180
7.2	<i>Recommendations for future research</i> .....	187
<b>CHAPTER 8</b>	.....	189

8	REFERENCES .....	189
---	------------------	-----

## **APPENDICES**

A	ROUGHNESS RESULTS AND PLOTTING.....	201
---	-------------------------------------	-----

B	OPTICAL MICROSCOPY IMAGES .....	238
---	---------------------------------	-----

## LIST OF TABLES

	Page
Table 1: Summary of carried out jet impingement tests and test parameters presented in this Chapter 5	77
Table 2: Normalized surface roughness data of before- and after- 7, 28, 240 and 408 hours of repeated tests (two trials) with a 3.5- m/s jet of reference fluid of distilled water. All normalized roughness values before test are unity, as previously explained.	83
Table 3: Summary of surface roughness modifications when roughness values were compared for measurements before- and after- tests with a 3.5- m/s, 10.7- m/s and 15.5- m/s jet of reference fluid of distilled water, and of the nanofluid of 2% nano-alumina in reference fluid	168
Table 4: Summary of surface roughness modifications when roughness values were compared for measurements before- and after- tests with a 3.5- m/s, 10.7- m/s and 15.5- m/s jet of reference fluid of 50% Ethylene glycol, and of the nanofluid of 2% nano-alumina in reference fluid.	168
Table 5: Summary of main surface modifications when comparing microscopy images before- and after-408 hours of testing with a 3.5m/s jet of reference fluid of distilled water, and of nanofluid of 2% nano-alumina in reference fluid	170
Table 6: Summary of surface modifications when comparing microscopy images before- and after-408 hours of testing with a 3.5m/s jet of reference fluid of 50/50% Ethylene Glycol in water, and of nanofluid of 2% nano-alumina in reference fluid	171
Table 7: Summary of main surface modifications when comparing microscopy images before- and after-112 hours of testing with a 10.7 m/s jet of reference fluid of distilled water, and of nanofluid of 2% nano-alumina in reference fluid	172

- Table 8: Summary of surface modifications when comparing microscopy images before- and after-112 hours of testing with a 10.7 m/s jet of reference fluid of 50/50% Ehtylene Glycol in water, and of nanofluid of 2% nano-alumina in reference fluid 174
- Table 9: Summary of surface modifications when comparing microscopy images before- and after-112 hours of testing with a 15.5 m/s jet of reference fluid of distilled water, and of nanofluid of 2% nano-alumina in reference fluid 175
- Table 10: Summary of surface modifications when comparing microscopy images before- and after-112 hours of testing with a 15.5 m/s jet of reference fluid of distilled water, and of nanofluid of 2% nano-alumina in reference fluid 179

## LIST OF FIGURES

	Page
Figure 1: Schematics and photograph of the single nozzle jet test rig to assess nanofluid wear by Molina et al [58].	51
Figure 2: Schematics (a) and photograph (b) of low speed side of the variable speed jet multiple nozzle test rig to assess nanofluid wear developed in this thesis research.	52
Figure 3: Schematics (a) and photograph (b) of high speed side of the variable speed jet multiple nozzle test rig to assess nanofluid wear developed in this thesis research.	55
Figure 4: Main chamber details of a) side view b) top view	57
Figure 5: Sample holder a) design and b) details	58
Figure 6: Piping network and instrumentation diagram for high speed jet multiple nozzle test rig	59
Figure 7: Components of (a) heating system and (b) cooling subsystem for the variable speed test-rig	68
Figure 8: Circuit diagram of thermal control subsystem for the variable speed test-rig	69
Figure 9: (a) Schematics and (b) photograph of the parallel-flow test rig to assess nanofluid wear.	71
Figure 10: Photograph of the parallel flow test sample holder in the parallel-flow test rig to assess nanofluid wear	72
Figure 11: Average Ra roughness for 3003-T3 aluminum before and after 3, 7, 14, 28, 56, 112, 240, 312 and 408 hour-treatments with the reference fluid distilled	79

water and its nanofluid of 2% nano-alumina in reference fluid and jet speed of 3.5 m/s and enlarged partial graph for 3 to 112 hours.

- Figure 12: Normalized Ra roughness for 3003-T3 aluminum before and after 3, 7, 14, 28, 56, 112, 240, 312 and 408 hour-treatments with the reference fluid of distilled water and its nanofluid of 2% nano-alumina in reference fluid and jet speed of 3.5 m/s and enlarged partial graph for 3 to 112 hours. 81
- Figure 13: Average weight change for 3003-T3 aluminum in before and after 3, 7, 14, 28, 56, 112, 240, 312 and 408 hour-treatments with the reference fluid of distilled water, and its nanofluid of 2% nano-alumina in reference fluid and jet speed of 3.5 m/s 84
- Figure 14: Optical microscopy images of 3003-T3 aluminum before and after (408-hour) test with (reference fluid, without nanoparticles) distilled water (Magnification: 500X). Pre-existing pitting and enlarged ones after treatment are circled. 85
- Figure 15: Optical microscopy images of 3003-T3 aluminum before and after (408-hour) test with nanofluid of 2% alumina in distilled water (Magnification: 500X). Pre-existing pitting and enlarged ones after treatment are circled. 87
- Figure 16: Average Ra roughness for copper alloy110 before and after 3, 7, 14, 28, 56, 112, 240, 312 and 408 hour-treatments with the reference fluid distilled water, and its nanofluid of 2% nano-alumina in reference fluid and jet speed of 3.5 m/s and enlarged partial graph for 3 to 112 hours. 89
- Figure 17: Normalized Ra roughness for alloy110 copper before and after 3, 7, 14, 28, 56, 112, 240, 312 and 408 hour-treatments with the reference fluid distilled water, and its nanofluid of 2% nano-alumina in reference fluid and jet speed of 3.5 m/s and enlarged partial graph for 3 to 112 hours. 91

- Figure 18: Average weight change for alloy110 copper in before and after 3, 7, 14, 28, 56, 112, 240, 312 and 408 hour-treatments with the reference fluid distilled water, and its 2% alumina nanofluid and jet speed of 3.5 m/s. 92
- Figure 19: Optical microscopy images of alloy110 copper before and after (408-hour) test with (reference fluid, without nanoparticles) distilled water (Magnification: 500X). Pre-existing pitting and enlarged ones after treatment are circled. 93
- Figure 20: Optical microscopy images of alloy110 copper before and after (408-hour) test with nanofluid of 2% alumina in distilled water (Magnification: 500X). Pre-existing pitting and seemingly clustered ones after treatment are circled. 95
- Figure 21: Average Ra roughness for 3003-T3 aluminum before and after 3, 7, 14, 28, 56, 112, 240, 312 and 408 hour-treatments with the reference fluid of 50/50% Ethylene Glycol in water, and its nanofluid of 2% nano-alumina in reference fluid and jet speed of 3.5 m/s. 96
- Figure 22: Normalized Ra roughness for 3003-T3 aluminum before and after 3, 7, 14, 28, 56, 112, 240, 312 and 408 hour-treatments with the reference fluid of 50/50% Ehtylene Glycol in water, and its nanofluid of 2% nano-alumina in reference fluid and jet speed of 3.5 m/s. 98
- Figure 23: Average weight change for 3003-T3 aluminum in before and after 3, 7, 14, 28, 56, 112, 240, 312 and 408 hour-treatments with the reference fluid of 50/50% Ehtylene Glycol in water, and its nanofluid of 2% nano-alumina in reference fluid and jet speed of 3.5 m/s. 99
- Figure 24: Optical microscopy images of 3003-T3 aluminum before and after (408-hour) test with (reference fluid, without nanoparticles) 50/50% Ethylene Glycol/water (Magnification: 5000X). 100



- Figure 25: Optical microscopy images of 3003-T3 aluminum before and after (408-hour) test with nanofluid of 2% alumina in 50/50% Ethylene Glycol/water (Magnification: 5000X). 102
- Figure 26: Average Ra roughness for copper alloy110 before and after 3, 7, 14, 28, 56, 112, 240, 312 and 408 hour-treatments with the reference fluid of 50/50% Ehtylene Glycol in water, and its 2% alumina nanofluid fluid and jet speed of 3.5 m/s. 103
- Figure 27: Normalized Ra roughness for alloy110 copper before and after 3, 7, 14, 28, 56, 112, 240, 312 and 408 hour-treatments with the reference fluid of 50/50% Ehtylene Glycol in water, and its nanofluid of 2% nano-alumina in reference fluid and jet speed of 3.5 m/s. 104
- Figure 28: Average weight change for alloy110 copper in before and after 3, 7, 14, 28, 56, 112, 240, 312 and 408 hour-treatments with the reference fluid of 50/50% Ehtylene Glycol in water, and its nanofluid of 2% nano-alumina in reference fluid and jet speed of 3.5 m/s. 105
- Figure 29: Optical microscopy images of alloy110 copper before and after (408-hour) test with (reference fluid, without nanoparticles) 50/50% Ethylene Glycol/water (Magnification: 5000X). 106
- Figure 30: Optical microscopy images of alloy110 copper before and after (408-hour) test with nanofluid of 2% alumina in 50/50% Ethylene Glycol/water (Magnification: 5000X). 108
- Figure 31: Average Ra roughness for 3003-T3 aluminum before and after 3, 7, 14, 28, 56 and 112 hour-treatments with the reference fluid distilled water and its nanofluid of 2% nano-alumina in reference fluid and jet speed of 10.7 m/s. 110

- Figure 32: Normalized Ra roughness for 3003-T3 aluminum before and after 3, 7, 14, 28, 56 and 112 hour-treatments with the reference fluid of distilled water and its nanofluid of 2% nano-alumina in reference fluid and jet speed of 10.7 m/s. 111
- Figure 33: Average weight change for 3003-T3 aluminum in before and after 3, 7, 14, 28, 56 and 112 hour-treatments with the reference fluid of distilled water and its nanofluid of 2% nano-alumina in reference fluid and jet speed of 10.7 m/s. 112
- Figure 34: Optical microscopy images of 3003-T3 aluminum before and after (112-hour) test with reference fluid of distilled water (Magnification: 500X). 114
- Figure 35: Optical microscopy images of 3003-T3 aluminum before and after (112-hour) test with nanofluid of 2% alumina in distilled water (Magnification: 500X). 116
- Figure 36: Average Ra roughness for copper alloy110 before and after 3, 7, 14, 28, 56 and 112 hour-treatments with the reference fluid distilled water and its nanofluid of 2% nano-alumina in reference fluid and jet speed of 10.7 m/s. 118
- Figure 37: Normalized Ra roughness for alloy110 copper before and after 3, 7, 14, 28, 56 and 112 hour-treatments with the reference fluid distilled water and its nanofluid of 2% nano-alumina in reference fluid and jet speed of 10.7 m/s. 119
- Figure 38: Average weight change for alloy110 copper in before and after 3, 7, 14, 28, 56 and 112 hour-treatments with the reference fluid distilled water and its nanofluid of 2% nano-alumina in reference fluid and jet speed of 10.7 m/s. 120
- Figure 39: Optical microscopy images of alloy110 copper before and after (112-hour) test with (reference fluid, without nanoparticles) distilled water (Magnification: 500X). Pre-existing pitting and slightly enlarged ones after treatment are circled. 121

- Figure 40: Optical microscopy images of alloy110 copper before and after (112-hour) test with nanofluid of 2% alumina in distilled water (Magnification: 500X). Pre-existing pitting and enlarged ones after treatment are circled. 123
- Figure 41: Average Ra roughness for 3003-T3 aluminum before and after 3, 7, 14, 28, 56 and 112 hour-treatments with the reference fluid Ethylene Glycol and its nanofluid of 2% nano-alumina in reference fluid and jet speed of 10.7 m/s. 125
- Figure 42: Normalized Ra roughness for 3003-T3 aluminum before and after 3, 7, 14, 28, 56 and 112 hour-treatments with the reference fluid of Ethylene Glycol and its nanofluid of 2% nano-alumina in reference fluid and jet speed of 10.7 m/s. 127
- Figure 43: Optical microscopy images of 3003-T3 aluminum before and after (112-hour) test with (reference fluid, without nanoparticles) 50/50% Ethylene Glycol/water (Magnification: 5000X). Pre-existing pitting and enlarged ones after treatment are circled. 128
- Figure 44: Optical microscopy images of 3003-T3 aluminum before and after (112-hour) test with nanofluid of 2% alumina in 50/50% Ethylene Glycol/water (Magnification: 5000X). Pre-existing pitting and enlarged ones after treatment are circled. 130
- Figure 45: Average Ra roughness for copper alloy110 before and after 3, 7, 14, 28, 56 and 112 hour-treatments with the reference fluid Ethylene Glycol and its nanofluid of 2% nano-alumina in reference fluid and jet speed of 10.7 m/s. 131
- Figure 46: Normalized Ra roughness for alloy110 copper before and after 3, 7, 14, 28, 56 and 112 hour-treatments with the reference fluid Ethylene Glycol and its nanofluid of 2% nano-alumina in reference fluid and jet speed of 10.7 m/s. 133

- Figure 47: Optical microscopy images of alloy110 copper before and after (112-hour) test with (reference fluid, without nanoparticles) 50/50% Ethylene Glycol/water (Magnification: 5000X). Pre-existing pitting and seemingly clustered ones after treatment are circled. 134
- Figure 48: Optical microscopy images of alloy110 copper before and after (112-hour) test with nanofluid of 2% alumina in 50/50% Ethylene Glycol/water (Magnification: 5000X). Pre-existing pitting and enlarged ones after treatment are circled. 135
- Figure 49: Average Ra roughness for 3003-T3 aluminum before and after 3, 7, 14, 28, 56 and 112 hour-treatments with the reference fluid distilled water and its nanofluid of 2% nano-alumina in reference fluid and jet speed of 15.5 m/s. 137
- Figure 50: Normalized Ra roughness for 3003-T3 aluminum before and after 3, 7, 14, 28, 56 and 112 hour-treatments with the reference fluid of distilled water and its nanofluid of 2% nano-alumina in reference fluid and jet speed of 15.5 m/s. 139
- Figure 51: Average weight change for 3003-T3 aluminum in before and after 3, 7, 14, 28, 56 and 112 hour-treatments with the reference fluid of distilled water and its nanofluid of 2% nano-alumina in reference fluid and jet speed of 15.5 m/s. 140
- Figure 52: Optical microscopy images of 3003-T3 aluminum before and after (112-hour) test with (reference fluid, without nanoparticles) distilled water (Magnification: 500X). 141
- Figure 53: Optical microscopy images of 3003-T3 aluminum before and after (112-hour) test with nanofluid of 2% alumina in distilled water (Magnification: 500X). 143

- Figure 54: Average Ra roughness for copper alloy110 before and after 3, 7, 14, 28, 56 and 112 hour-treatments with the reference fluid distilled water and its nanofluid of 2% nano-alumina in reference fluid and jet speed of 15.5 m/s. 141
- Figure 55: Normalized Ra roughness for alloy110 copper before and after 3, 7, 14, 28, 56 and 112 hour-treatments with the reference fluid distilled water and its nanofluid of 2% nano-alumina in reference fluid and jet speed of 15.5 m/s. 145
- Figure 56: Average weight change for alloy110 copper in before and after 3, 7, 14, 28, 56 and 112 hour-treatments with the reference fluid distilled water and its nanofluid of 2% nano-alumina in reference fluid and jet speed of 15.5 m/s. 146
- Figure 57: Optical microscopy images of alloy110 copper before and after (112-hour) test with (reference fluid, without nanoparticles) distilled water (Magnification: 500X). 148
- Figure 58: Optical microscopy images of alloy110 copper before and after (112-hour) test with nanofluid of 2% alumina in distilled water (Magnification: 500X). 150
- Figure 59: Average Ra roughness for 3003-T3 aluminum before and after 3, 7, 14, 28, 56 and 112 hour-treatments with the reference fluid distilled water and its nanofluid of 2% nano-alumina in reference fluid and parallel flow speed of 1 m/s. 151
- Figure 60: Normalized Ra roughness for 3003-T3 aluminum before and after 3, 7, 14, 28, 56 and 112 hour-treatments with the reference fluid of distilled water and its nanofluid of 2% nano-alumina in reference fluid and parallel flow speed of 1 m/s. 153
- Figure 61: Average weight change for 3003-T3 aluminum in before and after 3, 7, 14, 28, 56 and 112 hour-treatments with the reference fluid of distilled water and 154

- its nanofluid of 2% nano-alumina in reference fluid and parallel flow speed of 1 m/s.
- Figure 62: Optical microscopy images of 3003-T3 aluminum before and after (112-hour) test with reference fluid of distilled water (Magnification: 500X). 155
- Figure 63: Optical microscopy images of 3003-T3 aluminum before and after (112-hour) test with reference fluid of distilled water (Magnification: 500X). 157
- Figure 64: Average Ra roughness for copper alloy110 before and after 3, 7, 14, 28, 56 and 112 hour-treatments with the reference fluid distilled water and its nanofluid of 2% nano-alumina in reference fluid and parallel flow speed of 1 m/s. 158
- Figure 65: Normalized Ra roughness for alloy110 copper before and after 3, 7, 14, 28, 56 and 112 hour-treatments with the reference fluid distilled water and its nanofluid of 2% nano-alumina in reference fluid and parallel flow speed of 1 m/s. 159
- Figure 66: Average weight change for alloy110 copper in before and after 3, 7, 14, 28, 56 and 112 hour-treatments with the reference fluid distilled water and its nanofluid of 2% nano-alumina in reference fluid and parallel flow speed of 1 m/s. 160
- Figure 67: Optical microscopy images of alloy110 copper before and after (112-hour) test with (reference fluid, without nanoparticles) 50/50% Ethylene Glycol/water (Magnification: 5000X). Pre-existing pitting and seemingly clustered ones after treatment are circled. 161
- Figure 68: Optical microscopy images of alloy110 copper before and after (112-hour) test with (reference fluid, without nanoparticles) 50/50% Ethylene 163

Glycol/water (Magnification: 5000X). Pre-existing pitting and seemingly clustered ones after treatment are circled.

Figure 69: Foam produced in a) reference fluid of Ethylene Glycol jet test and b) its 2% alumin nanofluid jet test.

177

Figure 70: Normalized Ra roughness for 3003-T3 aluminum before and after 3, 7, 14, 28, 56, 112, 240, 312 and 408 hour-treatments with 3.5 m/s jet, and for 3, 7, 14, 28, 56 and 112 hour-treatments with 10.7 m/s and 15.5 m/s jet. All sets of data obtained for the reference fluid of distilled water, and for nanofluid of 2% nano-alumina in reference fluid.

185

## CHAPTER 1

### 1 INTRODUCTION

#### 1.1 Problem statement and rationale

Nanofluids are colloidal suspensions of nano-size-powders (of size 1 nm to 100 nm) in a base fluid. They have attracted a substantial amount of attention since Masuda et al [1] reported firstly, in 1993, their precursory observations on the thermal conductivity enhancement in liquid dispersions of nanoparticles and their potential as enhanced alternatives to ordinary cooling fluids these alternative cooling fluids. Addition of solid particles in flowing fluids is known to lead to higher erosion rates on conduit materials, but the effect of adding smaller size ones, as nanoparticles (1nm-100nm) are largely unknown. Use of nanofluids instead of conventional cooling fluids requires a better understanding of the likely wear and erosion effects when such nanofluids come in contact with typical cooling-system materials. The presence of nanoparticles in cooling fluids poses a challenging tribological problem, which require intensive theoretical and experimental investigations and exclusively novel solutions.

A number of nanofluid studies regarding thermal property enhancement, along with a variety of different nanoparticle types, have been reported during recent years. Metal oxides, pure metals, lamellar structures, and nanotubes have been examined as nanoparticles in nanofluids by different research teams as part of mainly lubrication studies, but there is no significant research on tribological behavior of nanoparticles in fluid conduits, especially in cooling systems. Research by Baxi [2] reveals that the deposition of particulate matter causes problems in many technical applications, for instance, in fouling of heat exchangers, contamination of nuclear reactors or blockage of membrane filters, and there is an interest in the optimum percentages of nano-particles



in cooling fluids for tolerable erosion and fouling rates. Material erosion in heat exchanger surface also depends on material hardness, angle of flow, flow velocity, particle volume fraction, and type of base fluid, pH of mixture and temperature of fluid, which makes this optimization more complex [2]. In particular, literature review in this thesis shows that fundamental experimental knowledge is needed on the erosion effects of nanofluids for jet impingement and in parallel flow cooling systems. Such knowledge can be of key importance in understanding the role of nano-particles in erosion mechanisms, and in particular for cooling systems.

The research work reported in this thesis includes the establishment of a methodology for testing and evaluating likely surface-change phenomena by nanofluid impact and by nanofluid flow through conduits. A combination of roughness change and removed-material (by weighing) measurements, and optical microscopy imaging and profilometry have been used for assessing the possible early surface changes of cooling-system materials subjected to nanofluids flows.

## **1.2 The research questions of interest**

Among the several unknowns regarding nanofluid tribological phenomena, the following research questions of interest are addressed by this research work:

- When nanofluids are set in contact with typical cooling-system materials, do they lead to different surface modifications than those produced by the reference fluids in same conditions?
- What are the testing conditions required for the assessment of material loss by nanofluids interaction with typical cooling system materials?

- What kind of instruments and methods are available for assessing the material surface changes in typical cooling system materials by fluid interaction? Are those methods and instruments appropriate for assessing material surface change by nanofluids action?
- What new instruments and methods are required for assessing the material surface changes in typical cooling system materials by fluid interactions? Are those methods and instruments appropriate for assessing material surface changes by nanofluids action?
- What are the factors and system parameters that control nanofluids tribological phenomena in cooling systems?
- Can roughness, weight loss and optical microscopy imaging and profilometry be assessing the effects of nanofluids on material surface?
- Do surface modifications result in accelerated short length laboratory tests as compared to fluid-flow tribological effects in actual heat exchanger systems?
- What are the relations between fluid flow speeds, test lengths and roughness changes when testing nanofluids affects on cooling systems surface?
- What are the mechanisms of possible material surface changes when nanofluids are set in contact with typical cooling-system materials?
- What are the possible roles of nanoparticle properties (i.e., nanopowder hardness as compared to that of impacted surface, and particle agglomeration and attachment to surfaces) in surface modifications when nanofluids are set in contact with typical cooling-system materials?

## CHAPTER 2

### 2 LITERATURE REVIEW

#### 2.1 Introduction

The word ‘Tribology’ is derived from the two Greek words ‘tribos’, meaning rubbing, and ‘logos’, meaning study [3]. In 1966 a working group set up by the Minister of State for Education of the UK, the Rt. Hon. Lord Bowden of Chesterfield first coined the word ‘Tribology’ in England [4]. The British Lubrication Engineering Working Group gave a specific definition of Tribology as the science and technology of interacting surfaces in relative motion and of related subjects and practices [5]. Tribology incorporate three interdisciplinary fields: friction, wear and lubrication. In any case the name is relatively new, but the engineering and economic importance of tribology is very old. It is applicable to many fields such as automotive, memory device technology, bioengineering, space engineering, nano-devices, etc. The study of wear, erosion and friction phenomenon at the nanometer scale is called nano-tribology. Nano-tribology can be defined as the investigation of interfacial processes, ranging in the molecular and atomic scale which are occurred during adhesion, friction, scratching, wear, nano indentation, and thin-film lubrication at sliding surfaces [6].

#### 2.2 Literature review on nanofluids

##### 2.2.1 Nanofluids

A new type of fluids called nanofluids, that is, liquids with nanometer size particles (1 nm to 10 nm size), are mainly studied for their abnormal thermal transport properties, and mainly as enhanced alternatives to ordinary cooling fluids. They have attracted a substantial amount of

attention since Masuda et al [1] reported firstly, in 1993, their precursory observations on the thermal conductivity enhancement in liquid dispersions of nanoparticles, their potential as enhanced alternatives to ordinary cooling fluids. Choi et al [7, 8] proposed the term “nanofluid” in 1995 for stable dispersions of nanoparticles. Since then nanofluids have been produced for many research purposes as mixtures of solid metal nano-particles (typically up to 5% of nanoparticles of size between 1 to 100 nm), as gold, oxides (as alumina, silica, titanium dioxide and copper oxide), carbides and nitrides nanoparticles, and of carbon nanotubes or nanofibers in continuous and saturated fluids (as water, ethanol and ethylene glycol) [9].

### **2.2.2 Properties of nanofluids and their promise as coolants**

Nanofluids are predicted to have higher thermal conductivity and heat transfer coefficients than those of the base fluids, because solids have much larger thermal conductivities than those of fluids, and nanoparticles have a much larger surface-to-volume ratio and larger mobility than those of larger solid particles.

The thermal conductivity of nanofluids would increase with volume concentration of particles, and the enhancement would be larger in, for instance, ethylene glycol solutions, which have typically a thermal conductivity lower than that of water [10]. Therefore, nanofluids are promising as coolants for critical-cooling systems, as nuclear systems [11], large engine radiators, microchips [12] and grinding [13], and are proposed for its use in compact heat exchanger for improved heat transfer performance. These and other potential uses of nanofluids, as applications for enhanced detergency, in the biomedical field, and as smart fluids, were discussed by Wong and De Leon [12]. Synthesis of nanopowders and preparation of nanofluids, and nanofluid performance as

transport- and electromagnetically-active-media, and as media for chemical reactions have been recently reviewed by Taylor et al [14].

Thermal and transport properties of nanofluids are predicted as substantially higher, but also addition of nanoparticles also produces larger viscosities than those of the base fluids [15-18]. The enhancement of heat transfer coefficient appears to go beyond a mere thermal-conductivity effect, because it cannot be predicted by traditional pure fluid correlations [11]. The measured thermal conductivities of nanofluids seem to depend on temperature, particle volume fraction, size, shape [17], and coating of nanoparticles [19], on type of base fluid [20], and on pH of mixtures [21]. Such dependencies and some larger than expected nanofluid viscosities can be partially explained [22-24] by aggregation of the nanoparticles, while the kinetics of deagglomeration may strongly depend also on suspension pH [25]. Witharana et al [26] recently suggested that the main mechanisms driving the thermal conductivity behavior are nanoparticle aggregation and the brownian motion in the particle suspension. A comprehensive review of heat transfer properties of nanofluids and their dependence on several factors was presented by Das et al. [27].

### **2.2.3 Other applications of nanofluids**

#### **2.2.3.1 Other heat transfer applications of nanofluids**

The remarkable capabilities of nanofluids in heat transfer improvement have encouraged researchers in recent years to develop advance concepts and technologies in, for instance, manufacturing of ultra-compact, miniaturized and smart electronic chips, and novel technical solutions for mechanical machineries. The uplifting demand for higher speed, multiple functions, more powerful and smaller size boards has almost doubled the number of transistors on electronic chips, with a production of localized heat flux of over 10 MW/m<sup>2</sup>, and the total power exceeding

300 W [28]. It was to solve this uncontrolled power-dissipation demand Choi et al [7, 8] proposed in 1995 the use of nanofluids, the stable dispersions of nanoparticles having abnormal thermal transport properties, as enhanced alternatives to ordinary cooling fluids.

In 2008 Ma et al. [29] and Philip et al [30] respectively developed the promising technologies of “Nanofluid in Oscillating Heat Pipe” and “Nanofluid with Tunable Thermal Properties”. According to Philip et al., tunable thermal property of nanofluids show the advantage of a 300% increase in thermal conductivity of the based fluid, and it may find many technological applications for these fluids in, for instance, nano-electromechanical system (NEMS) and micro-electromechanical system (MEMS) based devices. Routbort et al. [31] started a project in 2008 that employed nanofluids for industrial cooling which could result in large energy savings and resulting emissions reductions. In 2011, the US Department of Energy [32] conducted an experimental research from which they claimed that nanofluids achieved thermal conductivity enhancements of 10% to 50% compared to those of traditional fluids. They develop the chemistry to scale up from one liter to the pilot-production scale of 100 liters, from which they predicted significant energy savings and associated emissions reductions.

Alumina ( $\text{Al}_2\text{O}_3$ ) and copper oxide ( $\text{CuO}$ ) are the most common and inexpensive nanoparticles used by many researchers in their experimental investigations [38]. In most experiments, addition of nanoparticles in a base fluid resulted in enhancement of the thermal conductivity. In 1997, an experimental research [39] reported 60% improvement of the thermal conductivities as compared to those of corresponding base fluids for only 5-vol% of nanoparticles in nanofluids containing  $\text{Al}_2\text{O}_3$ ,  $\text{CuO}$ , and  $\text{Cu}$  nanoparticles with two different base fluids: water and HE-200 oil. Later in 1999, Lee et al [40] experimentally demonstrated an enhancement for heat transfer coefficient of

about 20% (as compared to base fluid) at 4 vol% of CuO-nanopowder nanoparticles in ethylene glycol nanofluid. Results suggested that not only particle shape but also size is to be considered dominant in enhancing the thermal conductivity of nanofluids. For instance, Leong et al [41] reported the heat transfer enhancement of an automotive car radiator using ethylene glycol with 2% copper as nanofluid (with ethylene glycol the base fluid for comparison); they observed that the overall heat transfer coefficient and bulk heat transfer were increased by about 3.8% with the use of the nanofluid as compared to the base fluid alone. More recently Heris et al [42] obtained an experimental enhancement for heat transfer coefficient of about 55% (as compared to base fluid) with a 0.8%-CuO-nanopowder in ethylene glycol nanofluid.

The work of Peyghambarzadeh et al [43] tested five different concentrations for nanofluid of alumina nanoparticles in water in the range of 0.1 to 1% volume, as they compare to pure water in an automobile radiator. Their results demonstrated that nanofluids with those low concentrations can enhance heat transfer efficiency up to 45% in comparison to pure water. Some follow-up work by the same researchers [44] measured the overall heat transfer coefficient (using the conventional 3-NTU technique) in a car radiator which was cooled by copper-oxide- and iron-oxide-nanofluids at concentrations of 0.15, 0.4, and 0.65 vol.% in water. They found that those nanofluids produced larger overall heat transfer coefficients (by up to 9%) as compared to those for water, and increasing the nanoparticle concentration enhanced the heat transfer. However, increasing the nanofluid inlet temperature led to lower overall heat transfer.

In an extensive research in 2009 on use of nanofluids in industrial application K. V. Wong et al [12] found that for U.S. industry, the replacement of cooling and heating water with nanofluids had the potential to conserve 1 trillion Btu of energy/per year. They also showed, for the U.S.

electric power industry, that using nanofluids in closed-loop cooling-cycles could save about 10–30 trillion Btu per year (equivalent to the annual energy consumption of about 50,000–150,000 households) and the associated emissions reductions would be approximately 5.6 million metric tons of carbon dioxide; 8,600 metric tons of nitrogen oxides; and 21,000 metric tons of sulfur dioxide. Donzelli et al. [38] demonstrated a smart application of nanofluid where a particular class of nanofluids can be used as a smart material working as a heat valve to control the flow of heat. The nanofluid can be readily configured either in a “low” state, where it conducts heat poorly, or in a “high” state, where the dissipation is more efficient.

Use of nanofluids has potential in nuclear power plants cooling [32]. Their application could enable significant power upgrades in current and future pressurize water reactors, thus enhancing their economic performance [45]. In 2012, M. G. M. Pop et al [46] published a patent on using nanoparticles in closed circuits of emergency systems and related methods. They claimed that using nanoparticles in solid or fluid form in a nuclear power plant cooling system can improve heat transfer and reduce corrosion. Kim et al. [47, 48] performed a study to assess the feasibility of nanofluids in nuclear applications by improving the performance of any water-cooled nuclear system that limited the heat removal. Possible applications include pressurized water reactor primary coolant, standby safety systems, accelerator targets, plasma divertors, and so forth, [45]. The use of nanofluids with at least 32% higher CHF (critical heat flux) could enable a 20% power density uprate in current plants without changing the fuel assembly design and without reducing the margin to CHF.



### 2.2.3.2 Simulation in nanofluids research

Computational fluid dynamics approaches (as lattice Boltzmann, Eulerian–Lagrangian, thermal dispersion, and Eulerian–Eulerian) have been applied [33] in the field of nanofluids to attempt understanding of the experimentally measured phenomena. In a simulated radial-flow cooling system of an alumina–water nanofluid at a Reynolds number of 1200, Roy et al. [34] found that the heat transfer rate increased by about 45% and 110% for respectively 5% - and 10%-volume concentrations of particles. In a similar cooling system Palm et al. [35] also numerically examined the heat transfer enhancement of alumina –water nanofluids, and their results predicted that 4% volume of  $\text{Al}_2\text{O}_3$  nanoparticles dispersed in water could produce a 25% increase in heat transfer coefficient as compared to water alone.

The cooling system of a Class 8 truck engine was modeled using the Flowmaster computer code. Numerical simulations were performed replacing the standard coolant, 50/50 mixture of ethylene-glycol and water, with nanofluids comprised of CuO nanoparticles suspended in a base fluid of a 50/50 mixture of ethylene-glycol and water. By using engine and cooling system parameters from the standard coolant case, the higher heat transfer coefficients of the nanofluids resulted in lower engine and coolant temperatures.

Another computational fluid dynamics simulation [36] of ideal nanofluid cooling (50/50 mixture of ethylene-glycol and water as base fluid and nanofluids comprised of CuO nanoparticles suspended in a base fluid) in a Cummins 500hp diesel engine showed that radiator size could be reduced by 5%. More recently Mehdi et al [37] used a two-phase Euler-Lagrange method and experimental data from various researchers to investigate the effect of various force (Brownian, thermophoretic, drag, lift, and virtual mass forces) on the particle distribution and thermal

characteristics of the water-base alumina nanofluid flowing inside a pipe under uniform wall heat flux. Their study suggested that the Brownian forces would make the particle distribution more uniform, whereas the thermophoretic forces would enhance nonuniformity of the particle distribution.

### **2.2.3.3 Automotive Applications**

Nanofluids have great potentials to improve automotive and heavy-duty engine cooling rates by increasing the efficiency, lowering the weight and reducing the complexity of thermal management systems. Researchers are trying to use nanofluids in automobile for various applications such as coolant, fuel additives, lubricant, shock absorber and refrigerant. Many conventional coolant-engine oils, automatic transmission fluids, coolants, lubricants, and other synthetic high temperature heat transfer fluids found in automotive thermal systems - radiators, engines, heating, ventilation and air-conditioning (HVAC) have characteristically showed poor heat transfer properties [12].

These systems could be more efficient by using nanofluids instead of conventional coolants [49, 50]. Ethylene glycol based nanofluids have attracted much attention in the application as engine coolant [51-53], due to the low pressure operation compared with a 50/50 mixture of ethylene glycol and water, which is the universally used automotive coolant. Nanofluids has a high boiling point, and it can be used to increase the normal coolant operating temperature and then reject more heat through the existing coolant system [54]. Leong et al [41] reported the heat transfer enhancement of an automotive car radiator using ethylene glycol with 2% copper as nanofluid (with ethylene glycol the base fluid for comparison); they observed that the overall heat transfer

coefficient and bulk heat transfer were increased by about 3.8% with the use of the nanofluid as compared to the base fluid alone.

At high speeds, approximately 65% of the total energy output from a truck is expended in overcoming the aerodynamic drag, and the large radiator in-front surface of the truck is partly responsible for this loss [12]. The use of high thermal conductivity nanofluids in radiators can potentially lead to reductions in the frontal area of radiators of up to 10% [55]. Due to the higher thermal efficiency and smaller size of the radiator there would be less cooling fluid and coolant pumps could be shrunk. Also, car engines could be operated at higher temperatures to produce more horsepower while meeting strict emission standards. The application of nanofluid could also contribute to a reduction of friction and wear, reducing parasitic losses, operation of components such as pumps and compressors and subsequently leading to more than 6% fuel savings [12].

An experimental investigation was carried out to improve the performance and emission characteristics of C.I engine using cerium oxide nanoparticles with diesel and biodiesel mixture fuel by Arul Mozhi Selven et al. [56]. The cerium oxide acted as an oxygen donating catalyst and provides oxygen for the oxidation of CO or absorbs oxygen for the reduction of NO<sub>x</sub>. They observed that combustion of the fuel will be improved and reduce the exhaust emission by using a cerium oxide nano particle catalyst. In another research, S. Senthilraja et al. [57], conclude that internal combustion engine performance will be improved by 5 ~ 10% by using nanoparticle suspended in commercial engine coolant.

It is plausible that using nanofluids in automobiles, higher thermal performance could be obtained in the future, but many practical, and in particular tribological, concerns remain about nanofluid effects on cooling system materials, as wear and erosion. There is little understanding of the

tribological impact of nanofluids on typical material surfaces. In order to determine whether nanofluids degrade radiator material, Molina et al [58, 59] presented preliminary work about the effects of jet-impingement on the roughness change (Ra, Rz and Rq) of 3003-T3 aluminum and copper specimens after 3, 7 and 14 hour treatments with suspensions of 2% nano-alumina in water, and in a solution of water plus ethylene glycol, as they compared to average initial roughness. They built and calibrated an apparatus that can create jet impingement coolant flow and are currently testing and measuring material loss of typical radiator materials by various nanofluids. In another research Singh et al. [59], measure nanofluid erosion effect on radiator material by weight loss-measurements as a function of fluid velocity and impact angle. They observed no erosion using nanofluids made from base fluids ethylene and tri-chloroethylene glycols with velocities as high as 9m/s and at 90°–30° impact angles. There was erosion observed with copper nanofluid at a velocity of 9.6 m/s and impact angle of 90°.

Use of nanofluid and tribological effect in automobile thermal system demand more research with a wider range of particle loadings in various base fluid. Extensive research and testing in this area will contribute in the design of efficient engine cooling and other thermal systems that contain nanofluids. Advance cooling system design using nanofluids would create a future generation engines that would be able to run at higher optimal temperatures with an increased power output. Engine, components would become smaller and less heavy allowing for higher speed, better gas mileage, saving consumers money and resulting in fewer emissions for a cleaner environment.

### **2.3 Wear, corrosion and abrasion**

Wear is a complex phenomenon. Almost all machines lose their durability and reliability due to wear, and the possibilities of new advanced machines are reduced because of wear problems [72].

In materials science, wear is the displacement or removal of material from its consequent and original position on a solid surface performed by the action of another surface. According to the German DIN standard 50-320, “the progressive loss of material from the surfaces of contacting body as a result of mechanical causes” is defined as wear. It is related to interactions between surfaces and more specifically the removal and deformation of material on a surface as a result of mechanical action of the opposite surface [73]. Loads, speed, temperature, contact type, type of environment etc are the parameters which effect wear of a material [74]. Furthermore, there are several types of wear [45]: erosive, corrosive, adhesive, abrasive, fatigue and impact wear.

Erosive wear can be defined as an extremely short sliding motion and is executed within a short time interval. Erosive wear is caused by the impact of particles of solid or liquid against the surface of an object [75]. The impacting particles gradually remove material from the surface through repeated deformations and cutting actions [76]. Momentum effect of impinged particles (solid, liquid or gaseous) remove fragments of materials from the surface cause erosive wear [77]. It is a widely encountered mechanism in industry. A common example is the erosive wear associated with the movement of slurries through piping and pumping equipment. Sand particles, nanoparticle and/or other solids will, in many applications, be present in the liquid, and may result in erosive wear of the pipe components; i.e. in the pipes, in pipe bends, blinded tees, connections etc. [78]. Erosive wear of engine bearings generally caused by cavitation in the lubrication oil [77]. The rate of erosive wear is dependent upon a number of factors. The material characteristics of the particles, such as their shape, hardness, impact velocity and impingement angle are primary factors along with the operation temperature and properties of the surface being eroded. The impingement angle is one of the most important factors and is widely recognized in literature [79]. For ductile materials the maximum wear rate is found when the impingement angle is approximately  $30^\circ$ ,

whilst for non-ductile materials the maximum wear rate occurs when the impingement angle is normal to the surface [80]. For aluminum and Cast iron maximum erosion rate is found at gradually  $20^{\circ}$  and  $80^{\circ}$  impingement angle [79].

Corrosion is the deterioration and loss of a material and its critical properties due to chemical, electrochemical and other reactions of the exposed material surface with the surrounding environment [81]. Corrosive wear is material degradation wherein both wear and corrosion mechanisms are present. Increased temperature and removal of the protecting oxide films from the surface during the friction or particle impingement promote the oxidation process. Friction and particle impingement provide continuous removal of the oxide film followed by continuous formation of new oxide film. Hard oxide particles removed from the surface and trapped between the sliding/rolling/impinged surfaces additionally increase the wear rate [80].

Impact wear is the wear of a solid surface that is due to percussion, which is a repetitive exposure to dynamic contact by another body [82]. This is a material loss/damage produced by a solid surface repeatedly impacting another solid surface [83]. Elastic and plastic deformation both produce relative slip of one surface on another-the requirement for sliding wear. Impact wear, however, is closely related to erosive wear.

## **2.4 Literature review on wear and erosion by nanofluids**

Over the recent years tribological investigation have done on variety of different nanoparticle types. Molina et al [58-60] conducted extensive research on tribological effect of alumina nanofluid on typical heat exchanger material 3003-T3 aluminum and alloy 110 copper. They measured weight loss, surface roughness, and microscopic image analysis to explore any possible erosion effect of nanofluid and base fluid on sample material. They concluded that those two fluids

produced neither significant roughness differences nor significant material removal. Thrush et al [61] conducted tribological experiment on nanofluids contact of different metal oxides, pure metals, lamellar structures, and nanotubes in lubricating systems. Particle concentration, size, and shape were primarily investigated. They also found tribological effects of nanoparticles in different combination of applications.

Gara and Zou [62], conducted research on tribological effects of zinc oxide and aluminum oxide nanoparticles in aqueous solutions with 0.1 to 50 wt% particle concentration range. The effects of nanoparticle type, particle concentration, and surface roughness of the specimen on the friction and wear characteristics were investigated. Tests were performed in a ball-on-disk tribometer with a 10 N applied load and at 100 mm/s sliding velocity. They found that nanoparticles had a beneficial effect on the friction and wear characteristics of lubricants. In a tribology test of copper nanoparticle (20 nm size) 0.2%wt in 50CC lubricating oil in a four ball tester with SAE52100 steel, 12.7 mm diameter balls, Yu et al [62] found that there was a wear-scar diameter reduction of 25% and a friction reduction of 20% at 140°C.

Undesirable abrasive effect may be eliminated if nanosized hard alumina particles are used as the filler (reinforcing phase) dispersed in a polymer matrix [63]. In that, friction and wear behavior of blended PTFE and 40 nm alumina particles composite was studied in [64]. This composite showed wear resistance up to 600 times higher than that of the reference samples (without nanoparticle filled) for a certain composition. In a comparative study [65] of the tribological properties of micrometer- and nanometer sized alumina particle filled in poly PPESK (phthalazine ether sulfone ketone) composites showed that 1 vol %-nano-alumina particles composite has the lowest wear rate. Tribological properties of nano-alumina reinforced Polyoxymethylene (POM) composites

were investigated in 2007 by Sun Lanhui et al [66]. They found that, under oil lubrication conditions alumina nanoparticles were more effective in enhancing tribological properties of the POM composites.

Shen et al. [67, 68] proposed in 2008 the concept of Minimum Quantity Lubrication (MQL) grinding using nanofluid. They found that the grinding force and surface roughness of nanofluid MQL grinding were decreased in comparison with those of pure oil MQL grinding. C. Mao et al [69] conducted a new research in 2014 on MQL grinding performance using nanofluids. Nanofluids showed superior grinding performance by reducing the grinding force and surface roughness in comparison with that of pure base fluid MQL grinding. They found that the addition of Al<sub>2</sub>O<sub>3</sub> nanoparticles in deionized water decreased the friction coefficient and the worn weight by 34.2% and by 43.4 %, respectively, as compared to those of pure deionized water. Sridharan et al [70] studied the characteristics of nanofluid MQL grinding process using MoS<sub>2</sub> and carbon nanotube nanoparticles. They also found that nanofluids can be effective to improve surface roughness and to reduce specific grinding energy.

In 2001, Eswaraiah et al [71] studied graphene based engine oil nanofluids for tribological applications. They prepared a graphene based engine oil nanofluids and their tested frictional characteristics (FC), antiwear (AW), and extreme pressure (EP) properties. The improvements in FC, AW, and EP properties of nanofluids are found of respectively 80, 33, and 40% as compared to those of base oil. They proposed this enhancement to explain the nanobearing mechanism of graphene in engine oil and ultimate mechanical strength of graphene.

Although nanofluid as coolant has several potential advantages, such as high heat transfer performance, smaller size and volume heat exchanger, a lower pressure drop and subsequently



lesser pumping power but many practical, and in particular tribological, concerns remain about nanofluid effects on cooling system materials, as wear and erosion, and there is little understanding of the tribological impact of nanofluids on typical material surfaces. Initial research at US Dept. of Energy facilities [84, 85] found no surface change to aluminum 3003 when jet-impacted for 750 hours by a 2 vol.-%-SiC- in-water nanofluid , and by nanofluids of Cu and Al oxides in the base fluids ethylene and trichloroethylene glycols, with velocities of 8 to 9 m/s and impact angle of 30°; also, the corresponding erosion rate in vehicle radiator was extrapolated to be of as low as 0.065 milligrams/year of typical vehicle operation.

The experimental research work of Celata et al [86, 87] tested effects on aluminum, copper, and stainless steel targets of nanofluid jets of TiO<sub>2</sub>, Al<sub>2</sub>O<sub>3</sub>, ZrO<sub>2</sub> (each at 9% concentration), and of SiC (at 3% concentration) in distilled water, as they compared to same materials impacted by a water-only jet. They reported no differences in material removal (by profilometer scanning) for stainless steel. But for aluminum and copper, some significant increase of nanofluid-erosion (as compared to base fluid) were observed on aluminum targets for the TiO<sub>2</sub>, Al<sub>2</sub>O<sub>3</sub>, and ZrO<sub>2</sub> nanofluids (of about three hundred difference), and for copper only in the case of ZrO<sub>2</sub> nanofluid. No effects were observed for any target material when impacted by the SiC nanofluid. From SEM analysis they concluded that for the used nanofluids most of the material would be removed by mechanical erosion, while for the water it would be worn mainly by intergranular corrosion (around the impurities of the metal matrix); SiC seemed to cause a very small corrosion effect, partly counterbalanced in the wear removal measurement by a deposition of metal oxides.

George et al [88] recently presented experimental work on erosion effects of a nanofluid of 0.1%-volume of TiO<sub>2</sub> in distilled water. They tested for up to 10 hours the jet-impingement effects at

5m/sec and 10m/sec and at different angles on aluminum and cast iron surfaces. They found that the rates of erosion (by specimen weighing) reached maximum at a 20° angle of impingement for aluminum, and at 90° for cast iron. Corrosion assisted erosion would be the mechanism of material removal in cast iron, and mild abrasive erosion in aluminum, while work hardening was observed for both materials. Nguyen et al [89] investigated the wear effect on an aluminum specimen subjected to the impinging of a jet of a 5% alumina-in-water nanofluid at a velocity of 9.6m/s. After 180 hours, a significant total mass loss of 14 mg was reported.

In 2014 Safaei et al [90] conducted a detail simulation research work on erosion prediction in 3-D, 90° elbow for two-phase (solid and liquid) turbulent flow with low volume fraction of copper. They studied for the influences of size and concentration of micro- and nanoparticles, shear forces, and turbulence on erosion behavior of fluid flow. They used a range of particle sizes from 10 nm to 100 microns and particle volume fractions from 0.00 to 0.04, the simulations were performed for the velocity range of 5–20 m/s. Their results indicate that the erosion rate is directly dependent on particles size and volume fraction as well as flow velocity. It has been observed that the maximum pressure has direct relationship with the particle volume fraction and velocity but has a reverse relationship with the particle diameter. It also has been noted that there is a threshold velocity as well as a threshold particle size, beyond which significant erosion effects kick in. The average friction factor is independent of the particle size and volume fraction at a given fluid velocity but increases with the increase of inlet velocities.

Laguna-Camacho et al [91] conducted an investigation on the effect of various microstructures and mechanical properties on the erosion resistance. In this research they design and developed a instrument to accelerate silicon carbide (SiC) particles from a nozzle by using a compressed air

stream that caused them to impact the surface of the target material. They used a constant velocity of 50 m/s for all the erosion tests. The target was impacted at an angle of 30° to the specimen surface, the particle feed rate was 20 g/min, SiC particles, 125 µm in size, were used as the abrasive. They concluded that erosion rate increases with increasing hardness and ultimate strength, but decreases with increasing ductility.

Harsha et al [92] conducted research on erosion behavior of ferrous (mild steel, stainless steel and cast iron) and non-ferrous (aluminium, brass, copper) materials and also examine the erosion model developed for normal and oblique impact angles by Hutchings [93]. They determined from the SEM studies that the worn surfaces had revealed various wear mechanisms such as microploughing, lip formation, platelet, small craters of indentation and microcracking. In addition to these studies, Morrison et al [94] carried out erosion tests on AISI 304 stainless steel. In this work, it was concluded from the SEM observations that similar morphologies for low and high impact angles could be observed in ductile metals when they were subjected to the impact of sharp particles. The surfaces displayed a peak-and valley topology together with attached platelet mechanisms. In addition, the physical basis for a mechanism to erosion in ductile metals was considered to be related to shear deformations that control material displacement within a process zone for a general set of impact events producing at all impact angles. These events included indentation, ploughing and cutting or micromachining.

In respect to the effect of the erodent particle shape on solid particle erosion, Hutchings showed differences in eroded surfaces due to a shape particle effect [93]. They observed that the shape of abrasive particles influences the pattern of plastic deformation around each indentation and the proportion of material displaced from each indentation, which forms a rim or lip. More rounded

particles led to less localized deformation, and more impacts were required to remove each fragment of debris.

Liebhard et al [96] conducted a study related to the effect of erodent particle characteristics on the erosion of 1018 steel. Spherical glass beads of four different diameter ranges between 53-600  $\mu\text{m}$  and angular SiC of nine different diameter ranges between 44-991  $\mu\text{m}$  were the erodents. The particle velocities were 20 and 60 m/s, an impact angle of  $30^\circ$  was used to conduct all the tests and the feed rate was varied from 0.6 to 6 g/min. The results showed that there was a big difference in the erosivity of the spherical and angular particles as a function of particle size. Angular particles generally were an order of magnitude more erosive than spherical particles. In addition, the erosivity of spherical particles increased with particle size to a peak and then decrease at even larger particle sizes. In respect to angular particle erosivity, it was increased with particle size to a level that became nearly constant with size at lower velocities, but increased continuously at higher particle velocities. Lower flow rates caused more mass loss than higher flow rates for both spherical and angular particles. In this work, the performance of different metallic materials has been analyzed. The aim of this experimentation was essentially to know the behavior of these materials against solid particle erosion and compare their erosion resistance. In addition, the functionality of both, the rig and the velocity measurement method was evaluated.

Molina et al [58] presented preliminary work about the effects of jet-impingement on the roughness change ( $R_a$ ,  $R_q$  and  $R_z$ ) of 3003-T3 aluminum and copper alloy 110 specimens after 3, 7 and 14 hour treatments with suspensions of 2% nano-alumina in water, and in a solution of water plus ethylene glycol, as they compared to average initial roughness. Some substantial increases of roughness were found for the jet-impinged aluminum specimens, while no significant change was

observed for copper. They also presented [97] dynamic viscosity measurements, showing that the addition of to 2%-volume of alumina nanopowders in ethylene glycol increased viscosity by about 30%, while a 5% of nanopowder can almost triple the alumina-nanofluid viscosity. The authors concluded that a 2%-volume concentration seemed to be a reasonable practical compromise (to enhance overall efficiency of cooling systems) between the likely improvements of heat transfer versus the increased viscosity. More recently, Molina et al [60] showed the same type of mild erosion effects by measuring surface roughness (Ra, Rq and Rz) and by microscopic observation (for magnifications of up 5000X) on aluminum and copper specimen after 112 hours of jet impingement of a 2% nano-alumina-50/50% ethylene glycol in water nanofluid at a velocity of 10.7 m/s.

## **2.5 Literature review on nanofluid test methodologies and used instruments**

Suspended solid particles in flowing fluids are likely to lead to higher erosion rates on conduit walls. A number of methodologies and test instruments are designed and have been developed for conventional fluid studies regarding their tribological interactions with solid surfaces.

The fundamental case of single-particle erosion on impacted surfaces is well known, and comprehensive reviews were presented by Engel [98] and Hutchins [99]. The latter author also presented a theoretical model of erosion by particles impacting at normal incidence [100]. That model employed a criterion of critical plastic strain, which was based on just two bulk properties of the impacted material, the dynamic hardness and the ductility of the metal, and on two dynamics parameters, the particle velocity and its mass. The model reasonably agreed with experiments for aluminum alloys, for example the Cousens and Hutchings' [101] study of material removal in aluminum alloys eroded at normal incidence by spherical particles. In that work scanning electron

microscopy and metallographic examinations showed that beneath the impacted surface a layer developed in the early stages of erosion, of approximately four times the hardness of the bulk, and before visible erosion occurred. That finding would explain early erosion, but as impact progressed and after the soft layer was removed, they suggested that bulk material underneath the hard layer would be forced through fissures in that layer to develop into softer surface platelets, and later detachment of them resulted in measurable erosion. However, an alternative explanation can be that micro-cracks in the underneath hard layer propagate and coalesce.

To assess the erosion rates for application purposes, the study of erosion involving multiple solid-particle impacts is required. It must include some aspects particular to this phenomenon, as the resulting wide range of simultaneous attack angles, and the effects of particle embedding in surfaces. The work of Brainard and Salik [102] for annealed copper and aluminum erosion produced by both single- and multiple-particle impacts agreed with the phenomenological findings of Cousens and Hutchings' work [101]. They tested aluminum specimens with 3.2-millimeter-diameter steel balls and microscopic brittle eroding particles at normal incidence and speeds of up to 140 m/s. Rao and Buckley [103] later investigated erosion and morphology of 6061-T6511 aluminum alloy eroded by normal impingement jets of a mix of spherical glass beads and angular crushed-glass particles. They showed that the time evolution for gas-jet erosion involved an "incubation period", an acceleration-deceleration period, and a final steady state period, and they correlated the increase of incubation and acceleration periods (with or without particle deposition) with a decreasing particle impact velocity.

The work of Gee and Hutchings [104] describes the four common erosion test systems (e.g., gas jet; centrifugal accelerator; wind tunnel; and whirling arm tests), and provides guidance for such

erosive wear testing. It also includes a discussion on the important variables in these “dry-type” erosion tests, as particle impact velocity, particle impact angle, particle size, shape and material, and ambient temperature.

The ASTM G76 - 07: Standard Test Method for Conducting Erosion Tests by Solid Particle Impingement Using Gas Jets [105] covers testing of material loss by solid particle impingement with gas-carrier jet-type erosion equipment. There is abundant data about this particle-in-gas-jet erosion of metals (including of copper and aluminum alloys) and of polymers [106]. The mechanisms of observed gas-jet erosion depend on the size of impacting particles, a fact that is relevant to the research work in this paper, and the logarithm of the volumetric erosion rate linearly relates to the logarithm of the impact velocity. For large particles impacting ductile materials, the erosion rates peak for a 20° angle of the incident jet with respect to surface, an effect that is attributed to particle ploughing and cutting by fragmented particles (for brittle materials, however, erosion peaks for the 90° angle, because of crack formation on the impacted crater). But for small particles, of less than one micrometer, flow patterns produce large disturbances from the nominal attack angle, and in particular for ductile materials the same erosion rates seem to occur for a wide range of attack angles around the 90° one.

Ives et al [107] observed, in case of impacted ductile metals, the impacting particle embedding can be of importance because a layer of deformed metal and embedded particles forms (on top of the deformed substrate underneath) and the mechanical properties of this mix layer would govern the erosion behavior. Interesting to this research, it seems that the average size of the embedded particles is much smaller than that of the average incident ones, likely because of particle fragmentation upon impact. It has also been suggested that below a particle-size threshold of about

five micrometers, erosion effects for ductile materials greatly diminish after an initial transient of mix layer formation (e.g., of a deformed metal and embedded particle interphase) [108]. For the case of large alumina particles impacting copper targets a mass gain (e.g., a negative volumetric wear) was observed during the initial particle-embedding transient [109].

In 2013 Celata et al [86, 87] designed experimental methodology called “HETNA” (Hydraulic Experiment on Thermo-Mechanical of Nanofluids) and an experimental facility to investigate and compare the behavior of the nanofluid and the base fluid (i.e., without nanoparticles). HETNA was designed as two identical loops working simultaneously under the same conditions, one filled with the nanofluid and the other with base fluid (without nanoparticles). The main advantage of their instrument was the comparison (of nanofluid interaction and base fluid interaction) is immediate, and an experimental matrix can be adjusted in real time.

A multiple nozzle jet impingement instrument was designed and fabricated by George et al [79]. Their apparatus was designed in such a way that a nominal amount of the nanofluid is used for the study and four different samples can be tested at a time, under different conditions. Sample holders of this instrument can be tilted to vary the angle of impingement. Its fluid flow velocity can be adjusted by means of rotameter and ball valves attached to each nozzle. Nguyen et al [89] investigated the wear effect on an aluminum specimen subjected to the impinging of a jet of a 5% alumina-in-water nanofluid at a velocity of 9.6m/s. They designed and fabricated a new experimental impinging jet system. Their system consists of a closed liquid circuit which is mainly composed of a 10-litre open reservoir and a high head all-plastic magnetically-driven centrifugal pump that forces a continuous circulation of liquid (of a reference fluid or of its nanofluids). They used a heated block in order to create a flat circular heated surface and 3 mm diameter nozzle was



used to create the fluid jet. The nozzle-to-surface distance was precisely adjusted by using three mechanical guides.

In 2013 a new jet impingement instrument was designed and developed by Molina et al [58, 97] to investigate nanofluids effects interaction with typical cooling-system materials. They designed and fabricated a single nozzle test rig, which allows controlling a fluid jet, that impacts a material target (the test specimen); nozzle to target distance, and target angle can be set within wide ranges, nanofluid is recirculated by the instrument pump. The recirculation (gear) pump of their instrument yields a maximum volume flow of 2.1 liter/minute at nozzle velocity of 10.7 m/s.

## CHAPTER 3

### 3 DESIGN, DEVELOPMENT AND CONSTRUCTION OF TEST INSTRUMENTS

One of the objectives of the research in this thesis is to make fundamental experimental measurements of possible early surface changes of cooling-system materials subjected to nanofluids flows. To accomplish these experimental measurements, new instruments were needed, as discussed in previous section 2.5. This chapter presents the design, construction and development of two new devices. Existing and commercial components are described briefly, and the newly developed instruments namely, a multiple nozzle jet impingement and a parallel flow setups, are discussed in detail.

#### 3.1 Motivation

Some instruments have been designed and developed over recent years for nanofluid studies, but mainly regarding thermal property enhancement. In this thesis work, because of the needed long experiment times, the need to test in different temperatures and to also test higher and lower speeds, a new multiple nozzle test-rig has been developed to explore the possible erosion effects of some typical nanofluid suspensions impacting some typical cooling-system materials.

This thesis is mainly based in the work of Molina et al [58, 60, 97] and their preliminary experimental results, by enhancing their experimental test methods. Therefore, two new instruments, a multiple-nozzle jet impingement test-rig, and a parallel-flow test rig were designed and developed for the purposes of this research work. These prototype instruments can be adequate platforms for further development of standard test-rigs.

### 3.2 Design and building process

The formulation of the design problem statement involved determining the requirements of the system, the given parameters, the design variables, any limitations or constraints, and any additional considerations arising from safety, environmental, or other concerns.

This chapter describes the design and development of two experimental test-rig for testing jet-impingement and parallel-flow nanofluids. These experimental setups were designed to meet several requirements that are following listed.

For jet impingement setup:

1. System must allow multiple identical fluid jets to allow simultaneous testing of different specimens, speeds and impingement angles.
2. System must hold multiple test specimens impacted by a fluid jet with adjustable nozzle to specimen distance and jet angle direction.
3. System must allow multiple velocity stages of jet impingement.
4. System must allow different temperatures of working fluid.

For parallel flow setup:

1. System must allow multiple velocity settings of flowing fluid.
2. System must allow holding multiple test specimens in flowing fluid.
3. System must allow and control different temperatures of working fluid. Single nozzle rig

### 3.3 Jet impingement test rigs

#### 3.3.1 Previous work: single nozzle test rig

Molina et al [58] carried out preliminary work in this research problem, they developed a test-rig to explore the possible erosion effects of some typical nanofluid suspensions impacting some typical cooling-system materials. Figure 1 shows a schematics and a photograph of Molina et al [58] developed test rig.

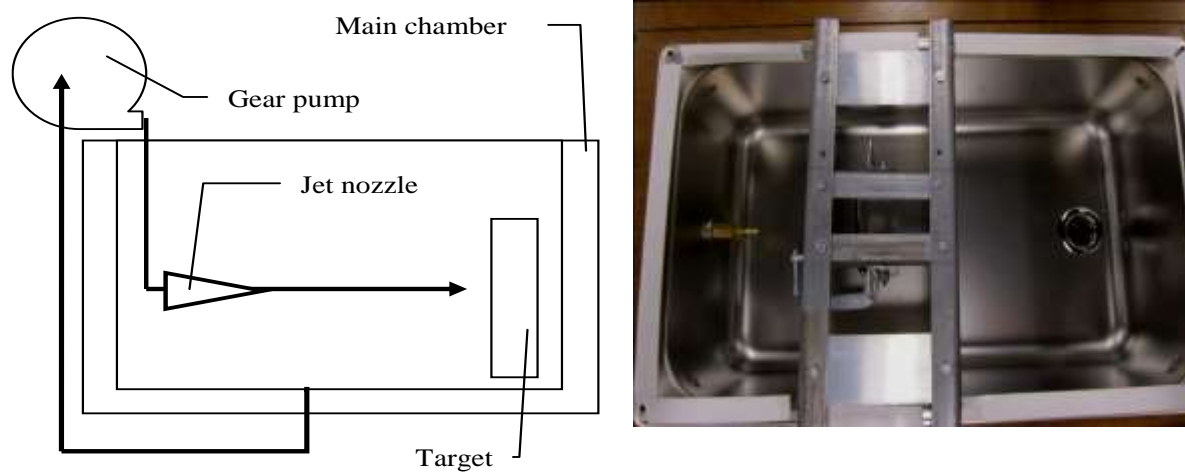


Figure 1. Schematics and photograph of the single nozzle jet test rig to assess nanofluid wear by Molina et al [58].

The test rig of Figure 1 allowed controlling a fluid jet, which impacts a material target (the test specimen); nozzle to target distance, and target angle can be set within wide ranges, nanofluid is recirculated by the instrument pump during each test, development of the instrument is presented elsewhere [58, 97]. The recirculation (gear) pump yields a maximum volume flow of 2.1 liter/minute at nozzle velocity of 10.7 m/s.

### 3.3.2 New variable speed jet multiple nozzle test rig

The experimental research problem of this thesis work required long experiment times and also to test higher and lower jet speeds than those of Molina et al [58]. The research work of this thesis developed a new multiple nozzle test-rig to explore the possible erosion effects of some typical nanofluid suspensions when they impact typical cooling-system materials.

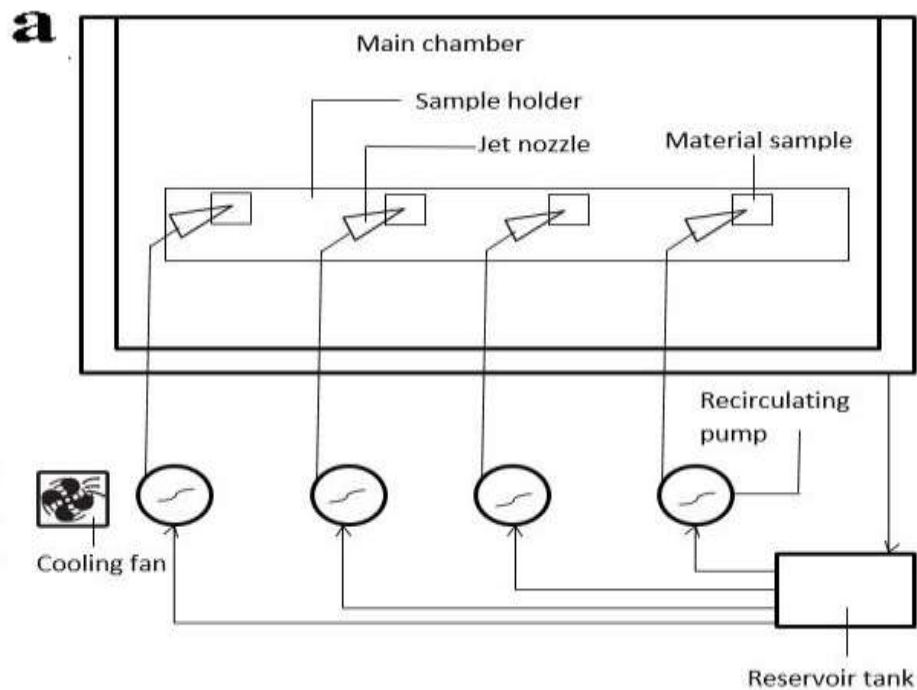


Figure 2a. Schematics of the low speed side of the variable speed jet multiple nozzle test rig to assess nanofluid wear developed in this thesis research.

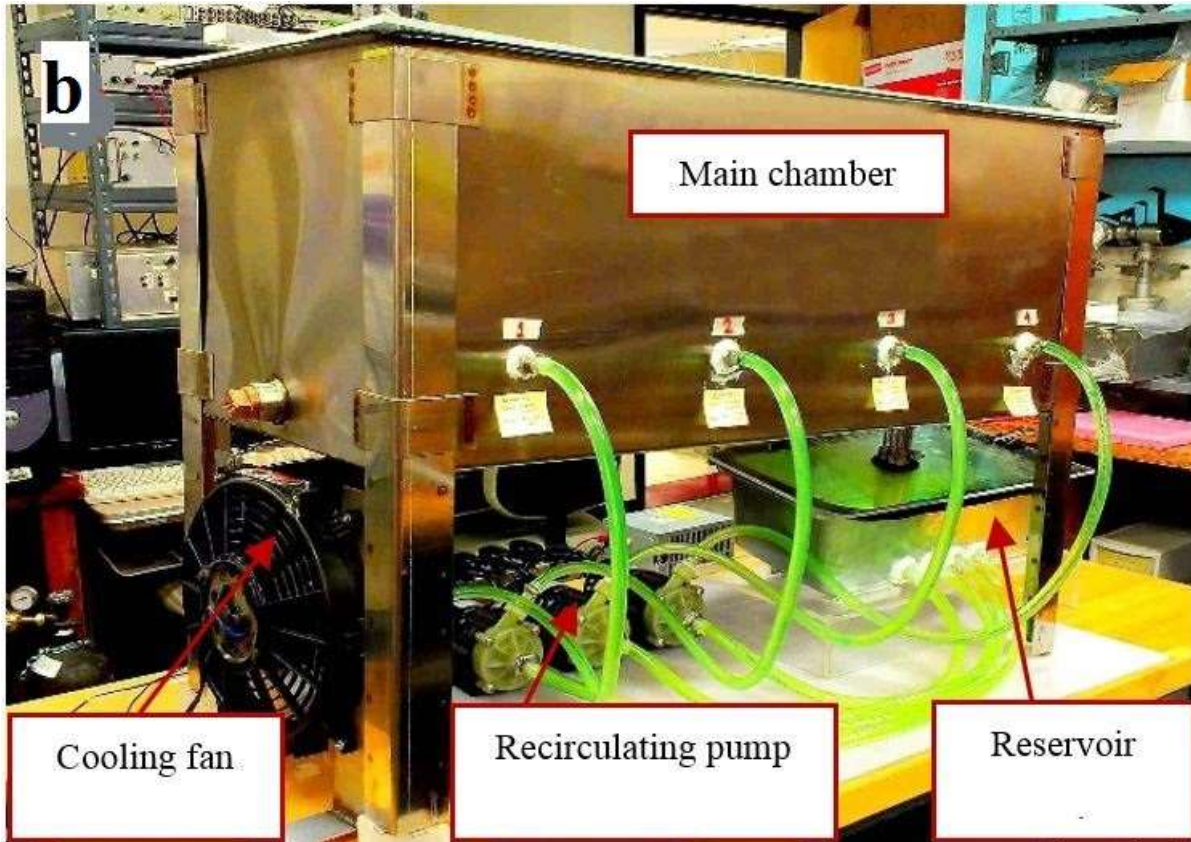


Figure 2. Schematics (a) and photograph (b) of the low speed side of the variable speed jet multiple nozzle test rig to assess nanofluid wear developed in this thesis research.

Figure 2 shows (a) schematics and (b) photograph of the newly developed test rig. This test rig consists of eight nozzles of same dimension. On the lower jet-speed (3.5 m/s) side, each one of four is fed by a pump, which supplies a flow of 2.08 liter/minute at a pressure of 6.5 kPa to the corresponding nozzle. On the higher jet-speed (5 m/s to 35 m/s) side four nozzles are fed by a high pressure centrifugal impeller with pump multiple stages boosts (of maximum pressure head 80m) and the fluid flow is distributed by a manifold to each nozzle; each flow is controlled by a flow control ball valve. Figure 3 shows the schematics and photograph of the high speed side of the variable-speed multiple-nozzle test rig. Two inline flow meters are used to set the required flow rates at the beginning of the experiment, depending on the chosen jet speed (a 0.2 to 2 gallons-per-

minute flow meter for low-speed jets setup, and a 2 to 20 gallons-per-minute flow meter for high-speed jet setup). Experimental fluids are recirculated by the instrument pumps during each test. A cooling fan is employed to remove heat generated from jet impingement, pipe friction, and pump impeller-casing friction, and to maintain a constant experimental temperature.

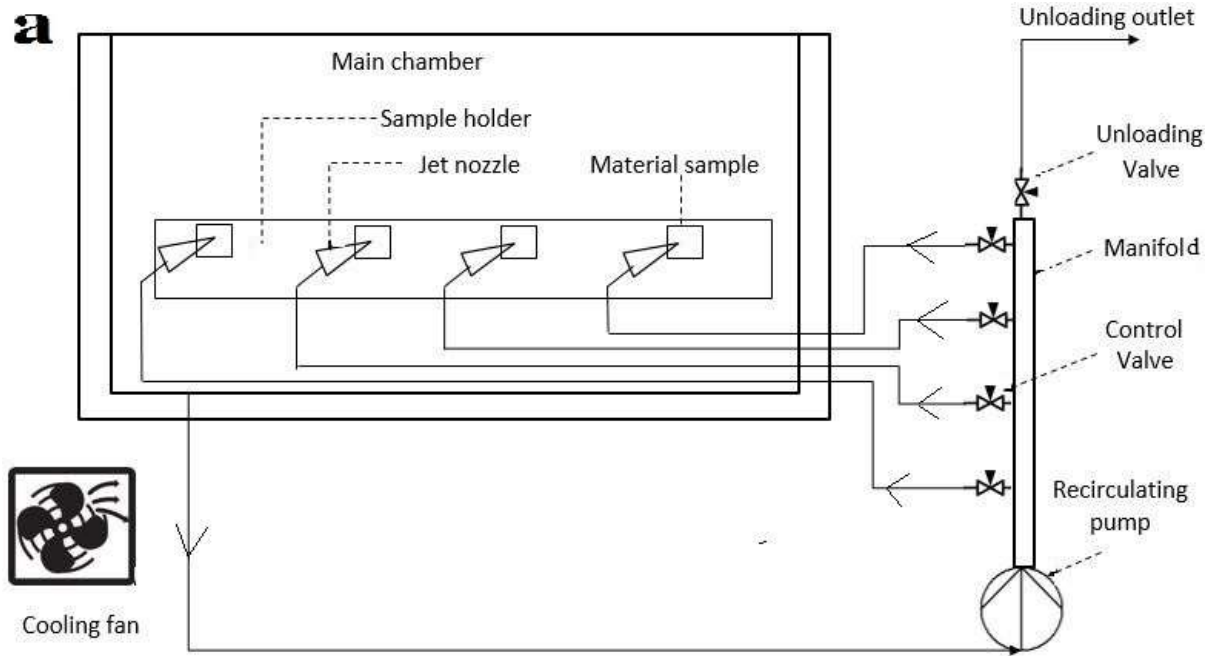


Figure 3a. Schematics of the high speed side of the variable speed jet multiple nozzle test rig to assess nanofluid wear developed in this thesis research.

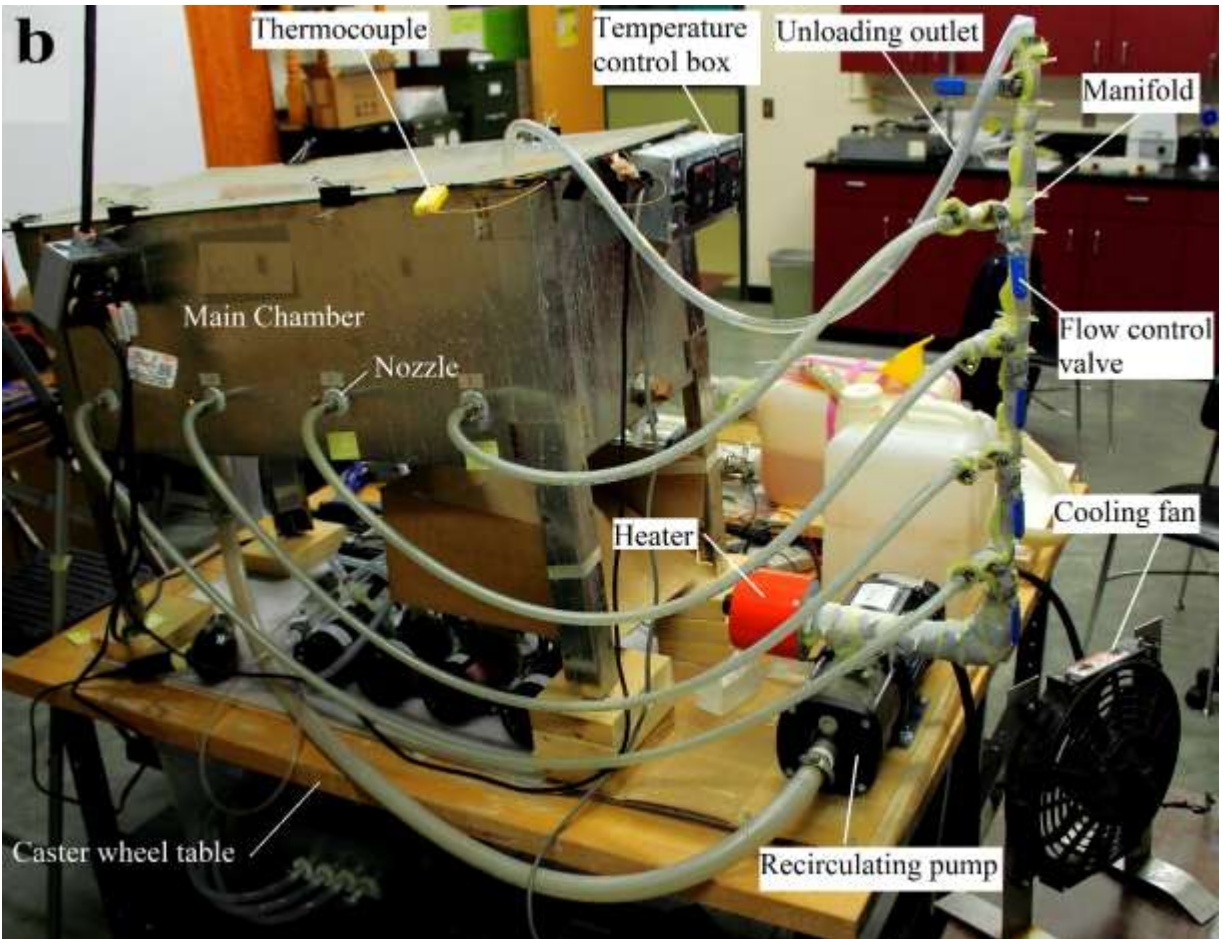


Figure 3. Schematics (a) and photograph (b) of the high speed side of the variable speed jet multiple nozzle test rig to assess nanofluid wear developed in this thesis research.

### 3.3.3 Components of the new test rigs

#### 3.3.3.1 Main chamber

Main chamber is a 36"x18"x14" stainless steel tank with 18" long leg (Figure 4). The tank that was selected from the design evaluation must be in incline configuration to create gravity feed of recirculating fluid towards tank outlet and enough space needed between basement and tank bottom for cooling purpose. The tank design also should be considered with proper safety and precautions. Eight nozzles of same dimension were attached in both walls of the tank long side.



Four of those were used for high speed (3- 35 m/s) and four others were used for low speed (3.5 m/s) jet test. Silicon seal was used to confirm no leakage form any through wall fittings (nozzle, tank outlet). A 38"x20"x1/8" optically clear acrylic sheet was used as top cover so that jet impingement operations can be observed in running condition.

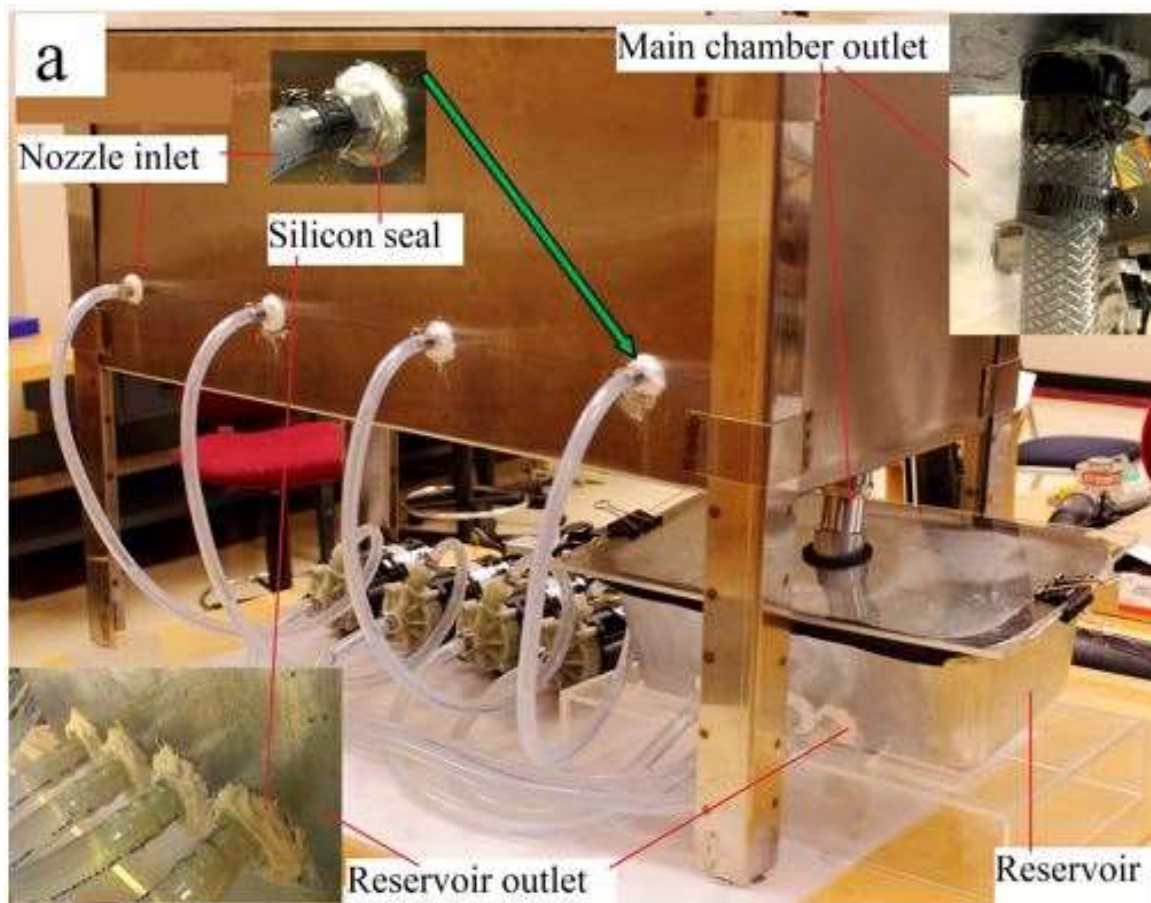


Figure 4a: Main chamber details of side view (low speed side).

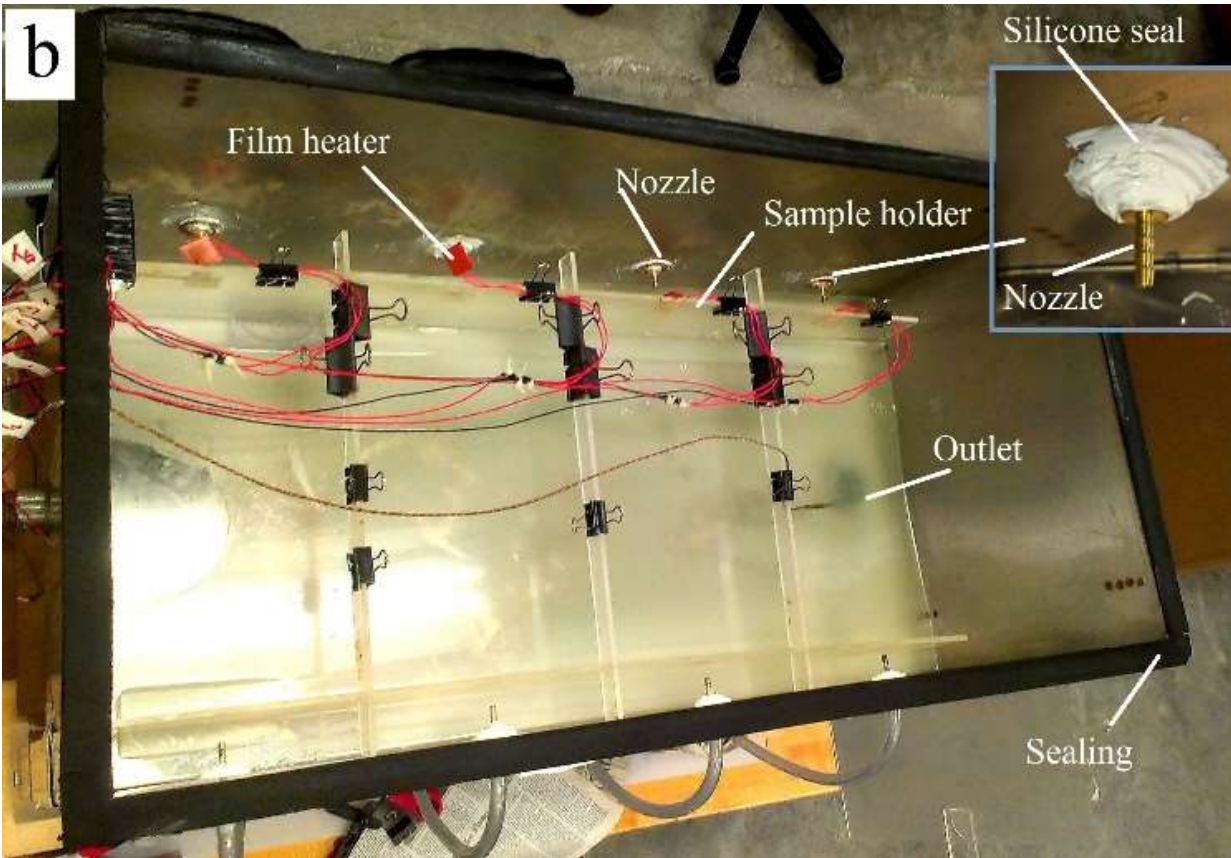


Figure 4: Main chamber details of a) side view b) top view

### 3.3.3.2 Jet impingement test sample holder

An optically clear acrylic sample holder was fabricated for the jet impingement experiment. This sample holder consists of five flanges through connections as shown in the Figure 5. The flanges were constructed from cast-acrylic sheet. Smaller flanges are connected to bigger flange through a slot in bigger flange. Length of bigger flanges and smaller flanges are the same as length and width (36"x18") of main chamber gradually. Sample holder can be placed inside of the main chamber tightly touching all walls. Jet length can be adjusted by adjusting the flange settings as shown in Figure 5. Eight sample inset slots has been cut on the bigger flanges to place sample. A small sample takeoff slots has also been cut off for each sample inset slot for easier sample

handling. Medium (1 inch) size paper clips were used to clamp sample with sample holder in sample inset slot.

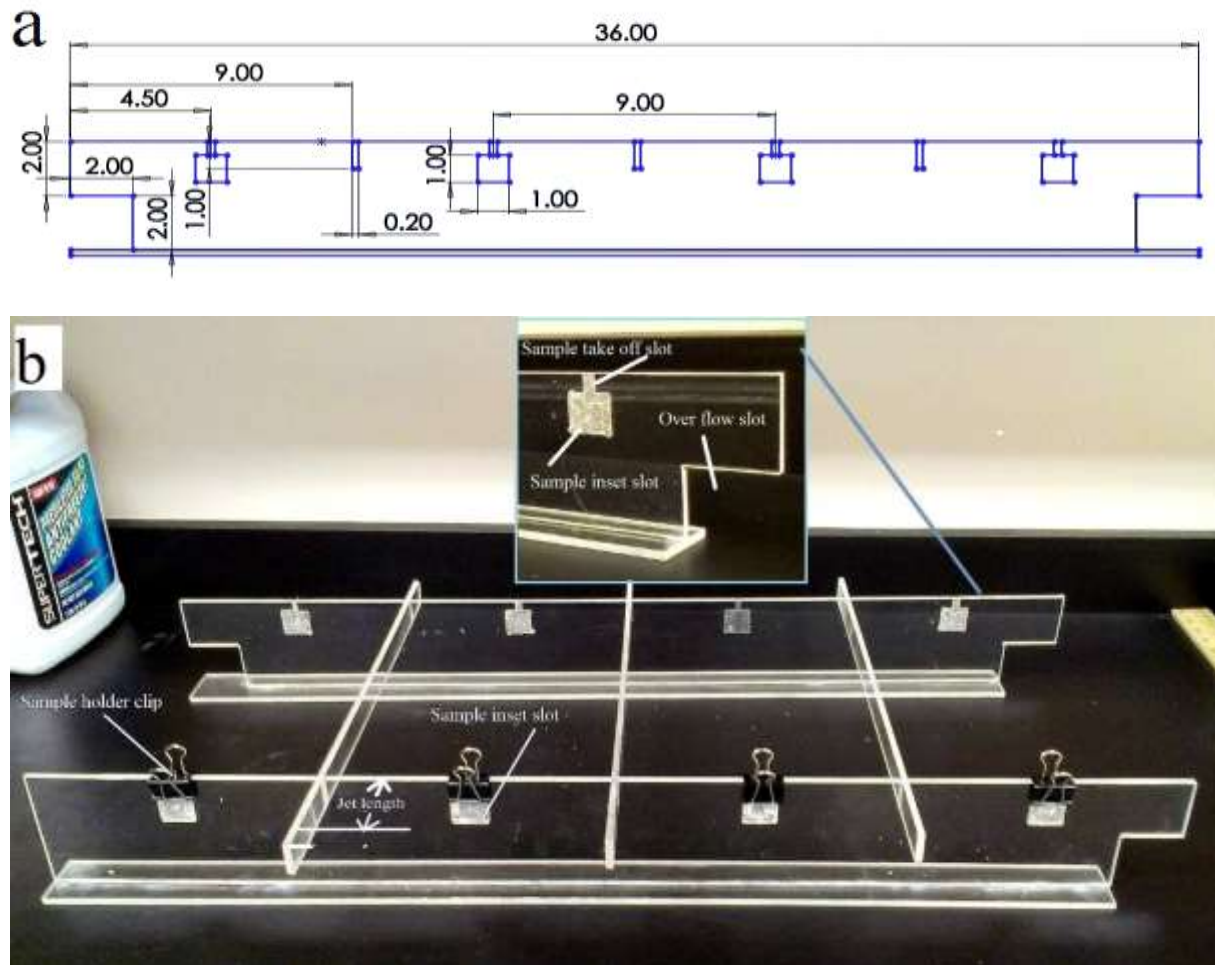


Figure 5: Jet impingement sample holder a) design and b) details

### 3.3.3.3 Pump-piping design and specification

The system is designed as piping network in which the flow of fluids is directed through the several items of equipment in Figure 6. If sufficient variables (flow rate and pressures) are specified on the network, the unknown variables can be calculated. Stainless steel metal pipe, pipe fittings and FDA-Compliant Resin tube were used in suction and discharge piping network. As FDA-

Compliant Resin and stainless steel exhibit high hardness, they show high wear resistance too. FDA-Compliant Resin has adequate clarity and toughness, which help to observe the fluid flow, while the thickness (4mm) helps to decrease the heat loss.

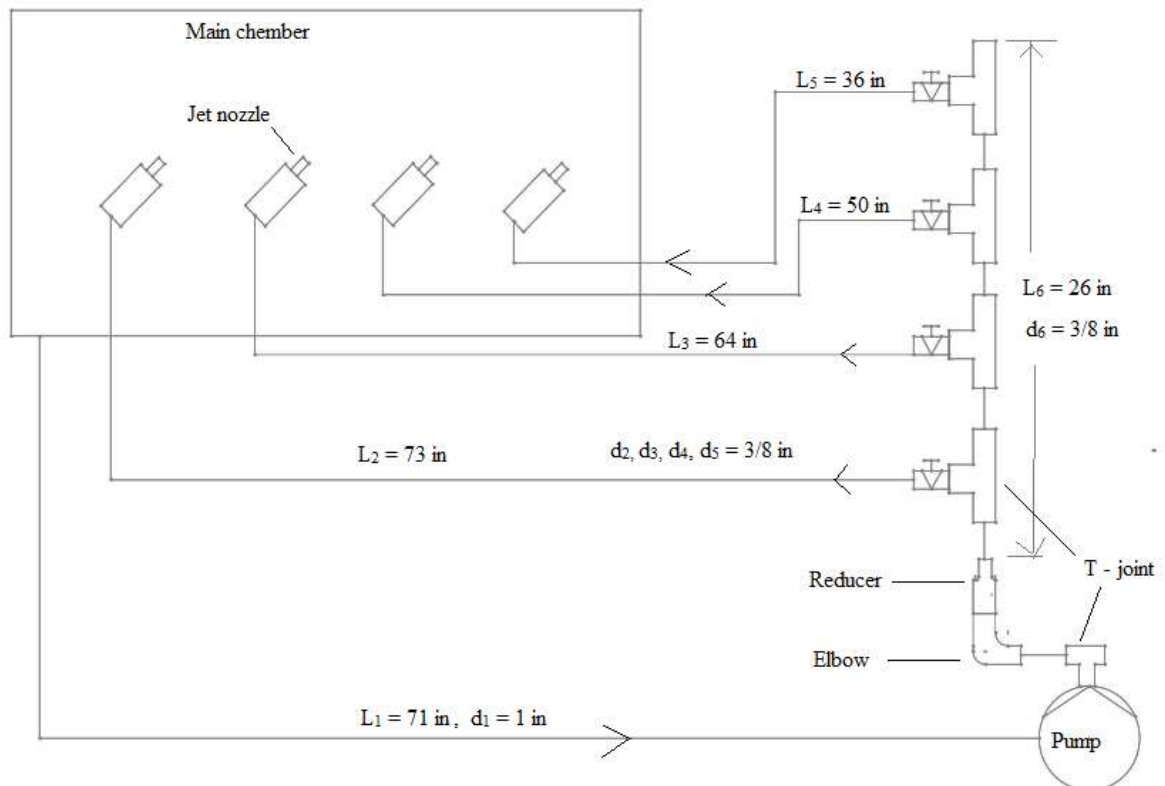


Figure 6: Piping network and instrumentation diagram for high speed jet multiple nozzle test rig (  $L$  = pipe length,  $d$  = pipe diameter)

In this designed system pumps do not suck; rather the pump pushes or throws the fluid out of the pump leaving a partial vacuum. A pump will not operate properly without sufficient inlet pressure, if so, the pump will cavitate. Cavitation is caused by the rapid formation of vapor pockets (bubbles) in a flowing liquid in regions of very low pressure and collapsing in higher pressure regions, often

a frequent cause of structural damage to the propellers or other parts of the pump [110]. Usually the atmospheric pressure pushes the fluid into the pump. For centrifugal pumps, this force is measured in Feet of Head. Atmospheric pressure at sea level is 14.7 psi. At sea level, this can also be stated in terms of 29.94 inches of mercury (barometers) or 33.9 feet of water. The convention with centrifugal pumps is measure pressure in Feet of Head.

### 3.3.3.3.1 Friction loss calculation and pump selection

#### Minor loss Calculation for low speed jet multiple nozzle test rig

Flowing fluid: Ethylene glycol

Properties of fluid:

$$\text{Density } \rho = 1.115 \text{ g/cc} = 1115 \text{ kg/m}^3 \text{ [111]}$$

$$\text{Dynamic viscosity } \mu = 4 \times 10^{-3} \text{ Ns/m}^2 \text{ [111]}$$

Expected maximum jet speed  $v = 3 \text{ m/s}$

Nozzle diameter  $d_n = 3.175 \text{ mm}$

$$\text{Flow rate } Q = Av = \pi d_n^2 v / 4$$

$$= 3.1415 \times 0.003175^2 \times 3 / 4$$

$$= 2.375 \times 10^{-5} \text{ m}^3/\text{s}$$

$$= 0.38 \text{ gpm.}$$

Minor loss in nozzle:

Nozzle diameter  $d_n = 3.175 \text{ mm}$ ,

Jet velocity  $v = 3 \text{ m/s}$

$$\text{Reynolds number } Re = \rho v d / \mu$$

$$= 1115 \times 3 \times 0.003175 / (4 \times 10^{-3})$$

$$= 2655 > 4000$$

= Flow is turbulent.

Minor loss in nozzle  $h_1 = k V^2 / 2g$  [112];

$$D_1/D_2 = (3/8)/0.125 = 3;$$

Resistance coefficient  $K = 0.25$  [100];

$$\text{Minor loss in nozzle } h_1 = (0.25 \times 3^2) / (2 \times 9.81)$$

$$= 0.115 \text{ m}$$

Minor loss in pipe:

$$\text{Pipe diameter} = 3/8 \text{ " } = 0.009525 \text{ m}$$

$$\text{Flow velocity} = Q/A = (2.375 \times 10^{-5}) / (\pi \times 0.009525^2 / 4) = 0.333 \text{ m/s}$$

Reynolds number  $Re = \rho v d / \mu$

$$= 1115 \times 0.333 \times 0.003175 / (4 \times 10^{-3})$$

$$= 295 < 4000$$

= Flow is laminar.

Friction factor  $f = 64/R$  [113];

$$= 64/295$$

$$= 0.22$$

Total pipe length = 20 + 20 = 40 in

$$\text{Minor loss in pipe } h_2 = f \frac{L v^2}{2gD}$$

$$= \frac{0.22 \times 40 \times 0.333^2}{\frac{2 \times 9.81 \times 3}{8}}$$

$$= 0.13 \text{ m}$$

Total minor loss  $H_L$

$$H_L = h_1 + h_2 = 0.115 + 0.13 = 0.25 \text{ m}$$

Total head required for pump:

HT = Static head + Friction head (minor loss)

$$= 0.4 \text{ m} + 0.25 \text{ m} = 0.65 \text{ m} = 2.13 \text{ ft}$$

According to the above calculation, the following pump is selected:

Vendor: McMaster, Part# 9925K71, Max head 7 ft

#### Minor loss Calculation for high speed jet multiple nozzle test rig

Flowing fluid: Ethylene glycol

Properties of fluid:

$$\text{Density } \rho = 1115 \text{ kg/m}^3$$

$$\text{Dynamic viscosity } \mu = 4 \times 10^{-3} \text{ Kg/m-s}$$

Expected maximum jet speed  $V = 25 \text{ m/s}$

Nozzle diameter  $d_n = 3.175 \text{ mm}$

Flow rate for each nozzle  $Q_1 = AV = \pi d_n V/4$

$$= 3.1415 * 0.0031752 * 25/4$$

$$= 1.98 \times 10^{-4} \text{ m}^3/\text{s}$$

$$= 3.135 \text{ gpm.}$$

For four nozzle, total flow rate  $Q = 4Q_1$

$$= 4 * 1.98 \times 10^{-4} \text{ m}^3/\text{s}$$

$$= 7.92 \times 10^{-4} \text{ m}^3/\text{s}$$

$$= 12.54 \text{ gpm.}$$

Minor loss in nozzle:

Nozzle diameter  $d_n = 3.175 \text{ mm}$ ,

Jet velocity  $V = 25 \text{ m/s}$

Reynolds number  $Re = \rho v d / \mu$

$$= (1115 \times 25 \times 0.003175) / (4 \times 10^{-3})$$

$$= 22125 > 4000$$

= Flow is turbulent.

Minor loss in nozzle  $h_1 = k V^2 / 2g$  [112];

$$D_1/D_2 = (3/8)/0.125 = 3;$$

Resistance coefficient  $K = 0.25$  [112]

Minor loss in each nozzle  $= (0.25 \times 25^2) / (2 \times 9.81)$

$$= 7.964 \text{ m (for each nozzle)}$$

Total minor loss in four nozzles  $h_1 = 4 \times 7.964$

$$= 31.856 \text{ m}$$

Minor loss in tube:

Tube diameter  $= 3/8 \text{ in}$

Total tube length  $= L_2 + L_3 + L_4 + L_5 = 73 + 64 + 50 + 36 = 223 \text{ in}$



$$\text{Flow velocity} = Q_1/A = (1.98 \times 10^{-4}) / (\pi \times 0.009525^2/4) = 2.78 \text{ m/s}$$

$$\text{Reynolds number } Re = \rho v d / \mu$$

$$= 1115 \times 2.78 \times 0.009525 / (4 \times 10^{-3})$$

$$= 7381 > 4000$$

$$= \text{Flow is turbulent.}$$

$$\text{Friction factor } f = 0.013 \text{ [113];}$$

$$\text{Minor loss in pipe } h_2 = f \frac{L v^2}{2gD}$$

$$= \frac{0.013 \times 223 \times 2.78^2}{2 \times 9.81 \times 3/8}$$

$$= 3.045 \text{ m}$$

Minor loss in T- joints:

$$\text{Joint diameter} = 3/8 \text{ "};$$

$$\text{Flow velocity} = Q_1/A = 1.98 \times 10^{-4} / (3.1415 \times 0.009525^2/4)$$

$$= 2.78 \text{ m/s};$$

$$\text{Reynolds number } Re = \rho v d / \mu$$

$$= 1115 \times 2.78 \times 0.009525 / (4 \times 10^{-3})$$

$$= 7381 > 4000$$

$$= \text{Flow is turbulent.}$$

$$\text{Minor loss in T-joint} = k V^2/2g \text{ [112];}$$

$$\text{Resistance coefficient } k = 0.15 \text{ [112];}$$

$$\text{Minor loss in T-joint} = 0.15 \times (2.778^2) / (2 \times 9.81)$$

$$= 0.0591 \text{ m}$$

Total minor loss in five T-joints  $h_3 = 0.0591 \times 5 = 0.296 \text{ m}$

Minor loss in manifold:

Manifold diameter =  $3/8 \text{ in} = 0.009525 \text{ m}$

Manifold length =  $26 \text{ in}$

Flow velocity =  $Q_1/A = (1.98 \times 10^{-4}) / (\pi * 0.009525^2/4) = 2.78 \text{ m/s}$

Reynolds number  $Re = \rho v d / \mu$

$$= 1115 \times 2.78 \times 0.009525 / (4 \times 10^{-3})$$

$$= 73811 > 4000$$

= Flow is turbulent.

Friction factor  $f = 0.013$  [113];

Minor loss in manifold  $h_4 = f \frac{L v^2}{2gD}$

$$= \frac{0.013 \times 26 \times 2.78^2}{2 \times 9.81 \times 3/8}$$

$$= 0.355 \text{ m}$$

Minor loss in suction pipe:

Suction pipe diameter  $d = 1" = 0.0254 \text{ m}$

Total pipe length  $L = 71 \text{ in} = 0.0254 \text{ m}$

Flow velocity =  $Q/A = (7.92 \times 10^{-4}) / (\pi * 0.0254^2/4) = 1.56 \text{ m/s}$

Reynolds number  $Re = \rho v d / \mu = (1115 \times 1.56 \times 0.0254) / (4 \times 10^{-3})$

$$= 11045 > 4000$$

= Flow is turbulent.

Friction factor  $f = 0.012$  [113];

$$\begin{aligned} \text{Minor loss in pipe } h_5 &= f \frac{L v^2}{2gD} \\ &= \frac{0.012 \times 71 \times 1.56^2}{2 \times 9.81 \times 1} = 0.1 \text{ m} \end{aligned}$$

Total minor loss  $H_L$

$$H_L = h_1 + h_2 + h_3 + h_4 + h_5 = 31.856 + 3.045 + 0.296 + 0.355 + 0.1 = 35.652 \text{ m} \approx 36 \text{ m}$$

Total head required for pump:

$$\begin{aligned} HT &= \text{Static head} + \text{Friction head (minor loss)} \\ &= 2 \text{ m} + 36 \text{ m} \\ &= 38 \text{ m} = 125 \text{ ft.} \end{aligned}$$

According to the above calculation, the following pump is selected:

Vendor: McMaster, Part # 8134k28, Max head 150 ft

### 3.3.3.4 Heating and cooling subsystem for the variable speed jet impingement test-rig

Heating is a thermodynamic process that uses an energy source to heat a fluid above its initial temperature. A heat exchanger is a device that is used for transfer of thermal energy (enthalpy) between two or more fluids, between a solid surface and a fluid, or between solid particulates and a fluid, at differing temperatures and in thermal contact, usually without external heat and work interactions [114]. The design and built heating and cooling subsystem are shown in Figure 7.

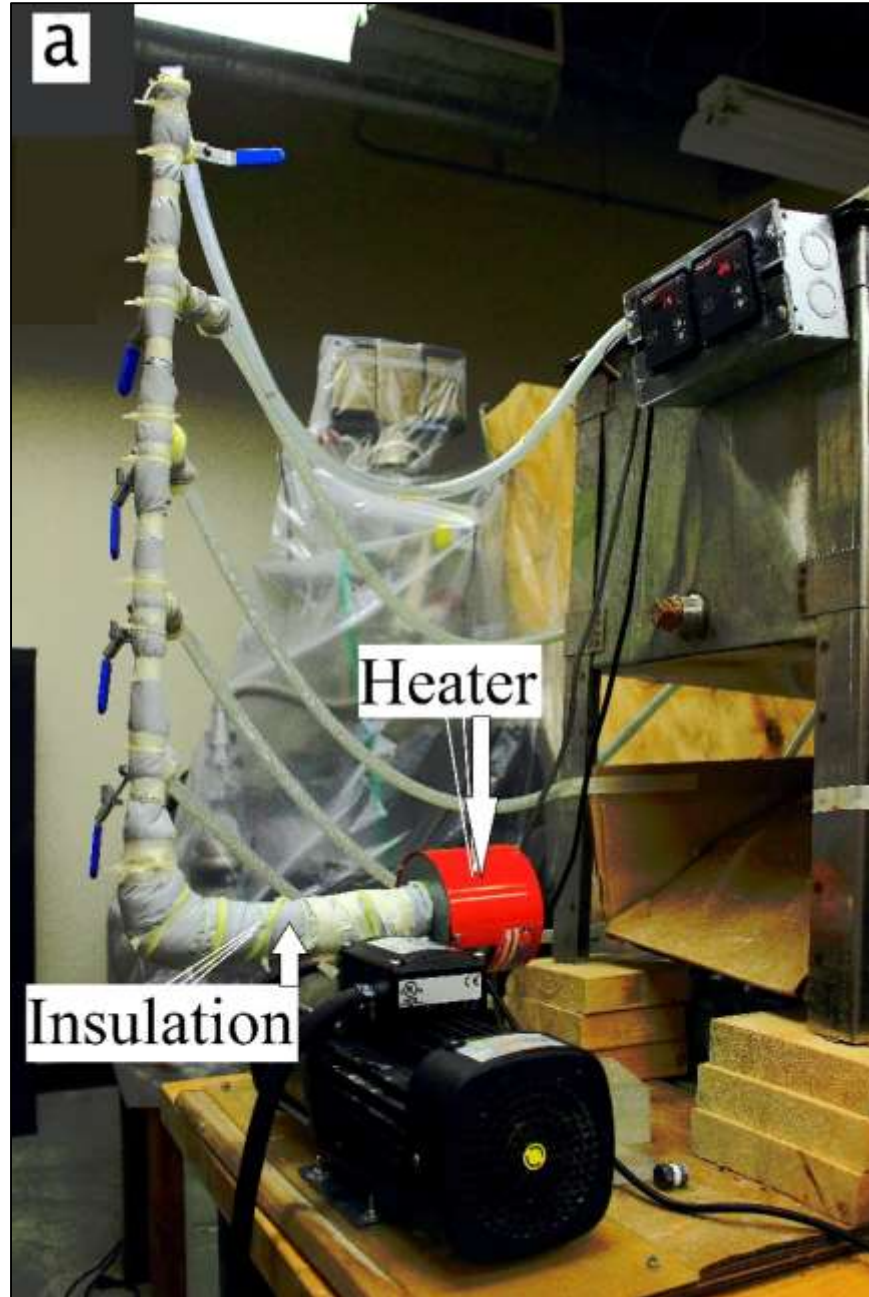


Figure 7a: Components of heating subsystem

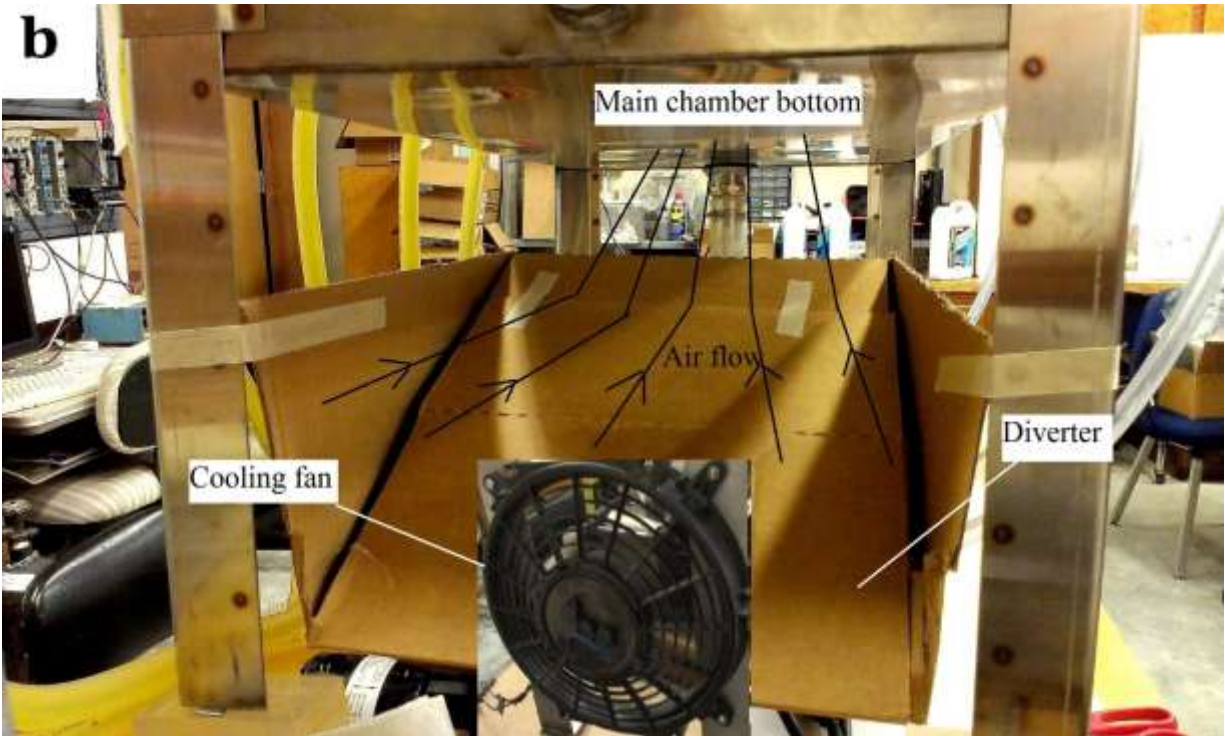


Figure 7: Components of (a) heating subsystem and (b) cooling subsystem for the variable speed jet impingement test-rig

An immersion heater (120 Volt, 500 Watts) was used for heating purpose in this experimental setup (showed in Figure 7a). It has a built-in thermocouple and a regulator to maintain the desired fluid temperature. It also has a threaded plug that was screwed through a threaded pipe fitting in the discharge pipe which is placed just next to the pump. The result is direct-contact heating of liquids which makes heating process faster and good control over system temperature.

Flexible fiberglass pipe wrap (1/2" Thick, 3" Width) insulation (Figure 7a) with vapor seal was used to create an adiabatic system. The wrap's vapor seal prevents heat loss by evaporation from hot water pipes and condensation on cold water pipes. All metal pipes were rapped by this fiberglass insulation and heat loss through FDA-Compliant resin tube, which was considered as negligible.

Heat can be dissipated through the main chamber walls. For faster response a cooling fan was used which was directed to the bottom surface of the main chamber. A cardboard maid diverter (figure 7b) has been used to divert air flow towards the hot surface (main chamber bottom).

### 3.3.3.5 Heating and cooling control subsystem

The designed and built heating and cooling subsystem for the variable speed test-rig is shown in Figure 8.

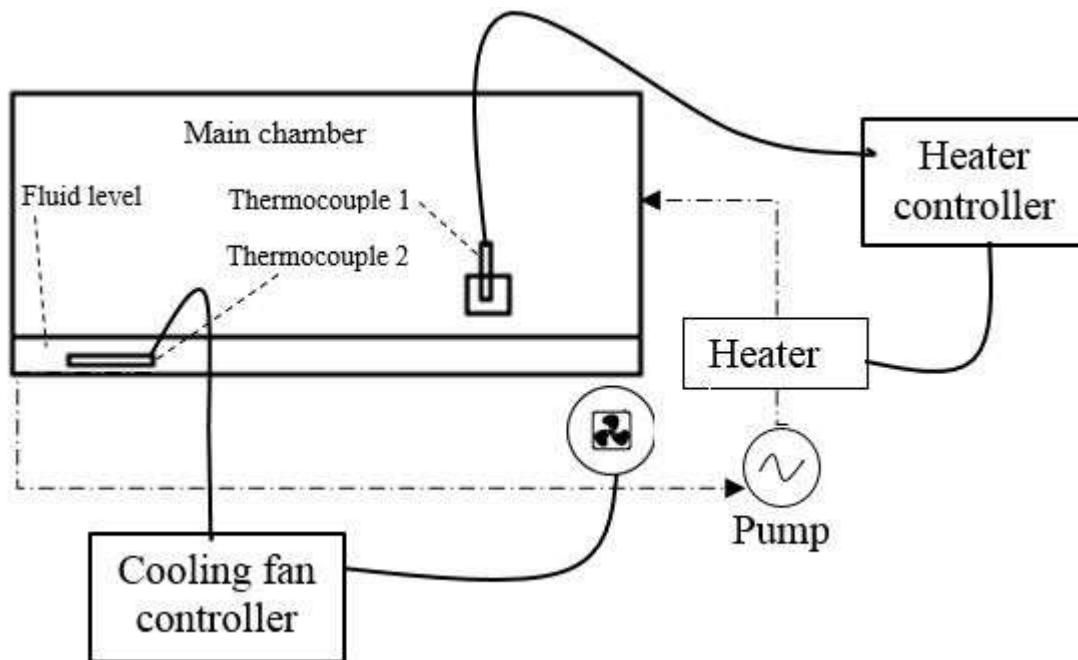


Figure 8 : Circuit diagram of thermal control subsystem for the variable speed jet impingement test-rig

Two K type immersion thermocouples (3 sec response time, temperature range 32<sup>0</sup> to 900<sup>0</sup>F) were used to maintain system temperature. Thermocouple 1 was placed under a test sample to measure jet temperature and thermocouple 2 was placed around tank outlet submerged under fluid but not touching the tank bottom surface to measure the pump inlet temperature. Two separate programmable temperature controller (for probe K thermocouple, temperature range 32° to 2192°

F) were used to operate cooling fan and heater to maintain desired temperature in system by using thermocouple feedback. Cooling fan controller takes temperature feedback from thermocouple 2 (figure 8) and operate cooling fan when fluid temperature goes above set temperature. Heater controller takes temperature feedback from thermocouple 1 (figure 8) operate heater as needed by set temperature.

### **3.4 Parallel flow setup**

To explore the possible erosion effect of typical nanofluid suspension in actual fluid flow systems, a new type of experimental setup was designed. Figure 9 shows a schematic and photograph of the newly developed test rig. A replica of fluid conduit system has been designed and developed where cooling fluid flow over the test sample inside a pipe. Coolant flow is fed by an instrumented pump and fluid flows are parallel to the test specimen length and to the specimen surface under test. A sample holder is used to hold specimens in coolant flow.

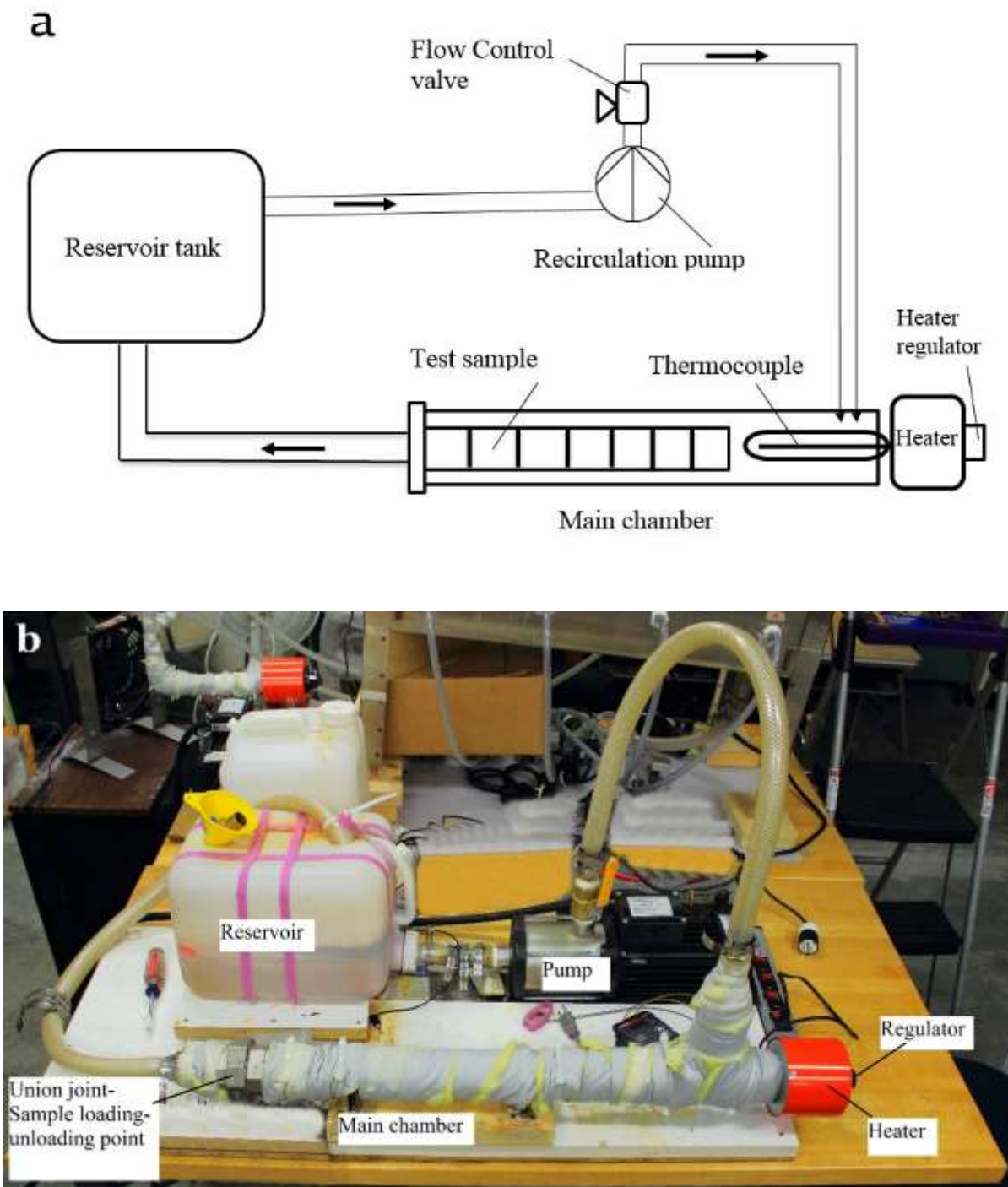


Figure 9: (a) Schematics and (b) photograph of the parallel-flow test rig to assess nanofluid wear.



### 3.4.1 Main chamber of the parallel-flow test-rig

Main chamber of the parallel flow system is a 2in diameter, 14 in length stainless steel pipe with a T-joint in one end and a union joint in other end. T-joint is for attaching inlet pipe and heating system together and union joint is for test sample loading-unloading purpose. Figure 9 shows the schematics and photograph of the main chamber.

### 3.4.2 Parallel flow test sample holder

A special type of sample holder was made for 1"x1" sample with thickness range of 0.5 mm to 4 mm. Figure 10 shows the photograph of the sample holder. It is a cartridge where maximum twelve sample can be loaded together. One end of the cartridge is open for sample loading-unloading and another end is fixed with a 1.8 inch wide end-flange. Cartridge can be closed by a 1.8 inch long bolt and nut after sample loading. Width of the end-flange and length of the closing bolt was designed 1.8 inch so that it can comfortably hold sample at the center of the 2 inch size main chamber.

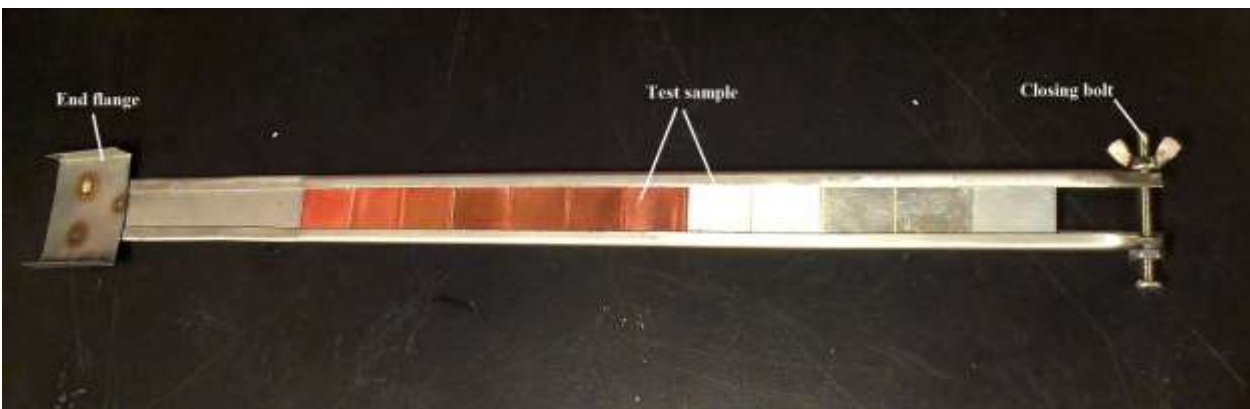


Figure 10: Photograph of the parallel flow test sample holder in the parallel-flow test rig to assess nanofluid wear

### **3.4.3 Heating subsystem of the parallel flow test-rig**

An immersion heater (120 Volt, 500 Watts) was used for heating purpose in this experimental setup. It has a built-in thermocouple and a regulator to maintain the desired fluid temperature. It also has a threaded plug that screwed directly in to main chamber inlet through T-joint. The result is direct-contact heating of liquid at inlet which makes heating process faster and good control over system temperature. Figure 9 shows the photograph of parallel-flow test rig, including the heating subsystem.

Flexible fiberglass pipe wrap (1/2" Thick, 3" Width) insulation with vapor seal was used to create an adiabatic system. The wrap's vapor seal prevents heat loss from hot water pipes and condensation on cold water pipes. All metal pipes were wrapped by this fiberglass insulation and heat loss through FDA-Compliant resin tube considered as negligible.

## CHAPTER 4

### 4 TEST METHODOLOGIES AND TESTED FLUIDS AND MATERIALS

The tests of this research work were carried out for (i) a commercial mixture of ethylene glycol in water (Prestone Super Tech 50/50 antifreeze/coolant [115]) and (ii) distilled water as reference fluids, and their nanofluid suspensions were obtained by adding a 2% volume concentration of alumina nanoparticles in those reference fluid. These mixtures were formulated by adding a commercial 20%-aluminum-oxide nanopowder dispersion in water (in which the employed nanopowders were of 99.99% gamma-alumina, 10nm original average particle size before aggregation in a 20% dispersion, proprietary dispersant not disclosed, supplied by US Research Nanomaterials Inc.) to each of the reference fluids.

#### 4.1 Test methodologies

Jet-impingement tests were carried out for 3, 7, 14, 28, 56, 112, 240, 312 and 408 hours with 3.5 m/s jet speed and for 3, 7, 14, 28, 56 and 112 hours with the 10.7 m/s and to 15.5 m/s jet speeds for each of the two fluids and those of nanofluids. Fluid jets were applied normal (e.g., at 90°) to test specimen surfaces, for constant distance from nozzle to target of 1 inch (25.4mm). Test target materials were copper alloy 110 (99.90% electrolytic heat exchanger quality, supplied by MSC Inc.) and aluminum 3003-T3 alloy (supplied by Kaiser Aluminum); each specimen was a plate of 1 inch by 1 inch (25.4mm by 25.4mm), 0.05inch (1.27 mm) thickness. Parallel flow tests were carried out for 3, 7, 14, 28, 56 and 112 hours for each of the two fluids and their nanofluids; in the parallel flow tests the fluid flows parallel (e.g., at 0°) to test specimen surfaces.

## 4.2 Test specimen preparation techniques

Each specimen was polished before test using flexible sand paper with distilled water in the sequence of 220, 600, 800, 1200, 2400 grit, to obtain a Ra roughness not greater than 5  $\mu$ inch. Specimens were then cleaned before tests by ultrasonic bath with micro-90 cleaning solution, and were air-dried before weight and roughness measurements. After test each specimen were rinsed with distilled water, and air-dried before weighing and roughness measurements.

Optical microscopy observations were carried out for the impacted material surfaces (of aluminum and copper specimens) before and after the jet-impingement and the parallel-flow tests, to assess surface modifications and to help elucidate the mechanisms of surface change. A Keyence VHX 1000 Digital Microscope of 54 Megapixel resolution was used. Surface images were captured by a high resolution zoom lens VH-Z500R/W for magnifications of 500x to 5000x (in the sequence 500x, 1000x, 2000x, 3000x, and 5000 x). A lower resolution lens (VH-Z20R) also was used at magnifications of 20x to 200x (in the sequence 20x, 30x, 50x, 100x, 150x and 200x). A VH-Z20R lens was employed for capturing images by three other lens angles (15°, 45°, and 90°).

Assessment of material-removal was carried out by pre- and post-test weighing of specimens, with a Shimadzu AUW120D balance of 0.1mg minimum readability in the used range. Further assessment of surface modifications was carried out by pre- and post-test roughness measurements; the employed instrument was a Mitutoyo Surfest SJ-201 surface roughness tester, and the recorded roughness parameters were Ra, Rq and Rz. Roughness was measured in two directions: along the lay (e.g., the predominant polishing direction), and across it. Three measurement of each Ra, Rq and Rz were made for each direction (for a total of six) and then these values were averaged for each Ra, Rq and Rz. Average values as per such procedure are displayed

in Chapter 5. For the employed measurement range of 14,400  $\mu\text{inch}$  (360  $\mu\text{m}$ ), the instrument resolution was of 1  $\mu\text{inch}$  (0.0254  $\mu\text{m}$ ) [116].

## CHAPTER 5

### 5 EXPERIMENTAL

Experimental results are presented on typical nanofluids (as 2%-volume of alumina nanopowders in 50/50 water/ethylene glycol solution and distilled water) which are jet-impinged (on aluminum and copper specimens) with 3.5 m/s to 15.5 m/s jet speeds, and for 1 m/s flow parallel to the test specimen surfaces. These treatments were applied during the long test periods ranging from 3 hours to up to 408 hours. Test temperature was kept within 31<sup>0</sup>C to 33<sup>0</sup>C in jet impingement tests. Table 1 is showing the test parameters of jet impingement tests.

Table 1: Summary of carried out jet impingement tests and test parameters presented in this Chapter 5

Jet speed Base fluid	3.5 m/s	10.7 m/s	15.5 m/s
Distilled water	done (section 5.1.1)	done (section 5.2.1)	done (section 5.3.1)
Ethylene glycol	done (section 5.1.1)	done (section 5.2.2)	Not done because of foaming problem (discussed in section 6.3.3)
Length of carried out tests (hours)	3, 7, 14, 28, 56, 112, 240, 312 and 408	3, 7, 14, 28, 56 and 112	3, 7, 14, 28, 56 and 112

In the parallel-flow test experimental work that followed the test-jet one, a set of test was carried out for 3, 7, 14, 28, 56 and 112 hours with a 1 m/s flow of the reference fluid of distilled water and of its 2% alumina nanofluid. Test temperature was kept within 85<sup>0</sup>C to 90<sup>0</sup>C.

The obtained surface modifications were assessed by roughness measurements, by weighing of removed-material, and by optical-microscopy. Roughness measurements (Ra, Rq, Rz) results are

plotted as time vs before- and after- test roughness for each test specimen. Weight measurements results are presented as time vs weight changes for test for specimens after test. Before- and after- test microscopic images of test samples are compared for each test specimen. The results also are presented on the observed surface modifications, as assessed by the used method (roughness measurements, optical microscopy and weight measurement) when same tests are conducted in aluminum and copper, and by both the base fluids and its alumina-nanofluids. The likely mechanisms of early erosion and abrasion, and the possibility of extrapolating the test-rig results and methodologies to typical cooling systems are later discussed in Chapters 6 and 7.

### **5.1.1 Summary of carried out jet impingement tests and test parameters**

#### **5.1.2 Test results of 3.5 m/s jet impingement with distilled water as base fluid and its nanofluid**

Figure 11 presents the measured average Ra roughness for 3003-T3 aluminum specimens before and after 3, 7, 14, 28, 56, 112, 240, 312 and 408 hour-treatments with the reference fluid of distilled water, and its nanofluid of 2%-volume of nano-alumina mixed in this reference fluid for 3.5 m/s jet speed. Initial values (without treatment), are called “before test”, while values after each treatment are called “after test” in following graphs.

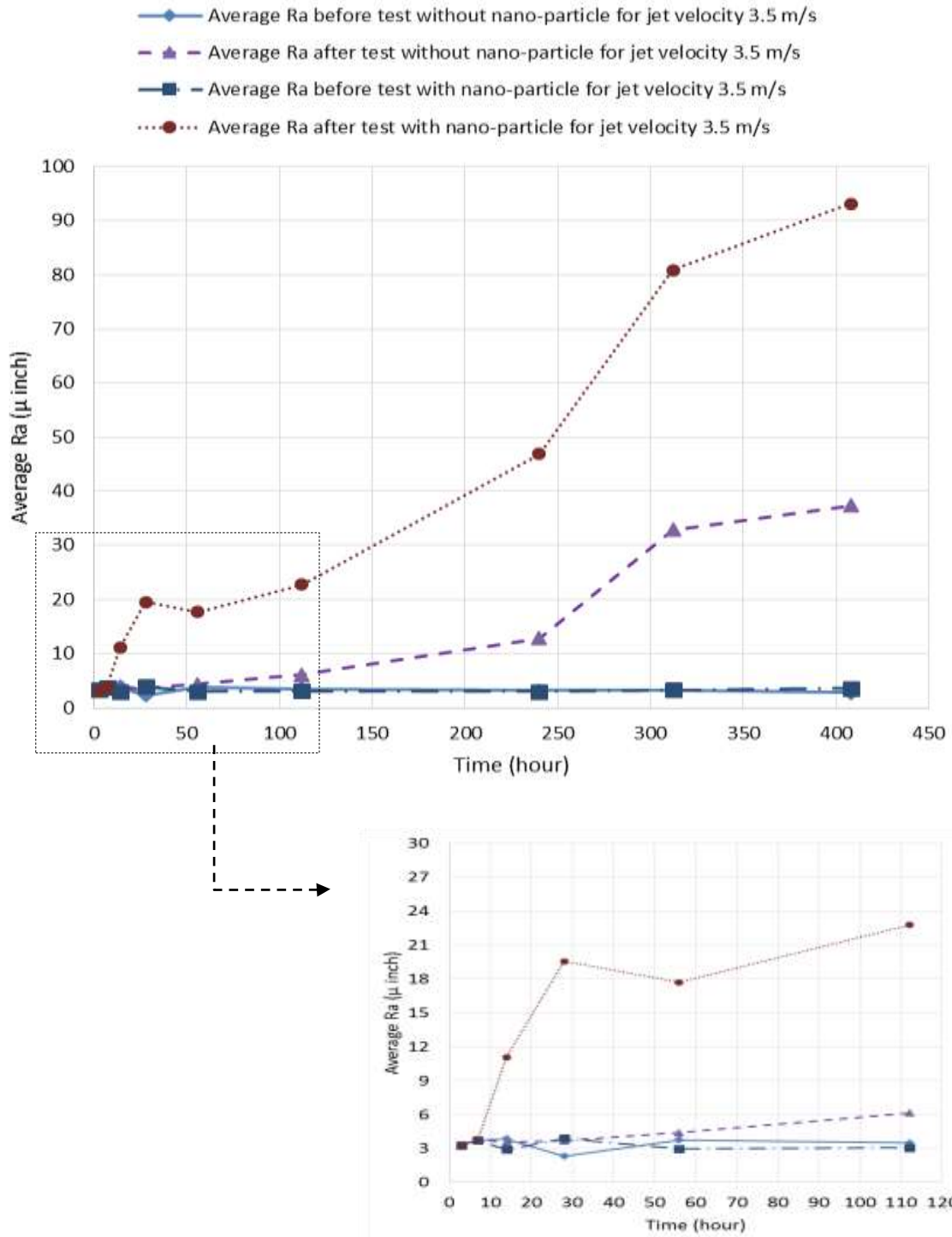


Figure 11. Average Ra roughness for 3003-T3 aluminum before and after 3, 7, 14, 28, 56, 112, 240, 312 and 408 hour-treatments with the reference fluid distilled water and its nanofluid of 2% nano-alumina in reference fluid and jet speed of 3.5 m/s and enlarged partial graph for 3 to 112 hours.



The measurements presented in Figure 11 indicate that aluminum-specimen roughness is affected by the jet impingements with both the reference fluid (distilled water), and its 2%-alumina-nanofluid. For reference fluid, initial (from 3 hour to 56 hour-test) Ra roughness values are not showing any significant increase, while minor increases are observed after test from 56 to 112 hours of testing which is followed by a monotonous increases after test from 240 hours to 408 hours of testing. Similar trends were observed for the two other measured roughness parameters, of Rq and Rz (presented in Appendix A). For the water base nanofluid, Ra roughness values in Figure 11 show increasing values for the whole span of testing, but there is a relatively lower increase after test from 28 hours to 112 hours of testing. For this nanofluid test the measured roughness changes are considerably higher as compare to each corresponding roughness changes for base fluid (distilled water). Similar trends were observed for the two other measured roughness parameters, Rq and Rz (presented in Appendix A).

Polishing of ductile materials as aluminum and copper cannot be controlled to obtain a single value of initial roughness but an interval of 2 to 4 microinches resulted in the low-range required for these tests. Therefore, there is a spread of initial values that was limited, after careful polishing, to 2 to 5 microinches (0.05 micrometer to 0.13 micrometer). To deal with the initial roughness spread within specimens presented in Figure 11 each of the Ra values was normalized and presented in Figure 12 for further analysis. Normalization of each after-test Ra-value was done by dividing it by the corresponding initial (before-test) Ra for the corresponding specimen.

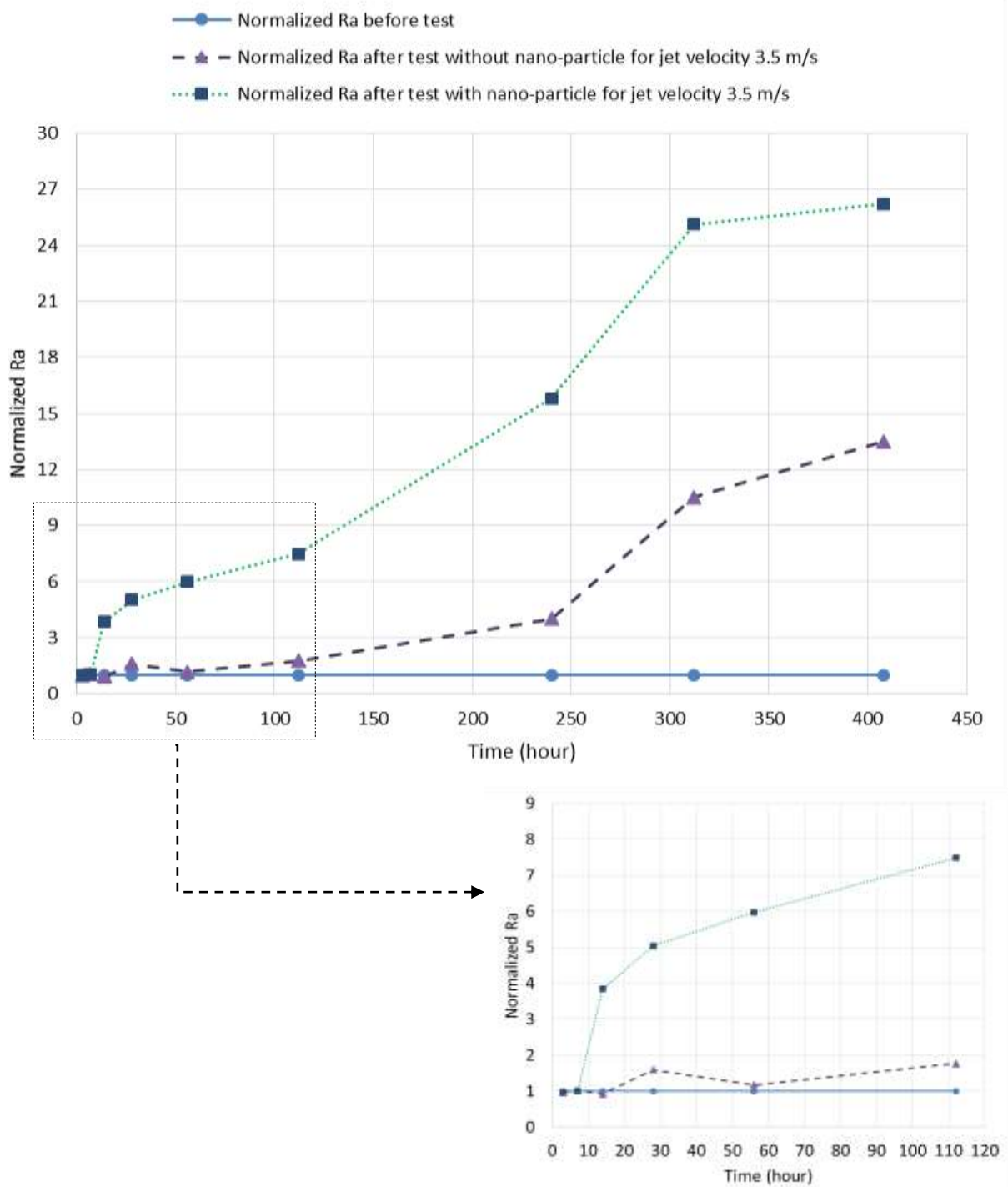


Figure 12. Normalized Ra roughness for 3003-T3 aluminum before and after 3, 7, 14, 28, 56, 112, 240, 312 and 408 hour-treatments with the reference fluid of distilled water and its nanofluid of 2% nano-alumina in reference fluid and jet speed of 3.5 m/s and enlarged partial graph for 3 to 112 hours.

Figure 12 more clearly shows the same trends suggested by Figure 11. The normalized roughness values increase up to eight-fold for the longest tested time of 408 hours as compared to initial ones. Figure 12 also suggests that surface treated with reference fluid (distilled water) undergone less surface modification as compared to that of treated by its 2%-alumina-nanofluid. The evolution of roughness in Figures 11 and 12 also suggests that some early cleaning of the surface may occur after tests from 3 hours to 56 hours tests (showing no significant increase of roughness in such interval), and that after 112 hours of test increased material erosion seems to proceed when impacted by the reference fluid jet impingement, while for the nanofluid, a monotonous increases starts from the beginning of the test and continues for up to the 408 hours of maximum testing.

Preliminary experiments were carried out for 3, 7, 14, 28, 56, 112, 240, 312 and 408 hour-treatments with the reference fluid of distilled water, and a nanofluid of 2%-volume of nano-alumina mixed in the reference fluid for 3.5 m/s jet speed. To access test and result respectabilities the tests for 7, 28, 240 and 408 hours were repeated twice for every set such of tests. Table 2 shows the normalized roughness data and average values for such repeated tests.

Table 2: Normalized surface roughness data of before- and after- 7, 28, 240 and 408 hours of repeated tests (two trials) with a 3.5- m/s jet of reference fluid of distilled water. All normalized roughness values before test are unity, as previously explained.

Test lengths in hours	Trial	After test		
		Ra	Rq	Rz
7	Trial 1	1.0082	1.458	1.00845
	Trial 2	1.0156	1.254	1.124
	Average	1.0119	1.356	1.066225
28	Trial 1	1.897	1.546	1.412
	Trial 2	1.281	1.354	1.298
	Average	1.589	1.45	1.355
240	Trial 1	3.876	4.7985	5.8678
	Trial 2	4.135	5.0124	5.7986
	Average	4.0055	4.90545	5.8332
408	Trial 1	13.571	12.3457	9.574
	Trial 2	13.398	12.546	9.378
	Average	13.4845	12.44585	9.476

Table 2 clearly shows a good repeatability of results and suggest that the developed test rigs and employed methodologies can lead to statistically significant results to assess the studied nanofluid effects.

Figure 13 presents the average weight changes for 3003-T3 aluminum in before and after 3, 7, 14, 28, 56, 112, 240, 312 and 408 hour-treatments with the reference fluid of distilled water, and its nanofluid of 2% nano-alumina mixed in this reference fluid. Weight measurements suggested a small increase in weight after treatments (the highest measured of 8mg) for 28-hour tests for both fluids, while no significant weight change was observed after test from 56 hours to 240 hours testing for both fluids. From 312 hours to 408 hours of testing, treatments with the reference fluid show a small decrease in weight (of 8 to 10 mg) after treatments, but

an abnormal weight decrease was measured when treated by its 2% nanofluid. Further investigation may be needed to confirm these observations.

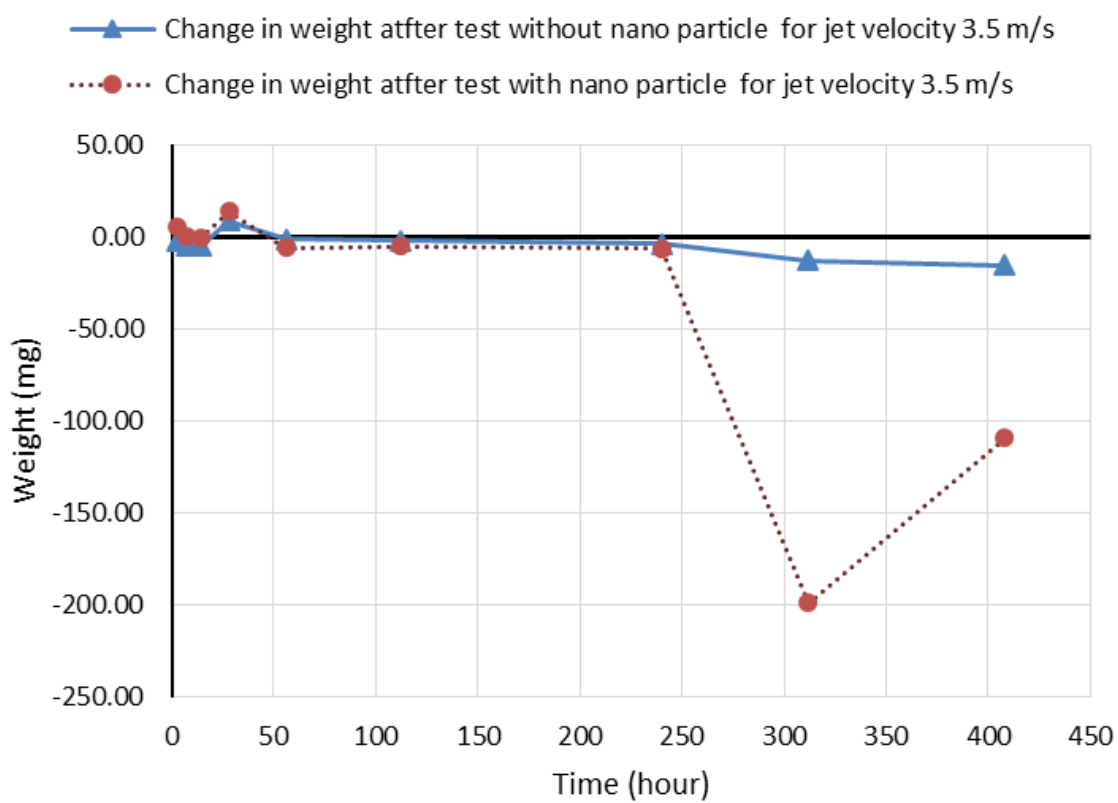


Figure 13. Average weight change for 3003-T3 aluminum in before and after 3, 7, 14, 28, 56, 112, 240, 312 and 408 hour-treatments with the reference fluid of distilled water, and its nanofluid of 2% nano-alumina in reference fluid and jet speed of 3.5 m/s

The measured roughness changes for aluminum samples suggest that significant surface modifications occur when jet-impinged. To study such modifications, optical microscopy was conducted for all the specimens after and before treatments. Figures 14 and 15 show microscopy images (for 500X magnification) for the aluminum specimens before and after jet-treatments for 408 hours with each corresponding fluid.

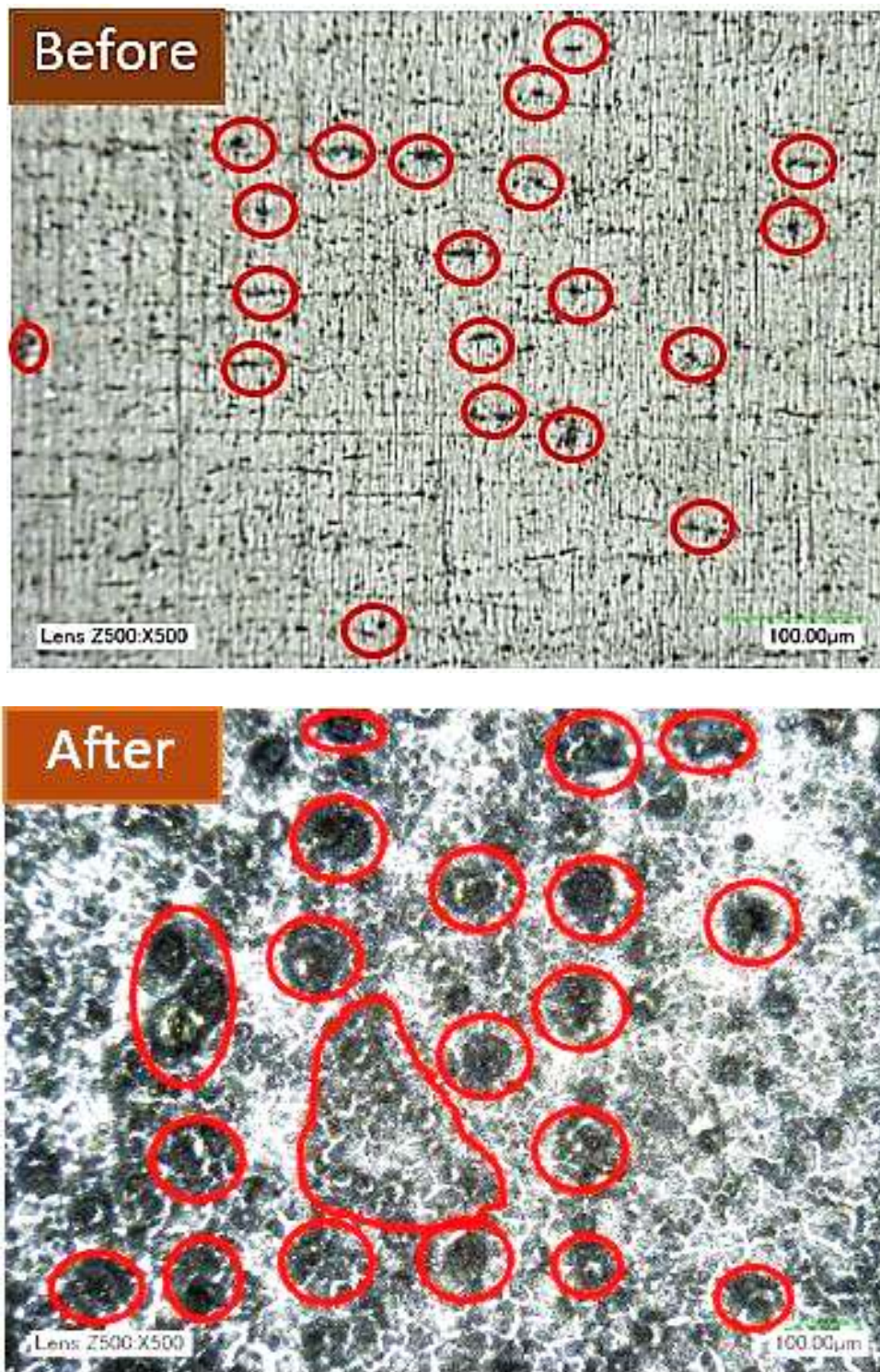


Figure 14. Optical microscopy images of 3003-T3 aluminum before and after (408-hour) test with (reference fluid, without nanoparticles) distilled water (Magnification: 500X). Pre-existing pitting and enlarged ones after treatment are circled.

Figure 14 allows comparison of before- and after-test images (Magnification: 500X) with reference fluid (distilled water), without nanoparticles. After treatment, polishing scratches have been removed (after test of 408 hours), small pitting (on average, smaller than 4 micrometers (150 microinches) becomes larger (to average of 20 to 25 micrometers (800 to 1000 microinches), which are showed as circled darker clusters in after-test image); some observed features also suggest that some larger areas (of about 35 to 40 micrometers) may have started some splinting.

Figure 15 allows comparison of before- and after-test images with nanofluid of 2% alumina in distilled water (Magnification: 500X). After 408-hour treatment, polishing scratches have been removed, small pitting (on average, smaller than 4 micrometers (150 microinches) becomes much larger (to average of 80 to 100 micrometers (3000 to 3100 microinches), showing as circled darker clusters in after-test image) and some irregular shape shallow splinting has been started. Growth of smaller pitting by nanofluid jet impingement is considerably larger as compared to those of reference fluid jet impingement.

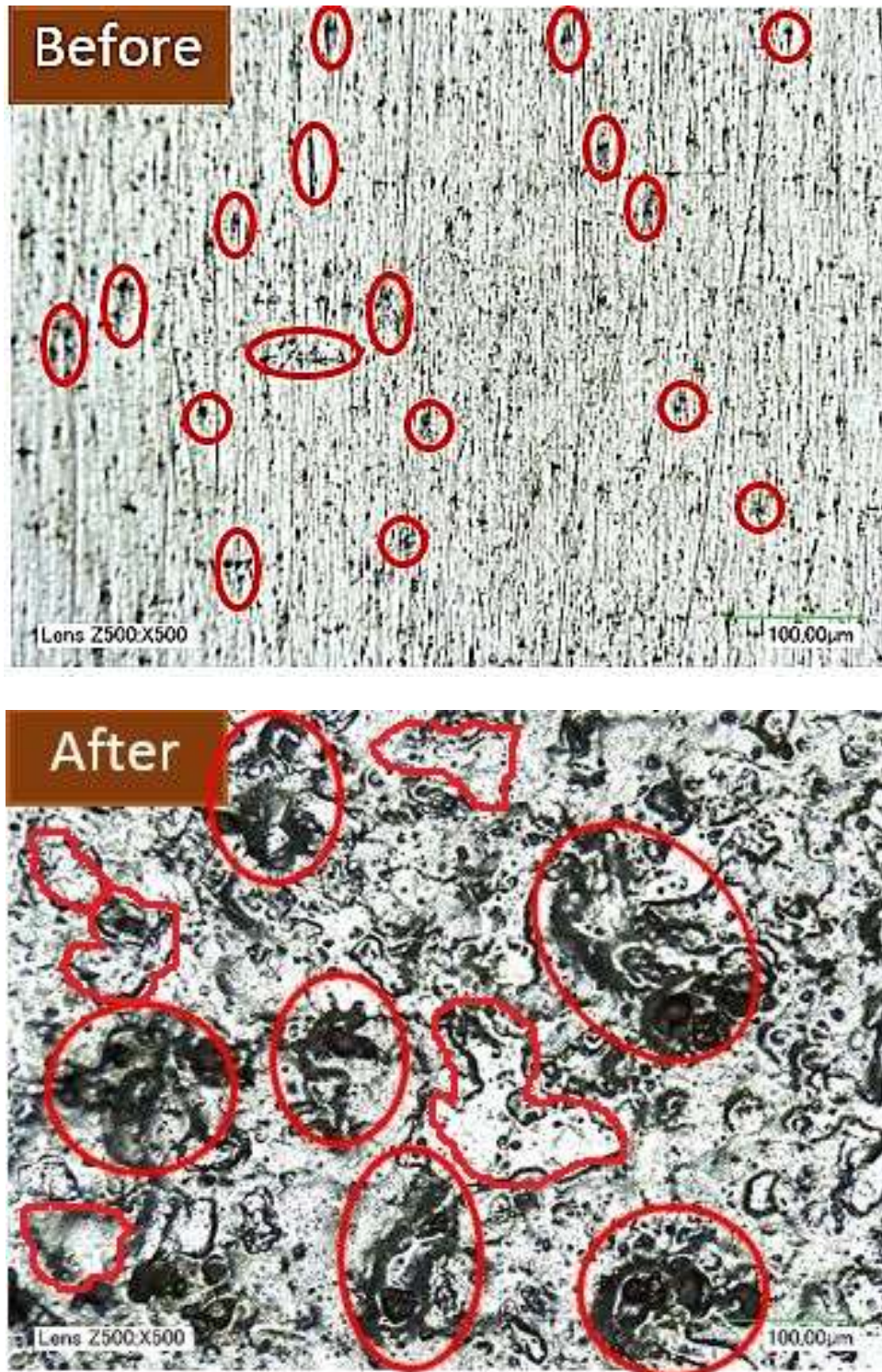


Figure 15. Optical microscopy images of 3003-T3 aluminum before and after (408-hour) test with nanofluid of 2% alumina in distilled water (Magnification: 500X). Pre-existing pitting and enlarged ones after treatment are circled.



Same jet-impingement treatments and subsequent measurements and analysis were carried out for copper alloy 110. Figure 16 presents the typically measured average Ra roughness for copper alloy 110 before and after 3, 7, 14, 28, 56, 112, 240, 312 and 408 hour treatments with the reference fluid of distilled water, and a nanofluid of 2% volume of nano-alumina mixed in the reference fluid. Initial values (without treatment), are called “before test”, while values after each treatment are called “after test” in following graphs.

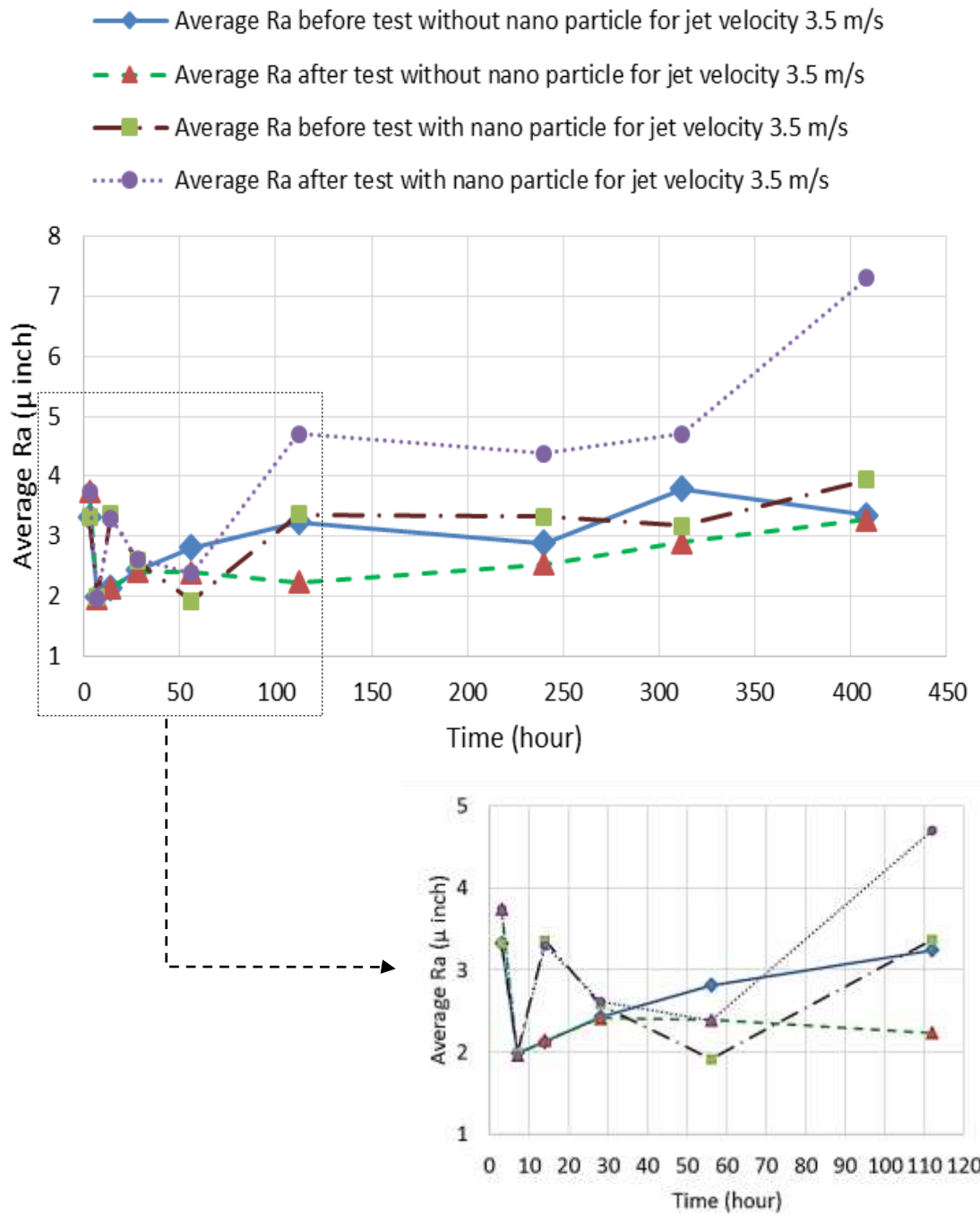


Figure 16. Average Ra roughness for copper alloy110 before and after 3, 7, 14, 28, 56, 112, 240, 312 and 408 hour-treatments with the reference fluid distilled water, and its nanofluid of 2% nano-alumina in reference fluid and jet speed of 3.5 m/s and enlarged partial graph for 3 to 112 hours.

Since the initial roughness for each specimen presented in Figure 16 was within the 2 to 5 microinches (0.05 micrometer to 0.13 micrometer) range, each of the Ra values is normalized and presented in Figure 17, where normalization of each after-test Ra-value was done as for data of Figure 12.

Figures 16 and 17 suggest that a minor surface modification (all roughness value differences were within 2 micro inch) were obtained when copper specimens were treated with 3.5 m/s speed jet of reference fluid (distilled water) and its 2% nanofluid. For reference fluid, Ra roughness values shows no significant change but a minor decreases (all roughness value difference are within 1 micro inch) for all the testes. For nanofluid, Ra roughness shows an increased value for 3 hours test but no change after test from 7 hours to 28 hours of testing followed by a little increase after test from 56 hours to 408 hours. Measured Rq and Rz (presented in Appendix A) roughness showed similar trends.

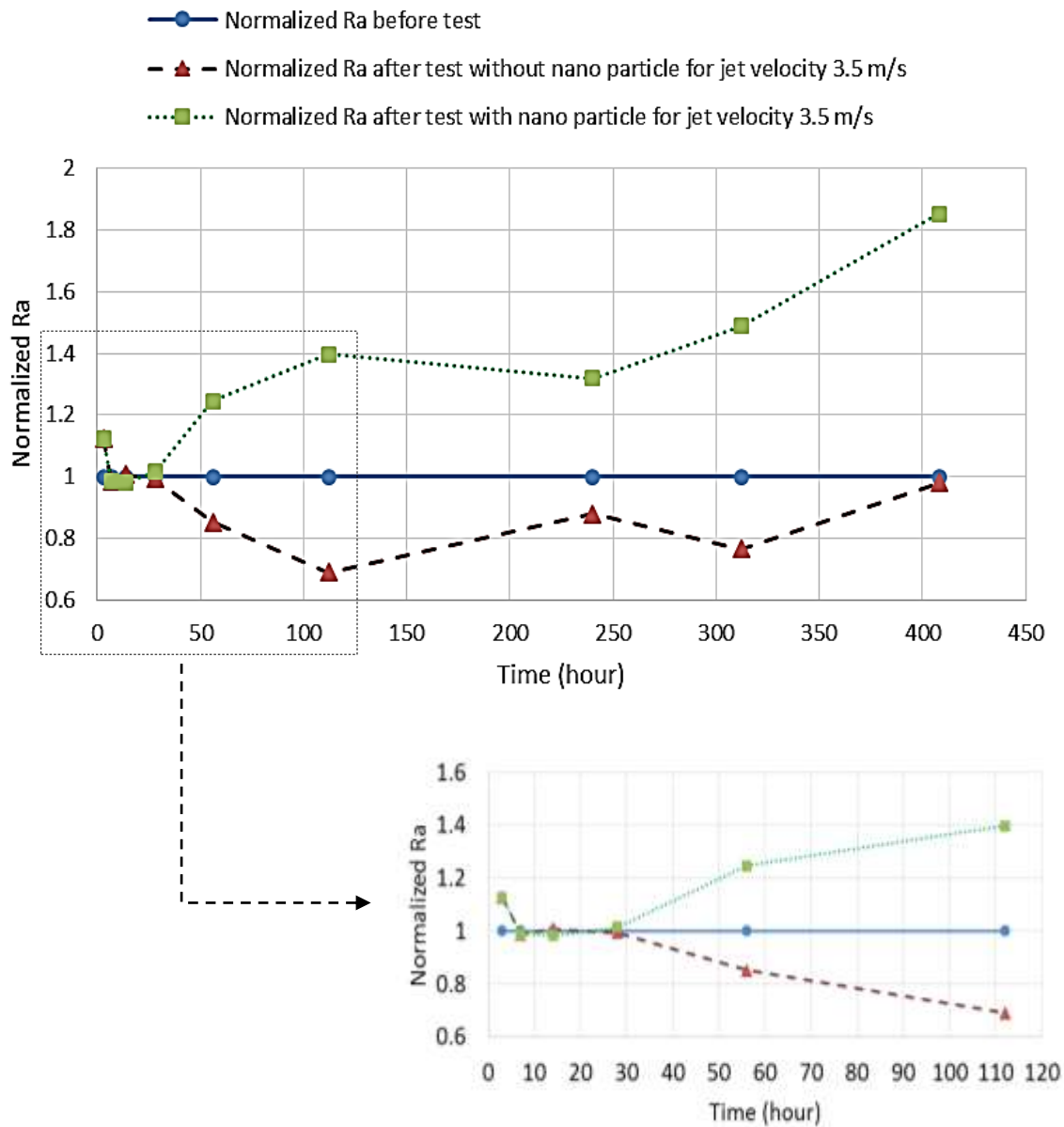


Figure 17. Normalized Ra roughness for alloy110 copper before and after 3, 7, 14, 28, 56, 112, 240, 312 and 408 hour-treatments with the reference fluid distilled water, and its nanofluid of 2% nano-alumina in reference fluid and jet speed of 3.5 m/s and enlarged partial graph for 3 to 112 hours.

Weight measurements of before- and after-tests also were conducted to investigate possible material-removal effects by the jet impingements. Figure 18 presents the measured change in weight for before and after 3, 7, 14, 28, 56, 112, 240, 312 and 408 hour-treatments for alloy110

copper specimens with both reference fluid (distilled water) and nanofluid (2%-volume of nano-alumina mixed). Weight measurements suggests a small increase in weight (the highest measured of 5mg) after 28-hour tests for reference fluid but no significant weight change has been observed after test from 56 hours to 408 hours jet impingements for the tested fluids and times.

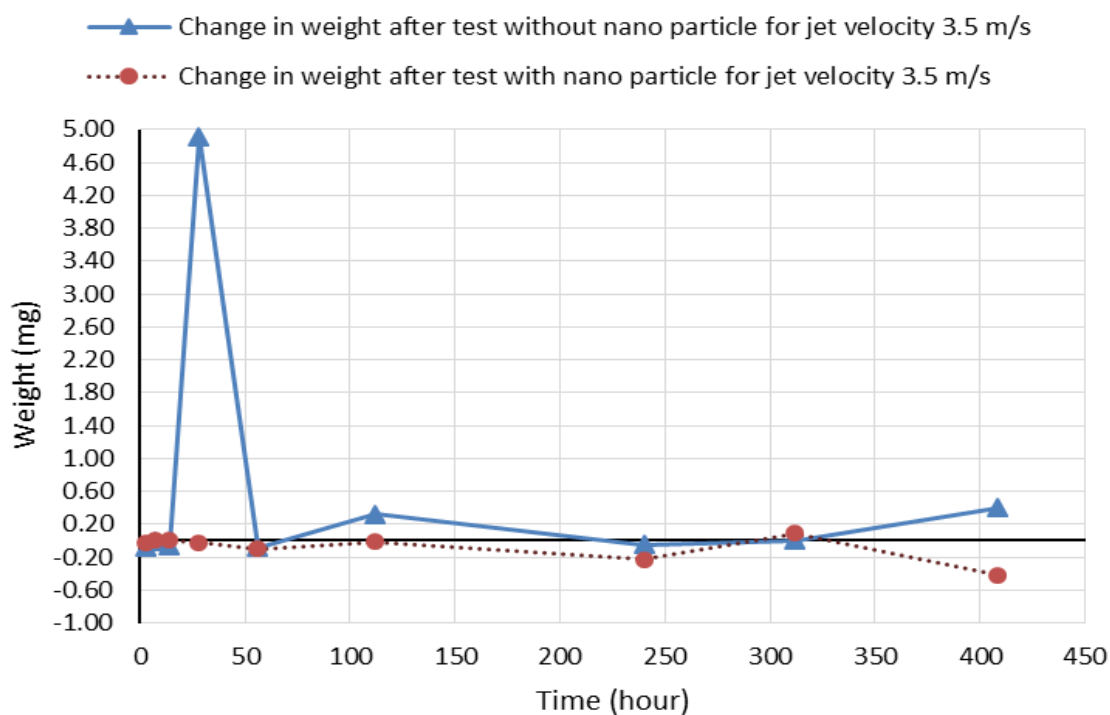


Figure 18. Average weight change for alloy 110 copper in before and after 3, 7, 14, 28, 56, 112, 240, 312 and 408 hour-treatments with the reference fluid distilled water, and its 2% alumina nanofluid and jet speed of 3.5 m/s.

Weight measurements of copper specimens found no significant weight change after jet impingements for the tested fluids and times. To study possible modifications non-detected by roughness or weight measurements, optical microscopy was conducted for all the specimens after and before treatments. Figures 19 and 20 show microscopy images (for 500X

magnification) for the copper specimens before and after jet-treatments with each corresponding fluid.

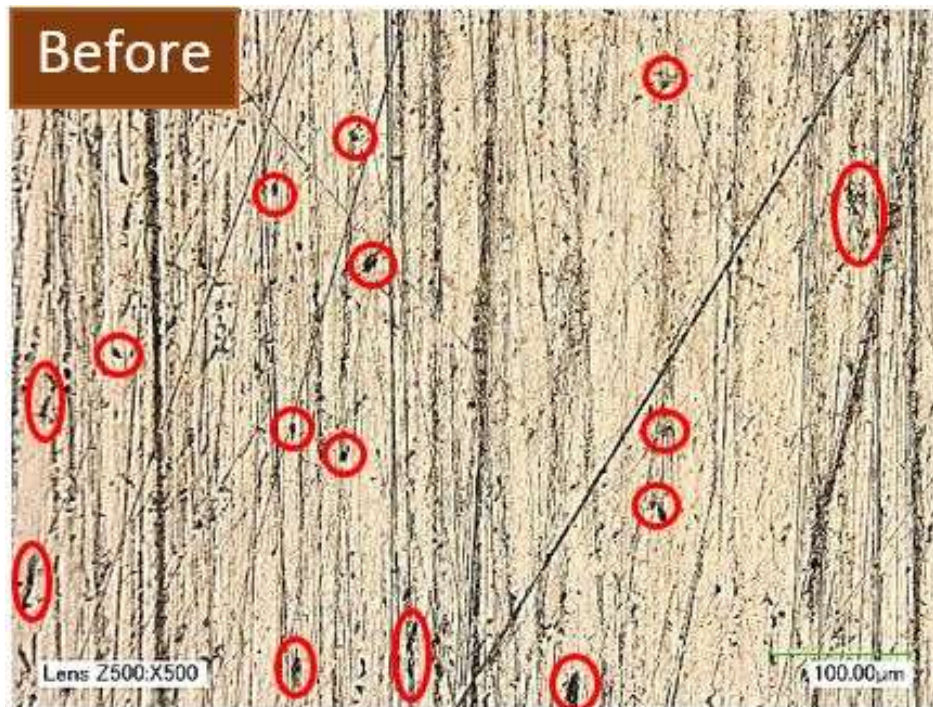


Figure 19. Optical microscopy images of alloy110 copper before and after (408-hour) test with (reference fluid, without nanoparticles) distilled water (Magnification: 500X). Pre-existing pitting and enlarged ones after treatment are circled.

Figure 19 allows comparison of before- and after-test images with reference fluid of distilled water (Magnification: 500X), without nanoparticles. Before treatment some limited pitting (circled in “before” image) and some sharp machining scratches were observed. After 408-hour treatment small pitting (on average, smaller than 5 micrometers (200 microinches) becomes larger (to average of 30 to 35 micrometers (1200 to 1400 microinches), showing as circled clusters in after-test image). Polishing scratches have not been removed but become shallow. Some material have been removed around those scratches in form of micro pitting and made those shallow. Many new micro-size pitting is observed in after treatment image.

Figure 20 allows comparison of before- and after-test (408 hours) images with nanofluid of 2% alumina in distilled water (Magnification: 500X). After 408-hour treatment, polishing scratches have completely been removed, and pre-existing pitting (circled in before image of above Figure 20) became much larger and widespread. Some pitting seems to clusters (circled in after image of above Figure 20) along original scratching lines and around the previous pitting (before test pitting).



Figure 20. Optical microscopy images of alloy 110 copper before and after (408-hour) test with nanofluid of 2% alumina in distilled water (Magnification: 500X). Pre-existing pitting and seemingly clustered ones after treatment are circled.



### 5.1.3 Test results of 3.5 m/s jet impingement with 50/50% Ethylene Glycol as base fluid and its nanofluid

Figure 21 presents the measured average Ra roughness for 3003-T3 aluminum specimens before and after 3, 7, 14, 28, 56, 112, 240, 312 and 408 hour-treatments with the reference fluid of 50/50% Ethylene Glycol in water (EG/Water), and a nanofluid of 2%-volume of nano-alumina mixed in the reference fluid of 50/50% water/Ethylene Glycol (initial values (without treatment), are called “before test”, while values after each treatment are called “after test” in following graphs).

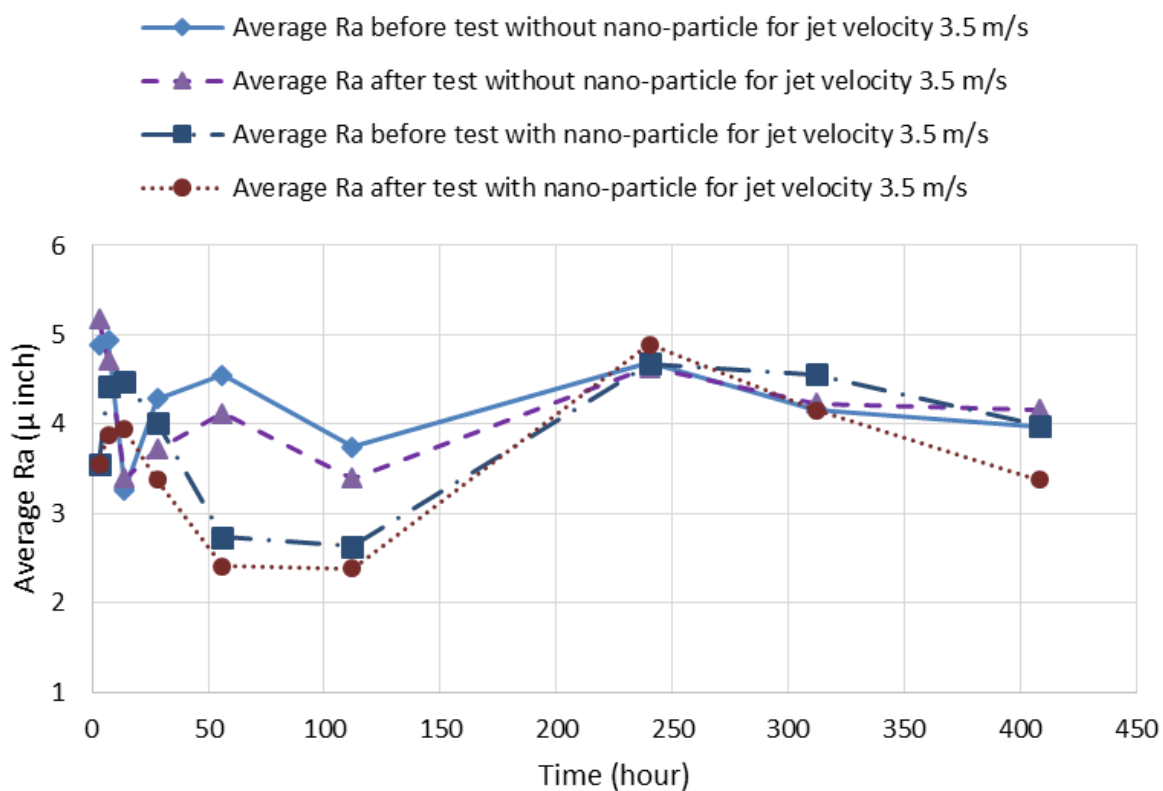


Figure 21. Average Ra roughness for 3003-T3 aluminum before and after 3, 7, 14, 28, 56, 112, 240, 312 and 408 hour-treatments with the reference fluid of 50/50% Ethylene Glycol in water, and its nanofluid of 2% nano-alumina in reference fluid and jet speed of 3.5 m/s.

The measurements presented in Figure 21 indicate that aluminum-specimen roughness may not be significantly affected by the jet impingements at 3.5 m/s speed with both the reference fluid (EG/water), and its 2%-alumina-nanofluid. For both of them, measured changes in Ra roughness values are within 1 microinch, which is the instrument resolution. Similar trends were observed for the two other measured roughness parameters, Rq and Rz (presented in Appendix A).

Since initial roughness for tested specimen presented in Figure 21 was within the 2 to 5 microinch range, each of the Ra values in Figure 21 are normalized and presented in Figure 22 to clarify any possible trend suggested by Figure 21. Normalization of each after-test Ra-value was done by dividing it by the corresponding initial (before-test) Ra for the corresponding specimen. Figure 22 shows that there are no significant changes for the roughness parameter Ra after the 3, 7, 14, 28, 56, 112, 240, 312 and 408 hours of test for both fluids. There is, however, a slight decreasing of roughness for the first 112 hours of test. Figures 21 and 22 are suggesting some early cleaning of the surface (shown as each small decrease of roughness), and removal of loose material (which was likely left from previous polishing), which may occurs within these test times. No clear trend follows which would suggest significant material erosion for the tested times.

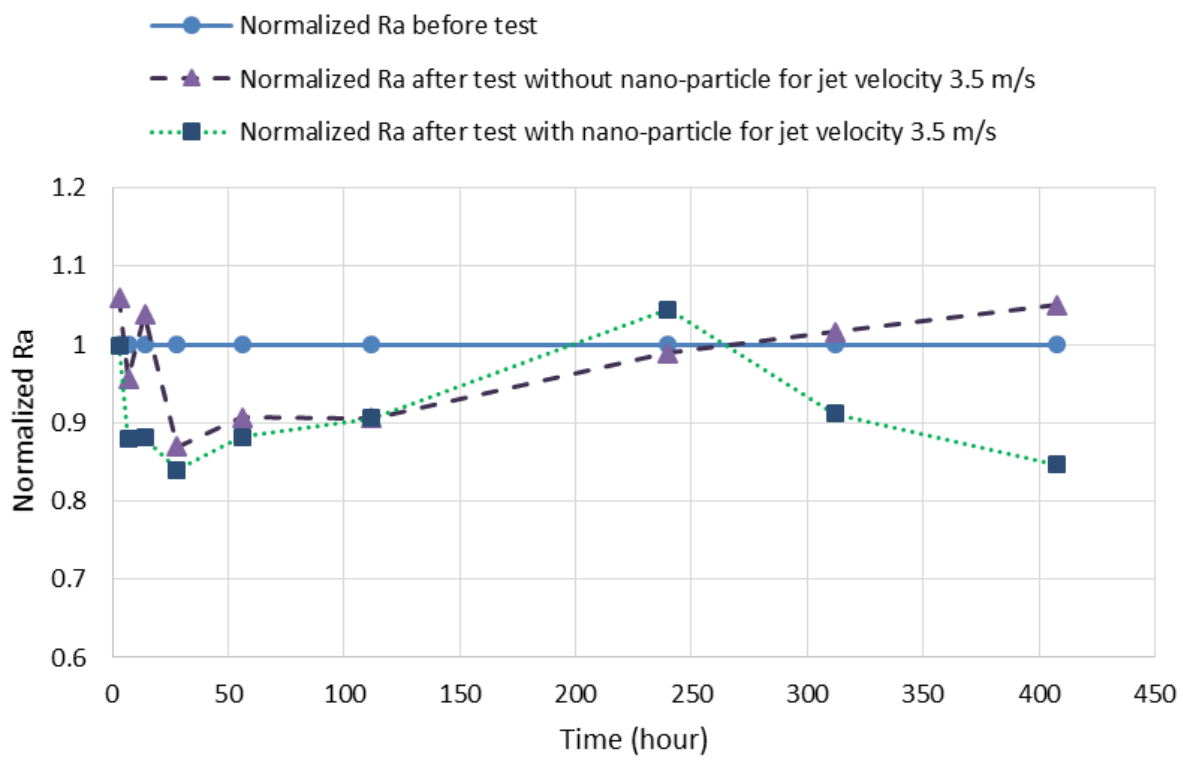


Figure 22. Normalized Ra roughness for 3003-T3 aluminum before and after 3, 7, 14, 28, 56, 112, 240, 312 and 408 hour-treatments with the reference fluid of 50/50% Ehtylene Glycol in water, and its nanofluid of 2% nano-alumina in reference fluid and jet speed of 3.5 m/s.

Weight measurements also were conducted before and after test to further investigate about possible erosion effects by the jet impingements. Figure 23 presents the measured average change in weight of before-and after- 3, 7, 14, 28, 56, 112, 240, 312 and 408 hour-treatments for 3003-T3 aluminum specimens with both reference fluid (50/50% Ethylene Glycol in water) and its nanofluid (of 2%-volume of nano-alumina).

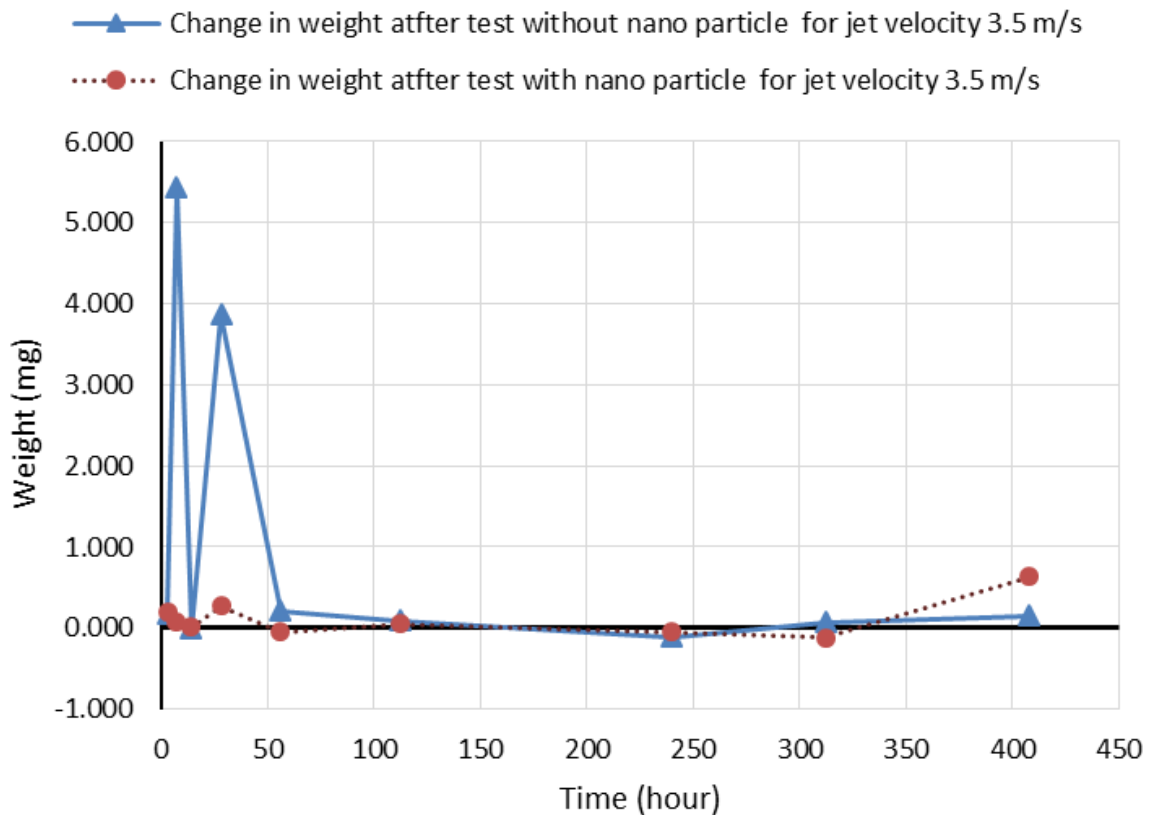


Figure 23. Average weight change for 3003-T3 aluminum in before and after 3, 7, 14, 28, 56, 112, 240, 312 and 408 hour-treatments with the reference fluid of 50/50% Ehtylene Glycol in water, and its nanofluid of 2% nano-alumina in reference fluid and jet speed of 3.5 m/s.

Weight measurements values of Figure 23 suggest a small increase in weight after treatments (the highest measured of 5mg) for 3- to 28-hour tests with reference fluid on aluminum, but not significant weight change was observed after 28 hour (to the maximum tested 408 hours) of jet impingement for both fluids.

The measured weight change and roughness changes for aluminum samples, however, suggested that minor surface modifications may occur when jet-impinged. To study such likely

modifications, optical microscopy was conducted for all the specimens before and after treatments for magnifications of 500x to 5000x (in the sequence 500x, 1000x, 2000x, 3000x, and 5000 x).

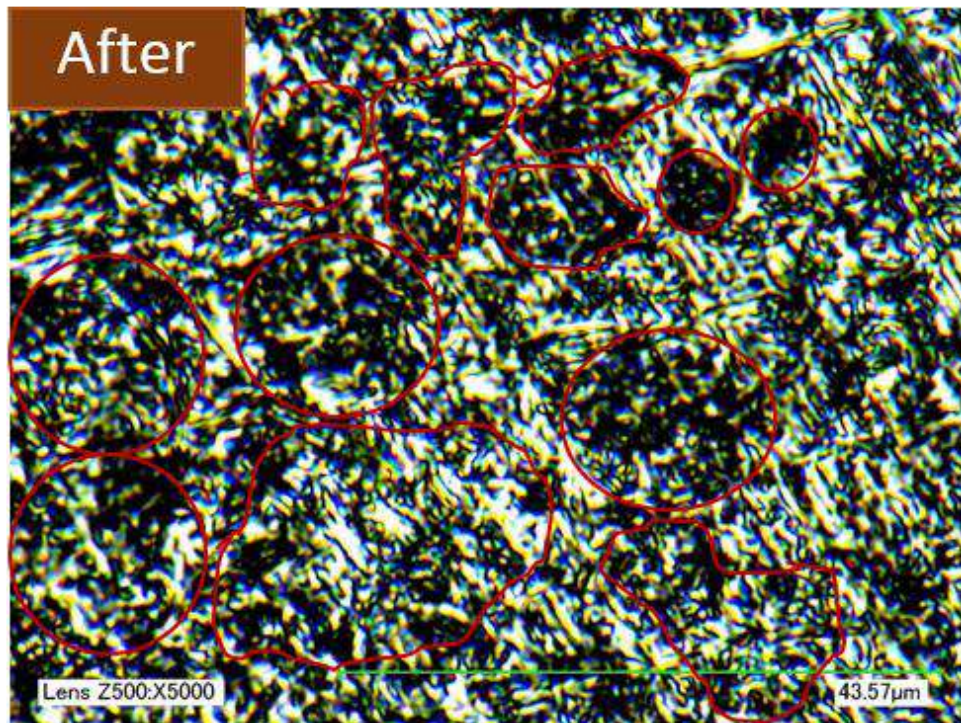
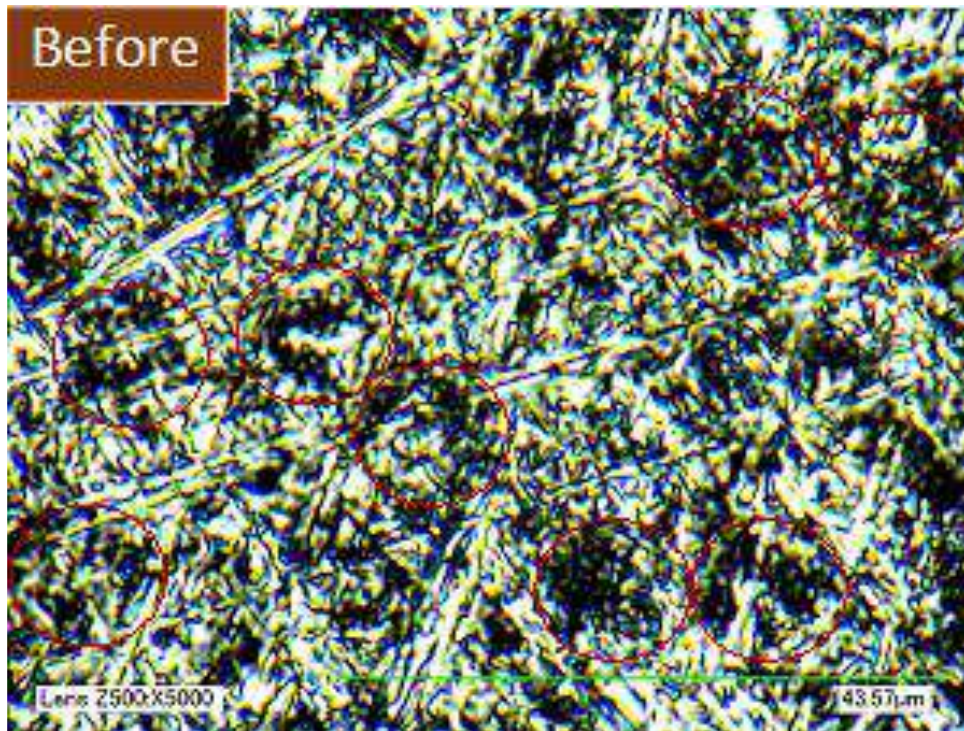


Figure 24: Optical microscopy images of 3003-T3 aluminum before and after (408-hour) test with (reference fluid, without nanoparticles) 50/50% Ethylene Glycol/water (Magnification: 5000X).

Figures 24 and 25 show microscopy images (for 5000X magnification) for the aluminum specimens before and after jet-treatments with each corresponding fluid. Figure 24 allows comparison of images for before- and after-test with (reference fluid) 50/50% Ethylene Glycol and water (Magnification: 5000X), without nanoparticles. After treatment, some short-length polishing scratches remain (after test of 408 hours). Small pitting before treatment (on average, smaller than 8 micrometers (300 micro inches)), becomes larger after treatment, to an average of 10 to 15 micrometers (400 to 600 micro inches), they are shown as circled darker clusters in after-test image. Some surface structures in after test image suggest that some larger areas (of about 30 micrometers) may have started some early erosion.

Figure 25 allows comparison of images for before- and after-test with nanofluid of 2% alumina in 50/50% Ethylene Glycol and water (Magnification: 5000X). After 408-hour treatment, most of the polishing scratches were removed except two bigger scratches (as compared to Figure 24 images, for reference fluid treatment, where some scratches remained), and before-test small-size pitting (on average, smaller than 8 micrometers (300 microinches), circled in figure 25) becomes widespread on after-treatment surface (on average, smaller than 20 micrometers (800 microinches), circled in Figure 25). Pitting seems to clusters along original scratching lines (circled in Figure 25) in after-treatment surface.

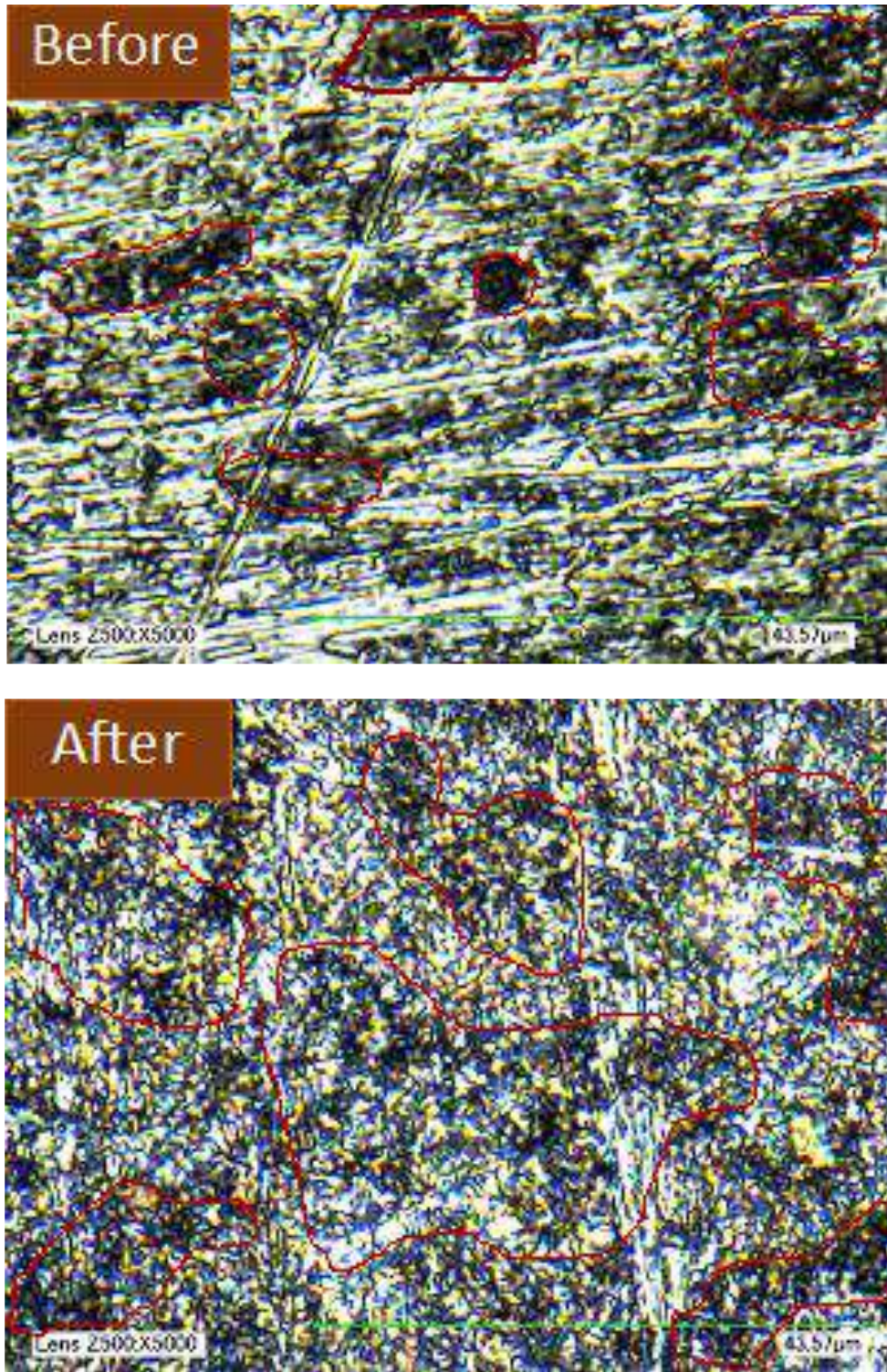


Figure 25: Optical microscopy images of 3003-T3 aluminum before and after (408-hour) test with nanofluid of 2% alumina in 50/50% Ethylene Glycol/water (Magnification: 5000X).

Same jet-impingement treatments and subsequent measurements and analysis were carried out for copper alloy 110. Figure 26 presents the typically measured average Ra roughness for copper alloy 110 before and after 3, 7, 14, 28, 56, 112, 240, 312 and 408 hour treatments with the reference fluid of 50% Ehtylene Glycol in water (EG/Water), and a nanofluid of 2% volume of nano-alumina mixed in the reference fluid (initial values (without treatment), are called “before test”, while values after each treatment are called “after test” in following graphs). Since the initial roughness for each specimen presented in Figure 26 was within the 2 to 5 micro-inch range, each of the Ra values is normalized and presented in Figure 27, where normalization of each after-test Ra-value was done as for data of Figure 22.

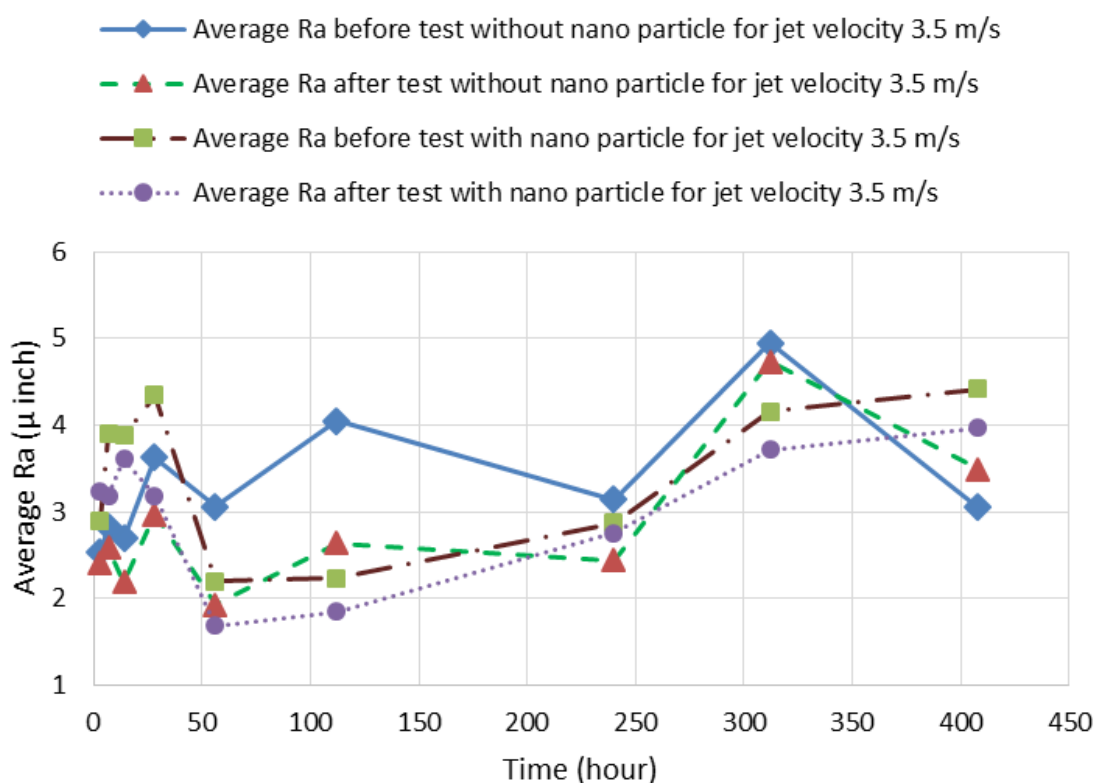


Figure 26. Average Ra roughness for copper alloy 110 before and after 3, 7, 14, 28, 56, 112, 240, 312 and 408 hour-treatments with the reference fluid of 50/50% Ehtylene Glycol in water, and its 2% alumina nanofluid fluid and jet speed of 3.5 m/s.



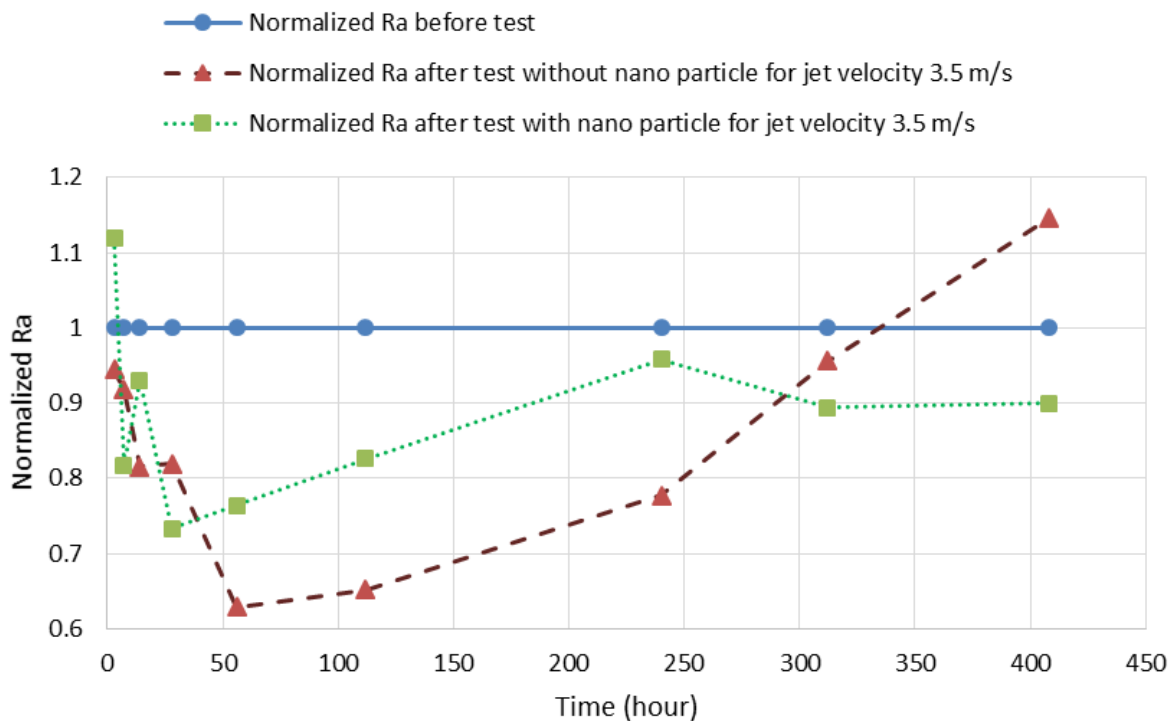


Figure 27. Normalized Ra roughness for alloy 110 copper before and after 3, 7, 14, 28, 56, 112, 240, 312 and 408 hour-treatments with the reference fluid of 50/50% Ethylene Glycol in water, and its nanofluid of 2% nano-alumina in reference fluid and jet speed of 3.5 m/s.

Figures 26 and 27 suggest that no significant roughness differences (all roughness value differences were within 1 micro inch) were obtained when copper specimens are treated for low-speed jet of reference fluid and its nanofluid. Measured  $R_q$  and  $R_z$  (presented in Appendix A) roughness showed similar trends. The small measured roughness differences are roughly within the instrument resolution of 1  $\mu$ inch.



Figure 28. Average weight change for alloy110 copper in before and after 3, 7, 14, 28, 56, 112, 240, 312 and 408 hour-treatments with the reference fluid of 50/50% Ehtylene Glycol in water, and its nanofluid of 2% nano-alumina in reference fluid and jet speed of 3.5 m/s.

Weight measurements of before- and after-tests also were conducted to investigate possible material-removal effects by the jet impingements. Figure 28 presents the measured change in weight for before vs. after 3, 7, 14, 28, 56, 112, 240, 312 and 408 hour-treatments for alloy110 copper specimens with both reference fluid (50/50% Ethylene Glycol in water) and nanofluid (2%-volume of nano-alumina mixed). No significant weight changes were found, however, after jet impingements for the tested fluids and times.

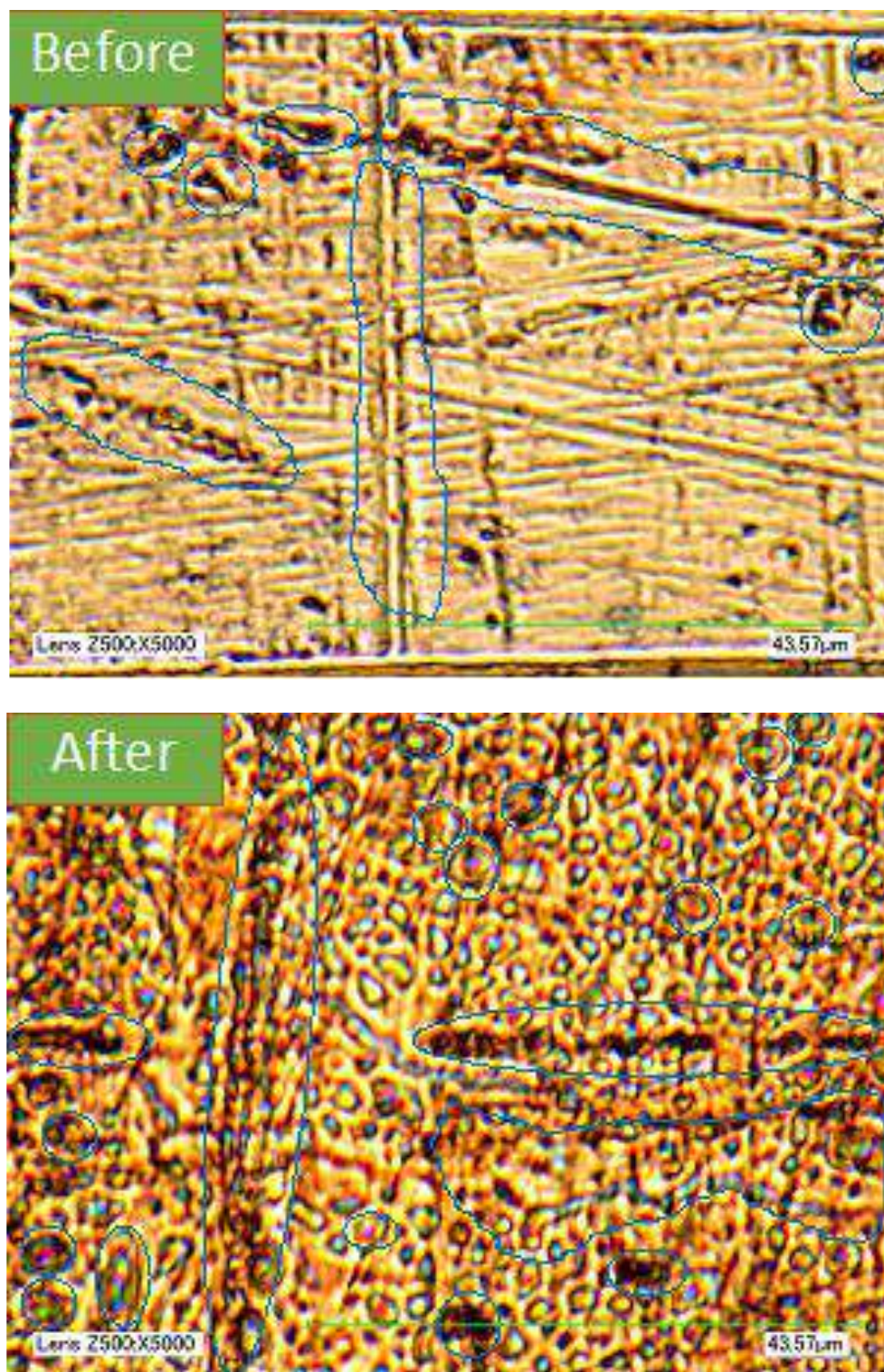


Figure 29: Optical microscopy images of alloy 110 copper before and after (408-hour) test with (reference fluid, without nanoparticles) 50/50% Ethylene Glycol/water (Magnification: 5000X).

To further study possible modifications, but non-detected by roughness or weight change measurements, optical microscopy was conducted for all the specimens after and before treatments. Figures 29 and 30 show microscopy images (for 5000X magnification) for the copper specimens before- and after jet-treatments with each corresponding fluid.

Figure 29 allows comparison of images before- and after-test with (reference fluid) of 50/50% Ethylene Glycol and water (Magnification: 5000X), without nanoparticles. Before treatment some limited pitting (circled in “before” image) and widespread machining scratches were observed, while after 408-hour treatment smaller polishing scratches have been completely removed but some deeper scratches remain, and widespread small-size pitting has occurred (some pitting after treatment seem to cluster around some bigger scratches, circled in “after” image).

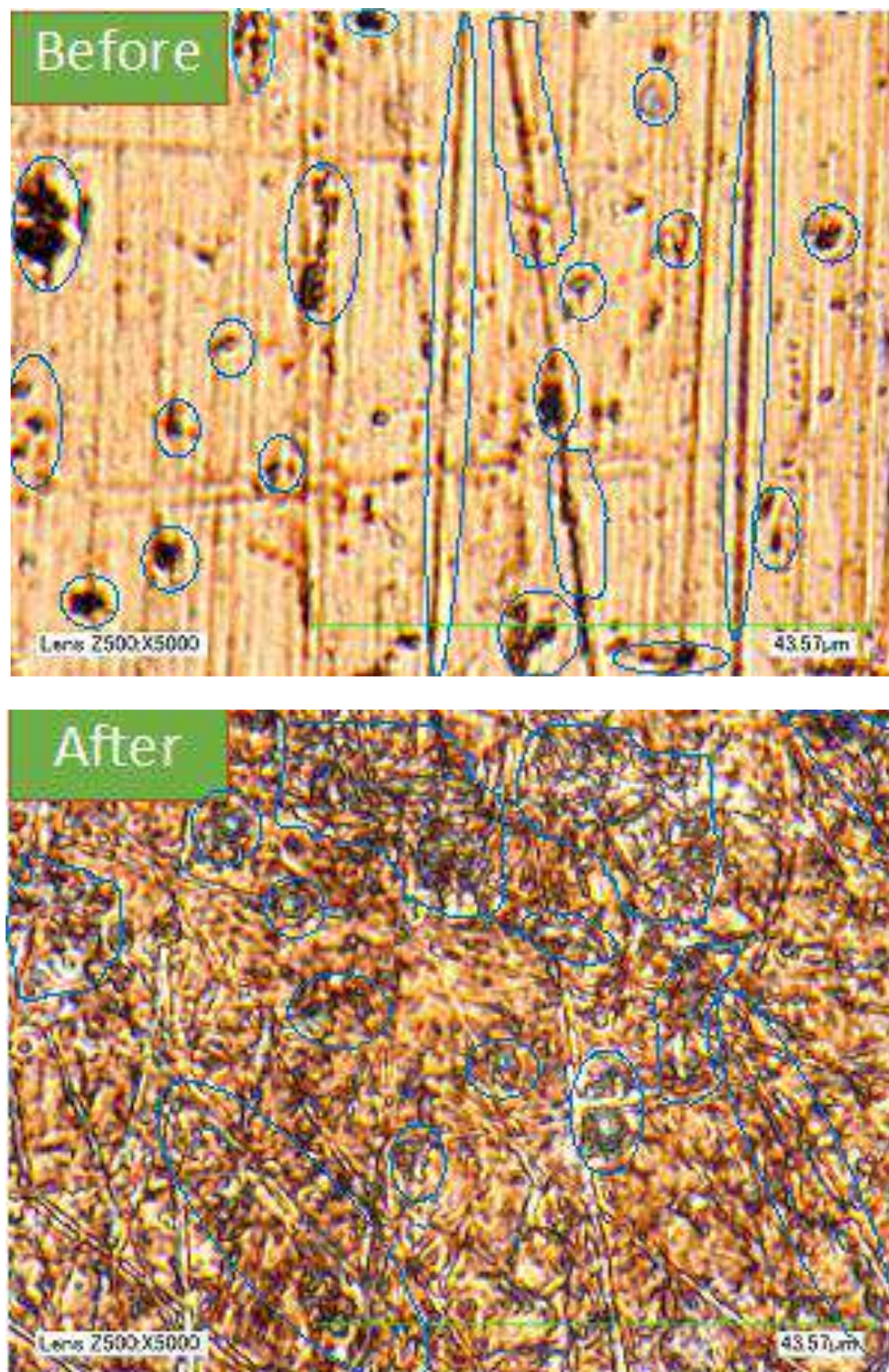


Figure 30: Optical microscopy images of alloy 110 copper before and after (408-hour) test with nanofluid of 2% alumina in 50/50% Ethylene Glycol/water (Magnification: 5000X).

Figure 30 allows comparison of images before- and after-test of copper treated with the nanofluid of 2% alumina in 50/50% Ethylene Glycol and water (Magnification: 5000X). After 408-hour treatment, polishing scratches were not fully removed, and pre-existing pitting (circled in “before” image of Figure 30) became much larger, some pitting seems to clusters along original scratching lines (circled in “after” image of Figure 30).

## **5.2 Test results for 10.7 m/s jet impingement treatments**

### **5.2.1 Test results of 10.7 m/s jet impingement with distilled water as base fluid and its nanofluid**

Figure 31 presents the measured average Ra roughness for 3003-T3 aluminum specimens before and after 3, 7, 14, 28, 56 and 112 hour-treatments with (i) the reference fluid of distilled water, and (ii) a nanofluid of 2%-volume of nano-alumina mixed in the (i) reference fluid (initial values (without treatment), are called “before test”, while values after each treatment are called “after test” in following graphs).

The measurements presented in Figure 31 indicate that aluminum-specimen roughness is affected by the jet impingements with both the reference fluid (distilled water), and its 2%-alumina-nanofluid. For reference fluid, the Ra roughness values initially increase (from the 3 hour-test) showing relatively lower increased value for 56 hours, to be followed by an increase after 112 hours testing. For nanofluid, the Ra roughness values start increase after test from 7 hours test and continue to increase up to 112 hours of test. Similar trends were observed for the two other measured roughness parameters, Rq and Rz (presented in Appendix A).

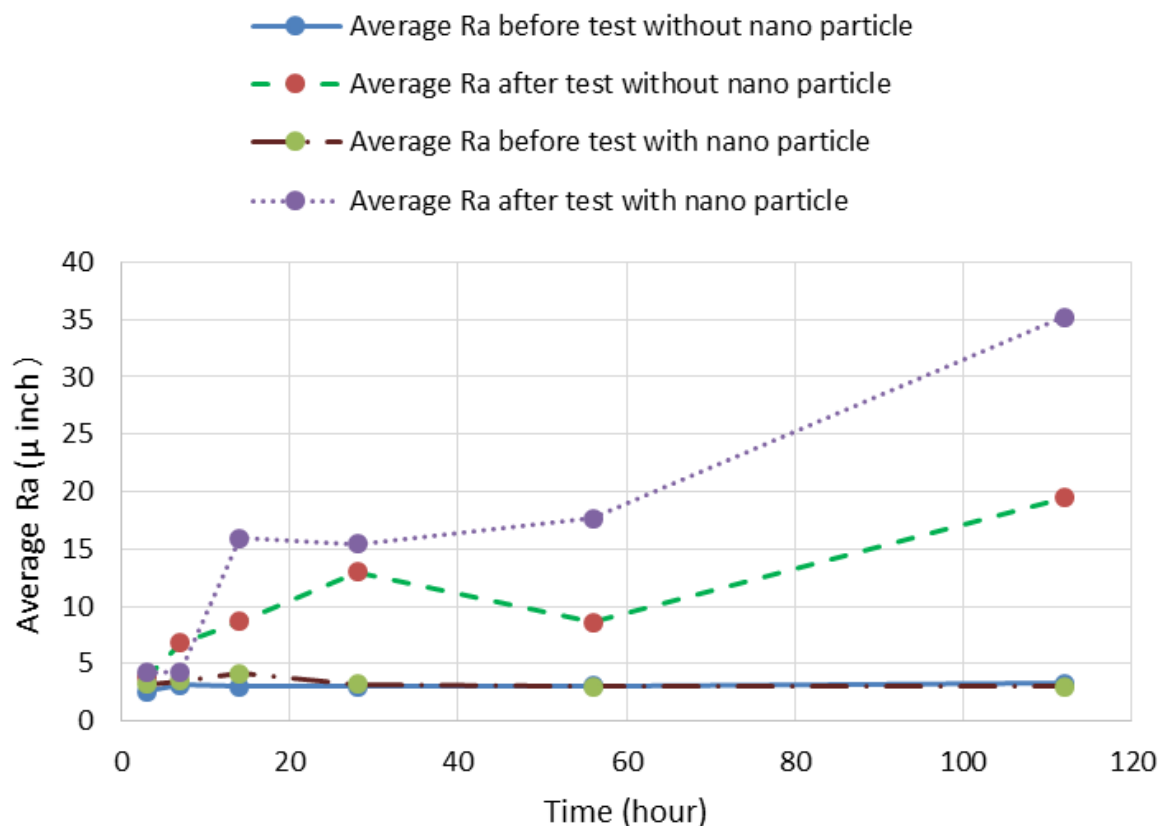


Figure 31. Average Ra roughness for 3003-T3 aluminum before and after 3, 7, 14, 28, 56 and 112 hour-treatments with the reference fluid distilled water and its nanofluid of 2% nano-alumina in reference fluid and jet speed of 10.7 m/s.

Since the initial roughness for each specimen presented in Figure 31 was within the 2 to 5 micro-inch range, each of the Ra values is normalized and presented in Figure 32. Normalization of each after-test Ra-value was done by dividing it by the corresponding initial (before-test) Ra for the corresponding specimen. Figure 32 clearly shows the trends suggested by Figure 31. For reference fluid, initial values increase (from the 3 hour-test) showing relatively lower increased value for 56 hours, to be followed by an increase after 112 hours testing. For nanofluid, the Ra roughness values start increase after test from 7 hours test and continued a slow increase up to 112 hours of test. After test from 56 hours to 112 hours of nanofluid test surface roughness changes are little higher

as compare to each corresponding roughness changes for base fluid (distilled water) test. Similar trends were observed for the two other measured roughness parameters, Rq and Rz (presented in Appendix A).

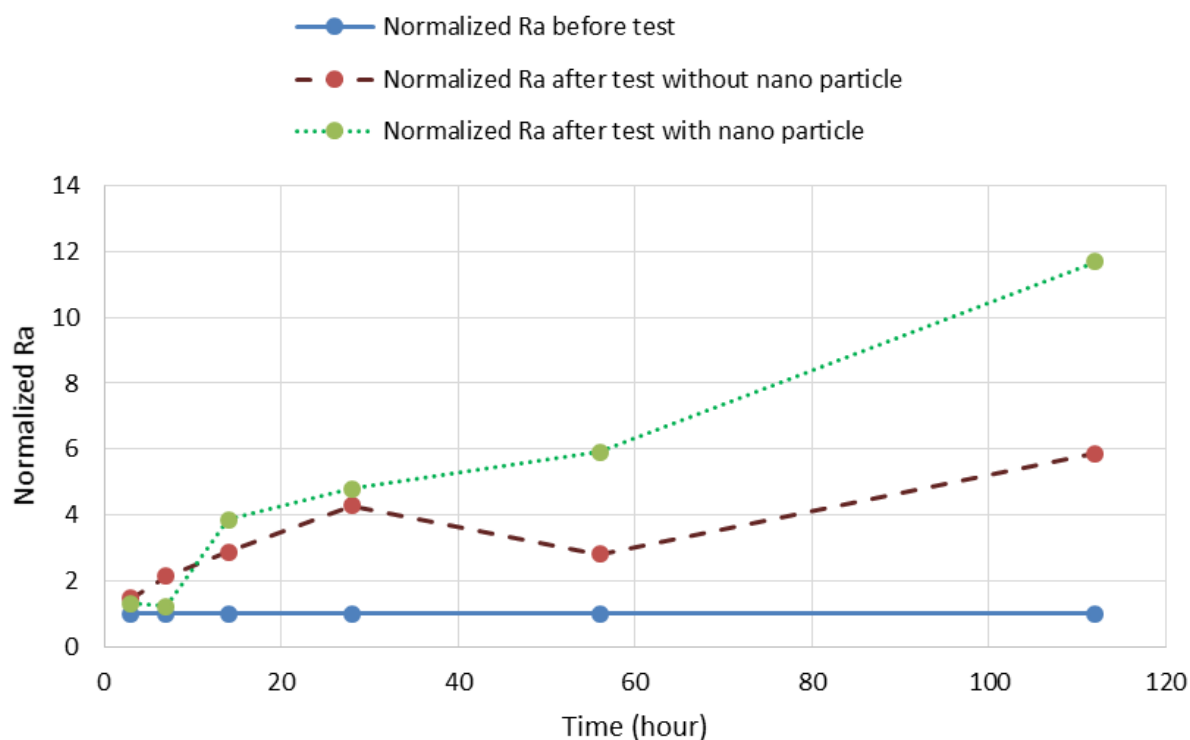


Figure 32. Normalized Ra roughness for 3003-T3 aluminum before and after 3, 7, 14, 28, 56 and 112 hour-treatments with the reference fluid of distilled water and its nanofluid of 2% nano-alumina in reference fluid and jet speed of 10.7 m/s.

Weight measurements also were conducted before and after test to further investigate about possible erosion effects by the jet impingements. Figure 33 presents the measured average change in weight of before-and after- 3, 7, 14, 28, 56 and 112 hour-treatments for 3003-T3 aluminum specimens with both reference fluid (distilled water) and its nanofluid (of 2%-volume of nano-alumina). No significant weight change (all measured weight changes are within 0.5 mg) was observed after jet impingements for the tested fluids and times.



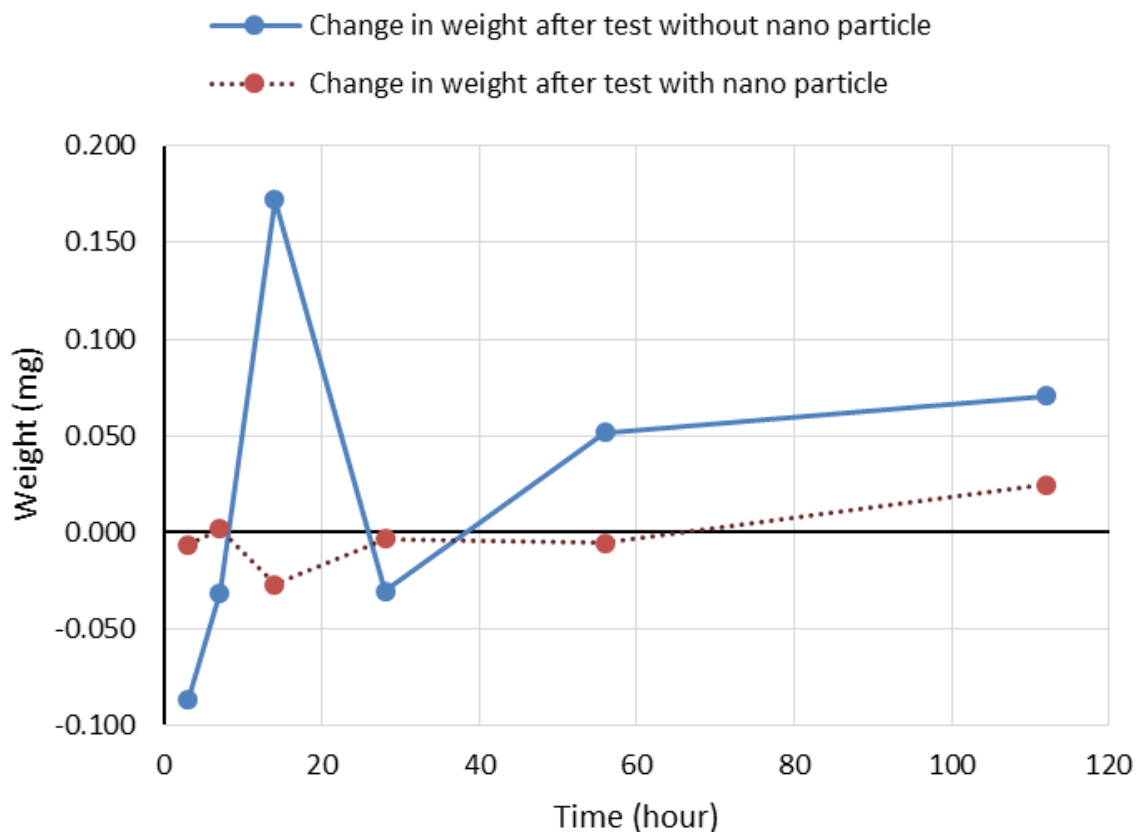


Figure 33. Average weight change for 3003-T3 aluminum in before and after 3, 7, 14, 28, 56 and 112 hour-treatments with the reference fluid of distilled water and its nanofluid of 2% nano-alumina in reference fluid and jet speed of 10.7 m/s.

The measured weight change and roughness changes for aluminum samples, however, suggested that a considerable surface modifications occur when jet-impinged. To study such modifications, optical microscopy was conducted for all the specimens before and after treatments for magnifications of 500x to 5000x (in the sequence 500x, 1000x, 2000x, 3000x, and 5000x). Figures 34 and 35 show microscopy images (for 500X magnification) for the aluminum specimens before and after jet-treatments with each corresponding fluid.

Figure 34 allows comparison of images (Magnification: 500X) for before- and after-test with (reference fluid) distilled water, without nanoparticles. After 112 hours treatment, all polishing

scratches has been removed. Small pitting before treatment (on average, smaller than 5 micrometers (200 micro inches)), becomes considerably larger and deeper (darker represent deeper) after treatment, to an average of 30 to 35 micrometers (1200 to 1400 micro inches), they are shown as circled darker clusters in after-test image. Darker spot represents the deeper pitting. Many small pitting spread around the bigger pitting in after image which represent the beginning of new erosion spot.



Figure 34: Optical microscopy images of 3003-T3 aluminum before and after (112-hour) test with reference fluid of distilled water (Magnification: 500X).

Figure 35 allows comparison of images for before- and after-test with nanofluid of 2% alumina in distilled water (Magnification: 5000X). After 112-hour treatment, all the polishing scratches were removed and before-test small-size pitting (on average, smaller than 5 micrometers (200 microinches), circled in figure 35) becomes larger and widespread on after-treatment surface (on average 40 to 45 micrometers (1600 to 1800 microinches), circled in Figure 35). Many medium size (on average 20 to 25 micrometers (800 to 1000 microinches)) micro pitting has been spread around the bigger pitting. Number of small, medium and large size pitting are higher in after-test image of nanofluid of 2% alumina in distilled water test as compare to after-test image of base fluid (distilled water) test.

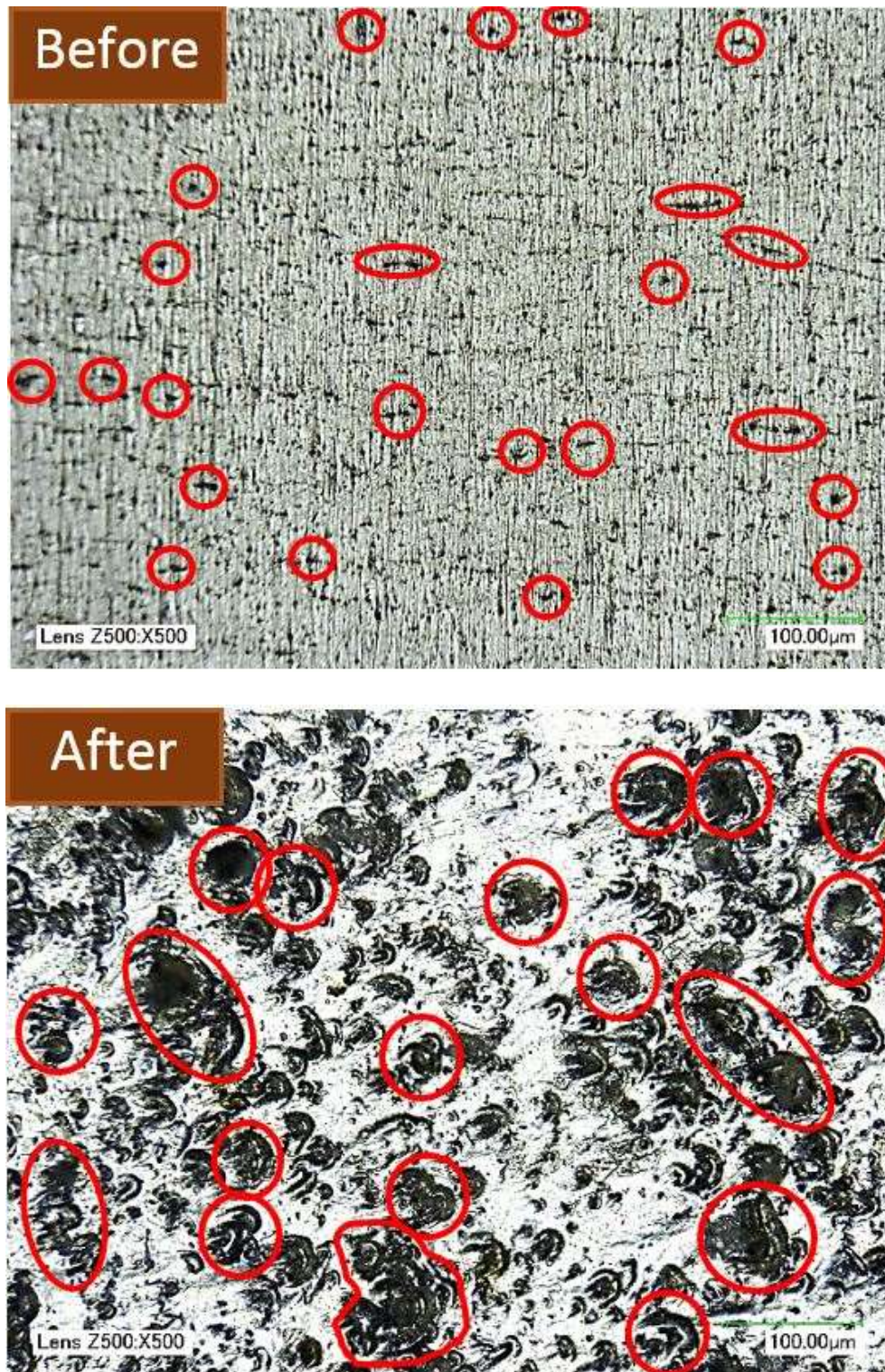


Figure 35: Optical microscopy images of 3003-T3 aluminum before and after (112-hour) test with nanofluid of 2% alumina in distilled water (Magnification: 500X).

Optical image analysis of Figures 34 and 35 also suggests a considerable erosion occurred in the form of micro pitting after 112 hours of jet impingement for both reference fluid and its nanofluid as it has been suggested by roughness measurement. Erosion loss on aluminum specimen surface has been occurred little more with nanofluid of 2% alumina in distilled water jet impingement as compare to base fluid (distilled water) jet impingement.

Same jet-impingement treatments and subsequent measurements and analysis were carried out for copper alloy 110. Figure 36 presents the typically measured average Ra roughness for copper alloy 110 before and after 3, 7, 14, 28, 56 and 112 hour treatments with the reference fluid of distilled water, and a nanofluid of 2% volume of nano-alumina mixed in the reference fluid (initial values (without treatment), are called “before test”, while values after each treatment are called “after test” in following graphs). Since the initial roughness for each specimen presented in Figure 36 was within the 2 to 5 micro-inch range, each of the Ra values is normalized and presented in Figure 37, where normalization of each after-test Ra-value was done as for data of Figure 32.

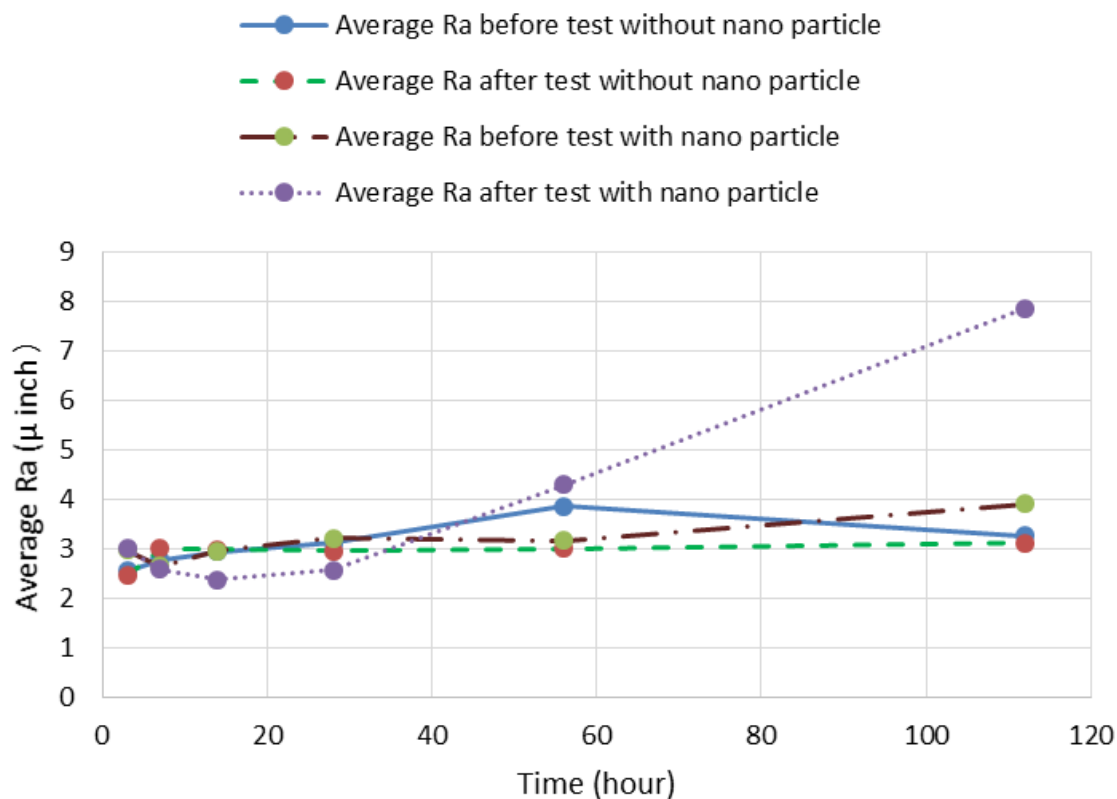


Figure 36. Average Ra roughness for copper alloy 110 before and after 3, 7, 14, 28, 56 and 112 hour-treatments with the reference fluid distilled water and its nanofluid of 2% nano-alumina in reference fluid and jet speed of 10.7 m/s.

Figures 36 and 37 suggest that no significant roughness differences (all roughness value differences were within 1 micro inch) were obtained when copper specimens are treated for 10.7 m/s speed jet of reference fluid (distilled water). A minor roughness change were obtained for 2% alumina in distilled water jet impingement. From 3 hours to 28 hours test there is no significant Ra roughness change, followed by a slow increases after test from 56 hours to 112 hours of test. Measured Rq and Rz (presented in Appendix A) roughness showed similar trends.

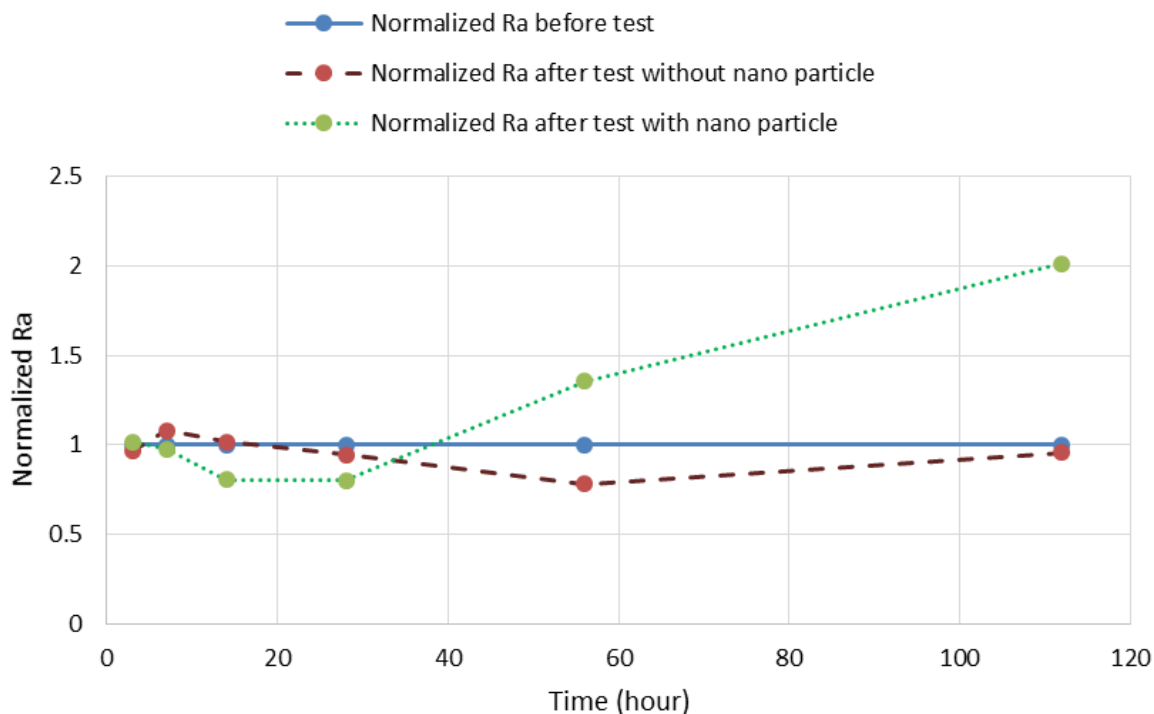


Figure 37. Normalized Ra roughness for alloy 110 copper before and after 3, 7, 14, 28, 56 and 112 hour-treatments with the reference fluid distilled water and its nanofluid of 2% nano-alumina in reference fluid and jet speed of 10.7 m/s.

Weight measurements also were conducted before and after test to further investigate about possible erosion effects by the jet impingements. Figure 38 presents the measured average change in weight of before-and after- 3, 7, 14, 28, 56 and 112 hour-treatments for 110 copper alloy specimens with both reference fluid (distilled water) and its nanofluid (of 2%-volume of nano-alumina). Weight measurements values of Figure 38 suggests no significant weight change (all weight changes are within 0.3 mg) after jet impingements for the tested fluids and times.



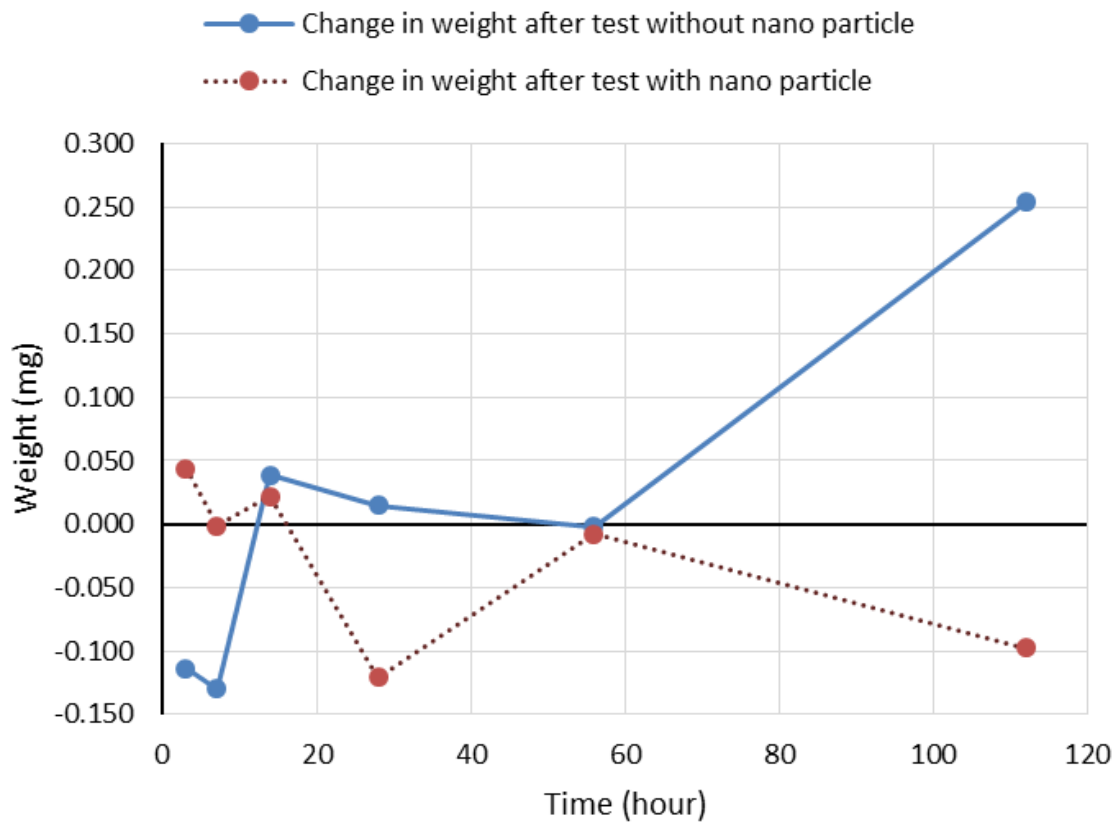


Figure 38. Average weight change for alloy110 copper in before and after 3, 7, 14, 28, 56 and 112 hour-treatments with the reference fluid distilled water and its nanofluid of 2% nano-alumina in reference fluid and jet speed of 10.7 m/s.

Weight measurements of copper specimens found no significant weight change (maximum change is 0.3 mg) after jet impingements for the tested fluids and times.

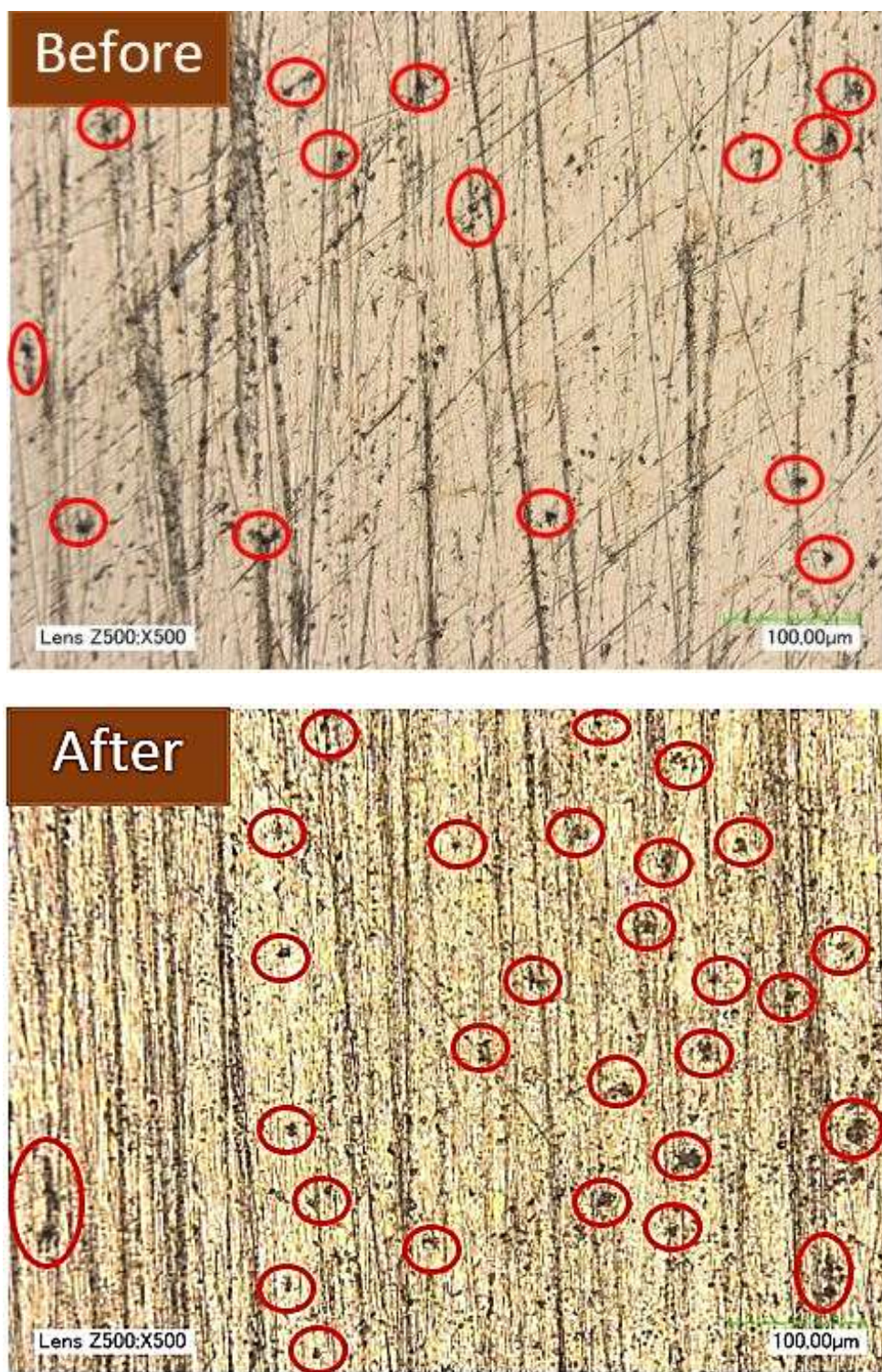


Figure 39. Optical microscopy images of alloy110 copper before and after (112-hour) test with (reference fluid, without nanoparticles) distilled water (Magnification: 500X). Pre-existing pitting and slightly enlarged ones after treatment are circled.

To study possible modifications non-detected by roughness or weight measurements, optical microscopy was conducted for all the specimens after and before treatments. Figures 39 and 40 show microscopy images (for 500X magnification) for the copper specimens before and after jet-treatments with each corresponding fluid.

Figure 39 allows comparison of before- and after-test images with reference fluid of distilled water (Magnification: 500X), without nanoparticles. Before treatment deeper (darker) polishing scratches and some limited pitting (circled in “before” image) were observed. After 112-hour treatment polishing scratches have not been removed but become shallow, and widespread small-size pitting is observed.

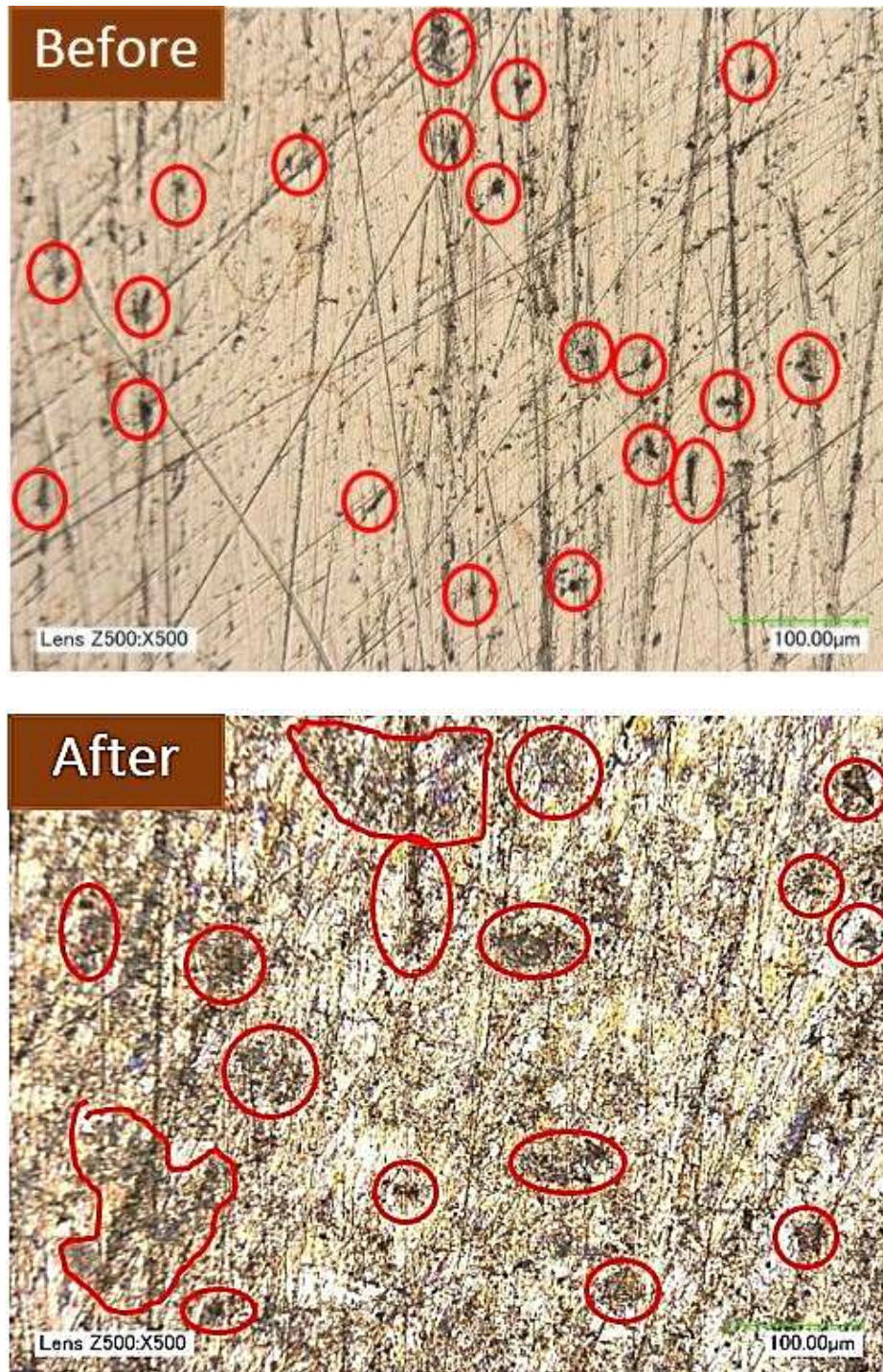


Figure 40. Optical microscopy images of alloy 110 copper before and after (112-hour) test with nanofluid of 2% alumina in distilled water (Magnification: 500X). Pre-existing pitting and enlarged ones after treatment are circled.

Figure 40 allows comparison of before- and after-test images with nanofluid of 2% alumina in distilled water (Magnification: 5000X). After 112-hour treatment, smaller polishing scratches were removed and bigger polishing scratches were become shallow (as compare to bigger polishing scratches in before image). Pre-existing pitting (circled in above Figure 40) became much larger and widespread, some pitting seems to clusters along original scratching lines (circled in above Figure 40).

### **5.2.2 Test results of 10.7 m/s jet impingement with 50/50% Ethylene Glycol as base fluid and its nanofluid**

Figure 41 presents the measured average Ra roughness for 3003-T3 aluminum specimens before and after 3, 7, 14, 28, 56 and 112 hour-treatments with (i) the reference fluid of 50/50% Ethylene Glycol in water (EG/Water), and (ii) a nanofluid of 2%-volume of nano-alumina mixed in the (i) reference fluid (initial values (without treatment), are called “before test”, while values after each treatment are called “after test” in following graphs).

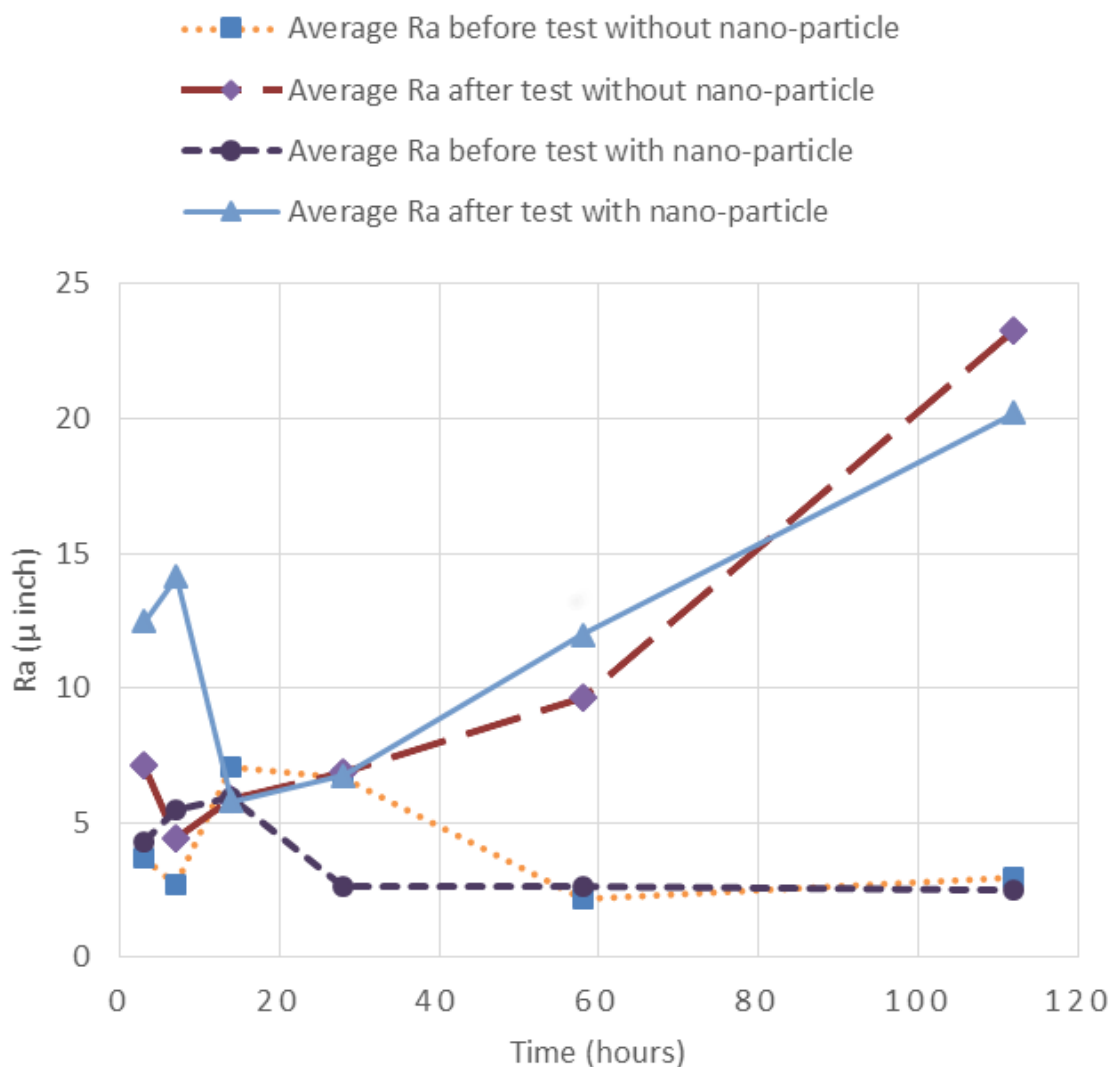


Figure 41. Average Ra roughness for 3003-T3 aluminum before and after 3, 7, 14, 28, 56 and 112 hour-treatments with the reference fluid Ethylene Glycol and its nanofluid of 2% nano-alumina in reference fluid and jet speed of 10.7 m/s.

The measurements presented in Figure 41 indicate that aluminum-specimen roughness is affected by the jet impingements with both the reference fluid (EG/water), and its 2%-alumina-nanofluid. For both of them, the Ra roughness values initially decrease (from the 3 hour-test) showing relatively lower values for 7 and 14 hours, to be followed by a monotonous increase after 28 hours (and longer) testing. Similar trends were observed for the two other measured roughness

parameters,  $R_q$  and  $R_z$  (presented in Appendix A). Weight measurements suggested a small increase in weight after treatments (the highest measured of 5mg) for 3- to 28-hour tests on aluminum, but not significant weight change was observed after 28 hours of jet impingement.

Since the initial roughness for each specimen presented in Figure 41 was within the 2 to 7 micro-inch range, each of the  $R_a$  values is normalized and presented in Figure 42. Normalization of each after-test  $R_a$ -value was done by dividing it by the corresponding initial (before-test)  $R_a$  for the corresponding specimen. Figure 42 clearly shows the trends suggested by Figure 41, of initial roughness increase, followed by a decrease for 7 and 14 hours, and by a monotonous increase after 28 hours of test. The roughness values increase up to eight-fold for the longest tested time of 112 hours. The evolution of roughness in Figures 41 and 42 suggests that some early cleaning of the surface may occur during the first three hours of test (shown as a small increase of roughness), while removal of loose material (left from previous polishing) occurs within the first 14 hours. After 28 hours of test, increased material erosion seems to proceed. Figure 42 also suggests that there were no significant differences on the measured roughness values after jet-impingement by the reference fluid (Ethylene Glycol/water), as compared to those by its 2%-alumina-nanofluid.

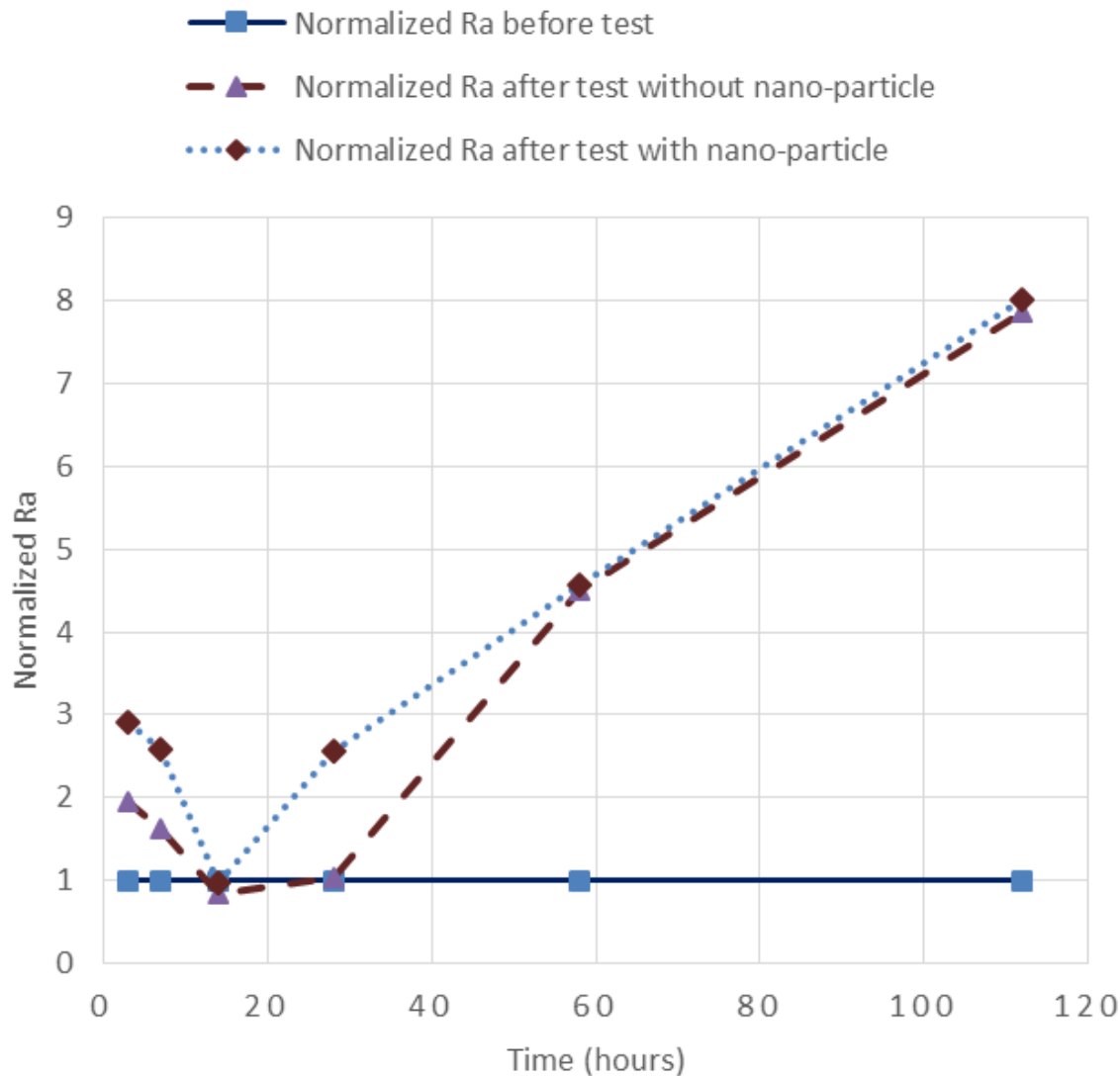


Figure 42. Normalized Ra roughness for 3003-T3 aluminum before and after 3, 7, 14, 28, 56 and 112 hour-treatments with the reference fluid of Ethylene Glycol and its nanofluid of 2% nano-alumina in reference fluid and jet speed of 10.7 m/s.

The measured roughness changes for aluminum samples suggest that significant surface modifications occur when jet-impinged. To study such modifications, optical microscopy was conducted for all the specimens after and before treatments. Figures 43 and 44 show microscopy images (for 5000X magnification) for the aluminum specimens before and after jet-treatments with each corresponding fluid.



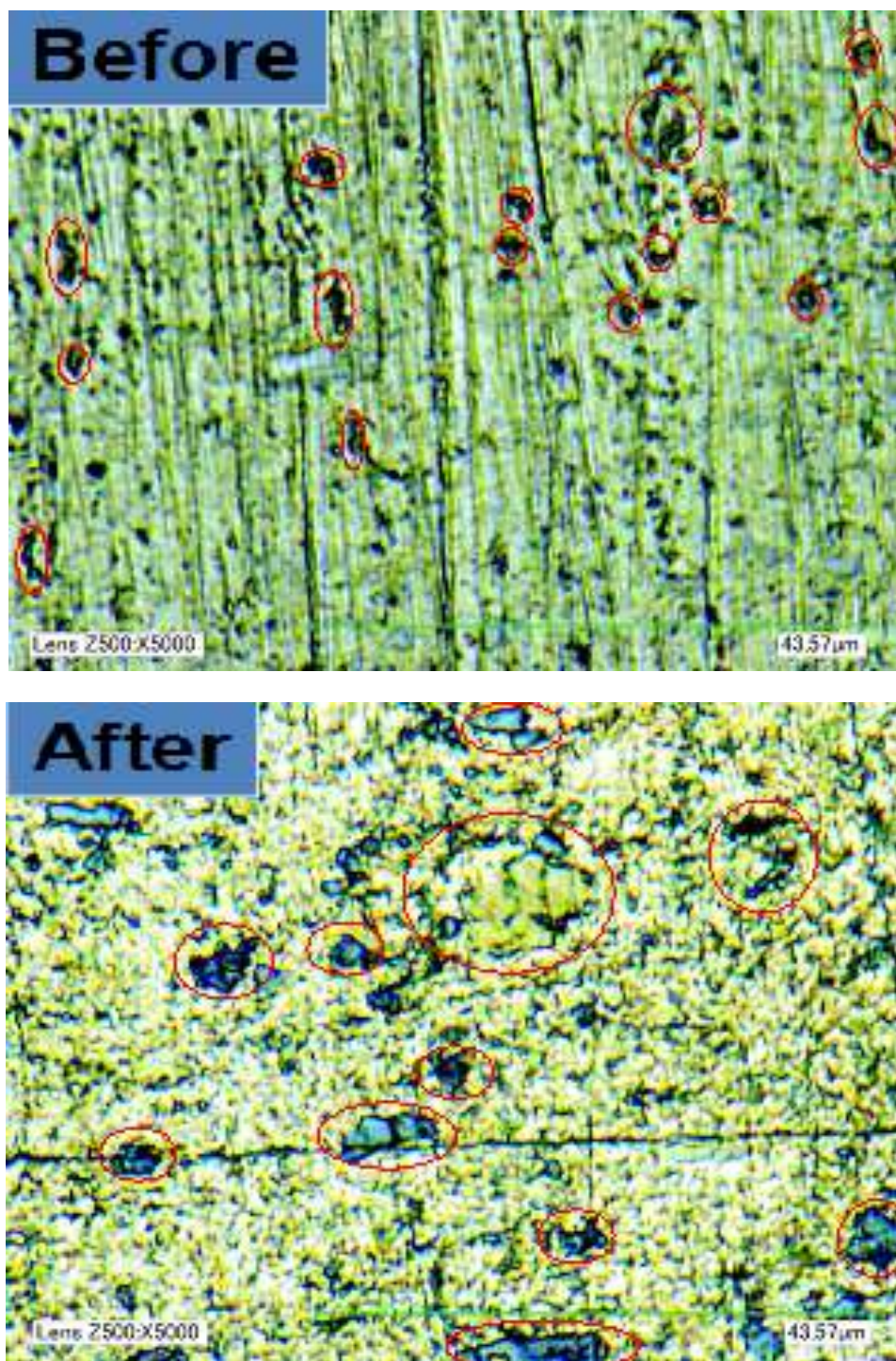


Figure 43. Optical microscopy images of 3003-T3 aluminum before and after (112-hour) test with (reference fluid, without nanoparticles) 50/50 Ethylene Glycol/water (Magnification: 5000X). Pre-existing pitting and enlarged ones after treatment are circled.

Figure 43 allows comparison of before- and after-test images with (reference fluid) of 50/50% Ethylene Glycol and water (Magnification: 5000X), without nanoparticles. After treatment, polishing scratches have been removed (after test of 112 hours), small pitting (on average, smaller than 5 micrometers (200 microinches) becomes larger (to average of 5 to 10 micrometers (200 to 400 microinches), showing as circled darker clusters in after-test image); some observed features also suggest that some larger areas (of about 20 micrometers, not shown in Figure 43) may have started some “spalling”.

Figure 44 allows comparison of before- and after-test images with nanofluid of 2% alumina in 50/50% Ethylene Glycol and water (Magnification: 5000X). After 112-hour treatment, some polishing scratches remain (as compared to Figure 43 images, where scratches were fully removed), small pitting-size is widespread (on average, smaller than 5 micrometers (200 microinches, circled in above figure 44) and pitting seems to clusters along original scratching lines (circled in above figure 44).

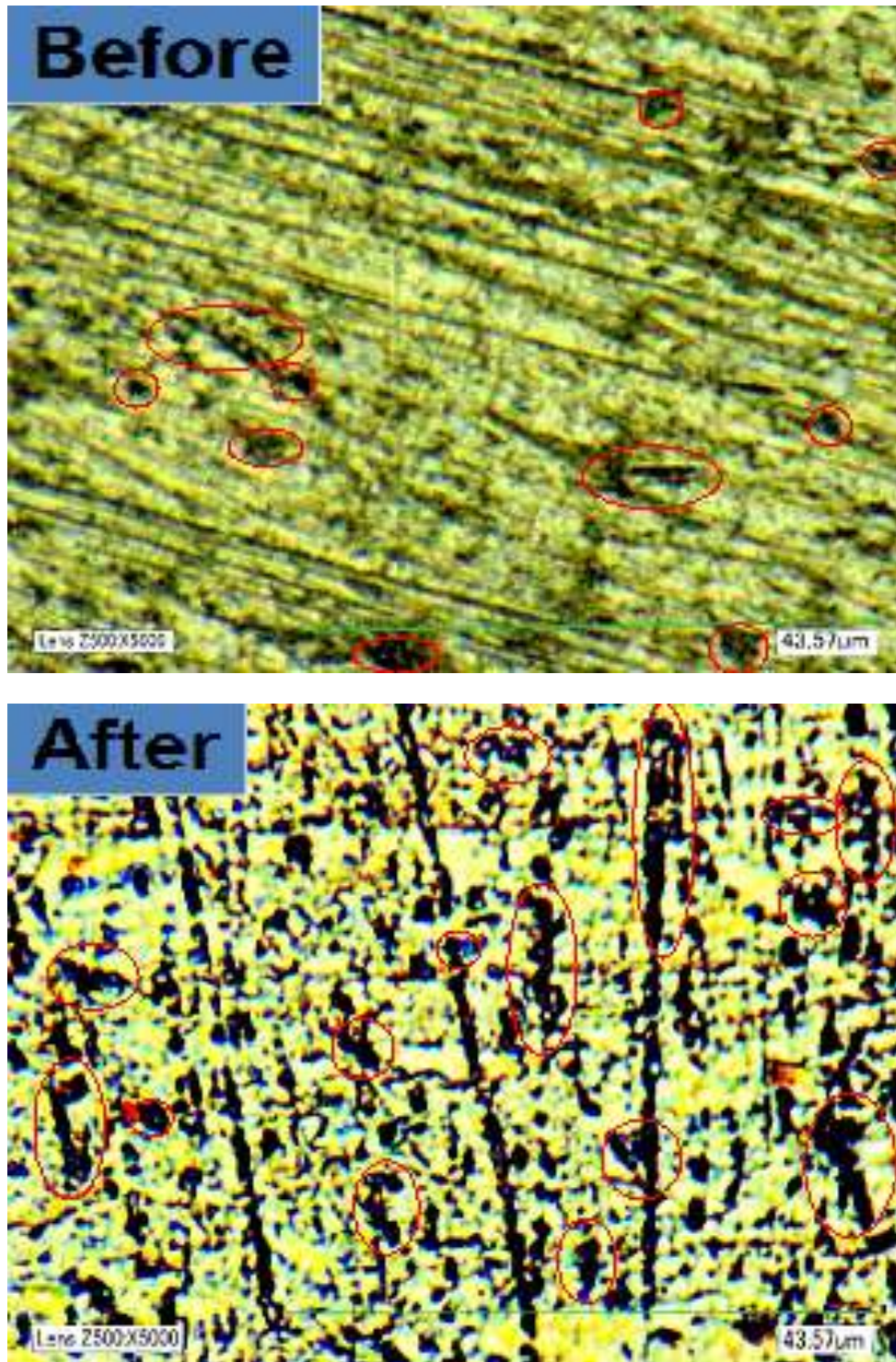


Figure 44. Optical microscopy images of 3003-T3 aluminum before and after (112-hour) test with nanofluid of 2% alumina in 50/50% Ethylene Glycol/water (Magnification: 5000X). Pre-existing pitting and enlarged ones after treatment are circled.

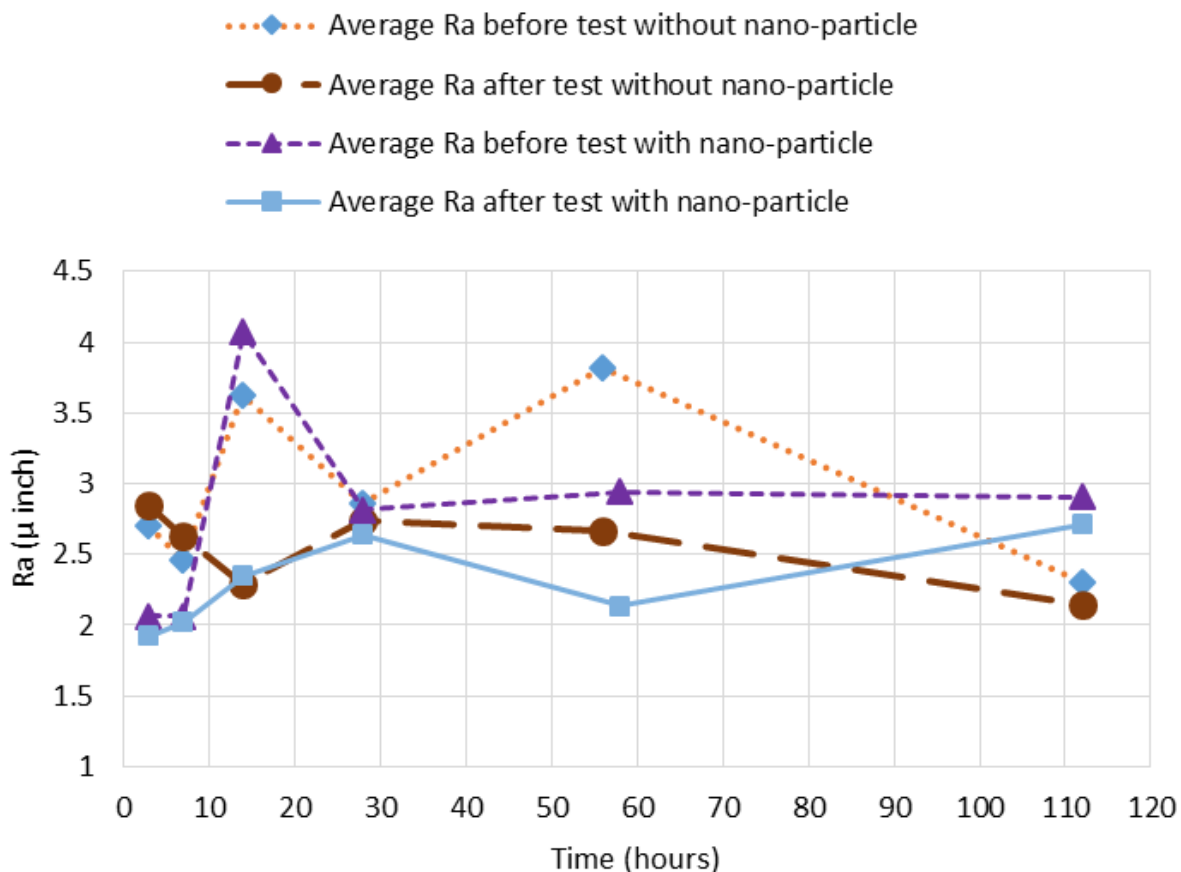


Figure 45. Average Ra roughness for copper alloy 110 before and after 3, 7, 14, 28, 56 and 112 hour-treatments with the reference fluid Ethylene Glycol and its nanofluid of 2% nano-alumina in reference fluid and jet speed of 10.7 m/s.

Figure 45 presents the typically measured average Ra roughness for copper alloy 110 before and after 3, 7, 14, 28, 56 and 112 hour treatments with (i) the reference fluid of 50% Ethylene Glycol in water (EG/Water), and (ii) a nanofluid of 2% volume of nano-alumina mixed in the (i) reference fluid (initial values (without treatment), are called “before test”, while values after each treatment are called “after test” in following graphs). Since the initial roughness for each specimen presented in Figure 45 was within the 2 to 4 micro-inch range, each of the Ra values is normalized and presented in Figure 46, where normalization of each after-test Ra-value was done as for data of

Figure 32. Measured  $R_q$  and  $R_z$  (presented in Appendix A) roughness showed similar trends. No significant roughness differences were measured, but normalized data of Figure 46 suggests a slight roughness decrease; however, these small observed differences are roughly within the instrument resolution of  $1 \mu\text{inch}$ , and they need further experimentation for validation.

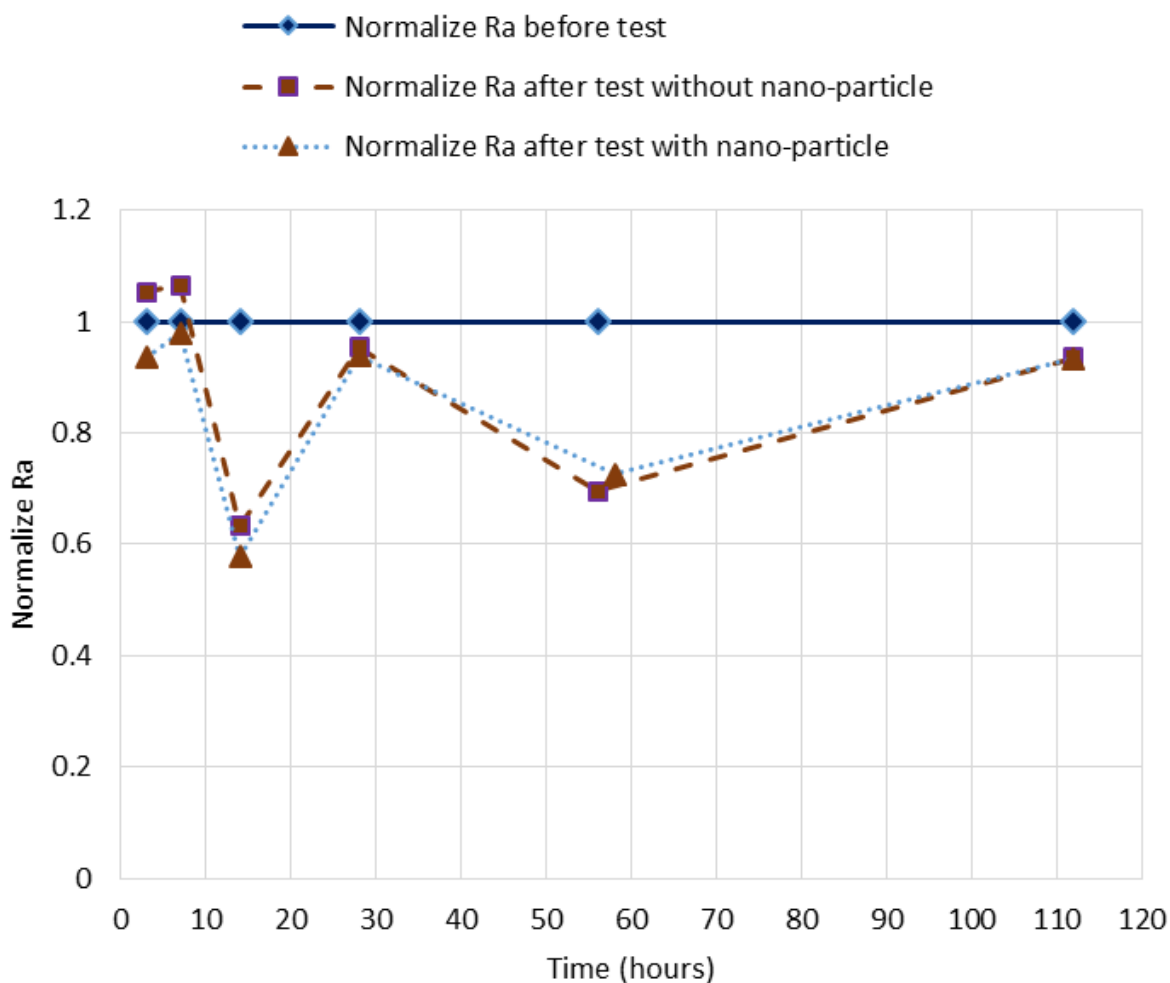


Figure 46. Normalized Ra roughness for alloy 110 copper before and after 3, 7, 14, 28, 56 and 112 hour-treatments with the reference fluid Ethylene Glycol and its nanofluid of 2% nano-alumina in reference fluid and jet speed of 10.7 m/s.

Weight measurements of copper specimens found no significant weight change after jet impingements for the tested fluids and times. To study possible modifications non-detected by

roughness or weight measurements, optical microscopy was conducted for all the specimens after and before treatments. Figures 47 and 48 show microscopy images (for 5000X magnification) for the copper specimens before and after jet-treatments with each corresponding fluid.

Figure 47 allows comparison of before- and after-test images with (reference fluid) of 50/50% Ethylene Glycol and water (Magnification: 5000X), without nanoparticles. Before treatment some limited pitting (circled in “before” image) and machining scratches were observed, while after 112-hour treatment polishing scratches have not been completely removed, and widespread small-size pitting is observed (some pitting after treatment seem to cluster around some areas (circled in “after” image)).

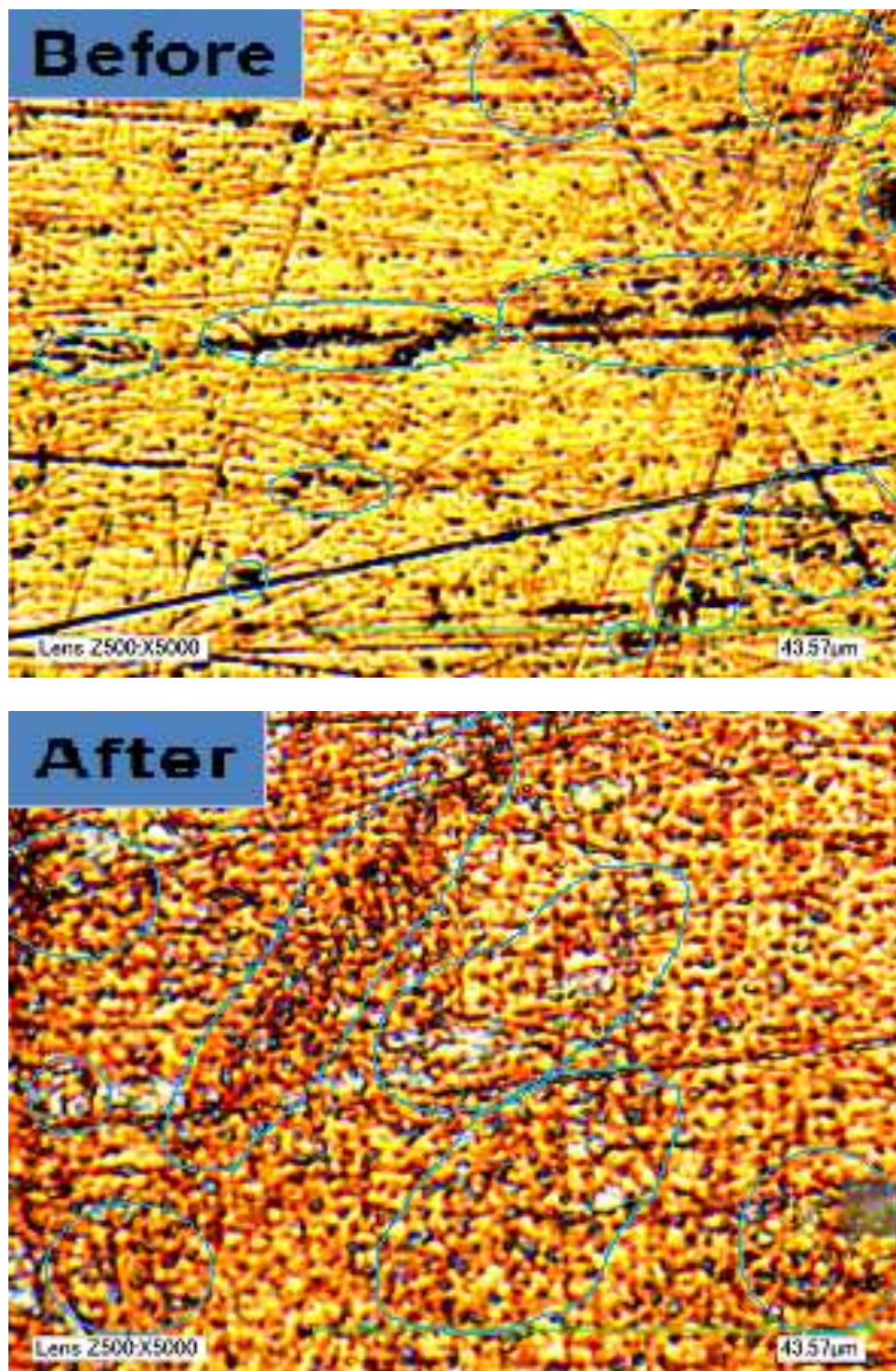


Figure 47. Optical microscopy images of alloy 110 copper before and after (112-hour) test with (reference fluid, without nanoparticles) 50/50% Ethylene Glycol/water (Magnification: 5000X). Pre-existing pitting and seemingly clustered ones after treatment are circled.

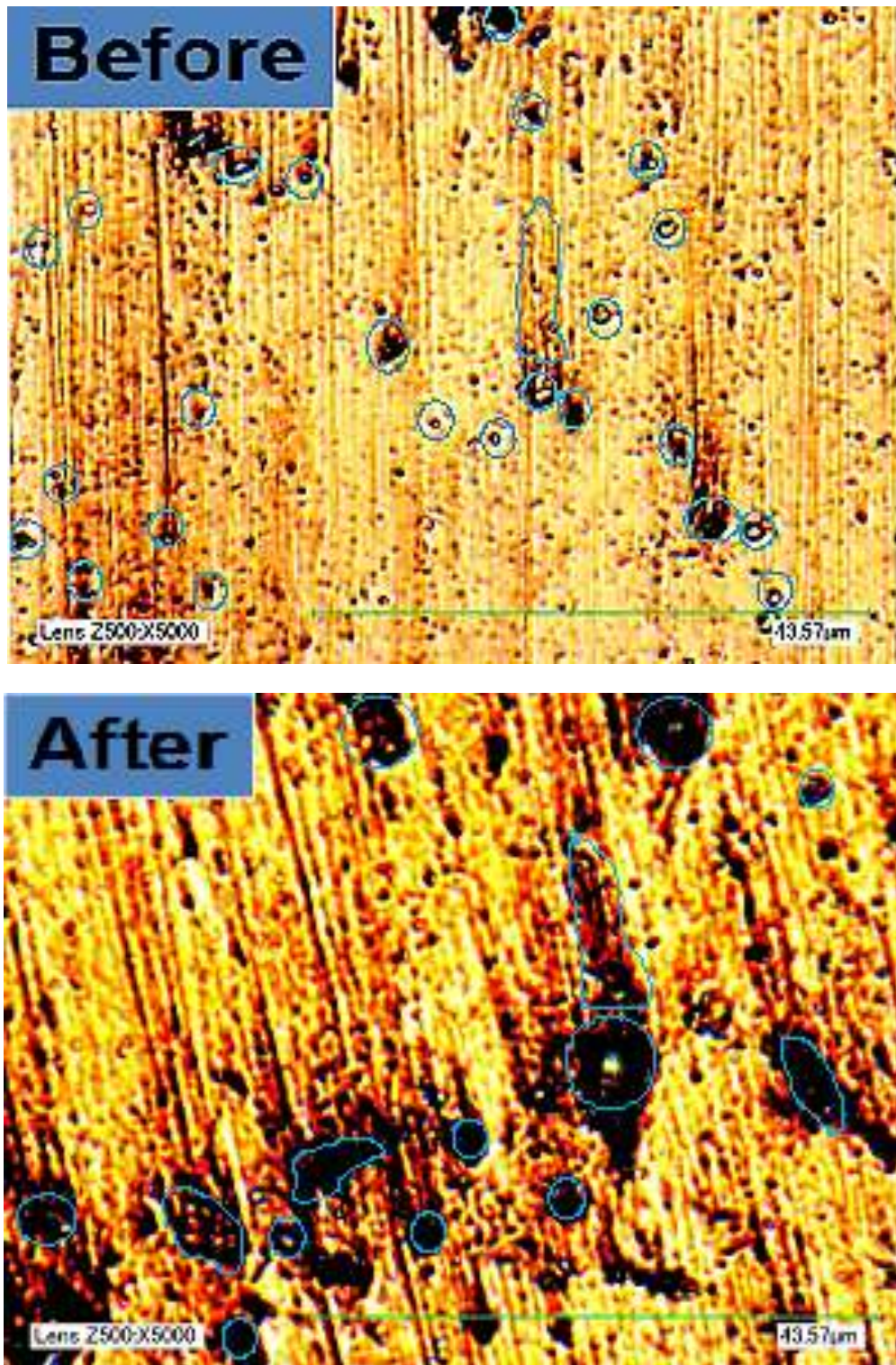


Figure 48. Optical microscopy images of alloy 110 copper before and after (112-hour) test with nanofluid of 2% alumina in 50/50% Ethylene Glycol/water (Magnification: 5000X). Pre-existing pitting and enlarged ones after treatment are circled.



Figure 48 allows comparison of before- and after-test images with nanofluid of 2% alumina in 50/50% Ethylene Glycol and water (Magnification: 5000X). After 112-hour treatment, polishing scratches were not removed, and pre-existing pitting (circled in above Figure 48) became much larger, some pitting seems to clusters along original scratching lines (circled in above Figure 48).

### 5.3 Test results for 15.5 m/s jet impingement treatments

#### 5.3.1 Test results of 15.5 m/s jet impingement with distilled water as base fluid and its nanofluid

Figure 49 presents the measured average Ra roughness for 3003-T3 aluminum specimens before and after 3, 7, 14, 28, 56 and 112 hour-treatments with the reference fluid of distilled water, and a nanofluid of 2%-volume of nano-alumina mixed in the reference fluid of distilled water. Initial values (without treatment), are called “before test”, while values after each treatment are called “after test” in following graphs.

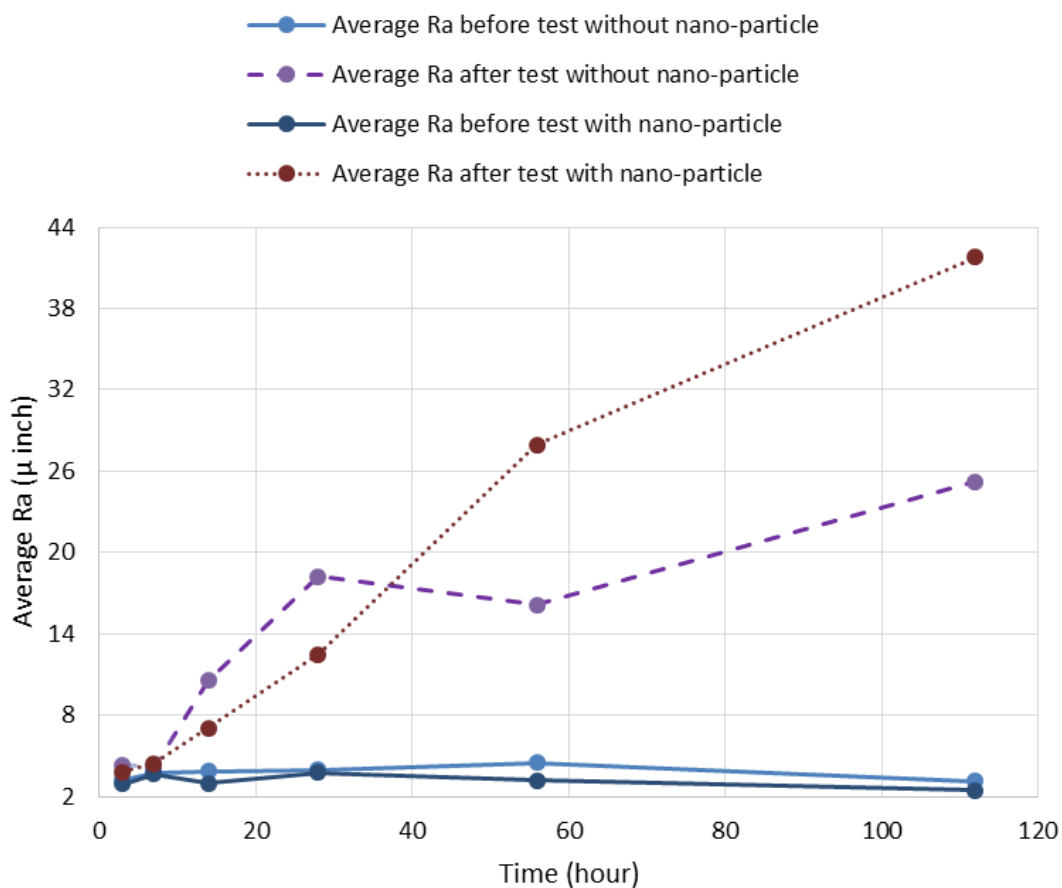


Figure 49. Average Ra roughness for 3003-T3 aluminum before and after 3, 7, 14, 28, 56 and 112 hour-treatments with the reference fluid distilled water and its nanofluid of 2% nano-alumina in reference fluid and jet speed of 15.5 m/s.

The measurements presented in Figure 49 indicate that aluminum-specimen roughness is significantly affected by the jet impingements with both the reference fluid (distilled water), and its 2%-alumina-nanofluid. For both of them, the Ra roughness values start increase after test from 7 hours test and almost similar increasing pattern shows until after 28 hours of test. After test from 56 hours of test roughness changes by base fluid (distilled water) jet impingement shows a slower increasing rate as compare to 2%-alumina nanofluid of distilled water. A significant higher roughness change obtained by 2%-alumina nanofluid of distilled water of 112 hours jet impingement testing as compare to obtained roughness change after 112 hours testing with base fluid (distilled water). Similar trends were observed for the two other measured roughness parameters, Rq and Rz (presented in Appendix A).

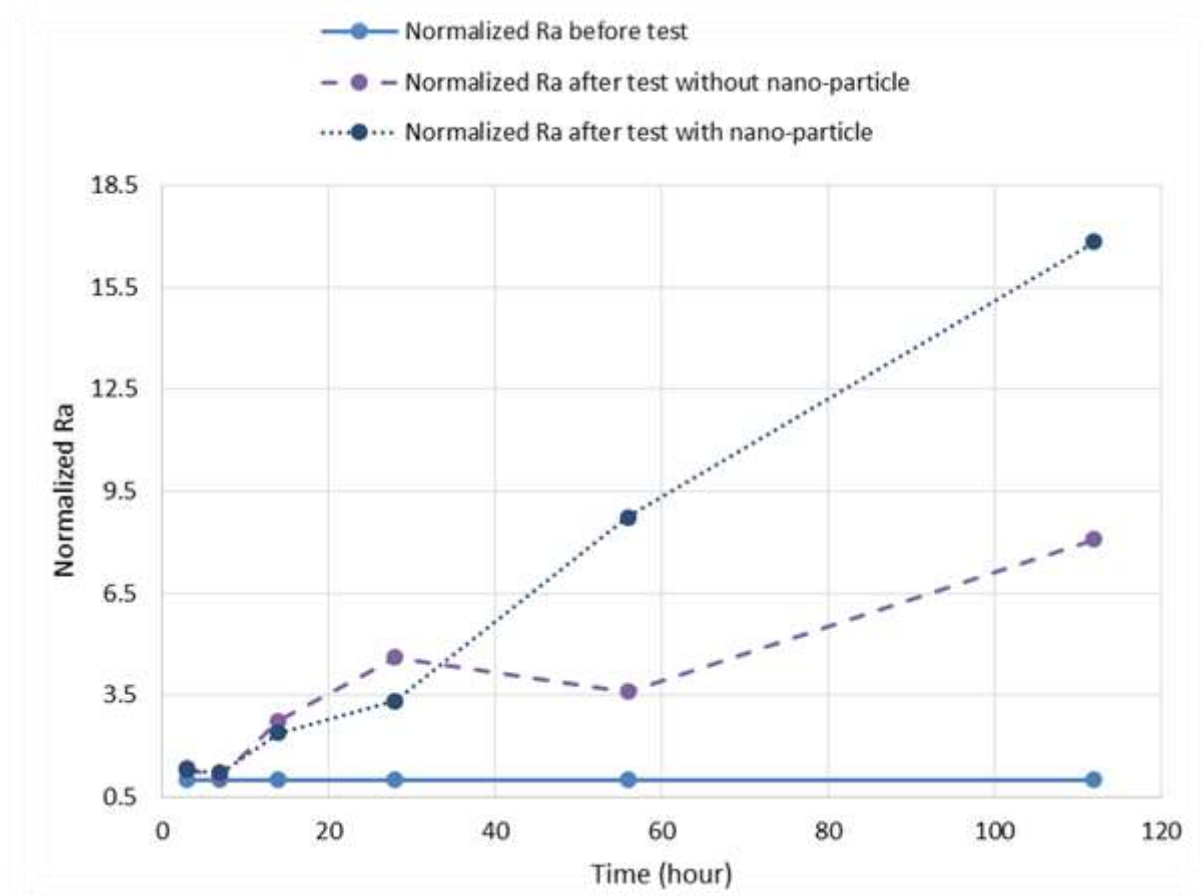


Figure 50. Normalized Ra roughness for 3003-T3 aluminum before and after 3, 7, 14, 28, 56 and 112 hour-treatments with the reference fluid of distilled water and its nanofluid of 2% nano-alumina in reference fluid and jet speed of 15.5 m/s.

Since initial roughness for tested specimen presented in Figure 49 was within the 2 to 4 micro-inch range, each of the Ra values in Figure 49 are normalized and presented in Figure 50 to clarify any possible trend suggested by Figure 49. Normalization of each after-test Ra-value was done by dividing it by the corresponding initial (before-test) Ra for the corresponding specimen. Figure 50 shows the similar trend as obtained in Figure 49.

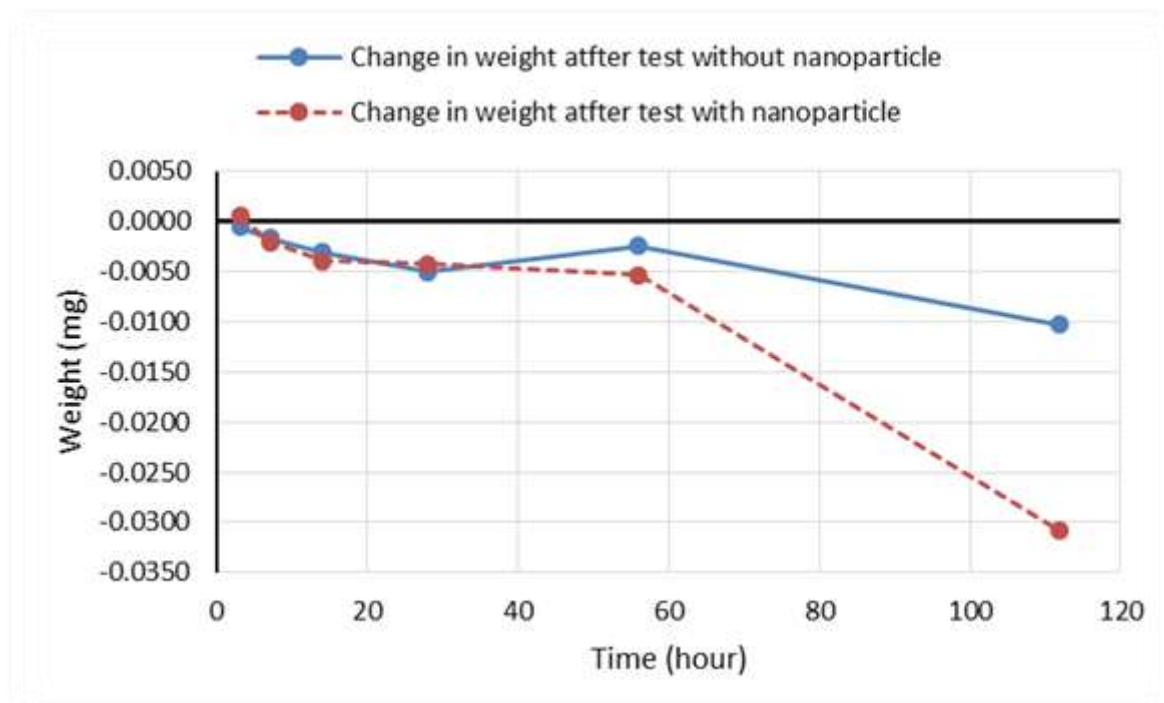


Figure 51. Average weight change for 3003-T3 aluminum in before and after 3, 7, 14, 28, 56 and 112 hour-treatments with the reference fluid of distilled water and its nanofluid of 2% nano-alumina in reference fluid and jet speed of 15.5 m/s.

Weight measurements were conducted before and after test to further investigate about erosion effects by the jet impingements. Figure 51 presents the measured average change in weight of before-and after- 3, 7, 14, 28, 56 and 112 hour-treatments for 3003-T3 aluminum specimens with both reference fluid (distilled water) and its nanofluid (of 2%-volume of nano-alumina). No significant weight change (all weight changes are within 0.04 mg) has been found by 15.5 m/s jet impingement of two tested fluids.

The measured roughness changes for aluminum samples suggest that significant surface modifications occur when jet-impinged. To study such modifications, optical microscopy was conducted for all the specimens after and before treatments. Figures 52 and 53 show microscopy images (for 500X magnification) for the aluminum specimens before and after jet-treatments with each corresponding fluid.

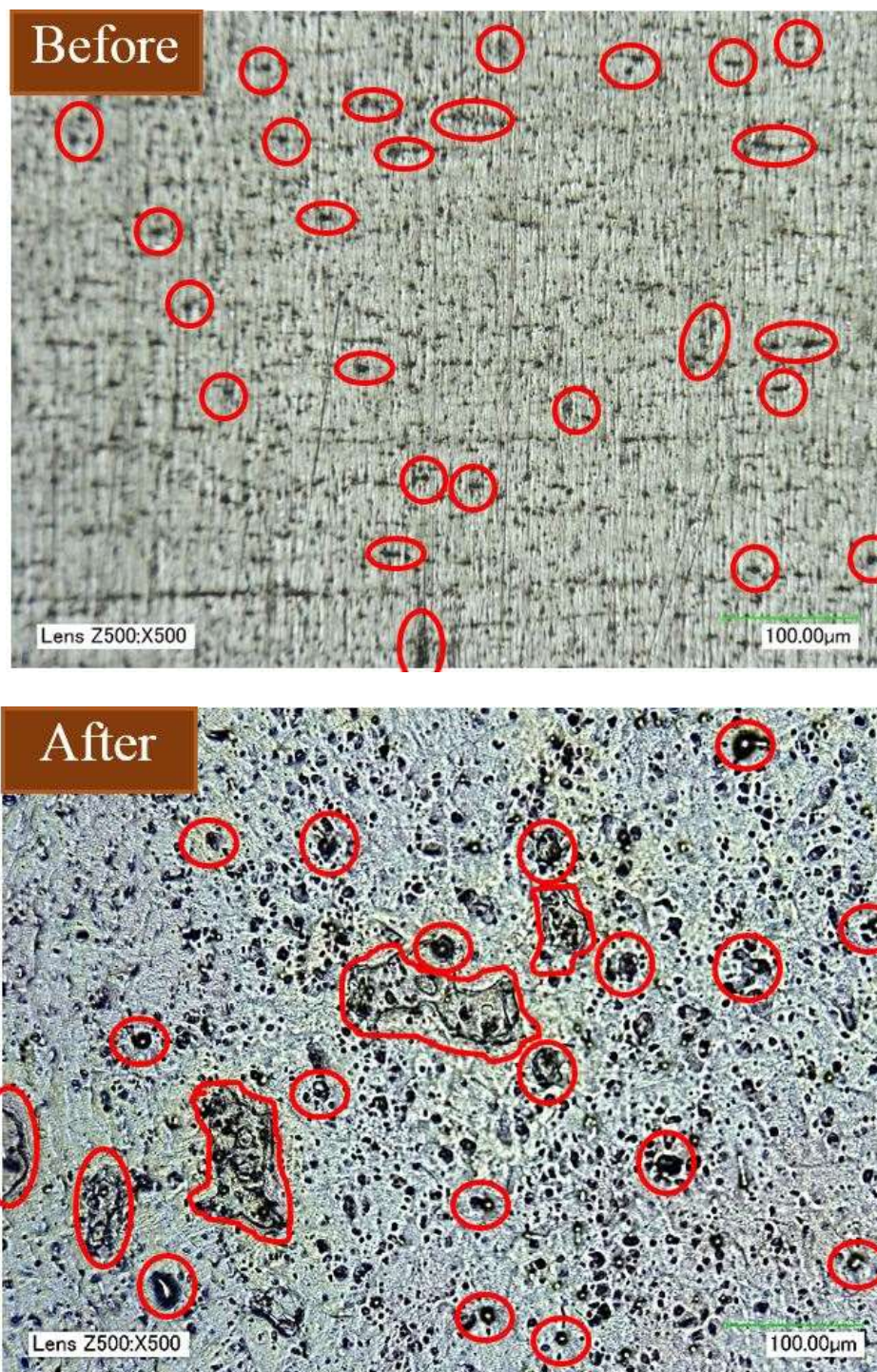


Figure 52: Optical microscopy images of 3003-T3 aluminum before and after (112-hour) test with (reference fluid, without nanoparticles) distilled water (Magnification: 500X).

Figure 52 allows comparison of before- and after-test images with (reference fluid) of distilled water (Magnification: 500X), without nanoparticles. After treatment, all polishing scratches have been removed (after test of 112 hours), small pitting (on average, smaller than 4 micrometers (150 microinches)) becomes larger (to average of 25 to 30 micrometers (1000 to 1200 microinches), showing as circled darker clusters in after-test image) and deeper (darker). Many small pitting (on average 10 micrometers (400 microinches)) spared around the whole image.

Figure 53 allows comparison of before- and after-test images with nanofluid of 2% alumina in distilled water (Magnification: 500X). After 112-hour treatment, all polishing scratches have been removed, small pitting (on average, smaller than 5 micrometers (200 microinches)) becomes larger (to average of 45 to 50 micrometers (1800 to 2000 microinches), showing as circled darker clusters in after-test image). Growth of pitting in after reference fluid (distilled water) test image is higher than that of in after 2% alumina nanofluid of reference fluid test image. Many medium size pitting (on average 20 micrometers (800 microinches)) spared around the whole image.

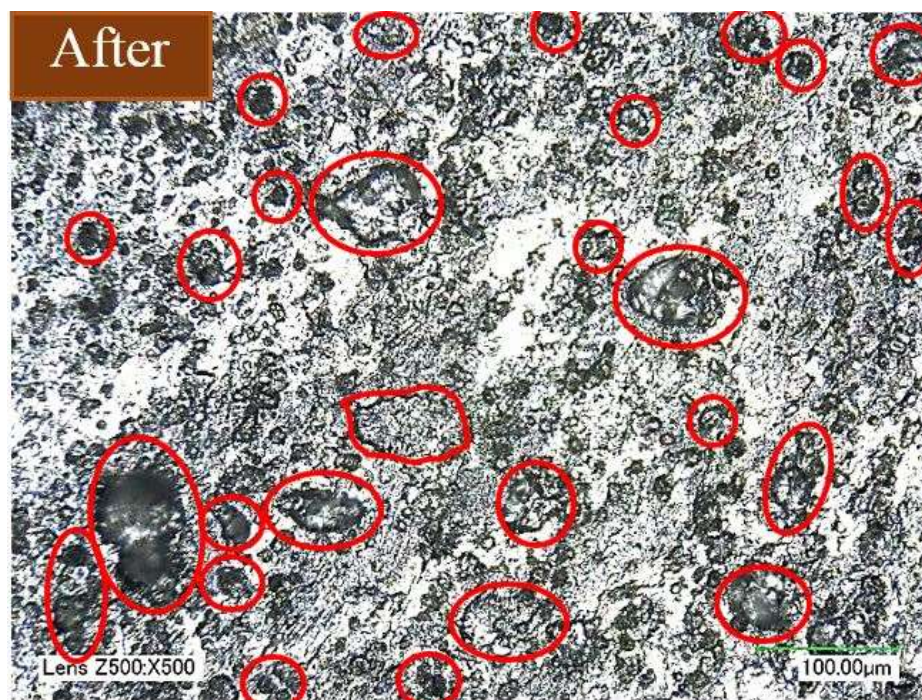
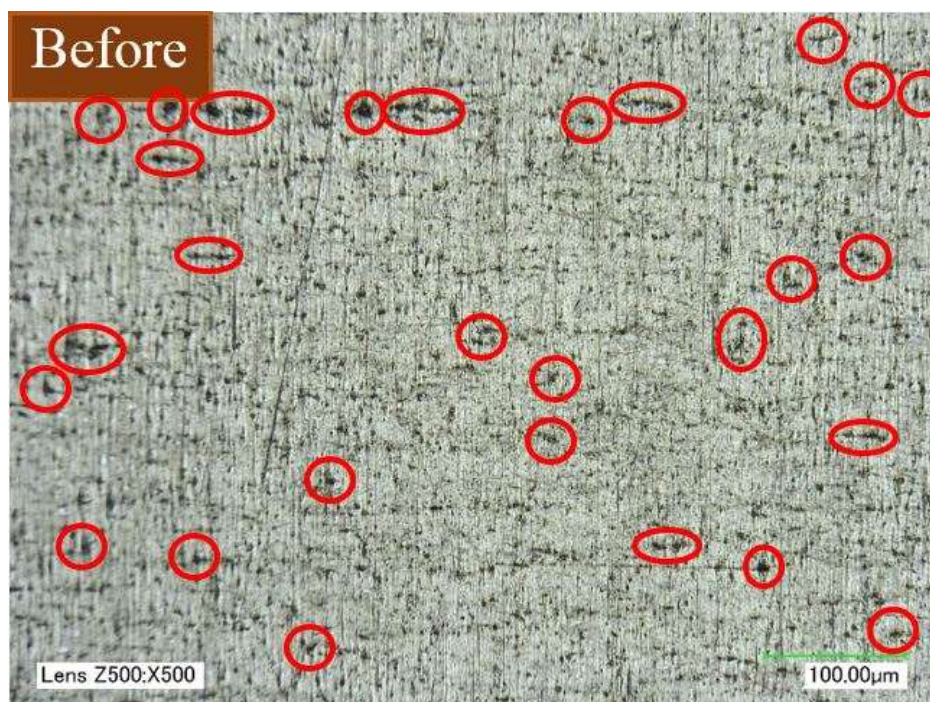




Figure 53: Optical microscopy images of 3003-T3 aluminum before and after (112-hour) test with nanofluid of 2% alumina in distilled water (Magnification: 500X).

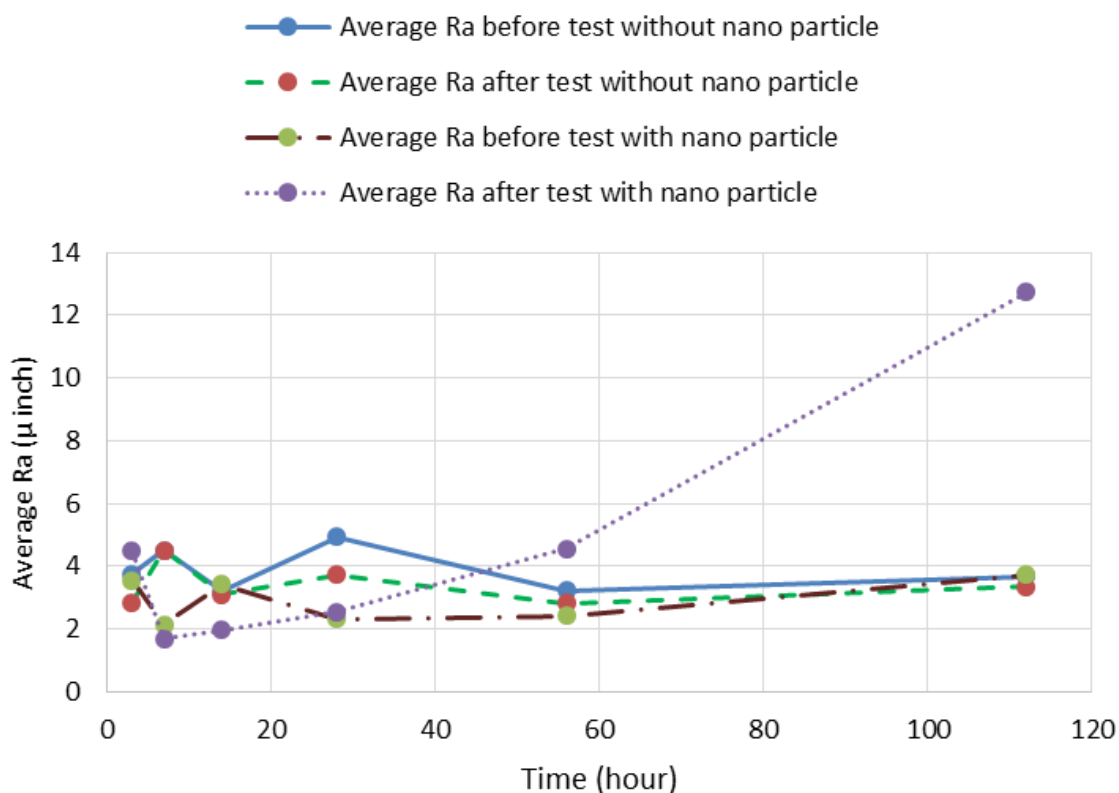


Figure 54. Average Ra roughness for copper alloy 110 before and after 3, 7, 14, 28, 56 and 112 hour-treatments with the reference fluid distilled water and its nanofluid of 2% nano-alumina in reference fluid and jet speed of 15.5 m/s.

Figure 54 presents the typically measured average Ra roughness for copper alloy 110 before and after 3, 7, 14, 28, 56 and 112 hour treatments with the reference fluid of distilled water and its 2% alumina nanofluid. Initial values (without treatment), are called “before test”, while values after each treatment are called “after test” in following graphs. Since the initial roughness for each specimen presented in Figure 54 was within the 2 to 4 micro-inch range, each of the Ra values is normalized and presented in Figure 55, where normalization of each

after-test Ra-value was done as for data of Figure 50. Measured Rq and Rz (presented in Appendix A) roughness showed similar trends. For base fluid (distilled water), no significant roughness differences were measured, but normalized data of Figure 55 suggests a slight roughness decrease (all roughness change values for reference fluid (distilled water) tests are within 1 micro inches).

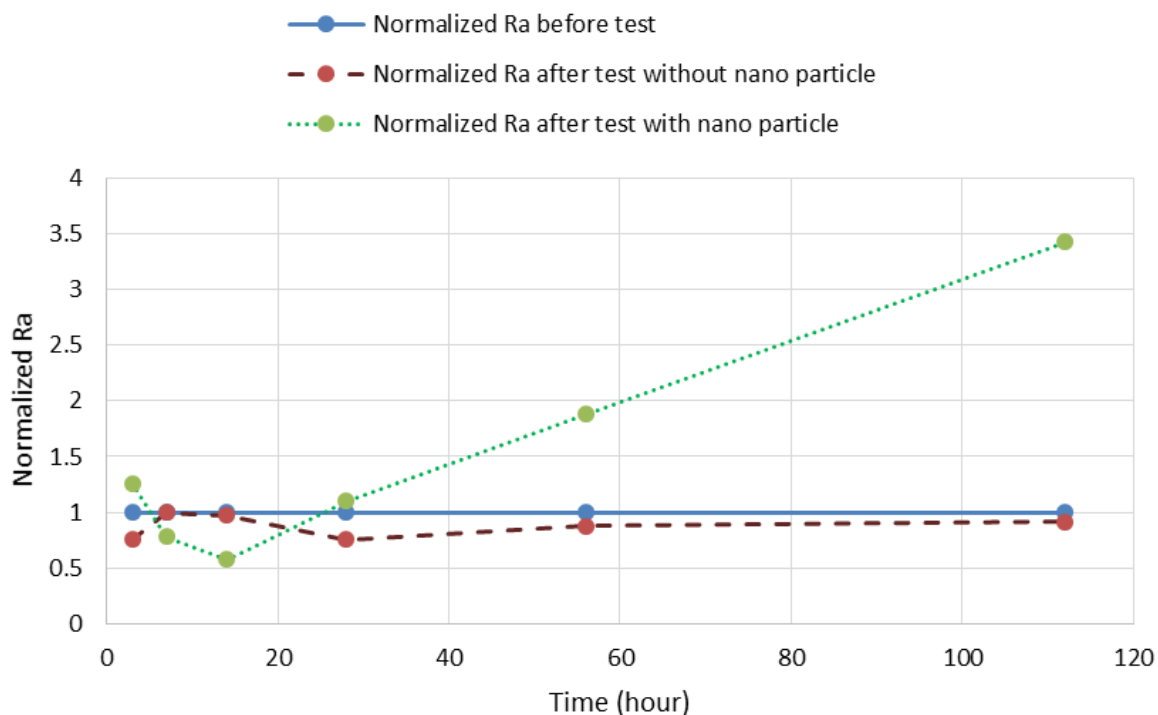


Figure 55. Normalized Ra roughness for alloy 110 copper before and after 3, 7, 14, 28, 56 and 112 hour-treatments with the reference fluid distilled water and its nanofluid of 2% nano-alumina in reference fluid and jet speed of 15.5 m/s.

For nanofluid (2% nano-alumina in distilled water) test, Ra roughness values initially decrease (from the 3 hour-test) showing decreased values for 7 and 14 hours, to be followed by a monotonous increase after 28 hours (and longer) testing. Similar trends were observed for the two other measured roughness parameters, Rq and Rz (presented in Appendix A). The evolution of roughness in Figures 54 and 55 suggests that some early cleaning of the surface

may occur during the first 28 hours of test (surface roughness shown as a small increase after 3 hours test followed by decrease after 7 hours to 28 hours), after 56 hours of test increased material erosion seems to proceed.

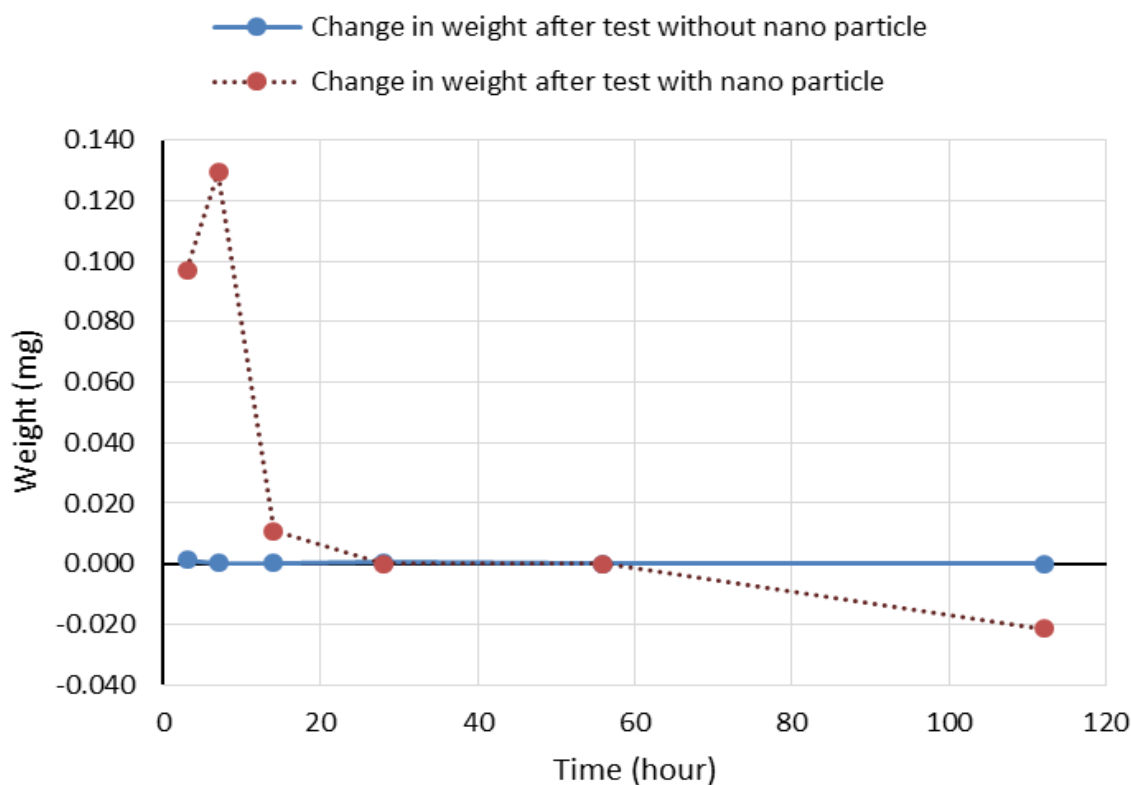


Figure 56. Average weight change for alloy 110 copper in before and after 3, 7, 14, 28, 56 and 112 hour-treatments with the reference fluid distilled water and its nanofluid of 2% nano-alumina in reference fluid and jet speed of 15.5 m/s.

Weight measurements were conducted before and after test to further investigate about erosion effects by the jet impingements. Figure 56 presents the measured average change in weight of before-and after- 3, 7, 14, 28, 56 and 112 hour-treatments for 3003-T3 aluminum specimens with both reference fluid (distilled water) and its nanofluid (of 2%-volume of nano-alumina). No significant weight change (all weight changes are within 0.04 mg) has been found by 15.5 m/s jet impingement of with and without nanoparticle of base fluid.

To study possible modifications non-detected by roughness or weight measurements, optical microscopy was conducted for all the specimens after and before treatments. Figures 57 and 58 show microscopy images (for 500X magnification) for the copper specimens before and after jet-treatments with each corresponding fluid.

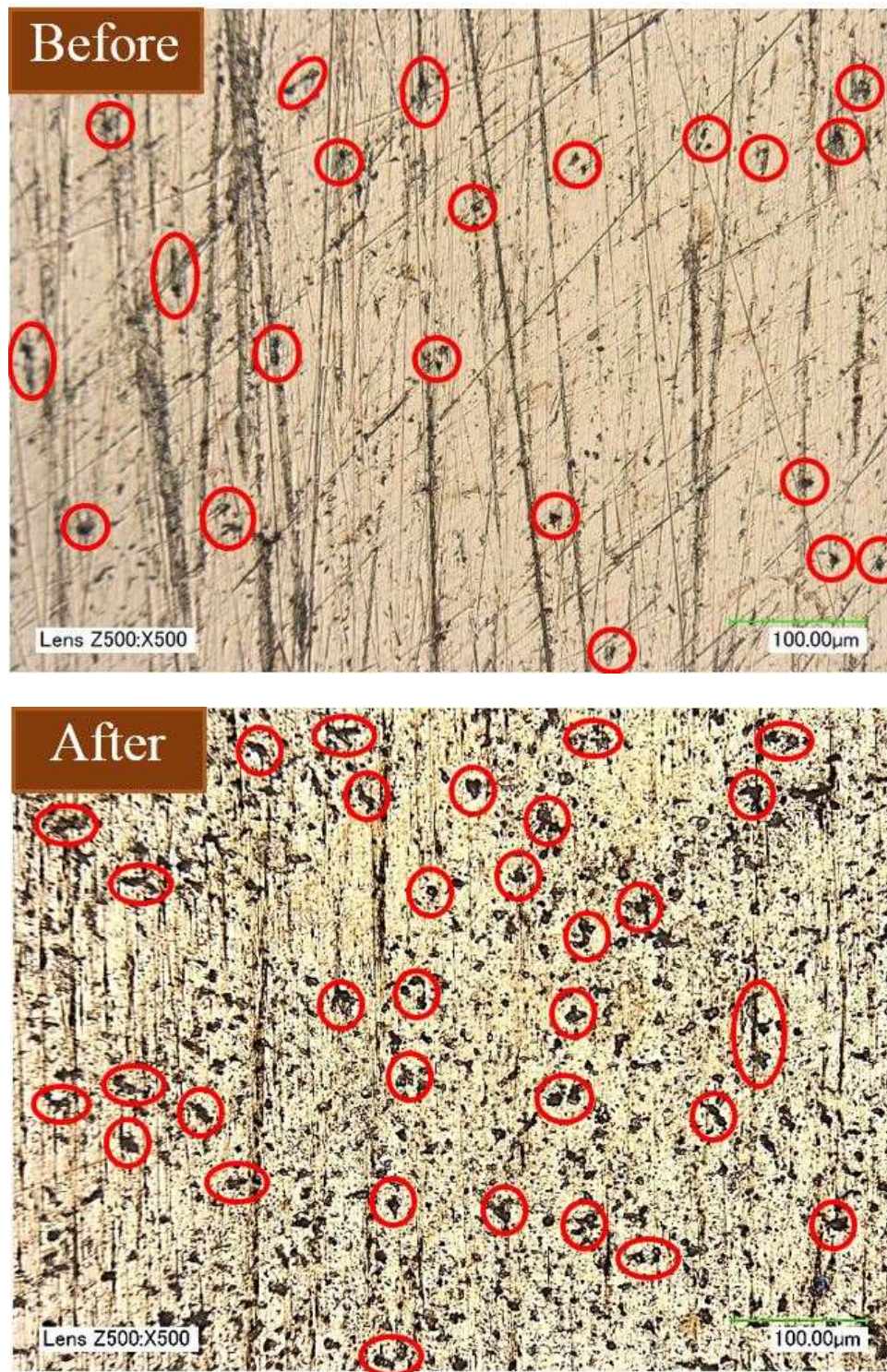


Figure 57: Optical microscopy images of alloy 110 copper before and after (112-hour) test with (reference fluid, without nanoparticles) distilled water (Magnification: 500X).

Figure 57 allows comparison of before- and after-test images with reference fluid of distilled water (Magnification: 500X), without nanoparticles. Before treatment some limited small pitting (on average 5 micrometer (200 microinches), circled in “before” image) and machining scratches were observed. After 112-hour treatment polishing scratches have not completely been removed but become shallow. Material has been removed around those before scratch in form of micro pitting and made those shallow. Previous small pitting (on average, smaller than 5 micrometers (200 microinches) become larger (to average of 15 to 20 micrometers (600 to 800 microinches), showing as circled darker clusters in after-test image). Widespread new small (on average 8 micrometer (300 microinches)) pitting is observed throughout the whole after image.

Figure 58 allows comparison of before- and after-test images with nanofluid of 2% alumina in distilled water (Magnification: 500X). After 112-hour treatment, all polishing scratches have been removed, and pre-existing pitting (circled in above Figure 58) became much larger. Some pitting seems to clusters around some previous pitting (before test pitting) and create some shallow spot on test specimen surface (marked in “after” image of figure 58).

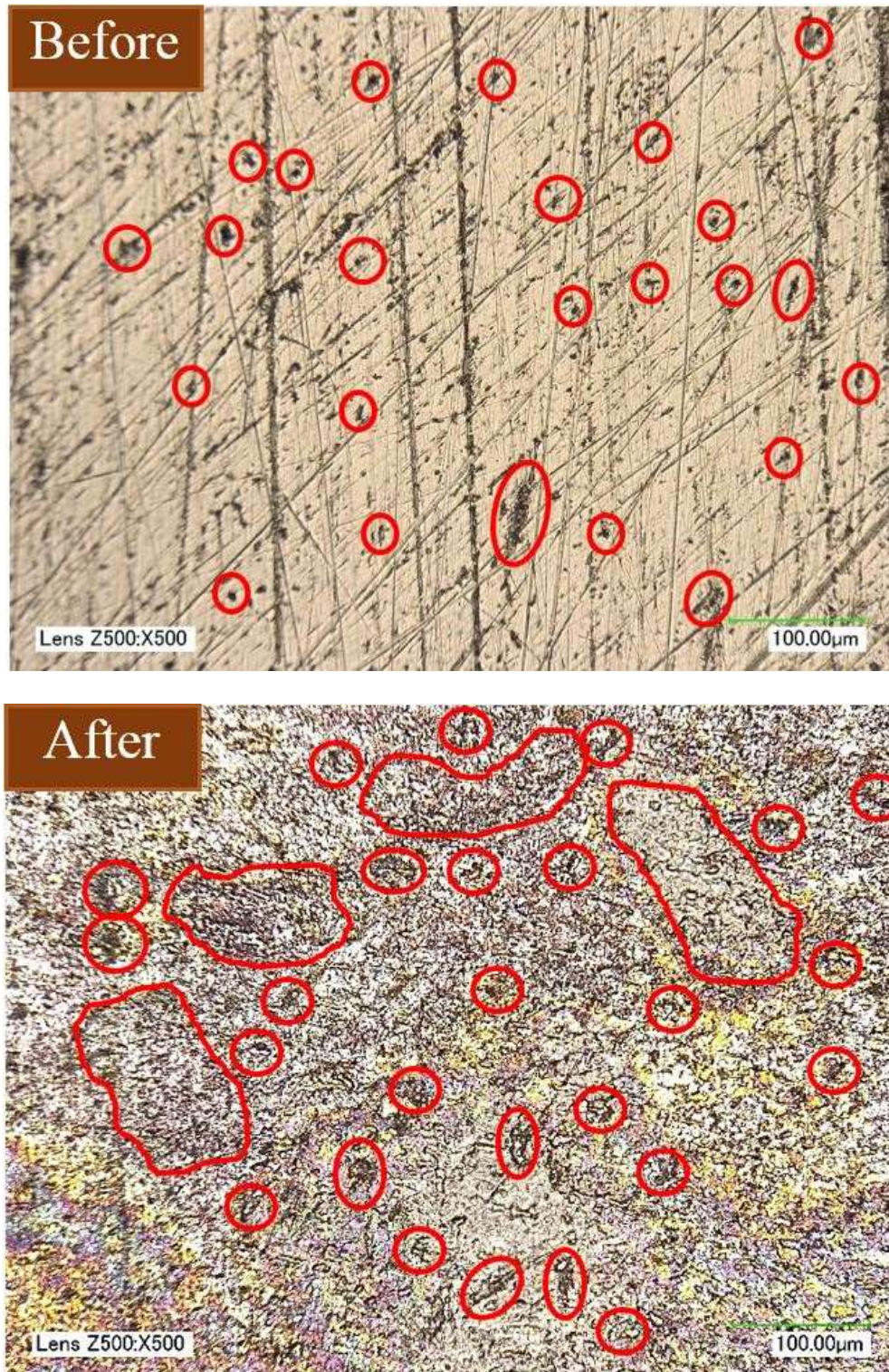


Figure 58: Optical microscopy images of alloy 110 copper before and after (112-hour) test with nanofluid of 2% alumina in distilled water (Magnification: 500X).

## 5.4 Test results for parallel flow treatments

Figure 59 presents the measured average Ra roughness for 3003-T3 aluminum specimens before and after 3, 7, 14, 28, 56 and 112 hour-treatments with the reference fluid of distilled water, and its nanofluid of 2%-volume of nano-alumina mixed in this reference fluid for 1 m/s flow parallel to the test specimen surfaces. Initial values (without treatment), are called “before test”, while values after each treatment are called “after test” in following graphs.

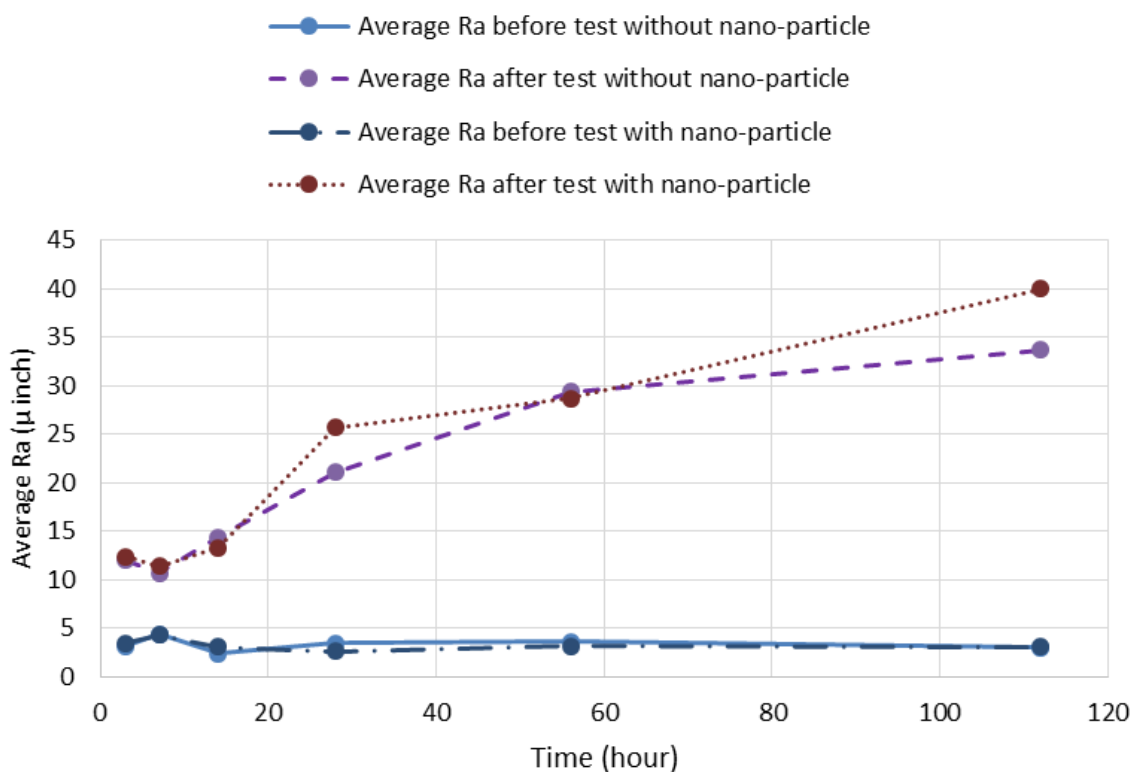


Figure 59. Average Ra roughness for 3003-T3 aluminum before and after 3, 7, 14, 28, 56 and 112 hour-treatments with the reference fluid distilled water and its nanofluid of 2% nano-alumina in reference fluid and parallel flow speed of 1 m/s.

The measurements presented in Figure 59 indicate that aluminum-specimen surface roughness is affected by the parallel flow of both the reference fluid (distilled water), and its 2%-alumina-nanofluid. For both fluid, initial (from 3 hour to 14 hour-test) Ra roughness values are not showing



any significant increase, while a monotonous increases after test from 28 hours to 112 hours of testing. Similar trends were observed for the two other measured roughness parameters, of Rq and Rz (presented in Appendix A) for both tested fluids.

Polishing of ductile materials as aluminum and copper cannot be controlled to obtain a single value of initial roughness but an interval of 2 to 4 microinch resulted in the low-range required for these tests. Therefore, there is a spread of initial values that was limited, after careful polishing, to 2 to 5 microinches (0.05 micrometer to 0.13 micrometer). To deal with the initial roughness spread within specimens presented in Figure 59 each of the Ra values was normalized and presented in Figure 60 for further analysis. Normalization of each after-test Ra-value was done by dividing it by the corresponding initial (before-test) Ra for the corresponding specimen.

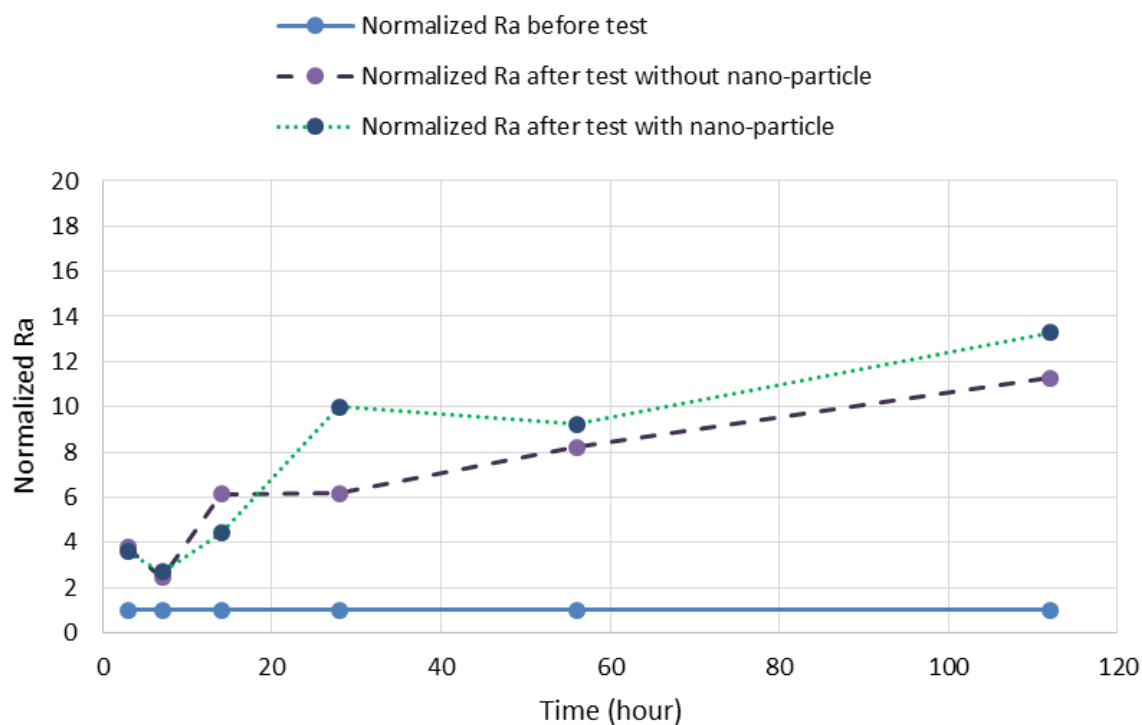


Figure 60. Normalized Ra roughness for 3003-T3 aluminum before and after 3, 7, 14, 28, 56 and 112 hour-treatments with the reference fluid of distilled water and its nanofluid of 2% nano-alumina in reference fluid and parallel flow speed of 1 m/s.

Figure 60 more clearly shows the same trends suggested by Figure 59. The normalized roughness values increase up to five-fold for the longest tested time of 112 hours as compared to initial ones. The evolution of roughness by parallel flow of both tested fluid shown in Figures 59 and 60 also suggests that some early cleaning of the surface may occur after tests from 3 hours to 14 hours tests (showing no significant increase of roughness in such interval), and that after 28 hours of test increased material erosion seems to proceed up to the 112 hours of maximum testing.

Figure 61 presents the average weight change for 3003-T3 aluminum in before and after 3, 7, 14, 28, 56 and 112 hours of parallel-flow treatments with the reference fluid of distilled water, and its nanofluid of 2% nano-alumina mixed in this reference fluid. No significant weight change (maximum change is 0.4 mg) was observed after test from 3 hours to 112 hours testing for both fluids.

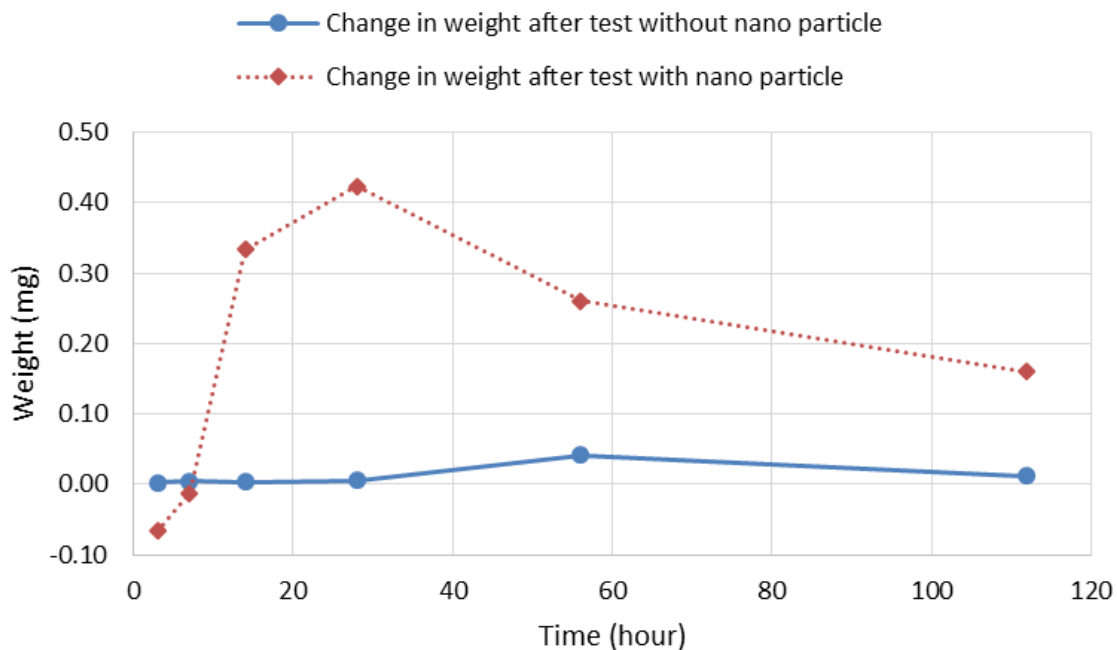


Figure 61. Average weight change for 3003-T3 aluminum in before and after 3, 7, 14, 28, 56 and 112 hour-treatments with the reference fluid of distilled water and its nanofluid of 2% nano-alumina in reference fluid and parallel flow speed of 1 m/s.

The measured roughness changes for aluminum samples suggest that significant surface modifications occur when tested fluid flow parallel to the test specimen surfaces. To study such modifications, optical microscopy was conducted for all the specimens after and before treatments. Figures 62 and 63 show microscopy images (for 500X magnification) for the aluminum specimens before and after parallel flow test for 112 hours with each corresponding fluid.

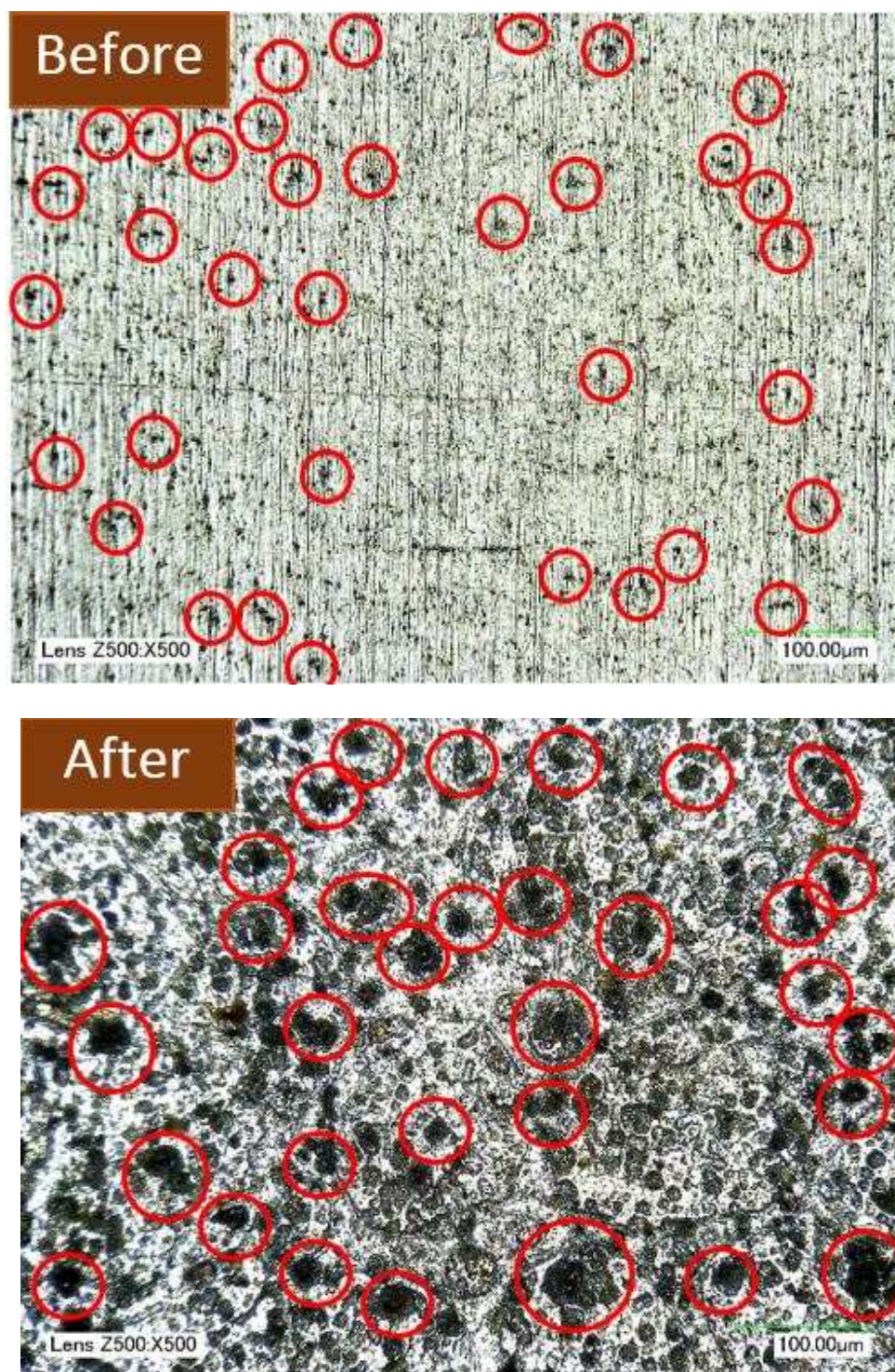


Figure 62: Optical microscopy images of 3003-T3 aluminum before and after (112-hour) test with reference fluid of distilled water (Magnification: 500X).

Figure 62 allows comparison of before- and after-test images (Magnification: 500X) with reference fluid (distilled water), without nanoparticles. After treatment, polishing scratches have been removed (after test of 112 hours), small pitting (on average, smaller than 4 micrometers (150 microinches) becomes larger (to average of 20 to 25 micrometers (800 to 1000 microinches), which are showed as circled darker clusters in after-test image); some observed features also suggest that some larger areas (of about 35 to 40 micrometers) may have started some splinting.

Figure 63 allows comparison of before- and after-test images with nanofluid of 2% alumina in distilled water (Magnification: 500X). After 112-hour treatment, polishing scratches have been removed, small pitting (on average, smaller than 4 micrometers (150 microinches) becomes much larger (to average of 60 to 80 micrometers (2400 to 3200 microinches), showing as circled darker clusters in after-test image) and some irregular shape shallow splinting has been started. Growth of smaller pitting by nanofluid flow is considerably larger as compared to those of reference fluid flow.

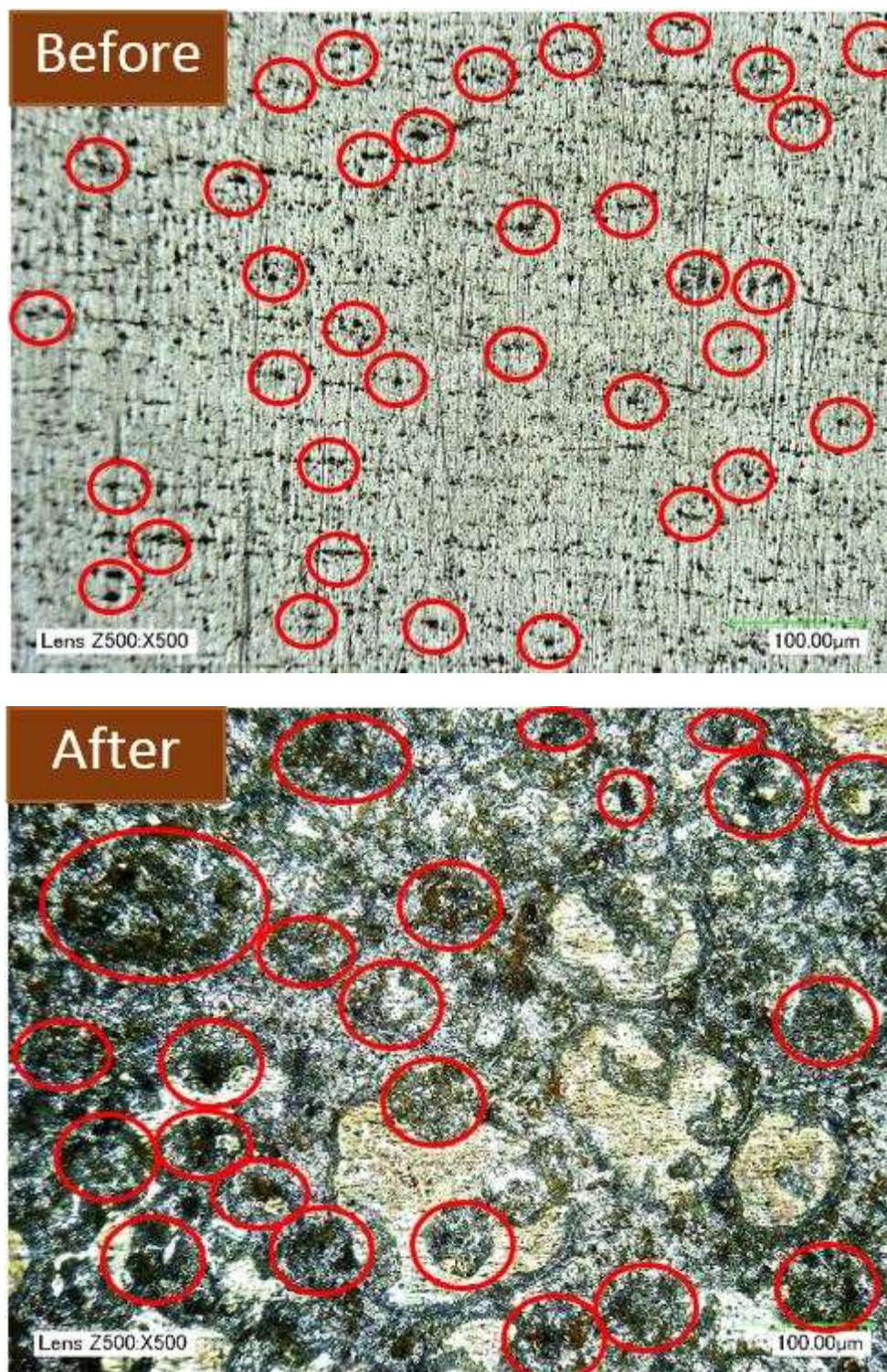


Figure 63: Optical microscopy images of 3003-T3 aluminum before and after (112-hour) test with reference fluid of distilled water (Magnification: 500X).

Same parallel flow treatments and subsequent measurements and analysis were carried out for copper alloy 110. Figure 64 presents the typically measured average Ra roughness for copper alloy 110 before and after 3, 7, 14, 28, 56 and 112 hour treatments with the reference fluid of distilled water, and a nanofluid of 2% volume of nano-alumina mixed in the reference fluid. Initial values (without treatment), are called “before test”, while values after each treatment are called “after test” in following graphs.

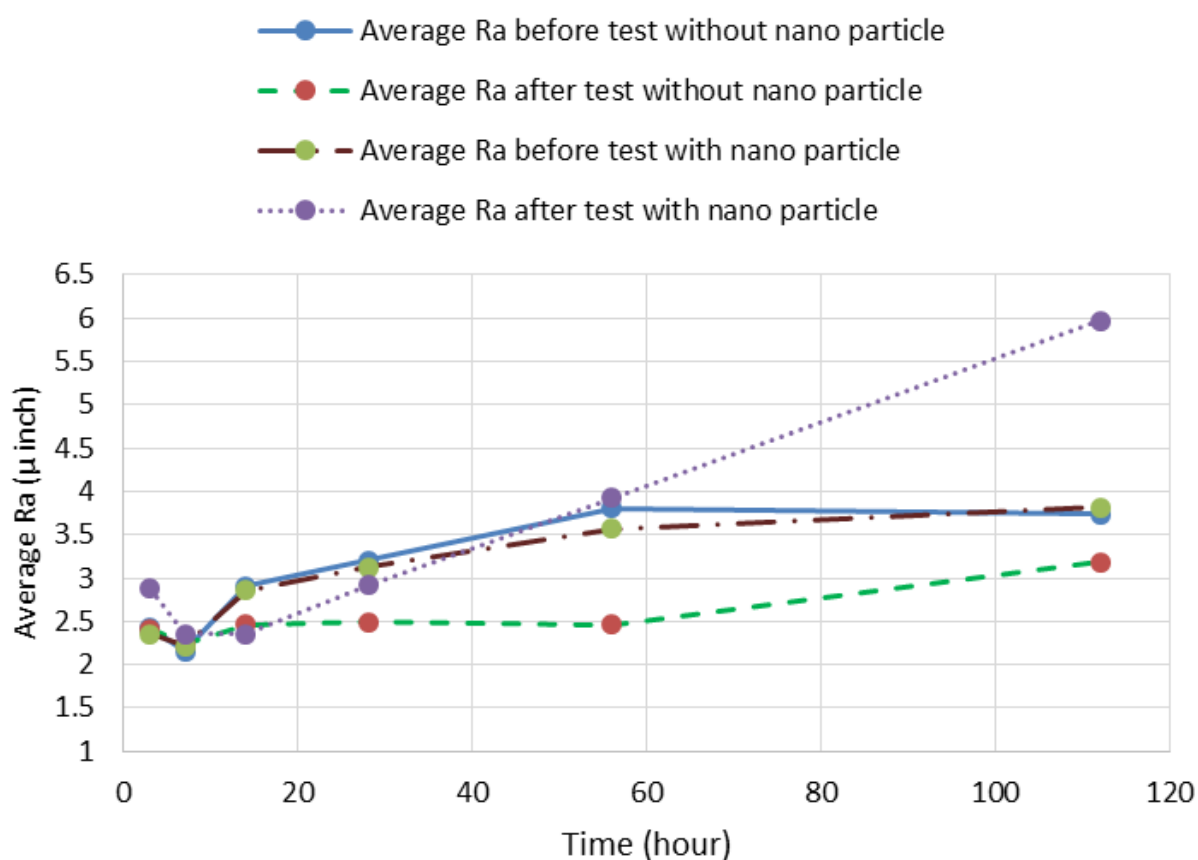


Figure 64. Average Ra roughness for copper alloy 110 before and after 3, 7, 14, 28, 56 and 112 hour-treatments with the reference fluid distilled water and its nanofluid of 2% nano-alumina in reference fluid and parallel flow speed of 1 m/s.

Since the initial roughness for each specimen presented in Figure 64 was within the 2 to 4 microinches (0.05 micrometer to 0.1 micrometer) range, each of the Ra values is normalized and

presented in Figure 65, where normalization of each after-test Ra-value was done as for data of Figure 60.

Figures 64 and 65 suggest that a minor surface modification (all roughness value differences were within 2 micro inch) were obtained when copper specimens were treated with 1 m/s flow parallel to the test specimen surfaces of reference fluid (distilled water) and its 2% nanofluid. For reference fluid, Ra roughness values shows no significant change but a minor decreases (all roughness value difference are within 1 micro inch) for all the testes. For nanofluid, Ra roughness shows an increased value for 3 hours test but decreased value after test from 7 hours to 14 hours of testing followed by a little increase after test from 28 hours to 112 hours. Measured Rq and Rz (presented in Appendix A) roughness showed similar trends.

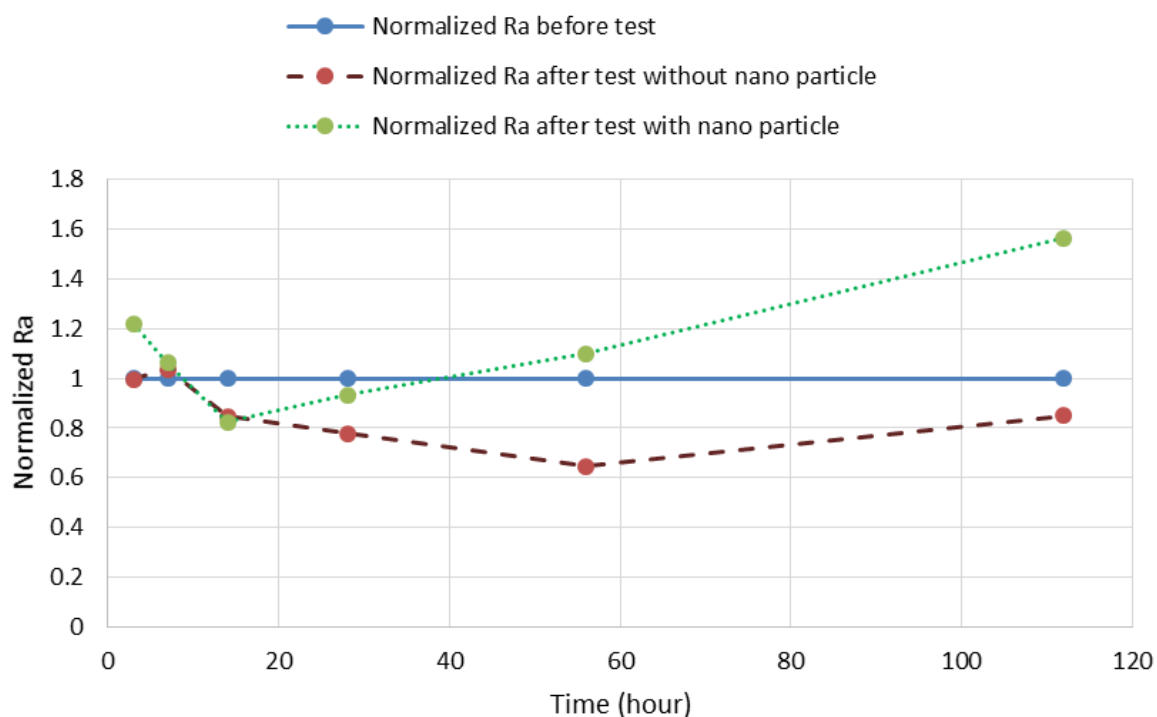


Figure 65. Normalized Ra roughness for alloy 110 copper before and after 3, 7, 14, 28, 56 and 112 hour-treatments with the reference fluid distilled water and its nanofluid of 2% nano-alumina in reference fluid and parallel flow speed of 1 m/s.



Weight measurements of before- and after-tests also were conducted to investigate possible material-removal effects by 1 m/s flow parallel to the test specimen surfaces. Figure 66 presents the measured change in weight for before and after 3, 7, 14, 28, 56 and 112 hour-treatments for alloy110 copper specimens with both reference fluid (distilled water) and nanofluid (2%-volume of nano-alumina mixed). Weight measurements of copper specimens found no significant weight change after 1 m/s flow parallel to the test specimen surfaces for the two tested fluids and times.

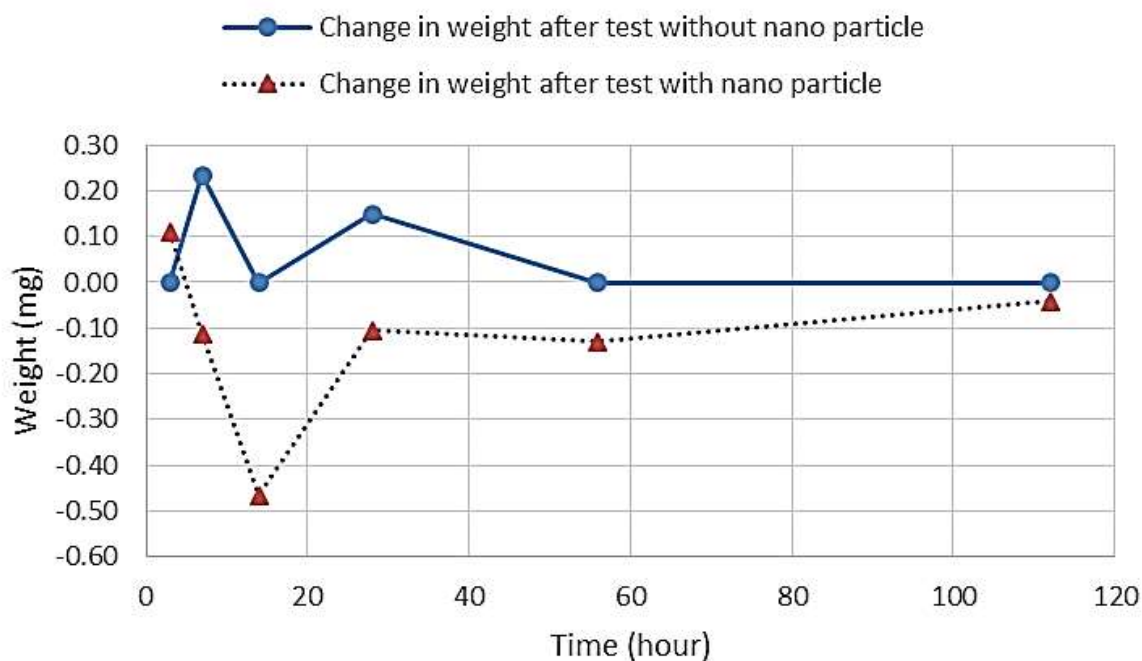


Figure 66. Average weight change for alloy110 copper in before and after 3, 7, 14, 28, 56 and 112 hour-treatments with the reference fluid distilled water and its nanofluid of 2% nano-alumina in reference fluid and parallel flow speed of 1 m/s.

To study possible modifications non-detected by roughness or weight measurements, optical microscopy was conducted for all the specimens after and before treatments. Figures 67 and 68 show microscopy images (for 500X magnification) for the copper specimens before and after parallel flow treatment with each corresponding fluid.

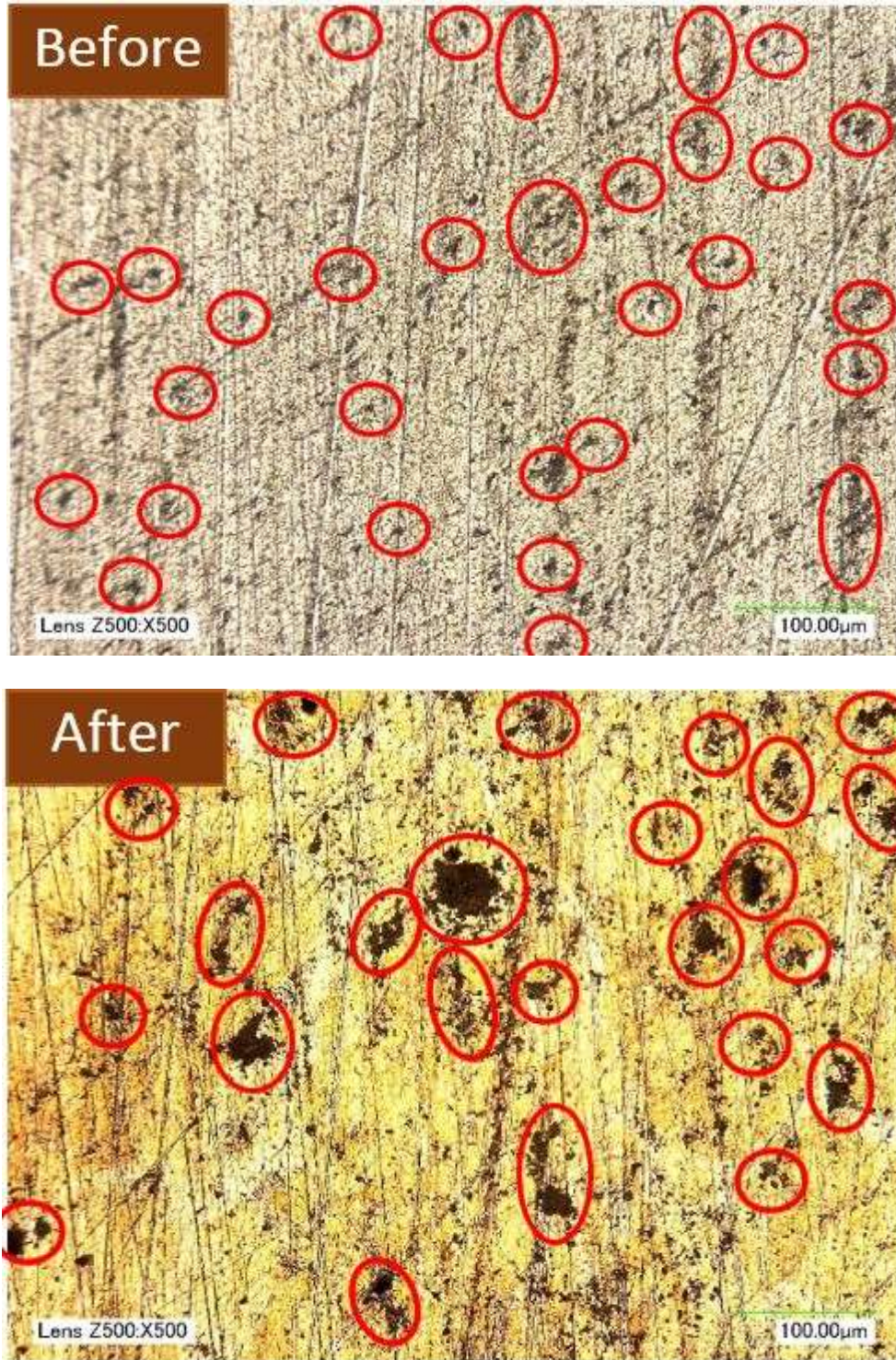


Figure 67. Optical microscopy images of alloy 110 copper before and after (112-hour) test with (reference fluid, without nanoparticles) distilled water (Magnification: 5000X). Pre-existing pitting and seemingly clustered ones after treatment are circled.

Figure 67 allows comparison of before- and after-test images with reference fluid of distilled water (Magnification: 500X), without nanoparticles. Before treatment some limited pitting (circled in “before” image) and some sharp machining scratches were observed. After 112-hour treatment small pitting (on average, smaller than 5 micrometers (200 microinches) becomes larger (to average of 30 to 35 micrometers (1200 to 1400 microinches), showing as circled clusters in after-test image). Polishing scratches have not been removed but become shallow. Some material have been removed around those scratches in form of micro pitting and made those shallow.

Figure 68 allows comparison of before- and after-test images with nanofluid of 2% alumina in distilled water (Magnification: 500X). After 112-hour treatment, pre-existing pitting (circled in before image Figure 68) became much larger and widespread. Some pitting seems to clusters (circled in after image Figure 68) along original scratching lines and around the previous pitting (before test pitting). Polishing scratches have not been removed but become shallow.

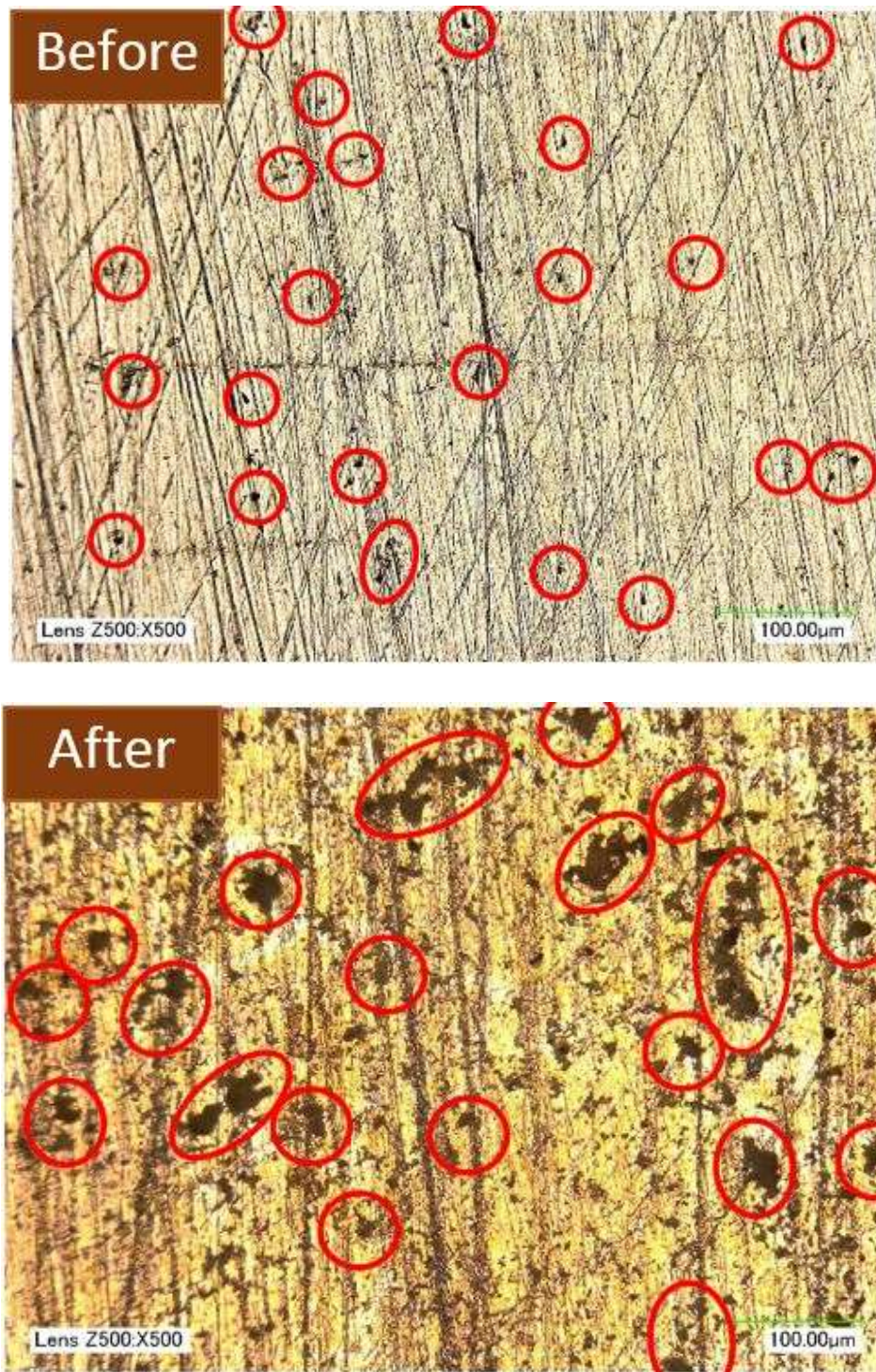


Figure 68. Optical microscopy images of alloy 110 copper before and after (112-hour) test with (reference fluid, without nanoparticles) distilled water (Magnification: 5000X). Pre-existing pitting and seemingly clustered ones after treatment are circled.

## CHAPTER 6

### 6 DISCUSSION

The main purpose of the research work reported in this thesis was to design, construct and develop new instruments for the experimental measurement of nanofluids effects when they interact with typical cooling-system materials, and to assess possible wear and erosion by nanofluids and prediction of such effects in cooling system materials. Development of instrument was presented in Chapter 3, test methodologies were introduced in Chapter 4, and experimental results were presented in Chapter 5.

#### 6.1 Discussion of instrument development

Two novel instruments have been designed and implemented to perform the investigations relevant to this work. A new multiple-nozzle test-rig has been designed to explore potential erosion effects of typical nanofluids suspensions impacted upon conventional cooling-system materials. A parallel-flow setup was also designed to replicate the typical flow in a fluid conduit system. The parallel flow setup was designed and developed to explore the possible erosion effects of typical nanofluids suspensions in such real fluid-conduit systems (e.g., a radiator/heat exchanger system). These prototype instruments can be implemented as adequate platforms for further development of standard test-rigs.

#### 6.2 Discussion of jet impingement instrument design and development

The designed, built and developed jet impingement instrument showed the feasibility of testing the surface modification effects of nanofluids by a jet impinged on flat specimen in the range of 3.5 m/s- and 15.5 m/s- jet speeds. The designed test rig showed to be appropriate to test the

tribological phenomenon for the required long test-times (up to 408 hours of test). Preliminary work related to this research method and instrument design was carried out by Molina et al [58]. They designed and fabricated a single nozzle test rig which allows controlled flow of a fluid jet, which impacts a material target (the test specimen). The nozzle to target distance and target angle can be set within wide ranges, while the nanofluid is recirculated by the instrument pump. The recirculation (gear) pump of their instrument yields a maximum volume flow of 2.1 liter/minute at nozzle velocity of 10.7 m/s.

Issues such as the long experiment times and the need to test higher and lower jet speeds, prompted the design and development of an ad-hoc methodology and suitable instruments to explore the possible erosion effects of typical nanofluids suspensions impacting on conventional cooling-system materials. The setup implemented in this work is capable of testing eight different samples simultaneously under various conditions. The main test chamber, pump-piping, sealing and sample holder were designed in such a way that, multiple identical fluid jets can be adjusted to allow simultaneous testing of different specimens., Parameters such as jet speed, jet length and impingement angle can be controlled while using a nominal amount of nanofluid. Features of this instrument are similar to those of an instrument recently presented by George et al [79] for their nanofluid tribology research but it is this thesis instrument that has better capacity.

Feasibility of using this instrument to assess erosion effect of nanofluid on typical cooling system material is in good agreement with the ASTM G76 - 07: standard test method [105], which concerns erosion tests by solid particle impingement using gas jets and covers testing of material loss by solid particle impingement with gas-carrier jet-type erosion equipment.

### **6.2.1 Discussion of parallel flow instrument design and development**

To explore the erosion effects of typical nanofluids suspensions in real fluid-conduit systems (e.g., a radiator/heat exchanger system) a parallel-flow setup was designed and developed where the cooling fluid flows parallel to the test sample inside a pipe. The designed, built and developed parallel-flow instrument showed the feasibility of testing the surface modification effects of nanofluids in fluid-conduit systems on flat specimen surfaces at  $0^0$  (parallel) to the flow. The designed test rig showed to be appropriate to test the tribological phenomenon for the required long test-times (up to 112 hours of test).

In the new test-rig, coolant flow is fed by an instrument pump and fluid flows parallel to the test sample length. A sample holder is used to hold the sample in coolant flow. An immersion heater was used for heating which has a built-in thermocouple and a regulator to maintain the desired fluid temperature. A relatively similar instrument was used by Celata et al [86, 87] called “HETNA” (Hydraulic Experiment on Thermo-mechanical of Nanofluid) to investigate and compare the erosion behavior of the nanofluid and the base fluid (without nanoparticles). HETNA was designed as two identical loops working simultaneously under the same conditions, one filled with the nanofluid and the other with base fluid (without nanoparticles). The advantage of this thesis work parallel-flow instrument over HETNA is that a large number of tests can be simultaneously carried out for different test lengths on different test specimens. This instrument can be a good testing analogy of real fluid conduit system (e.g., a radiator) to explore erosion behavior of nanofluid in a fluid-conduit systems. This parallel flow instrument shows some similarities to that of Peyghambarzadeh et al [43, 44] for nanofluid heat transfer. They used an actual car radiator as a cross flow heat exchanger which was a good testing analogy of real fluid conduit system (e.g., a radiator/heat exchanger), but the instrument of this

thesis work was designed with a focus on nanofluid erosion test and therefore, has better control of some parameters, as temperature, and facilities to accommodate material samples inside flow.

In following sections of this Chapter, the results will be discussed of using these two instruments (multiple nozzle jet impingement and parallel flow instrument) to test nanofluid interactions with material surfaces, and using roughness measurements, optical microscopy and weight measurement for assessing early surface changes.

### **6.3 Discussion of wear and erosion data for jet impingement tests**

The possible material surface modifications were presented in Chapter 5 of jet impingement (at 90° on test specimen surface) and parallel flow (at 0° with test specimen surface) on two typical heat exchanger materials- aluminum and copper, with conventional coolants (of 50% Ethylene Glycol in water, and distilled water), and the nanofluids obtained by adding of 2%-volume of nano-alumina mixed in the coolants. Possible surface erosion was quantified by measuring surface roughness and weight loss, and further qualitative analysis was performed by surface microscopy of the specimens before and after tests. The extensive data obtained by these exploratory tests was presented and plotted in Chapter 5. The following Tables 3 and 4 summarize the surface roughness modifications obtained by 3.5 m/s-10.7 m/s- and 15.5 m/s-jet impingement on the tested materials (aluminum and copper) with the tested fluids (50% Ethylene Glycol in water and distilled water and those of 2%-volume of nano-alumina nanofluids).



Table 3: Summary of surface roughness modifications when roughness values were compared for measurements before- and after- tests with a 3.5- m/s, 10.7- m/s and 15.5- m/s jet of reference fluid of distilled water, and of the nanofluid of 2% nano-alumina in reference fluid

Jet speed (m/s)	Initial roughness interval Ra ( $\mu$ inch)	Surface roughness changed after:			
		Aluminum was tested with:		Copper was tested with:	
		Reference fluid	Nanofluid	Reference fluid	Nanofluid
3.5	2 to 4	Slightly Changed	Significantly changed	Not changed	Slightly Changed
10.7	2 to 5	Slightly Changed	Significantly changed	Not changed	Slightly Changed
15.5	2 to 5	Significantly changed	Significantly higher changes than those from reference fluid testing	Not changed	Slightly Changed

Table 4: Summary of surface roughness modifications when roughness values were compared for measurements before- and after- tests with a 3.5- m/s, 10.7- m/s and 15.5- m/s jet of reference fluid of 50/50% Ethylene glycol in water, and of the nanofluid of 2% nano-alumina in reference fluid.

Jet speed (m/s)	Initial roughness interval Ra ( $\mu$ inch)	Surface roughness changed after:			
		Aluminum was tested with:		Copper was tested with:	
		Reference fluid	Nanofluid	Reference fluid	Nanofluid
3.5	2 to 5	Not changed	Not changed	Not changed	Not changed
10.7	2 to 7	Changed	Changed	Not changed	Not changed
15.5	2 to 5	No experiment conducted because of foaming problem (discussed in section 6.3.3).			

For low speed (3.5 m/s) jet-test of reference fluid of distilled water and its 2% nanofluid the results indicate that nanofluids may lead to higher roughness-value modification effects than those produced by reference fluid at same speed, for the two tested materials (aluminum and copper). However, 3.5 m/s jet test of reference of 50/50 ethylene glycol/water and its 2% nanofluid did not produce any significant surface modification for both tested materials. The tests for 10.7 m/s and 15.5 m/s jet test of reference fluid of distilled water and its 2% nanofluid also show that nanofluid lead to higher roughness-value modification effects than those

produced by its reference fluid on the two tested materials (aluminum and copper). Similar trends were found in Celata et al [86, 87] research by profilometer scanning; they reported some significant increase (of about three hundred times) of nanofluid-lead modification (as compare to those from reference fluid of distilled water) on aluminum targets for 9% concentration of TiO<sub>2</sub>, Al<sub>2</sub>O<sub>3</sub>, and ZrO<sub>2</sub> nanofluids, and for copper only in the case of ZrO<sub>2</sub> nanofluid. All these research results for 10.7 m/s jet test of reference fluid of 50/50 ethylene glycol/water and its 2% nanofluid, which suggest no effect of nanofluid on surface-roughness modification for both tested materials, are in good agreement with the findings of D. Singh's nanofluid research [85] at US Dept. of Energy facilities.

### **6.3.1 Discussion of surface roughness, weight measurement data and image analysis of 3.5 m/s jet impingement tests**

After the carried-out 3, 7, 14, 28, 56, 112, 240, 312 and 408 hours of 3.5m/s-jet impingement tests with distilled water and its 2% nanofluid, the measured roughness parameters (Ra, Rq and Rz) revealed significant changes of roughness for the tested materials (aluminum and copper) or fluids (presented in section 5.1.1). No significant changes of specimen-weight were measured, however, for any of the tested materials and fluids.

The trends suggested by the roughness increases (particularly for the longest tested times of 408 hours) were reflected by the substantial surface modifications observed by optical microscopy images (for 500x magnification). Table 5 summarizes the surface modifications observed by image analysis (presented in section 5.1.1) before- and after-408-hour-testing with both fluids (reference fluid and its 2%-alumina nanofluid) on both tested materials (aluminum and copper).

Table 5: Summary of main surface modifications when comparing microscopy images before- and after-408 hours of testing with a 3.5m/s jet of reference fluid of distilled water, and of nanofluid of 2% nano-alumina in reference fluid

Surface texture	When aluminum was tested		When copper was tested	
	With reference fluid	With nanofluid	With reference fluid	With nanofluid
Initial scratches	Removed	Removed	Partially removed	Removed
Initial pitting	Enlarged	Enlarged and deeper	Enlarged	Enlarged and widespread

Table 5 shows that initial scratches from pre-test specimen-polishing were removed, but the depth of scratch removal seems to depend on both the used fluid and the impacted material; it may be possible that the combination of both factors would lead to different nascent modifications, but further research is needed to understand the scratch removal mechanisms. Pre-test slight initial-pitting becomes enlarged for the two-tested fluids and materials, but nanofluid increases the depth of pitting in aluminum, while development of widespread small surface-pitting occur for copper for the nanofluid test.

These results suggest that 2% alumina nanofluid in distilled water produces more surface modification effects than those from its reference fluid (distilled water) for the 3.5 m/s speed jet impingement in the tested times. It is also shown that aluminum is a more likely to be eroded material than copper for the conducted jet impingement tests, times and speeds.

After 3, 7, 14, 28, 56, 112, 240, 312 and 408 hours of 3.5m/s-jet impingement tests with 50/50 Ethylene Glycol/Water and its 2% alumina nanofluid, the measured roughness parameters (Ra, Rq and Rz) did not produce any significant changes of roughness for the tested materials (aluminum and copper) or fluids (presented in section 5.1.2). No significant changes of

specimen-weight were measured, however, for any of the tested materials and fluids. These results suggest that some nascent surface modifications started to occur for the low-speed jet impingement in the investigated tested times.

Measured roughness increases (particularly for the longest tested times of 408 hours) were reflected by the substantial surface modifications observed by optical microscopy images (for 5000x magnification). Table 6 summarizes the surface modifications observed by image analysis (presented in section 5.1.2) before- and after-408-hour-testing with both fluids (reference fluid and its 2%-alumina nanofluid) on both tested materials (aluminum and copper).

Table 6: Summary of surface modifications when comparing microscopy images before- and after-408 hours of testing with a 3.5m/s jet of reference fluid of 50/50% Ethylene Glycol in water, and of nanofluid of 2% nano-alumina in reference fluid

Surface texture	When aluminum was tested		When copper was tested	
	With reference fluid	With nanofluid	With reference fluid	With nanofluid
Initial scratches	Partially removed	Mostly removed	Mostly removed	Partially removed
Initial pitting	Enlarged	Enlarged and widespread	Not enlarged but widespread	Enlarged and widespread

Table 6 shows that initial scratches from pre-test specimen-polishing were removed, but the depth of scratch removal seems to depend on both the used fluid and the impacted material; it may be possible that the combination of both factors would lead to different nascent modifications, but further research is needed to understand the scratch removal mechanisms. Pre-test slight initial pitting becomes enlarged for the two-tested fluids in aluminum, but reference fluid does not seem to enlarge pitting in copper, while development of widespread small surface-pitting occur for copper for the two-tested fluids, but not for aluminum for

reference fluid; in general the tested nanofluid seems to lead to stronger pitting than the reference 50/50%-Ehtylene Glycol/water.

### 6.3.2 Discussion of surface roughness, weight measurement data and image analysis of 10.7 m/s jet impingement tests

After the 3, 7, 14, 28, 56 and 112 hours of 10.7 m/s-jet impingement tests with distilled water and its 2% nanofluid, the measured roughness parameters ( $R_a$ ,  $R_q$  and  $R_z$ ) revealed a significant changes of roughness for the tested materials (aluminum and copper) or fluids (presented in section 5.2.1). No significant changes of specimen-weight were measured, however, for any of the tested materials and fluids.

Measured roughness increases (particularly for the longest tested times of 112 hours) were reflected by the substantial surface modifications observed by optical microscopy images (for 500x magnification). Table 7 summarizes the surface modifications observed by image analysis (presented in section 5.2.1) before- and after-112-hour-testing with both fluids (reference fluid and its 2%-alumina nanofluid) on both tested materials (aluminum and copper).

Table 7: Summary of main surface modifications when comparing microscopy images before- and after-112 hours of testing with a 10.7 m/s jet of reference fluid of distilled water, and of nanofluid of 2% nano-alumina in reference fluid

Surface texture	When aluminum was tested		When copper was tested	
	With reference fluid	With nanofluid	With reference fluid	With nanofluid
Initial scratches	Removed	Removed	Partially removed	Partially removed
Initial pitting	Enlarged and deeper	Enlarged and widespread	Not enlarged but widespread	Enlarged and widespread

Table 7 shows that initial scratches from pre-test specimen-polishing were removed, but the depth of scratch removal seems to depend on the impacted material. For both fluid tests on aluminum all scratches have been removed but for similar tests on copper, scratches were removed partially. Pre-test slight initial pitting becomes enlarged for both fluids treatment on aluminum and for nanofluid treatment on copper. Initial pitting widespread for both fluids treatment on copper and for nanofluid treatment on aluminum. But reference fluid treatment on aluminum increases the depth of initial pitting as well as make it enlarged.

These results suggest that 2 % alumina nanofluid in distilled water have more surface modification effect than its reference fluid (distilled water) for the 10.7 m/s speed jet impingement for the tested times and aluminum is more likely erosive cooling system material than copper for those jet impingement tests.

Jet impingement tests were carried out for 3, 7, 14, 28, 56 and 112 hours with 10.7 m/s jet with 50/50 Ethylene Glycol/Water and its 2% alumina nanofluid. Similar increasing roughness change trend has been observed for two tested fluids on aluminum. No significant roughness changes were found for 3- to 112- hour interval of jet impingement tests on copper with both reference fluid (ethylene glycol/water) and its nanofluid.

The trends suggested by the roughness increases (particularly for the longest tested times of 112 hours) were reflected by the substantial surface modifications observed by optical microscopy images (for 5000x magnification). Table 8 summarizes the surface modifications observed by image analysis (presented in section 5.2.2) before- and after-112-hour-testing with both fluids (reference fluid and its 2%-alumina nanofluid) on both tested materials (aluminum and copper).

Table 8: Summary of surface modifications when comparing microscopy images before- and after-112 hours of testing with a 10.7 m/s jet of reference fluid of 50/50% Ehtylene Glycol in water, and of nanofluid of 2% nano-alumina in reference fluid

Surface texture	When aluminum was tested		When copper was tested	
	With reference fluid	With nanofluid	With reference fluid	With nanofluid
Initial scratches	Removed	Partially removed	Partially removed	Not removed
Initial pitting	Enlarged	Enlarged and widespread	Not enlarged but widespread	Enlarged

Table 8 summarizes the possible surface modifications observed by microscopy imaging for tests. Optical microscopy imaging (magnification 5000x) showed different surface-modification mechanisms: while reference fluid completely removed polishing scratches and enlarged original small pitting for the 112-hour test on aluminum, the 2%-alumina-nanofluid did not completely remove polishing scratches and it led to enlarged and widespread small pitting, which seems to cluster along some original scratching lines. For reference fluid test on copper, initial scratches has been removed partially and initial pitting did not enlarged but widespread. For nanofluid test on copper, initial scratches have not been removed and initial pitting became enlarged but was not widespread.

### 6.3.3 Discussion of surface roughness, weight measurement data and image analysis of 15.5 m/s jet impingement tests

Another set of tests was carried out for 3, 7, 14, 28, 56 and 112 hours with 15.5 m/s-jet impingement with distilled water, and with its 2% nanofluid. The measured roughness parameters ( $R_a$ ,  $R_q$  and  $R_z$ ) revealed a significant changes of roughness for the tested materials (aluminum and copper) or fluids (presented in section 5.3.1). For both materials, after 112 hours of test, nanofluid treatment shows higher surface roughness change than its reference

fluid. No significant changes of specimen-weight were measured, however, for any of the tested materials and fluids.

The trends suggested by the roughness increases (particularly for the longest tested times of 112 hours) were reflected by the substantial surface modifications observed by optical microscopy images (for 500x magnification). Table 9 summarizes the surface modifications observed by image analysis (presented in section 5.3.1) before- and after-112-hour-testing with both fluids (reference fluid and its 2%-alumina nanofluid) on both tested materials (aluminum and copper)

Table 9: Summary of surface modifications when comparing microscopy images before- and after-112 hours of testing with a 15.5 m/s jet of reference fluid of distilled water, and of nanofluid of 2% nano-alumina in reference fluid

Surface texture	When aluminum was tested		When copper was tested	
	With reference fluid	With nanofluid	With reference fluid	With nanofluid
Initial scratches	Removed	Removed	Partially removed	Removed
Initial pitting	Enlarged	Enlarged and widespread	Enlarged and widespread	Enlarged and widespread

Table 9 summarizes different surface-modification mechanisms: while initial polishing scratches were completely removed by both fluids test on aluminum. For the test on copper, initial polishing scratches were completely removed by nanofluid test but partially removed by reference fluid test. Pre-test initial micro pitting becomes enlarged for the two-tested fluids and materials. Pitting were widespread for both fluids test on copper but pitting were widespread for only nanofluid test on aluminum.



These results suggest that 2 % alumina nanofluid in distilled water produces deeper surface modification effects than those from its reference fluid (distilled water) for the 15.5 m/s speed jet impingement for the tested times, and that aluminum is more easily eroded cooling-system material than copper for those jet impingement tests.

Jet impingement tests of 15.5 m/s jet with 50/50% Ethylene Glycol/water and its 2% alumina nanofluid was not completed because of some practical problems. Excessive foam generation was the main problem for this set of experiments. Figure 69 shows a picture of the foaming conditions for 15.5 m/s jet impingement tests with reference fluid of 50/50% Ethylene Glycol/water and its 2% alumina nanofluid. Foam was formed by trapping pockets of air/gas in tested liquid. Three inches of foam layer were created inside the main chamber within just 30 minutes of 15.5 m/s jet impingement of reference fluid (50/50% Ethylene Glycol/water) test. For nanofluid (2% nano-alumina in 50/50% Ethylene Glycol/water) test same amount of foam was created within 20 minutes of test.



Figure 69. Foam produced in jet impingement test of a) reference fluid of 50/50% Ethylene Glycol/water and b) its 2% alumina nanofluid.

In most foams produced in reference fluid (50/50% Ethylene Glycol/water) jet test, the volume of trapped air/gas is large with thin films of liquid separating the regions of gas. Smaller size foams (as compare to reference fluid foam) were produced in nanofluid (2% nano-alumina in

50/50% Ethylene Glycol/water) jet tests in same conditions of tests. In atmospheric condition, it takes five hours for natural dissolving of all foams created during 30 minutes of reference fluid test, and it was observed that after twelve hours foams created by 20 minutes nanofluid test were not fully dissolved.

The foaming production with 50% Ethylene Glycol in water-alumina nanofluid is not likely to occur in actual cooling systems, in which flow speeds are much smaller than the used 15.5 m/s jet-speed. But this foaming problem clearly set a practical limit to the use of jet-impingement test at speeds of 15.5 m/s and higher, at least for some nanofluids.

#### **6.4 Discussion of surface roughness, weight measurement data and image analysis of parallel flow tests**

In parallel flow tests a set of test was carried out for 3, 7, 14, 28, 56 and 112 hours with 1 m/s flow of reference fluid of distilled water and its 2% nanofluid. The measured roughness parameters (Ra, Rq and Rz) revealed significant changes of roughness for the two tested fluid on aluminum (presented in section 5.4.1). Tests on aluminum samples shows similar increasing trend of roughness change for both reference fluid (distilled water) and its 2% nanofluid after test from 7 hours to 112 hours. No significant changes of specimen-weight (all weight changes were within 0.5 mg) were measured, however, for any of the tested materials and fluids.

The trends suggested by the roughness increases (particularly for the longest tested times of 112 hours) were reflected by the substantial surface modifications observed by optical microscopy images (for 500x magnification). Table 10 summarizes the surface modifications observed by image analysis (presented in section 5.4.1) before- and after-112-hour-testing with

both fluids (reference fluid and its 2%-alumina nanofluid) on both tested materials (aluminum and copper)

Table 10: Summary of surface modifications when comparing microscopy images before- and after-112 hours of testing with a 15.5 m/s jet of reference fluid of distilled water, and of nanofluid of 2% nano-alumina in reference fluid

Surface texture	When aluminum was tested		When copper was tested	
	With reference fluid	With nanofluid	With reference fluid	With nanofluid
Initial scratches	Removed	Removed	Not removed	Not Removed
Initial pitting	Enlarged and widespread	Enlarged and widespread	Enlarged	Enlarged

Table 10 shows different surface-modification mechanisms: while initial polishing scratches were completely removed by both fluids test on aluminum. For the test on copper, initial polishing scratches were not removed by two tested fluid. Pre-test initial micro pitting becomes enlarged for the two-tested fluids and materials. Pitting were widespreded for both fluids test on aluminum.

These results suggest that reference fluid of distilled water and its 2 % alumina nanofluid have similar surface modification effect for 1 m/s speed parallel flow tests for the tested times on aluminum and no surface roughness modification has been found by those tests on copper samples.

## CHAPTER 7

### 7 CONCLUSIONS

#### 7.1 Conclusions

A main purpose of this research was to establish a methodology for testing and evaluating surface-change phenomena by nanofluid interaction with cooling system material and to design, construct and develop instruments for such purpose. Two new test-rigs were designed and developed: a multiple nozzle jet impingement test rig and a parallel flow test rig. Appropriate experimental techniques, which accounted for assessment of the wear effects of fluid jet impact on material surface and of parallel flow effect on fluid-conduit walls, were also designed and developed.

These instruments and corresponding methodology were employed for experimental measurement of possible material surface modification by jet impingement (at  $90^\circ$  to test specimen surface) and parallel flow (at  $0^\circ$  with test specimen surface) on typical heat exchanger materials (aluminum and copper) with conventional coolant (of 50% Ethylene Glycol in water and distilled water), and those of nanofluids of 2%-volume of nano-alumina mixed in the coolant. The possible surface erosion effects were quantified by measuring surface roughness and weight loss, and further analysis was performed by surface microscopy of specimens before and after carrying out the specified tests. In this chapter, conclusions from the design and development of the new instrument are presented. Also, main conclusions from the surface modification measurements of Chapter 5 and the discussions of Chapter 6 are included.

Addition of solid particles in flowing fluids is known to lead to higher erosion rates on conduit materials, but the effect of adding very small size of the nanoparticles (1nm-100nm) and their

small volumetric fraction in the suspension, negligible secondary effects were expected. It is hypothesized that – since alumina (nanoparticle used in this research) is fairly chemically inert, and based on the smaller momentum transferred by the particles to the fluid conduit walls, material removal in early surface-modifying mechanism is a mainly mechanical process (such as erosion and abrasion). No noticeable experimental investigations have been carried out on this topic so far, and data available in the literature is insufficient (as discussed in Chapter 2).

It is concluded that new experimental systems of jet impingement and parallel flow testing were required to assess the possible surface modification when nanofluids are set in contact with typical cooling-system materials. The newly designed systems allow multiple identical fluid jets to facilitate simultaneous testing of different specimens, jet lengths, speeds and impingement angles. Both jet impingement and parallel systems allow multiple velocity stages of fluid flow. The sample holder is able to hold multiple test specimens. The systems also allows testing at different temperatures of working fluid.

Methodologies and required instruments found by literature review of these topics [58-60, 79, 86-90, 106] were inadequate for the purposes of this research, due to the lack of essential features, such as – inadequate number of identical fluid jets, jet speed staging, variable jet angle and temperature variability of circulating fluid. The previous instrument design of Molina et al [58] showed some operational limits. For instance, smaller size of main chamber and reservoir tank of the preliminary setup limited the capacity of circulating fluid, and the single nozzle prevented simultaneous tests. It was concluded that a new jet impingement instrument with higher capacities in all features was required for this nanofluid tribology research. Also, a new type of experimental

setup, named parallel flow setup, was required to replicate the typical fluid flow in a fluid conduit system (e.g. a radiator or heat exchanger).

Two new tests rigs were designed and developed: a multiple nozzle test rig and a parallel flow test rig. Appropriate experimental techniques were also designed and developed to explore the feasibility of employing fluid jet impact and parallel flow on material surface, and of using roughness and wear measurement for assessing the possible surface changes. The instruments proved appropriate to investigate tribological effects of nanofluid interaction with typical cooling system materials. In particular, assessment of possible surface changes (which may precede erosion and abrasion) by the developed instruments and by roughness measurements of Ra, Rq and Rz seems to be a suitable technique. This prototype instruments can be an adequate platforms for further development of a standard test rigs.

Tests were carried out of jet impingement (at 90° on test specimen surface) and parallel flow (at 0° with test specimen surface) on typical heat exchanger materials (aluminum and copper) with conventional coolant (of 50% Ethylene Glycol in water and distilled water), and those of nanofluids of 2%-volume of nano-alumina mixed in the coolant. The possible surface erosions were quantified by measuring surface roughness and weight loss, and further analysis was performed by surface microscopy of specimens before and after tests.

For all sets of jet impingement and parallel flow tests, surface change measurements suggest that, the material removal rate is mostly dependent on impacted fluid, fluid jet speed and on impacted material. These findings reasonably agreed with the recent research [79, 80, and 89] findings.

Alumina nanoparticle of 2% volume suspension in typical coolant of 50% Ethylene Glycol in water and in distilled water have shown significant wear effects on aluminum surface for both jet impingement and parallel flow tests as compare to those of base fluid tests. For copper, no significant wear effect has been found by adding 2% volume of alumina nanoparticle in typical coolant of 50% Ethylene Glycol in water and distilled water for both jet impingement and parallel flow tests as compared to those of base fluid tests. These findings suggest that, aluminum is more likely to be eroded than copper for the conducted tests.

Distilled water as cooling fluid was shown to be a more erosive fluid than 50% Ethylene Glycol in water for two tested materials and fluids. For each set of test at same jet speed, tests with distilled water as reference fluid showed higher surface modification effect than those from 50% Ethylene Glycol in water as reference fluid, as confirmed from roughness measurements ( $R_a$ ,  $R_q$  and  $R_z$ ) and microscopy image analysis (initial pitting and surface texture change), conducted for both reference fluid and 2% alumina nanofluid. Nanofluid of 2% alumina in distilled water showed significantly higher surface changes than its reference fluid (distilled water) in each set of tests but these effects were not significant when 2% alumina was added in 50/50 Ethylene Glycol/water and utilized for the same set of tests. Parallel flow tests were carried out for only reference fluid of distilled water and its 2% alumina nanofluid at 90°C and showed significantly higher material surface modification effect (by surface roughness measurement and microscopy imaging) of nanofluid than its reference fluid.

Jet speed has shown significant effects on surface modifications for all tested fluids and materials. Faster surface modifications occurred with higher jet speed tests. Longer tests of lower jet speed shows equivalent surface modifications as compared to shorter tests of higher jet speed by





Figure 70: Normalized Ra roughness for 3003-T3 aluminum before and after 3, 7, 14, 28, 56, 112, 240, 312 and 408 hour-treatments with 3.5 m/s jet, and for 3, 7, 14, 28, 56 and 112 hour-treatments with 10.7 m/s and 15.5 m/s jet. All sets of data obtained for the reference fluid of distilled water, and for nanofluid of 2% nano-alumina in reference fluid.

The data comparison of Figure 70 shows that jet-speed has a substantial effect on the roughness modifications of aluminum surfaces by jet-impingement for the two tested fluids. In order to assess the effects of Ra roughness of the test factors jet speed and test-time, the plot of Figure 70 shows for one chosen value of Ra roughness, the corresponding test time required for the three used jet-speeds. Tests with 2% alumina nanoparticles in distilled water for 3.5 m/s, 10.7 m/s and 15.5 m/s jet speed took respectively 180 hours, 112 hours and 75 hours of tests respectively for increases of Ra roughness of 12 times from its initial Ra roughness value (corresponding changes also observed for Rq and Rz). Tests with reference fluid of distilled water for 3.5 m/s, 10.7 m/s and 15.5 m/s jet speed took 260 hours, 112 hours and 85 hours of tests respectively for increase of Ra roughness of 6 times of its initial Ra roughness value (corresponding changes also observed for Rq and Rz). Similar comparisons were formulated using microscopy image analysis. Further research is required to confirm those findings by repeating the specified tests. Safaei et al [90] also reached a similar conclusion in their work on a computational simulation of erosion effects of nanofluids. They concluded that, the erosion rate is directly dependent on particle size and volume fraction as well as flow velocity inside of a 90° elbow for two-phase (solid and liquid) turbulent flow.

Since alumina is fairly chemically inert, material removal in this early surface-modifying mechanism in aluminum and copper surfaces should be attributed to mainly mild abrasion mechanisms, with no significant chemical erosion component. These mechanisms are in good agreement with the findings of George et al. [79], which were obtained for titanium-dioxide nanofluid jet-impinged on aluminum. Further research by altering the experimental factors (jet

speed steps, test lengths), are needed to confirm the actual surface modification mechanism in real heat exchanger systems.

Roughness change measurements, weight losses and optical microscopy imaging and profilometry were proven as adequate methods to assess the effects of nanofluids on material surface when nanofluids are set in contact with typical cooling-system materials. Roughness changes (roughness measurement of Ra, Rq and Rz) and microscopy image analysis (initial pitting and surface texture change) show all possible surface modifications in all set of jet impingement and parallel flow tests but weight losses and optical profilometry did not show any significant difference in those tests. Weight measurement and optical profilometry are useful in the measurement of surface modification for higher speed (higher than the maximum speed test of 15.5 m/s) and longer length (longer than the maximum test length of 408 hours) jet impingement and parallel flow tests.

The author is aware of the possible roles of many factors, not yet considered in this work, in the erosion by typical nanofluid-coolants, and that they will require further research, They are, for instance, material properties (i.e., hardness), nanopowder properties (i.e., particle size, nanopowder hardness as compared to that of impacted surface, and particle agglomeration and attachment to surfaces), and cooling system parameters (i.e., effects of material heating and cooling in actual heat-exchanger systems).

These instruments proved appropriate to investigate tribological effects of nanofluid interaction with typical cooling system materials. In particular, assessment of possible surface changes (which may precede erosion) by the developed instrument and by roughness measurements of Ra, Rq and Rz, weight loss measurement, microscopy image analysis and microscopy profilometry seems to

be suitable techniques. These prototype instruments are suitable platform for further research and development of a standard test rig.

## **7.2 Recommendations for future research**

This thesis presents research to establish methodologies for testing and evaluating surface-change by nanofluid impact. The work is presented on development of novel test rigs and testing methodologies, and on the use of typical surface analysis tools for assessment of wear and erosion that may be produced by nanofluids; prediction of such effects in cooling systems is discussed. However, the experimental picture describing tribological effects of nanofluids in contact with typical cooling-system materials is still incomplete. Two new instruments, data acquisition systems, and adequate measurement methodologies are made available from this research work to investigate such unknowns regarding tribological effects of nanofluids. Further knowledge on tribological phenomena will be of importance for a deeper understanding of the role of nanoparticle in surface modification mechanism inside a heat exchanger system.

Robust control system should be designed to connect all parameters of those instruments for precise and automated operation. An improved heating system may need to be introduced to heat sample surfaces, to replicate the actual cooling operation of heat exchangers, so that the tested experimental tribological phenomenon can be analogous to that of real cooling systems. Robust insulation should be applied to minimize the unwanted heat loss.

Possible effects of jet impingement angles, longer length tests and higher jet speed tests should be experimentally explored. Different types of nanoparticles, size of them and other cooling system materials should be tested in future research to find the tribologically favorable combinations of

nanoparticles, base fluids and cooling system materials. All set of tests should be replicated to assess test and result repeatability and design of experiments could be applied to investigate the effects of important factors, as test length flow speed, jet angle and temperature, and of their possible interactions.

## CHAPTER 8

### 8 REFERENCES

- [1] H. Masuda, A. Ebata, K. Teramae, N. Hishinuma, Alternation of thermal conductivity and viscosity of liquid by dispersing ultra-fine particles (dispersion of  $\gamma$ -Al<sub>2</sub>O<sub>3</sub>, SiO<sub>2</sub> and TiO<sub>2</sub> ultra-fine particles), *Netsu Bussei*, 4, 227–233, (1993).
- [2] J. Baxi, Tribological characterization of coatings and nanofluids. Diss. Texas A&M University, (2008).
- [3] J. E. Pope, Rules of thumb for mechanical engineering, Gulf Professional Publishing, Houston, 227, (1996).
- [4] H. P. Jost, Tribology: How a word was coined 40 years ago, *Tribology & lubrication technology*, 24-28, (2006).
- [5] S.K. Basu, S.N. Sengupta, B.B. Ahuja, Fundamentals of tribology, Prentice-Hall of India Pvt. Ltd., New Delhi, (2005).
- [6] R. Khandelwal, S. Sahni, Nanotribology - The road to no WEAR, DST Unit of Nanoscience, (online) Available: <http://www.dstuns.iitm.ac.in/teaching-and-presentations/teaching/undergraduate%20courses/vy305-molecular-architecture-and-evolution-of-functions/presentations/presentations-2006/P5.pdf>. (Accessed: 26- Mar- 2015).
- [7] S.U.S. Choi, J.A. Eastman, Enhancing thermal conductivity of fluids with nanoparticles, Proceedings of the ASME 1995 International Mechanical Engineering Congress and Exhibition, San Francisco, CA, 99-106, (1995).
- [8] S.U.S. Choi, Development and applications of non-newtonian flows, D.A.Siginer and H.P.Wang, Editors, ASME Publisher, 9-105, (1995).
- [9] A.K. Singh, Thermal conductivity of nanofluids, *Defense Sc. Journal*, 58 (5), 600-607, (2008).

- [10] J. A. Eastman, S. U. S. Choi, S. Li, W. Yu, L. J. Thompson, Anomalously increased effective thermal conductivities of ethylene glycol-based nanofluids containing copper nanoparticles, *Applied Physics Letters*, 78 (6), 718–720, (2001).
- [11] J. Buongiorno, Convective transport in nanofluids, *J. Heat Transfer*, 128 (3), 240-250, (2006).
- [12] K.V. Wong, O. De Leon, Applications of nanofluids: current and future, *Advances in Mechanical Engineering*, 2010, 11, (2010).
- [13] Y. Hou, C. Li, D. Zhang, D. Jia, S. Wang, Grinding temperature with nanoparticle jet minimum quantity lubrication, *Bentham Science* 7 (2), 149-161, (2014).
- [14] R. Taylor, S. Coulombe, T. Otanicar, P. Phelan, A. Gunawan, W. Lv, G. Rosengarten, R. Prasher, H. Tyagi, Small particles, big impacts: a review of the diverse applications of nanofluids, *J. Appl. Phys.* 113, (2013).
- [15] J. Eastman, S.U.S. Choi, S. Li, W. Yu, L. J. Thompson, Anomalously increased effective thermal conductivities of ethylene glycol-based nanofluids containing copper nanoparticles, *Appl. Phys. Lett.*, 78 (6), 718-720, (2001).
- [16] B.C. Pak, Y. Cho, Hydrodynamic and heat transfer study of dispersed fluids with submicron metallic oxide particles, *Exp. Heat Transfer*, 11, 151-170, (1998).
- [17] P.E. Phelan, P. Bhattacharya, R.S. Prasher, Nanofluids for heat transfer applications, *Annual Rev. Heat Transfer*, 14, 255-275, (2005).
- [18] S.M.S. Murshed, K.C. Leong, C. Yang, Investigations of thermal conductivity and viscosity of nanofluids, *Intl Journal. of Thermal Sc.*, 47 (5), 560-568, (2008).
- [19] V. Trisaksri, S. Wongwises, Critical review of heat transfer characteristics of nanofluids, *Renewable and Sustainable Energy Rev.*, 11 (3), 512-523, (2007).
- [20] H. Xie, J. Wang, T. Xi, Y. Liu, F. Ai, Q. Wu, Thermal conductivity enhancement of suspensions containing nanosized alumina particles, *J. App. Physics*, 91 (7), 4568-4572, (2002).

- [21] R. Prasher, P.E. Phelan, P. Bhattacharya, Effect of aggregation kinetics on the thermal conductivity of nanoscale colloidal solutions (nanofluids), *Nano Letters*, 6 (7), 1529-1534, (2006).
- [22] R. Prasher, D. Song, J. Wang, P. Phelan, Measurement of nanofluid viscosity and its implications for thermal applications, *App. Phys. Lett.*, 89 (13), 3108, (2006).
- [23] J. Chevalier, O. Tillement, F. Ayela, Structure and rheology of SiO<sub>2</sub> nanoparticle suspensions under very high shear rates, *Phys.Rev.E*, 80 (5), 1403, (2009).
- [24] A.J. Schmidt, M. Chiesa, D.H. Torchinsky, J.A. Johnson, A. Boustani, G.H. McKinley, K.A. Nelson, G. Chen, Experimental investigation of nanofluid shear and longitudinal viscosities, *App. Phys. Lett.*, 92(24), 4107, (2008).
- [25] P. Ding, A.W. Pacek, Effect of pH on deagglomeration and rheology/morphology of aqueous suspensions of goethite nano-powder, *J. Colloid and Interface Science*, 325 (1), 165-172, (2008).
- [26] S. Witharana, J.A. Weliwita, H. Chen, L. Wang, Recent advances in thermal conductivity of nanofluids, *Recent Patents on Nanotechnology*, 7 (3), 198-207, (2013).
- [27] S. K. Das, S.U.S. Choi, H. Patel, Heat transfer in nanofluids-a review, *Heat Transfer Engineering*, 27(10), 3–19, (2006).
- [28] A. Baharanchi, Introduction to nanotechnology, Engineering Information Center, FIU, (2013). (Online). Available: <http://web.eng.fiu.edu/~vlassov/EEE-5425/Abbasi-Heat-transfer.pdf>. (Accessed: 26- Mar- 2015).
- [29] H. Ma, C. Wilson, B. Borgmeyer, K. Park, Q. Yu, S. Choi and M. Tirumala, Effect of nanofluid on the heat transport capability in an oscillating heat pipe, *Applied Physics Letters*, 88 (14), 3116, (2006).
- [30] J. Philip, P. D. Shima, R. Baldev, Nanofluid with tunable thermal properties, *Applied Physics Letters* 92 (4), 3108, (2008).



- [31] J. Routbort, Nanomanufacturing portfolio: manufacturing processes and applications to accelerate commercial use of nanomaterials, Argonne National Lab, Michellin North America, St. Gobain Corp. 1-12, (2009).
- [32] G. Varga, Development and demonstration of nanofluids for industrial cooling applications, U.S. Department of Energy, Industrial Technologies Program, 1-2, (2011).
- [33] M. Bahiraei, Comprehensive review on different numerical approaches for simulation in nanofluids: traditional and novel techniques, *Journal of Dispersion Science and Technology*, 35 (7), 984-996, (2014).
- [34] G. Roy, C.T. Nguyen, P.R. Lajoie, Numerical investigation of laminar flow and heat transfer in a radial flow cooling system with the use of nanofluids, superlattices and microstructures, 35, 497–511, (2004).
- [35] S.J. Palm, G. Roy, C. T. Nguyen, Heat transfer enhancement with the use of nanofluids in radial flow cooling systems considering temperature- dependent properties, *Applied Thermal Engineering*, 26, 2209–2218, (2006).
- [36] S.K. Saripella, W. Yu, J. Routbort, D. France, U. Rizwan, Effects of nanofluid coolant in a class 8 truck engine, *SAE Technical Paper*, 01, 2141, (2007).
- [37] M. Bahiraei, S.M. Hosseinalipour, Effects of various forces on particle distribution and thermal features of suspensions containing alumina nanoparticles, *Journal of Dispersion Science and Technology*, 35 (9), 859-867, (2014).
- [38] X. Wang, A. S. Mujumdar, A review on nanofluids-part II: experiments and applications, *Brazilian Journal of Chemical Engineering* 25 (4), 631-648, (2008).
- [39] J. A. Eastman, U. S. Choi, S. Li, L. J. Thompson, S. Lee, Enhanced thermal conductivity through the development of nanofluids, *Materials Research Society Symposium - Proceedings*, 457, 3–11, (1997).

- [40] S. Lee, S.U.S. Choi, S.Li, J. A. Eastman, Measuring thermal conductivity of fluids containing oxide nanoparticles, *Journal of Heat Transfer*, 121, 280–289 (1999).
- [41] K.Y. Leong, R. Saidur, S.N. Kazi, A.H. Mamun, Performance investigation of an automotive car radiator operated with nanofluid-based coolants (nanofluid as a coolant in a radiator), *Applied Thermal Engineering*, 30, 2685-2692, (2010).
- [42] S.Z. Heris, M. Shokrgozar, S. Poorpharhang, M. Shanbedi, S. H. Noie, Experimental study of heat transfer of a car radiator with CuO/Ethylene Glycol- water as a coolant, *Journal of Dispersion Science and Technology*, 35 (8), 677-684, (2014).
- [43] S.M. Peyghambarzadeh, S.H. Hashemabadi, M. J. Seifi, S.M. Hoseini, Improving the cooling performance of automobile radiator with Al<sub>2</sub>O<sub>3</sub>/water nanofluid, *Applied Thermal Engineering*, 1833-1838, (2011).
- [44] S.M. Peyghambarzadeh, S.H. Hashemabadi, M. Naraki, Y. Vermahmoudi, Experimental study of overall heat transfer coefficient in the application of dilute nanofluids in the car radiator, *Applied Thermal Engineering*, 52, 8-16, (2013).
- [45] J. Buongiorno, Nanofluids for enhanced economics and safety of nuclear reactors: an evaluation of the potential features, issues, and research gaps. *Nuclear Technology* 162 (1), 80-91, (2008).
- [46] M.G. Pop, B.G. Lockamon, Nuclear power plant using nanoparticles in closed circuits of emergency systems and related method. U.S. Patent 8,160,197, issued April 17, (2012).
- [47] S. J. Kim, I. C. Bang, J. Buongiorno, L. W. Hu, Study of pool boiling and critical heat flux enhancement in nanofluids, *Bulletin of the Polish Academy of Sciences—Technical Sciences*, 55(2), 211–216, (2007).
- [48] S. J. Kim, I. C. Bang, J. Buongiorno, L. W. Hu, Surface wettability change during pool boiling of nanofluids and its effect on critical heat flux, *International Journal of Heat and Mass Transfer*, 50 (19), 4105–4116, (2007).

- [49] W. Yu, D. M. France, J. L. Routbort, S.U.S. Choi, Review and comparison of nanofluid thermal conductivity and heat transfer enhancements, *Heat Transfer Engineering*, 29 (5), 432–460, (2008).
- [50] M. Chopkar, P. K. Das, I. Manna, Synthesis and characterization of nanofluid for advanced heat transfer applications, *Scripta Materialia*, 55(6), 549–552, (2006).
- [51] S. Lee, S.U.S. Choi, Application of metallic nanoparticle suspensions. Argonne National Laboratory Energy Technology Division; CONF-961105-20, (1996).
- [52] V. Sridhara, B.S. Gowrishanka, S.L.N. Snehalatha, Nanofluids a new promising fluid for cooling. *Trans Indian Ceram Soc*, 68, 1–17, (2009).
- [53] S.S. Botha, Synthesis and characterization of nanofluids for cooling applications. PhD thesis. University of the Western Cape, (2007).
- [54] Yu. Wei, H. Xie. A review on nanofluids: preparation, stability mechanisms, and applications. *Journal of Nanomaterials* 2012 (1), 1687-4129, (2012)
- [55] D. Singh, J. Toutbort, G. Chen, Annual report Argonne National Lab (2006).
- [56] V. A. M. Selvan, R. B. Anand, M. Udayakumar, *J. Eng. Appl. Sci.* 4, 1, (2009).
- [57] S. Senthilraja, M. Karthikeyan, R. Gangadevi. Nanofluid applications in future automobiles: comprehensive review of existing data, *Nano-Micro Letters* 2 (4), 306-310, (2010).
- [58] G.J. Molina, M. Hulett, V. Soloiu, M. Rahman, Erosion effects of nanofluids on selected cooling-system materials, Third International Symposium on Tribo-Corrosion, ASTM STP 1563, P. J. Blau, F. E. Schmidt, D. Drees, and J.-P. Celis, Eds., ASTM Intl, West Conshohocken, PA, 47-65, (2012).
- [59] D. Singh, J. Toutbort, G. Chen, Heavy vehicle systems optimization merit review and peer evaluation, Annual Report, Argonne National Laboratory, 23, 405-411, (2006).

- [60] G.J. Molina, F. Aktaruzzaman, W. Stregles, V. Soloiu, and M. Rahman, Jet-impingement effects of alumina-nanofluid on aluminum and copper, *Advances in Tribology*, 2014 (2014).
- [61] S. J. Thrush, Investigation of dispersion, stability, and tribological performance of oil-based aluminum oxide nanofluids, Oakland University Dept. of Mechanical Engineering, (2012).
- [62] L. Gara, Q. Zou, Friction and wear characteristics of water-based ZnO and Al<sub>2</sub>O<sub>3</sub> nanofluids, *Tribology Transactions*, 55 (3), 345–350, (2012).
- [62] H. Yu, Y. Xu, P. Shi, B. Xu, X. Wang, Q. Liu, Tribological properties and lubricating mechanisms of Cu nanoparticles in lubricant, *Transactions of Nonferrous Metals Society of China (English Edition)*, 18 (3), 636–641, (2008).
- [63] D. Kopeliovich, Tribological properties and applications of alumina, Substech, (2013). (Online). Available: [http://www.substech.com/dokuwiki/doku.php?id=tribological\\_properties\\_and\\_applications\\_of\\_alumina](http://www.substech.com/dokuwiki/doku.php?id=tribological_properties_and_applications_of_alumina). (Accessed: 26- Mar- 2015).
- [64] W. G. Sawyer, K. D. Freudenberg, P. Bhimaraj, L. S. Schadler, A study on the friction and wear behavior of PTFE filled with alumina nanoparticles, *Wear*, 254, 573–580, (2003).
- [65] X. Shao, Q. Xue, W. Liu, M. Teng, H. Liu, X. Tao, Tribological behavior of micrometer- and nanometer-Al<sub>2</sub>O<sub>3</sub>-particle-filled poly(phthalazine ether sulfone ketone) copolymer composites used as frictional materials, *Journal of applied polymer science*, 95(5), 993-1001, (2005).
- [66] S. Lanhui, Y. Zhenguo, L. Xiaohui, Tribological properties of nano-Al<sub>2</sub>O<sub>3</sub> modified POM nanocomposites, *Chinese Journal of materials Research*, 21(6), 654-658, (2007).
- [67] S. Bin, A. J. Shih, S. C. Tung. Application of nanofluids in minimum quantity lubrication grinding, *Tribology Transactions*, 51(6), 730-737, (2008).
- [68] B. Shen, A.P. Malshe, P. Kalita, A.J. Shih, Performance of novel MoS<sub>2</sub> nanoparticles based grinding fluids in minimum quantity lubrication grinding. *Transactions of NAMRI/SME* 36, 357–364, (2008).

- [69] M. Cong, The tribological properties of nanofluid used in minimum quantity lubrication grinding, *The International Journal of Advanced Manufacturing Technology*, 71(5-8), 1221-1228, (2014).
- [70] U. Sridharan, S. Malkin, Effect of minimum quantity lubrication (MQL) with nanofluid on grinding behavior and thermal distortion, *Transactions of NAMRI/SME*, 37, 629–636, (2009).
- [71] E. Varrla, V. Sankaranarayanan, S. Ramaprabhu, Graphene-based engine oil nanofluids for tribological applications, *ACS applied materials & interfaces*, 3(11), 4221-4227, (2011).
- [72] K. Koji, K. Adachi, Wear mechanisms, *Modern tribology handbook*, 1, 273-300, (2001).
- [73] E. Rabinowicz, Friction and wear of materials, Wiley, Technology & Engineering, John Wiley and Sons, New York, 244, (1965).
- [74] J. Black, Handbook of biomaterial properties, Garth Hastings Springer Science & Business Media, 590, (1998).
- [75] G. Stachowiak, A. W. Batchelor, Engineering tribology, Butterworth-Heinemann, University of Western Australia, Perth, Australia, 871, (2013)
- [76] P. M. Kumari, R. P. Saini, A review on silt erosion in hydro turbines, *Renewable and Sustainable Energy Reviews*, 12(7), 1974-1987, (2008).
- [77] D. Kopeliovich, Mechanisms of wear, Substech.com, (2015). (Online). Available: [http://www.substech.com/dokuwiki/doku.php?id=mechanisms\\_of\\_wear](http://www.substech.com/dokuwiki/doku.php?id=mechanisms_of_wear). (Accessed: 27- Mar- 2015).
- [78] Exchange.dnv.com, Recommended Practice, RP O501: Erosive Wear in Piping Systems, (2011). (Online). Available: <https://exchange.dnv.com/servicedocuments/currentVersion/dnv?DNV-RP-O501>. (Accessed: 27- Mar- 2015).
- [79] G. Gibin, Experimental investigation of material surface erosion caused by TiO<sub>2</sub> nanofluid impingement, *Journal of Nanofluids*, 3(2), 97-107, (2014).

- [80] S. Tamer, İ. Taşkıran, Erosive wear behavior of polyphenylenesulphide (PPS) composites, *Materials & design*, 28(9), 2471-2477, (2007).
- [81] Efcweb.org, EFC Working Party 7: Corrosion Education' (2012). (online) <http://www.efcweb.org/Definition+of+Corrosion.html>. (Accessed: 26- Mar- 2015).
- [82] ASTM International. Handbook Committee. *ASTM handbook: Friction, lubrication, and wear technology*, ASTM International, West Conshohocken, PA, 18, (1992).
- [83] K. G. Budinski, *Guide to friction, wear and erosion testing*, ASTM International, West Conshohocken, PA, 132, (2007).
- [84] J.L. Routbort, D. Singh, Annual progress report for advanced vehicle technology analysis and evaluation activities and heavy vehicle systems optimization program, U.S. Department of Energy, AVTAE Activities and HVSO Program, USA, 261-264, (2008).
- [85] D. Singh, E. Timofeeva, Y. Wen, R. K. Smith, Erosion of radiator materials by nanofluids, *Vehicle Technologies—Annual Review*, 18-22, (2009).
- [86] G.P. Celata, F. D'Annibale, A. Mariani, Nanofluid flow effects on metal surfaces, *EAI - Energia Ambiente e Innovazione*, 4, 94-98, (2011).
- [87] G.P. Celata, F. D'Annibale, A. Mariani, S. Sau, E. Serra, R. Bubbico, C. Menale, H. Poth, Experimental results of nanofluids flow effects on metal surfaces, *Chemical Engineering Research and Design*, 92(9), 1616-1628, (2014).
- [88] G. George, R.K. Sabareesh, S. Thomas, V. Sajith, T. Hanas, S. Das, C. B. Sobhan, Experimental investigation of material surface erosion caused by TiO<sub>2</sub> nanofluid impingement, *Journal of Nanofluids*, 3, 1–11, (2014).
- [89] C.T. Nguyen, G. Laplante, M. Cury, G. Simon, Experimental investigation of impinging jet heat transfer and erosion effect using Al<sub>2</sub>O<sub>3</sub>-water nanofluid, 6th IASME/WSEAS International Conference on Fluid Mechanics and Aerodynamics (FMA'08), Rhodes, Greece, 1790-5095, (2008).

- [90] M. R. Safaei, Investigation of micro-and nanosized particle erosion in a 90° pipe bend using a two-phase discrete phase model. *The Scientific World Journal* 2014, (2014).
- [91] J. Laguna-Camacho, Solid particle erosion on different metallic materials. *Tribol Eng*, 5, 63-77, (2013).
- [92] A. P. Harsha, D. K. Bhaskar, Solid particle erosion behavior of ferrous and non-ferrous materials and correlation of erosion data with erosion models, *Materials and Design*, 29, 1745-1754, (2008).
- [93] I. M. Hutchings, *Tribology: friction and wear of engineering materials*, London, Edward Arnold, 273, (1992).
- [94] C.T. Morrison, R. O. Scattergood, Erosion of 304 stainless steel, *Wear*, 111, 1- 13, (1986).
- [95] A. V. Levy, P. Chik, The effects of erodent composition and shape on the erosion of steel, *Wear*, 89, 151-162, (1983).
- [96] M. Liebhard, A. Levy, The effect of erodent particle characteristics on the erosion of metals, *Wear*, 151, 381-390, (1991).
- [97] G.J. Molina, M. Hulett, V. Soloiu, M. Rahman, On the surface effects of nanofluids in cooling-system materials, *Materials Research Society Spring Meeting, San Francisco, CA, April* MRS Online Proceedings Library, Cambridge University Press, 1558, 1-5, (2013).
- [88] P.A. Engel, *Impact wear of materials*, Elsevier, New York, NY, 89, (1976).
- [99] I.M. Hutchings, Mechanisms of the erosion of metals by solid particles, *Proc of ASTM Symp. on Erosion: Prevention and its Useful Applications*, ASTM STP 664, Alder, W., Eds., ASTM International, West Conshohocken, PA, 59-76, (1979).
- [100] I. M. Hutchings, A model for the erosion of metals by spherical particles at normal incidence, *Wear*, 70, 269-281, (1981).

[101] A.K. Cousins, I.M. Hutchings, A critical study of the erosion of an aluminium alloy by solid particles at normal impingement, *Wear*, 88, 335-348, (1983).

[102] W. A. Brainard, J. Salik, Scanning-electron-microscope study of normal-impingement erosion of ductile metals, Lewis Research Center, Cleveland, Ohio, National Aeronautics and Space Administration Scientific and Technical, Information Office, NASA Technical Paper 1609, (1980).

[103] R. P. Veerabhadra, D. H. Buckley, Time dependence of solid-particle impingement erosion of an aluminum alloy, National Aeronautics and Space Administration Scientific and Technical Information Branch, Lewis Research Center, Cleveland, Ohio, NASA Technical Paper 2169, (1983).

[104] M.G. Gee, I. M. Hutchings, General approach and procedures for erosive wear testing, National Physical Laboratory, NPL Measurement Good Practice Guide No. 56, ISSN: 1368-6550, (2002).

[105] ASTM Standard G76–07: Standard test method for conducting erosion tests by solid particle impingement using gas jets, Annual Book of ASTM Standards, ASTM International, West Conshohocken, PA, (2007).

[106] A.W. Ruff, S.M. Wiederhorn, Erosion by solid particle impact, *Treatise on Materials Science and Technology*, Volume 16-Erosion, C. M. Preece, Ed., Academic Press , New York, NY, 69-126, (1979).

[107] L.K. Ives, A.W. Ruff, Transmission and scanning electron microscopy studies of deformation at erosion impact sites, *Wear*, 46, 149-162, (1978).



- [108] J.E. Goodwin, W. Sage, G.P. Tilly, A study of erosion by solid particles, Proc.of the Institute of Mechanical Engineers, 184 (15), 279-292, (1969).
- [109] L.K. Ives, A.W. Ruff, Electron microscopy study of erosive wear damage in copper, Proc. of ASTM Symp. on Erosion: Prevention and its Useful Applications, ASTM STP 664, PA, 5-35 (1979) .
- [110] J.E. Edwards, Chemstations CHEMCAD piping systems user's guide and tutorial. 73, (2010).
- [111] Engineeringtoolbox.com, Ethylene Glycol heat-transfer fluid, (2013). (Online). Available: [http://www.engineeringtoolbox.com/ethylene-glycol-d\\_146.html](http://www.engineeringtoolbox.com/ethylene-glycol-d_146.html). (Accessed: 26- Mar- 2015).
- [112] University of Delaware, Minor losses in pipes, (2015) (Online). Available: [http://udel.edu/~inamdar/EGTE215/Minor\\_loss.pdf](http://udel.edu/~inamdar/EGTE215/Minor_loss.pdf). (Accessed: 26- Mar- 2015).
- [113] C. Wu, V. Kumar, J. Liao, F. L'Esperance, G. Baker, Pipe friction calculation for fluid flow in a pipe, (2015). (Online) [http://www.efunda.com/formulae/fluids/calc\\_pipe\\_friction.cfm](http://www.efunda.com/formulae/fluids/calc_pipe_friction.cfm), (Accessed: 26- Mar- 2015).
- [114] R. K. Shah, D. R Sekuli, Heat exchangers, Delphi harrison thermal systems, Lockport, New York. (Online) Available: [http://razifar.com/cariboost\\_files/Heat\\_20Exchangers.pdf](http://razifar.com/cariboost_files/Heat_20Exchangers.pdf). (Accessed: 26- Mar- 2015).
- [115] MSDS503. Custom brand antifreeze/coolant. Material data safety sheet, <http://msds.walmartstores.com/client/document?productid=5f456c08-9657-4abf-afb2-6926434ce2e7&action=MSDS&subformat=NAM>, 7, (2008).
- [116] Surface roughness measuring tester surftest SJ-210 User's Manual, No. 99MB122A, Series No.178, Mitutoyo Corp., Japan.

## APPENDIX A

### ROUGHNESS RESULTS AND PLOTTING

#### A.1 Jet impingement test results

This Appendix includes all the roughness measurements carried out as part of the research work of this thesis. Roughness parameters Ra, Rq and Rz were measured three times in each of the longitudinal direction (along the texture lay) and of the transversal direction (perpendicular of the texture lay). These six values are averaged to obtain each of Ra, Rq and Rz values for each sample. Same procedure is used before-test and after-test.

##### A.1.1 Test results for 3.5 m/s jet impingement treatments

##### A.1.1.1 Test results of 3.5 m/s jet impingement with distilled water as base fluid and its nanofluid on aluminum

Table A.1. Surface roughness data for before- and after- 3 hours of tests with a 3.5- m/s jet of reference fluid of distilled water

Surface roughness ( $\mu$ inch)	Before test			After test		
	Ra	Rq	Rz	Ra	Rq	Rz
Longitudinal	3.63	4.52	26.5	3.21	4.23	27.38
	3.3	4.27	29.78	3.29	4.29	26.34
	3.19	4.18	25.97	3.09	3.92	26.73
Transvers	3.09	4.28	36.55	3.78	6.71	35.72
	3.13	4.12	28.98	3.28	4.18	26.83
	3.35	4.71	29.01	3.08	4.12	26.85
Average	3.28	4.34	29.46	3.18	4.14	26.84

Table A.2. Surface roughness data for before- and after- 7 hours of tests with a 3.5- m/s jet of reference fluid of distilled water

Surface roughness ( $\mu$ inch)	Before test			After test		
	Ra	Rq	Rz	Ra	Rq	Rz
Longitudinal	3.69	4.73	29.88	3.12	4.24	36.59
	3.92	5.03	36.2	4.94	6.39	36.73
	3.96	5.1	35.38	3.35	4.29	33.79
Transvers	3.87	5.01	35.77	3.71	11.95	35.77
	3.29	4.87	29.11	3.72	6.81	35.59
	3.57	5.11	34.21	3.82	6.60	35.83
Average	3.71	4.97	33.42	3.78	6.71	35.72

Table A.3. Surface roughness data for before- and after- 14 hours of tests with a 3.5- m/s jet of reference fluid of distilled water

Surface roughness ( $\mu$ inch)	Before test			After test		
	Ra	Rq	Rz	Ra	Rq	Rz
Longitudinal	4.62	5.86	38.32	3.58	4.97	38.28
	4.17	5.57	35.11	3.79	5.14	41.3
	3.44	4.43	28.36	3.55	4.63	33.44
Transvers	3.14	4.35	29.12	3.25	4.91	37.89
	4.04	5.25	29.98	3.19	3.92	36.83
	3.57	4.98	31.27	3.58	6.71	35.82
Average	3.83	5.7	32.03	3.54	4.91	37.73

Table A.4. Surface roughness data for before- and after- 28 hours of tests with a 3.5- m/s jet of reference fluid of distilled water

Surface roughness ( $\mu$ inch)	Before test			After test		
	Ra	Rq	Rz	Ra	Rq	Rz
Longitudinal	2.34	3.03	20.05	2.55	3.46	29.85
	2.24	3.31	21.13	2.71	3.8	31.32
	2.2	2.92	24.24	6.15	6.08	33.42
Transvers	2.44	3.18	23.95	4.22	5.51	30.15
	2.51	3.22	22.34	2.72	3.62	26.25
	2.22	3.01	22.34	3.87	4.60	30.30
Average	2.31	3.11	22.34	3.67	4.50	30.20

Table A. 5. Surface roughness data for before- and after- 56 hours of tests with a 3.5- m/s jet of reference fluid of distilled water.

Surface roughness ( $\mu$ inch)	Before test			After test		
	Ra	Rq	Rz	Ra	Rq	Rz
Longitudinal	3.21	4.23	30.31	4.26	6	53.85
	3.94	5.18	38.39	3.81	5.51	50.41
	4.14	5.42	37.04	4.32	6.05	49.36
Transvers	3.22	4.21	31.31	5.12	6.67	49.36
	3.89	5.88	37.77	4.36	6.51	50.53
	4.01	5.87	38.08	4.49	6.15	50.65
Average	3.735	5.13	35.48	4.37	6.06	50.74

Table A. 6. Surface roughness data for before- and after- 112 hours of tests with a 3.5- m/s jet of reference fluid of distilled water

Surface roughness ( $\mu$ inch)	Before test			After test		
	Ra	Rq	Rz	Ra	Rq	Rz
Longitudinal	3.24	4.3	29.16	4.77	8.06	77.11
	3.32	4.53	30.11	9.56	13.56	106.32
	2.34	3.32	29.27	5.28	7.4	66.42
Transvers	3.13	4.32	30.21	4.86	7.07	64.84
	4.34	5.52	37	6.36	9.21	78.21
	4.44	5.69	37.21	6.01	8.87	78.53
Average	3.46	4.61	32.16	6.12	9.02	78.67

Table A. 7. Surface roughness data for before- and after- 240 hours of tests with a 3.5- m/s jet of reference fluid of distilled water.

Surface roughness ( $\mu$ inch)	Before test			After test		
	Ra	Rq	Rz	Ra	Rq	Rz
Longitudinal	3.38	4.36	27.61	11	17.42	144.1
	2.74	3.59	24.28	15.75	25.19	194.2
	3.61	4.67	34.54	14.42	23.81	196.98
Transvers	3.59	4.77	34.58	9.97	15.5	129.42
	2.98	3.78	25.01	12.56	20.81	166.71
	2.85	3.88	24.89	12.89	20.15	166.01
Average	3.19	4.175	28.48	12.78	20.48	166.17

Table A. 8. Surface roughness data for before- and after- 312 hours of tests with a 3.5- m/s jet of reference fluid of distilled water.

Surface roughness ( $\mu$ inch)	Before test			After test		
	Ra	Rq	Rz	Ra	Rq	Rz
Longitudinal	2.9	3.88	27.99	38.22	51	295.26
	3.15	4.08	26.71	30.85	41.64	242.45
	3.12	4.06	26.17	31.17	41.95	242.78
Transvers	2.91	3.87	26.92	31.21	42.13	244.12
	3.54	4.79	33.75	32.16	44.01	256.24
	3.14	4.29	32.98	32.99	44.25	256.13
Average	3.12	4.16	29.08	32.86	44.18	256.15

Table A. 9. Surface roughness data for before- and after- 408 hours of tests with a 3.5- m/s jet of reference fluid of distilled water.

Surface roughness ( $\mu$ inch)	Before test			After test		
	Ra	Rq	Rz	Ra	Rq	Rz
Longitudinal	3.26	4.42	34.02	41.38	55.97	304.24
	3.27	4.92	34.22	32.84	45.02	263.01
	3.4	4.36	27.38	38.77	51.39	280.52
Transvers	2.25	4.44	35.21	36.31	46.94	248.83
	2.29	2.98	21.47	37.13	49.75	274.36
	2.13	2.87	20.98	37.24	49.68	274.01
Average	2.76	3.99	28.88	37.32	49.83	274.15

Table A. 10. Surface roughness data for before- and after- 3 hours of tests with a 3.5- m/s jet of 2% alumina nanofluid of distilled water.

Surface roughness ( $\mu$ inch)	Before test			After test		
	Ra	Rq	Rz	Ra	Rq	Rz
Longitudinal	2.53	3.04	23.55	7.56	11.34	75.21
	3.15	3.95	24.44	12.81	18.88	106.11
	3.26	3.19	25.51	12.21	18.31	124.68
Transvers	2.31	3.04	23.81	7.61	11.35	75.21
	3.11	3.58	24.45	12.81	18.18	106.23
	3.15	3.78	25.11	12.01	18.31	124.38
Average	2.88	3.53	24.43	11.05	16.14	102.06

Table A. 11. Surface roughness data for before- and after- 7 hours of tests with a 3.5- m/s jet of 2% alumina nanofluid of distilled water.

Surface roughness ( $\mu$ inch)	Before test			After test		
	Ra	Rq	Rz	Ra	Rq	Rz
Longitudinal	2.35	3.05	25.51	11.68	19.44	95.21
	3.12	3.86	24.45	12.81	18.68	106.11
	3.24	4.69	25.51	12.21	18.31	124.68
Transvers	4.35	5.14	28.57	11.64	19.34	105.21
	3.14	3.95	24.41	12.81	18.78	106.21
	3.23	4.79	25.51	12.71	18.3	124.78
Average	3.88	4.53	25.43	12.05	18.14	112.56

Table A.12. Surface roughness data for before- and after- 14 hours of tests with a 3.5- m/s jet of 2% alumina nanofluid of distilled water.

Surface roughness ( $\mu$ inch)	Before test			After test		
	Ra	Rq	Rz	Ra	Rq	Rz
Longitudinal	2.33	3.04	23.5	7.66	11.34	75.2
	3.1	3.96	24.4	12.8	18.78	106.21
	3.21	3.59	25.41	12.71	18.3	124.78
Transvers	3.15	3.95	24.44	12.81	18.88	106.11
	3.26	3.19	25.51	12.21	18.31	124.68
	2.31	3.04	23.81	7.61	11.35	75.21
Average	2.87	3.56	24.33	11.15	16.34	112.16

Table A. 13. Surface roughness data for before- and after- 28 hours of tests with a 3.5- m/s jet of 2% alumina nanofluid of distilled water.

Surface roughness ( $\mu$ inch)	Before test			After test		
	Ra	Rq	Rz	Ra	Rq	Rz
Longitudinal	3.43	4.34	27.38	23.19	32.63	196.57
	4.74	6.09	36.14	25.07	36.83	197.98
	3.48	4.55	31.26	21.86	30.36	189.86
Transvers	3.24	3.69	24.41	12.8	18.78	106.21
	2.35	3.14	25.51	12.71	18.3	124.78
	3.14	3.95	24.43	11.05	16.14	102.06
Average	3.88	4.99	31.59	24.37	34.27	195.80

Table A. 15. Surface roughness data for before- and after- 112 hours of tests with a 3.5- m/s jet of 2% alumina nanofluid of distilled water.

Surface roughness ( $\mu$ inch)	Before test			After test		
	Ra	Rq	Rz	Ra	Rq	Rz
Longitudinal	2.93	3.75	25.53	20.1	30.85	175.58
	2.99	3.09	26.92	15.73	23.84	160.76
	3.21	4.29	26.07	17.26	27.05	155.54
Transvers	3.48	4.55	31.26	25.07	36.83	197.98
	3.24	3.69	24.41	21.86	30.36	189.86
	2.35	3.14	25.51	12.21	18.31	124.68
Average	3.04	3.71	26.17	17.70	27.25	163.96

Table A.17. Surface roughness data for before- and after- 312 hours of tests with a 3.5- m/s jet of 2% alumina nanofluid of distilled water.

Surface roughness ( $\mu$ inch)	Before test			After test		
	Ra	Rq	Rz	Ra	Rq	Rz
Longitudinal	3.33	3.04	23.5	72.31	103.43	555.07
	3.12	3.96	24.4	74.74	95.89	499.08
	3.21	3.59	25.5	95.56	125.25	642.58
Transvers	3.43	3.64	22.51	82.31	113.53	565.08
	3.32	3.85	19.4	76.74	105.79	489.09
	3.81	3.69	29.48	55.56	135.15	652.18
Average	3.22	3.53	24.43	80.87	108.19	565.58

Table A. 14. Surface roughness data for before- and after- 56 hours of tests with a 3.5- m/s jet of 2% alumina nanofluid of distilled water.

Surface roughness ( $\mu$ inch)	Before test			After test		
	Ra	Rq	Rz	Ra	Rq	Rz
Longitudinal	2.45	3.24	22.97	24.19	22.63	156.57
	3.17	4.52	33.01	22.07	36.83	187.98
	3.27	4.78	38.02	23.86	20.36	199.86
Transvers	3.26	3.19	25.51	19.8	28.78	156.21
	2.31	3.04	23.81	22.71	28.3	194.78
	2.88	3.53	24.43	31.05	21.14	162.06
Average	2.96	4.18	31.33	23.37	33.27	194.80

Table A. 16. Surface roughness data for before- and after- 240 hours of tests with a 3.5- m/s jet of 2% alumina nanofluid of distilled water.

Surface roughness ( $\mu$ inch)	Before test			After test		
	Ra	Rq	Rz	Ra	Rq	Rz
Longitudinal	3.26	4.11	26.33	25.97	42.02	265.8
	3.34	4.32	31.01	21.84	32.15	216.26
	2.67	3.4	22.57	20.51	29.9	188.7
Transvers	3.16	3.11	36.33	31.97	32.02	165.8
	2.35	4.92	21.01	25.84	31.15	296.26
	3.67	2.98	25.57	18.51	39.9	198.7
Average	2.95	3.95	26.64	22.77	34.69	223.59

Table A. 18. Surface roughness data for before- and after- 408 hours of tests with a 3.5- m/s jet of 2% alumina nanofluid of distilled water.

Surface roughness ( $\mu$ inch)	Before test			After test		
	Ra	Rq	Rz	Ra	Rq	Rz
Longitudinal	3.43	4.34	27.38	95.35	124.92	639.46
	3.74	5.09	32.14	107.08	143.45	843.74
	3.48	4.55	31.26	76.86	97.51	579.57
Transvers	4.53	6.34	25.38	75.35	114.92	439.48
	2.64	3.19	28.16	86.18	133.45	743.75
	3.58	5.65	31.28	96.76	117.51	679.58
Average	3.55	4.66	30.26	93.09	121.96	654.25

Following Figures A.1 and A.2 displays plots of average and normalized values of Rq and Rz roughness for 3003-T3 aluminum before and after 3, 7, 14, 28, 56, 112, 240, 312 and 408 hour-treatments with the reference fluid distilled water and its 2% alumina nanofluid with 3.5 m/s jet speed respectively.

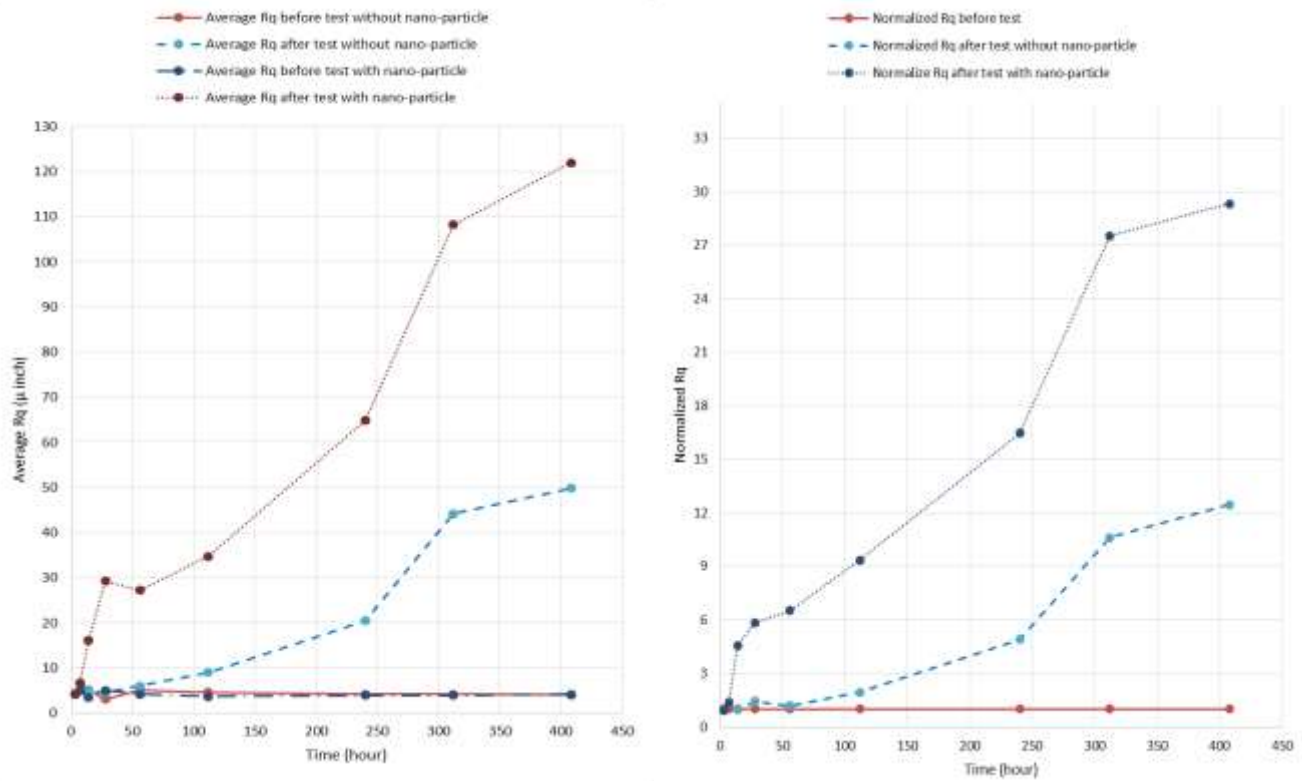


Figure A. 1. Average and normalized Rq roughness for 3003-T3 aluminum before and after 3, 7, 14, 28, 56, 112, 240, 312 and 408 hour-treatments with the reference fluid distilled water and its 2% alumina nanofluid and jet speed of 3.5 m/s.

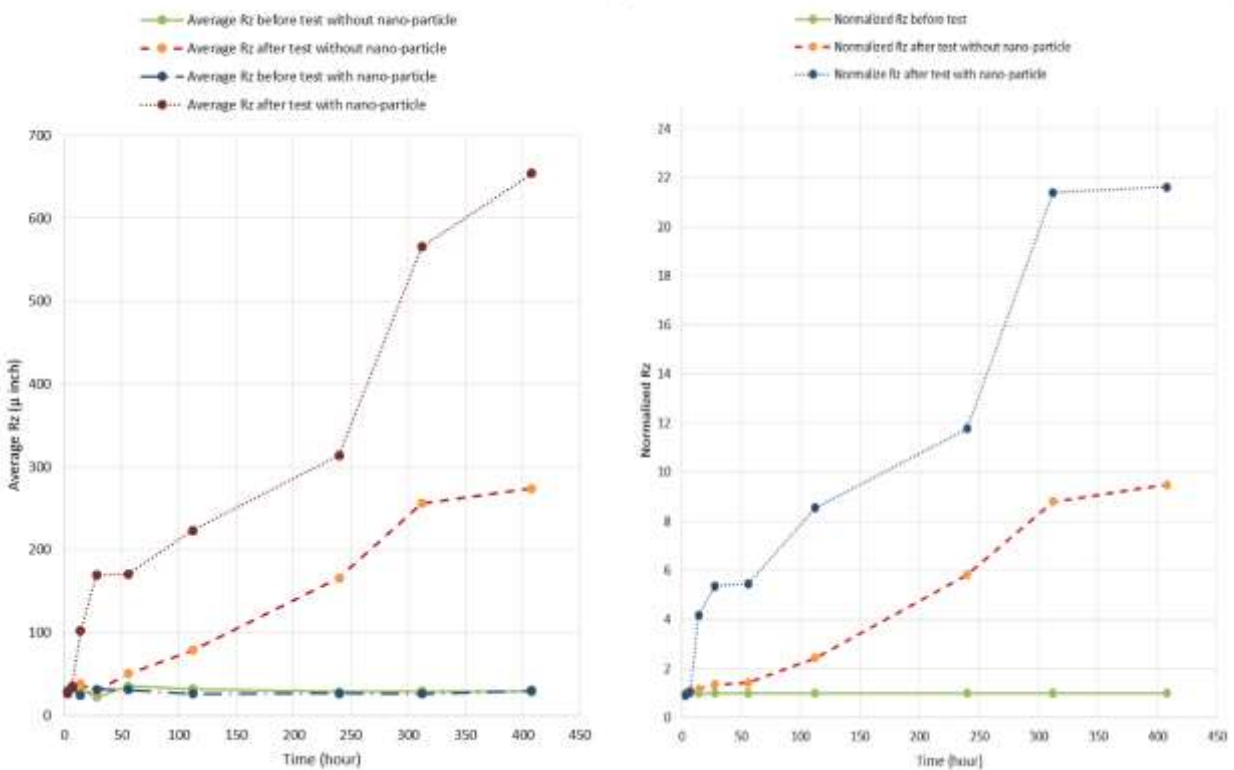


Figure A. 2. Average and normalized Rz roughness for 3003-T3 aluminum before and after 3, 7, 14, 28, 56, 112, 240, 312 and 408 hour-treatments with the reference fluid distilled water and its 2% alumina nanofluid and jet speed of 3.5 m/s.

## A.1.1.2 Test results of 3.5 m/s jet impingement with distilled water as base fluid and its nanofluid on Copper

Table A. 19. Surface roughness data for copper alloy110 before- and after- 3 hours of tests with a 3.5- m/s jet of distilled water.

Surface roughness ( $\mu$ inch)	Before test			After test		
	Ra	Rq	Rz	Ra	Rq	Rz
Longitudinal	1.88	2.86	24.86	2.31	3.4	29.66
	1.94	3.12	28.26	1.21	1.71	13.78
	2.06	3.09	22.3	2.48	3.71	31.46
Transvers	1.95	3.22	27.26	1.86	2.9	23.56
	2.01	3.07	21.31	1.21	1.71	13.78
	2.11	3.05	20.31	2.48	3.71	31.46
Average	1.99	3.07	24.05	1.96	2.93	24.62

Table A. 21. Surface roughness data for copper alloy110 before- and after- 14 hours of tests with a 3.5- m/s jet of distilled water.

Surface roughness ( $\mu$ inch)	Before test			After test		
	Ra	Rq	Rz	Ra	Rq	Rz
Longitudinal	2.35	3.51	33.2	1.85	3.22	27.1
	1.85	2.82	25.34	2.81	3.68	25.24
	2.26	3.33	23.86	2.27	3.15	24.11
Transvers	1.98	2.78	25.31	1.63	2.43	21.27
	2.21	3.47	32.98	1.85	3.22	27.1
	2.11	3.23	30.12	2.81	3.68	25.24
Average	2.13	3.19	28.47	2.14	3.12	24.43

Table A. 23. Surface roughness data for copper alloy110 before- and after- 56 hours of tests with a 3.5- m/s jet of distilled water.

Surface roughness ( $\mu$ inch)	Before test			After test		
	Ra	Rq	Rz	Ra	Rq	Rz
Longitudinal	2.2	3.18	26.66	3.07	4.13	31.47
	3.11	4.92	41.11	6.14	8.41	43.82
	1.89	2.81	22.45	2.05	2.98	20.1
Transvers	2.45	3.57	27.01	2.31	2.91	20.07
	3.01	4.12	40.11	4.14	6.41	33.82
	2.41	3.17	25.18	2.05	2.98	20.1
Average	2.52	3.63	30.42	3.39	4.61	28.87

Table A. 25. Surface roughness data for copper alloy110 before- and after- 240 hours of tests with a 3.5- m/s jet of distilled water.

Surface roughness ( $\mu$ inch)	Before test			After test		
	Ra	Rq	Rz	Ra	Rq	Rz
Longitudinal	2.78	3.98	32.76	2.71	3.54	21.05
	2.7	4.26	37.25	2.81	3.62	21.23
	2.95	4.18	26.4	2.71	3.54	21.05
Transvers	2.97	4.78	29.12	2.08	2.86	16.88
	3.01	5.12	38.52	2.81	3.62	21.23
	2.88	4.12	35.25	2.08	2.86	16.88
Average	2.88	4.41	33.22	2.53	3.34	19.72

Table A. 20 Surface roughness data for copper alloy110 before- and after- 7 hours of tests with a 3.7- m/s jet of distilled water.

Surface roughness ( $\mu$ inch)	Before test			After test		
	Ra	Rq	Rz	Ra	Rq	Rz
Longitudinal	4.98	7.18	39.04	4.15	6.01	47.27
	1.98	2.99	22.83	3.43	5.03	39.93
	2.67	4.03	29.71	2.99	4.06	27.13
Transvers	3.89	6.81	29.05	4.41	6.53	45.38
	2.67	4.01	28.77	3.43	5.03	39.93
	3.78	6.87	29.15	2.99	4.06	27.13
Average	3.33	5.32	29.76	3.75	5.41	39.93

Table A. 22. Surface roughness data for copper alloy110 before- and after- 28 hours of tests with a 3.5- m/s jet of distilled water.

Surface roughness ( $\mu$ inch)	Before test			After test		
	Ra	Rq	Rz	Ra	Rq	Rz
Longitudinal	2.24	3.51	28.33	2.1	3.56	30.33
	4.54	5.87	44.68	2.76	4.41	33.97
	1.71	2.44	20.48	2.22	3.29	29.29
Transvers	2.17	3.25	27.13	2.56	3.79	30.88
	1.89	2.14	22.18	2.1	3.56	30.33
	2.01	3.15	28.23	2.76	4.41	33.97
Average	2.43	3.39	28.51	2.41	3.76	31.12

Table A. 24. Surface roughness data for copper alloy110 before- and after- 112 hours of tests with a 3.5- m/s jet of distilled water.

Surface roughness ( $\mu$ inch)	Before test			After test		
	Ra	Rq	Rz	Ra	Rq	Rz
Longitudinal	2.97	5.22	42.33	2.21	3.55	28.63
	2.3	3.76	33.09	2.3	3.41	25.45
	3.94	5.71	41.62	2.32	3.38	24.71
Transvers	3.56	5.21	41.26	2.1	3.11	25.3
	2.89	3.67	33.19	2.3	3.41	25.45
	3.78	5.72	42	2.32	3.38	24.71
Average	3.24	4.88	38.92	2.23	3.36	26.02

Table A. 26. Surface roughness data for copper alloy110 before- and after- 312 hours of tests with a 3.5- m/s jet of distilled water.

Surface roughness ( $\mu$ inch)	Before test			After test		
	Ra	Rq	Rz	Ra	Rq	Rz
Longitudinal	2.58	4.08	37.97	3.03	4.58	39.05
	4.01	6.1	31.46	2.65	4.08	33.75
	4.43	6.37	47.27	2.45	3.01	29.1
Transvers	3.89	5.88	41.01	3.45	4.68	27.22
	4.02	6.01	32.11	2.65	4.08	33.75
	3.77	5.98	40.12	2.45	3.01	29.1
Average	3.78	5.74	38.33	2.89	4.09	32.28

Table A. 27. Surface roughness data for copper alloy110 before- and after- 408 hours of tests with a 3.5- m/s jet of distilled water.

Surface roughness ( $\mu$ inch)	Before test			After test		
	Ra	Rq	Rz	Ra	Rq	Rz
Longitudinal	3.1	4.99	40.88	2.28	3.46	23.95
	3.83	5.61	41.2	3.12	5.31	41.06
	3.25	4.96	37.44	2.44	4.02	29.33
Transvers	3.51	4.98	41.11	5.9	9.88	60.96
	3.11	4.87	40.89	2.63	3.95	29.28
	3.25	4.69	37.41	3.12	5.31	41.06
Average	3.34	5.02	39.83	3.27	5.33	36.92

Table A. 28. Surface roughness data for copper alloy110 before- and after- 3 hours of tests with a 3.5- m/s jet of 2% nano-alumina nanofluid of distilled water.

Surface roughness ( $\mu$ inch)	Before test			After test		
	Ra	Rq	Rz	Ra	Rq	Rz
Longitudinal	2.73	3.84	31.85	3.7	5.29	41.54
	3.61	5.13	34.99	2.91	3.98	26.52
	3.85	5.64	49.99	3.28	4.59	33.81
Transvers	2.42	3.64	30.96	2.62	3.69	27.35
	2.67	4.01	31	2.72	3.9	28.05
	2.53	3.79	32.33	2.5	3.59	28.48
Average	2.48	3.59	33.85	2.81	3.83	31.96

Table A. 29. Surface roughness data for copper alloy110 before- and after- 7 hours of tests with a 3.5- m/s jet of 2% nano-alumina nanofluid of distilled water.

Surface roughness ( $\mu$ inch)	Before test			After test		
	Ra	Rq	Rz	Ra	Rq	Rz
Longitudinal	3.51	4.13	34.99	2.91	3.98	26.52
	3.85	5.64	49.99	3.28	4.59	33.81
	2.42	3.64	30.96	2.62	3.69	27.35
Transvers	3.85	5.64	49.99	3.28	4.59	33.81
	2.61	3.84	31.85	3.7	5.29	41.54
	3.61	5.13	34.99	2.91	3.98	26.52
Average	3.26	4.97	35.94	3.89	4.82	36.96

Table A. 30. Surface roughness data for copper alloy110 before- and after- 14 hours of tests with a 3.5- m/s jet of 2% nano-alumina nanofluid of distilled water.

Surface roughness ( $\mu$ inch)	Before test			After test		
	Ra	Rq	Rz	Ra	Rq	Rz
Longitudinal	3.85	5.64	49.99	3.28	4.59	33.81
	2.61	3.84	31.85	3.7	5.29	41.54
	3.61	5.13	34.99	2.91	3.98	26.52
Transvers	3.85	5.64	49.99	3.28	4.59	33.81
	2.61	3.84	31.85	3.7	5.29	41.54
	3.61	5.13	34.99	2.91	3.98	26.52
Average	3.36	4.87	38.94	3.29	4.62	33.96

Table A. 31. Surface roughness data for copper alloy110 before- and after- 28 hours of tests with a 3.5- m/s jet of 2% nano-alumina nanofluid of distilled water.

Surface roughness ( $\mu$ inch)	Before test			After test		
	Ra	Rq	Rz	Ra	Rq	Rz
Longitudinal	2.42	3.64	30.96	2.62	3.69	27.35
	2.67	4.01	31	2.72	3.9	28.05
	2.53	3.79	32.33	2.5	3.59	28.48
Transvers	2.42	3.64	30.96	2.62	3.69	27.35
	2.67	4.01	31	2.72	3.9	28.05
	2.53	3.79	32.33	2.5	3.59	28.48
Average	2.58	3.89	31.85	2.61	3.73	27.96

Table A. 32. Surface roughness data for copper alloy110 before- and after- 56 hours of tests with a 3.5- m/s jet of 2% nano-alumina nanofluid of distilled water.

Surface roughness ( $\mu$ inch)	Before test			After test		
	Ra	Rq	Rz	Ra	Rq	Rz
Longitudinal	1.86	2.99	30.78	2.09	3.45	28.69
	1.93	3.12	29.19	1.98	3.22	27.59
	1.95	3.81	35.55	3.08	3.81	24.11
Transvers	1.86	2.99	30.78	2.09	3.45	28.69
	1.93	3.12	29.19	1.98	3.22	27.59
	1.95	3.81	35.55	3.08	3.81	24.11
Average	1.91	3.31	31.84	2.38	3.49	26.80

Table A. 33. Surface roughness data for copper alloy110 before- and after- 112 hours of tests with a 3.5- m/s jet of 2% nano-alumina nanofluid of distilled water.

Surface roughness ( $\mu$ inch)	Before test			After test		
	Ra	Rq	Rz	Ra	Rq	Rz
Longitudinal	3.83	5.17	31.12	5.45	7.52	50.9
	4.15	6.67	41.05	4.89	6.71	36.26
	2.61	3.76	27.95	3.76	5.08	39.43
Transvers	3.83	5.17	31.12	5.45	7.52	50.9
	4.15	6.67	41.05	4.89	6.71	36.26
	2.61	3.76	27.95	3.76	5.08	39.43
Average	3.36	4.88	32.56	4.7	6.44	42.20

Table A. 34. Surface roughness data for copper alloy110 before- and after- 240 hours of tests with a 3.5- m/s jet of 2% nano-alumina nanofluid of distilled water.

Surface roughness ( $\mu$ inch)	Before test			After test		
	Ra	Rq	Rz	Ra	Rq	Rz
Longitudinal	4.01	6.14	52.74	5.74	7.37	50.42
	3.07	4.89	43.53	4.32	5.96	44.78
	2.87	3.94	36.89	4.86	6.63	40.21
Transvers	4.01	6.14	52.74	5.74	7.37	50.42
	3.07	4.89	43.53	4.32	5.96	44.78
	2.87	3.94	36.89	4.86	6.63	40.21
Average	3.32	4.75	41.69	4.98	6.65	45.14

Table A. 35. Surface roughness data for copper alloy110 before- and after- 312 hours of tests with a 3.5- m/s jet of 2% nano-alumina nanofluid of distilled water.

Surface roughness ( $\mu$ inch)	Before test			After test		
	Ra	Rq	Rz	Ra	Rq	Rz
Longitudinal	4.03	5.3	39.43	5.08	6.59	39.51
	3.03	4.39	35.67	5.51	7.14	46.24
	2.44	3.45	38.26	3.54	5.02	53.25
Transvers	4.03	5.3	39.43	5.08	6.59	39.51
	3.03	4.39	35.67	5.51	7.14	46.24
	2.44	3.45	38.26	3.54	5.02	53.25
Average	3.17	4.38	37.77	4.71	6.25	46.33

Table A. 36. Surface roughness data for copper alloy110 before- and after- 408 hours of tests with a 3.5- m/s jet of 2% nano-alumina nanofluid of distilled water.

Surface roughness ( $\mu$ inch)	Before test			After test		
	Ra	Rq	Rz	Ra	Rq	Rz
Longitudinal	4.01	5.74	41.29	6.62	8.54	50.4
	4.73	7.15	53.92	6.25	8.1	55.77
	3.09	4.84	41.63	7.54	9.55	61.9
Transvers	4.01	5.74	41.29	6.62	8.54	50.4
	4.73	7.15	53.92	6.25	8.1	55.77
	3.09	4.84	41.63	7.54	9.55	61.9
Average	3.94	5.91	45.61	6.80	8.73	56.02



Following Figures A.3 and A.4 displays plots of average and normalized values of Rq and Rz roughness for copper alloy110 before and after 3, 7, 14, 28, 56, 112, 240, 312 and 408 hour-treatments with the reference fluid distilled water and its 2% alumina nanofluid with 3.5 m/s jet speed respectively.

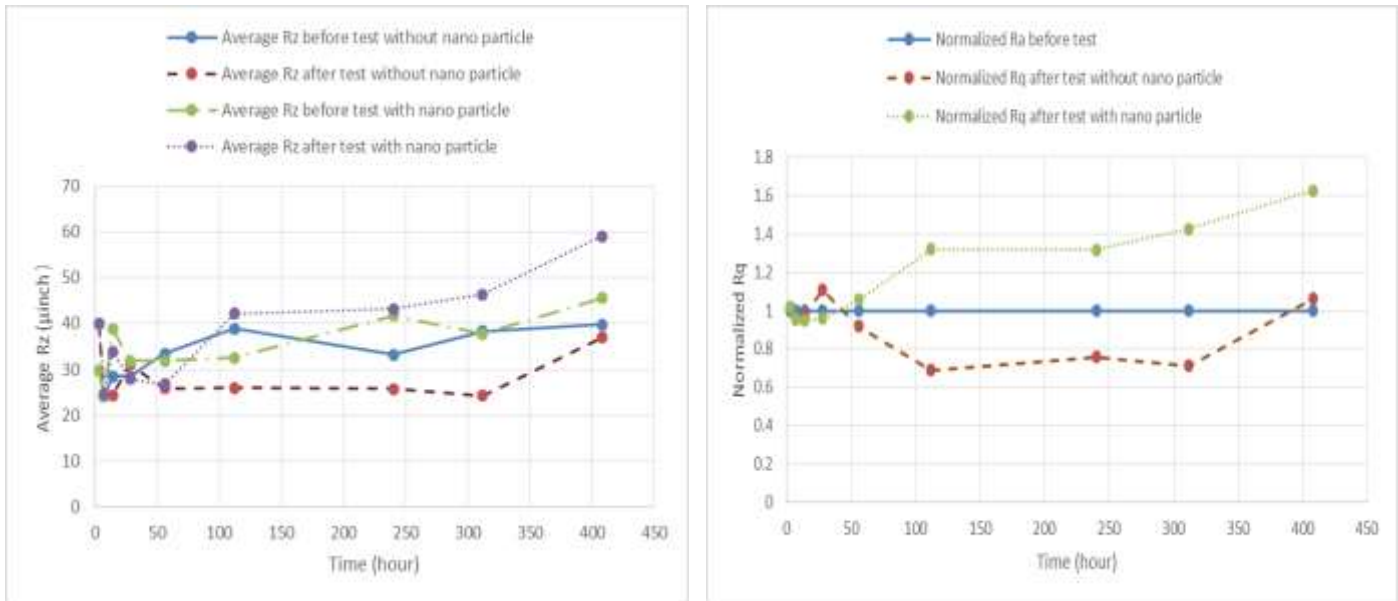


Figure A. 3. Average and normalized Rq roughness for copper alloy110 before and after 3, 7, 14, 28, 56, 112, 240, 312 and 408 hour-treatments with the reference fluid distilled water, and with nanofluid of 2% nano-alumina in reference fluid and jet speed of 3.5 m/s.

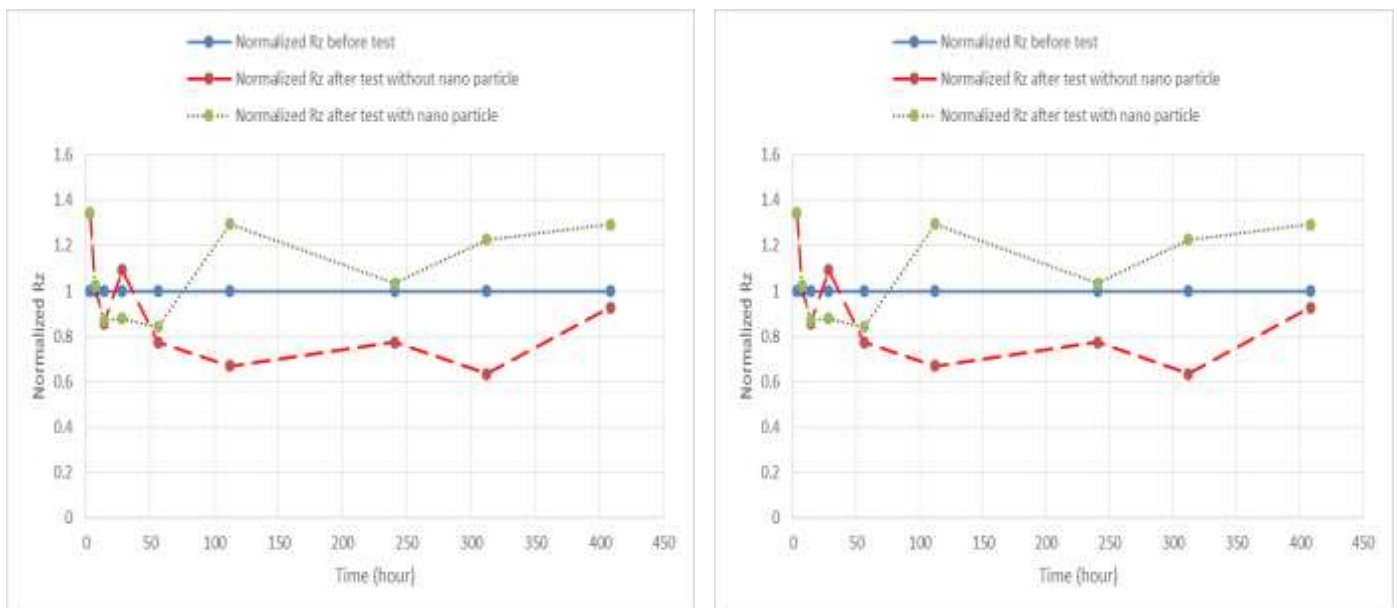


Figure A. 4. Average and normalized Rz roughness for copper alloy110 before and after 3, 7, 14, 28, 56, 112, 240, 312 and 408 hour-treatments with the reference fluid distilled water, and with nanofluid of 2% nano-alumina in reference fluid and jet speed of 3.5 m/s.

### A.1.1.3 Test results of 3.5 m/s jet impingement with 50/50% Ethylene Glycol as base fluid and its 2% alumina nanofluid on aluminum

Table A. 37. Surface roughness data for 3003-T3 aluminum before- and after- 3 hours of tests with a 3.5- m/s jet of 50% Ethylene Glycol in water.

Surface roughness ( $\mu$ inch)	Before test			After test		
	Ra	Rq	Rz	Ra	Rq	Rz
Longitudinal	4.69	6.09	42.35	4.91	6.22	35.17
	5.32	6.86	44.67	5.16	6.46	36.16
	5.09	6.59	40.74	5.24	6.76	41.81
Transvers	5.55	7.26	43.37	5.52	6.91	37.85
	4	6.48	42.53	5.14	6.78	42.97
	4.65	6.12	41.12	5.07	6.57	45.25
Average	4.88	6.57	42.46	5.17	6.62	39.87

Table A. 39. Surface roughness data for 3003-T3 aluminum before- and after- 14 hours of tests with a 3.5- m/s jet of 50% Ethylene Glycol in water.

Surface roughness ( $\mu$ inch)	Before test			After test		
	Ra	Rq	Rz	Ra	Rq	Rz
Longitudinal	6.21	7.91	43.98	7.55	9.72	56.26
	6.19	9.58	57.2	5.74	7.18	37.69
	4.29	5.94	37.51	4.58	6.26	38.69
Transvers	5.93	7.87	46.58	5.28	7.17	46.2
	4.59	6.95	36.11	4.98	5.99	38.18
	5.44	7.65	44.27	5.62	7.264	43.40
Average	6.21	7.91	43.98	7.55	9.72	56.26

Table A. 41. Surface roughness data for 3003-T3 aluminum before- and after- 56 hours of tests with a 3.5- m/s jet of 50% Ethylene Glycol in water.

Surface roughness ( $\mu$ inch)	Before test			After test		
	Ra	Rq	Rz	Ra	Rq	Rz
Longitudinal	4.52	6.29	47.3			
	4.95	7.1	52.33	3.35	4.57	31.48
	4.23	5.62	35.98	3.95	5.14	31.62
Transvers	4.52	6.29	47.3	4.31	6.15	41.55
	4.96	7.06	41.35	4.89	6.32	39
	4.09	5.71	40.64	3.95	5.14	31.62
Average	4.55	6.36	43.52	4.13	5.55	35.91

Table A. 38. Surface roughness data for 3003-T3 aluminum before- and after- 7 hours of tests with a 3.5- m/s jet of 50% Ethylene Glycol in water.

Surface roughness ( $\mu$ inch)	Before test			After test		
	Ra	Rq	Rz	Ra	Rq	Rz
Longitudinal				5.39	7.19	44.92
	5.68	7.59	50.32			
	4.57	6.01	40.51	4.67	6.67	50.48
Transvers	6.13	8.14	56.24	4.29	5.78	40.4
	4.18	6.27	40.19	4.64	6.32	45.98
	4.12	5.35	34.23	4.62	6.05	41.55
Average	4.94	6.67	44.30	4.72	6.40	44.67

Table A. 40. Surface roughness data for 3003-T3 aluminum before- and after- 28 hours of tests with a 3.5- m/s jet of 50% Ethylene Glycol in water.

Surface roughness ( $\mu$ inch)	Before test			After test		
	Ra	Rq	Rz	Ra	Rq	Rz
Longitudinal	4.02	5.4	34.35	4.15	5.79	36.84
	3.17	4.17	27.88	4.57	6.73	50.61
	5.92	6.92	41.7	4.4	6.81	45.75
Transvers	5.14	7.09	44.4	3.53	4.72	27.49
	3.04	4.18	26.98	2.45	3.13	20.3
	4.41	6.46	43.93	3.25	4.31	27.57
Average	4.28	5.71	36.54	3.73	5.25	34.76

Table A. 42. Surface roughness data for 3003-T3 aluminum before- and after- 112 hours of tests with a 3.5- m/s jet of 50% Ethylene Glycol in water.

Surface roughness ( $\mu$ inch)	Before test			After test		
	Ra	Rq	Rz	Ra	Rq	Rz
Longitudinal	3.59	4.75	33.97	3.3	4.45	33.91
	3.68	4.88	33.03	3.29	4.15	25.82
	3.59	4.55	27.67	3.3	4.27	28.21
Transvers	3.59	4.75	33.97	3.3	4.45	33.91
	3.67	4.97	35.75	3.29	4.15	25.82
	4.22	5.74	35.84	3.7	4.79	31.94
Average	3.75	4.98	33.25	3.40	4.42	29.97

Table A. 43. Surface roughness data for 3003-T3 aluminum before- and after- 240 hours of tests with a 3.5- m/s jet of 50% Ethylene Glycol in water.

Surface roughness ( $\mu$ inch)	Before test			After test		
	Ra	Rq	Rz	Ra	Rq	Rz
Longitudinal	4.21	5.18	27.93	4.83	5.96	32.34
	4.14	5.12	28.94	4.33	5.53	29.5
	6.88	8.88	49.2	4.58	5.58	27.7
Transvers	4.21	5.19	28.73	4.45	5.51	29.5
	4.54	5.38	27.99	4.6	5.58	28.9
	4.14	5.18	27.25	5.01	6.11	20.86
Average	4.69	5.82	31.67	4.63	5.71	28.13

Table A. 45. Surface roughness data for 3003-T3 aluminum before- and after- 408 hours of tests with a 3.5- m/s jet of 50% Ethylene Glycol in water.

Surface roughness ( $\mu$ inch)	Before test			After test		
	Ra	Rq	Rz	Ra	Rq	Rz
Longitudinal	3.45	4.46	30.75	4.46	5.61	34.75
	4.06	5.17	29.69	5.75	7.09	39.83
	3.79	5.02	36.8	3.64	4.78	33.45
Transvers	4.98	6.48	46.37	3.77	4.88	33.71
	3.41	4.44	30.71	3.6	4.72	36.02
	4.1	5.2	29.69	3.77	4.88	36.02
Average	3.67	5.13	34.00	4.17	5.33	35.63

Table A. 47. Surface roughness data for 3003-T3 aluminum before- and after- 7 hours of tests with a 3.5- m/s jet of 2% alumina nanofluid of 50% Ethylene Glycol in water.

Surface roughness ( $\mu$ inch)	Before test			After test		
	Ra	Rq	Rz	Ra	Rq	Rz
Longitudinal	4.33	5.65	40.61	3.92	4.92	35.17
	5.32	7.11	47.21	3.79	4.89	34.29
	4.31	5.5	33.88	3.99	5.16	35.16
Transvers	3.97	5.42	42.87	3.87	5.26	36.01
	4.13	6.5	32.81	3.95	5.12	34.08
	4.45	5.59	34.04	3.77	5.21	34.28
Average	4.42	5.96	38.57	3.88	5.09	34.83

Table A. 49. Surface roughness data for 3003-T3 aluminum before- and after- 28 hours of tests with a 3.5- m/s jet of 2% alumina nanofluid of 50% Ethylene Glycol in water.

Surface roughness ( $\mu$ inch)	Before test			After test		
	Ra	Rq	Rz	Ra	Rq	Rz
Longitudinal	3.93	5.09	32.78	3.15	4.25	32.17
	3.71	4.7	29.12	3.52	4.53	29.99
	4.44	5.62	32.28	3.59	4.58	28.3
Transvers	4.13	5.61	30.18	3.15	4.25	27.73
	3.91	4.62	29.71	3.39	4.52	28.11
	3.93	5.09	32.78	3.47	4.85	31.01
Average	4.02	5.13	30.81	3.38	4.50	29.55

Table A. 44. Surface roughness data for 3003-T3 aluminum before- and after- 312 hours of tests with a 3.5- m/s jet of 50% Ethylene Glycol in water.

Surface roughness ( $\mu$ inch)	Before test			After test		
	Ra	Rq	Rz	Ra	Rq	Rz
Longitudinal	3.1	3.52	30.88	3.33	4.74	32.61
	4.59	7.23	49.19	4.46	6.23	39.89
	3.45	5.01	31.17	4.5	6.33	41.55
Transvers	4.96	6.83	43.09	4.93	6.83	42.96
	4.73	7.18	45.35	3.94	5.73	37.7
	4.59	7.12	49.19	3.74	5.83	37.17
Average	4.16	5.91	39.94	4.23	5.97	38.94

Table A. 46. Surface roughness data for 3003-T3 aluminum before- and after- 3 hours of tests with a 3.5- m/s jet of 2% alumina nanofluid of 50% Ethylene Glycol in water.

Surface roughness ( $\mu$ inch)	Before test			After test		
	Ra	Rq	Rz	Ra	Rq	Rz
Longitudinal	4.03	5.43	36.97	3.35	4.5	35.03
	3.07	4.01	29.77	3.94	5.32	37.21
	3.11	4.18	28.58	3.82	4.86	32.91
Transvers	4.12	5.34	36.96	3.29	4.51	35.32
	3.32	4.41	35.33	3.71	4.72	32.81
	3.7	4.76	32.85	3.21	4.11	29.78
Average	3.56	4.69	33.41	3.55	4.67	33.84

Table A. 48. Surface roughness data for 3003-T3 aluminum before- and after- 14 hours of tests with a 3.5- m/s jet of 2% alumina nanofluid of 50% Ethylene Glycol in water.

Surface roughness ( $\mu$ inch)	Before test			After test		
	Ra	Rq	Rz	Ra	Rq	Rz
Longitudinal	3.15	4.05	27.07	3.48	4.92	36.41
	4.57	5.78	35.62	3.7	4.85	34.71
	5.17	6.61	40.34	3.89	5.77	31.29
Transvers	5.17	7.45	45.35	3.8	4.93	32.2
	4.67	5.79	35.63	4.12	5.97	39.27
	4.15	5.17	35.63	4.69	5.87	35.79
Average	4.48	5.81	36.61	3.95	5.39	34.95

Table A. 50. Surface roughness data for 3003-T3 aluminum before- and after- 56 hours of tests with a 3.5- m/s jet of 2% alumina nanofluid of 50% Ethylene Glycol in water.

Surface roughness ( $\mu$ inch)	Before test			After test		
	Ra	Rq	Rz	Ra	Rq	Rz
Longitudinal	2.45	3.2	22.71	2.87	3.06	23.14
	3.23	4.26	27.79	2.13	2.77	17.99
	2.36	3.17	22.3	2.25	3.13	21.19
Transvers	2.78	3.21	22.17	2.43	3.12	22.13
	2.81	3.17	22.77	2.39	2.78	19.88
	2.81	3.11	21.98	2.46	2.99	20.67
Average	2.74	3.35	23.29	2.42	2.98	20.83

Table A. 51. Surface roughness data for 3003-T3 aluminum before- and after- 112 hours of tests with a 3.5- m/s jet of 2% alumina nanofluid of 50% Ethylene Glycol in water.

Surface roughness ( $\mu$ inch)	Before test			After test		
	Ra	Rq	Rz	Ra	Rq	Rz
Longitudinal	3.33	4.36	27.23	2.86	3.78	24.1
	2.31	3.02	21.4	2.65	3.4	20.98
	2.41	3.88	30.38	2.32	3.87	30.38
Transvers	3.13	4.16	27.22	2.05	2.64	17.05
	2.21	3.01	21.22	2.12	3.11	22.21
	2.44	3.89	30.01	2.34	3.59	28.11
Average	2.64	3.72	26.24	2.39	3.40	23.81

Table A. 53. Surface roughness data for 3003-T3 aluminum before- and after- 312 hours of tests with a 3.5- m/s jet of 2% alumina nanofluid of 50% Ethylene Glycol in water.

Surface roughness ( $\mu$ inch)	Before test			After test		
	Ra	Rq	Rz	Ra	Rq	Rz
Longitudinal	4.86	6.22	33.5	3.79	4.82	31.38
	3.68	5.51	38.52	4.68	4.58	32.84
	5.18	6.38	35.36	3.78	4.87	33.9
Transvers	3.17	4.15	38.12	4.23	6.31	42.21
	5.91	6.83	45.73	4.56	6.57	43.12
	3.68	5.51	38.52	3.91	5.47	42.19
Average	4.56	5.82	38.25	4.16	5.44	37.61

Table A. 52. Surface roughness data for 3003-T3 aluminum before- and after- 240 hours of tests with a 3.5- m/s jet of 2% alumina nanofluid of 50% Ethylene Glycol in water.

Surface roughness ( $\mu$ inch)	Before test			After test		
	Ra	Rq	Rz	Ra	Rq	Rz
Longitudinal	4.24	5.69	36.94	3.96	5.71	42.98
	3.81	5.04	35.5	4.87	6.11	38.17
	5.87	6.85	51.17	4.83	5.36	37.99
Transvers	5.63	7.46	48.39	5.62	6.93	47.99
	4.42	5.96	36.49	5.89	6.97	42.17
	4.12	5.61	36.44	4.92	6.89	49.17
Average	4.68	6.10	40.82	5.02	6.33	43.08

Table A. 54. Surface roughness data for 3003-T3 aluminum before- and after- 408 hours of tests with a 3.5- m/s jet of 2% alumina nanofluid of 50% Ethylene Glycol in water.

Surface roughness ( $\mu$ inch)	Before test			After test		
	Ra	Rq	Rz	Ra	Rq	Rz
Longitudinal	4.43	5.58	34.88	4.68	4.45	34.68
	3.79	4.82	29.85	2.77	3.92	25.98
	3.88	4.78	27.58	3.18	4.86	25.38
Transvers	3.91	4.87	26.59	2.95	3.85	25.43
	4.13	5.68	33.91	3.45	4.92	27.36
	3.79	4.83	29.81	3.23	4.12	38.01
Average	3.99	5.09	30.44	3.38	4.35	29.47

Following Figures A.5 and A.6 displays plots of average and normalized values of Rq and Rz roughness for 3003-T3 aluminum before and after 3, 7, 14, 28, 56, 112, 240, 312 and 408 hour-treatments with the reference fluid of 50/50% Ethylene Glycol in water and its 2% alumina nanofluid with 3.5 m/s jet speed respectively.

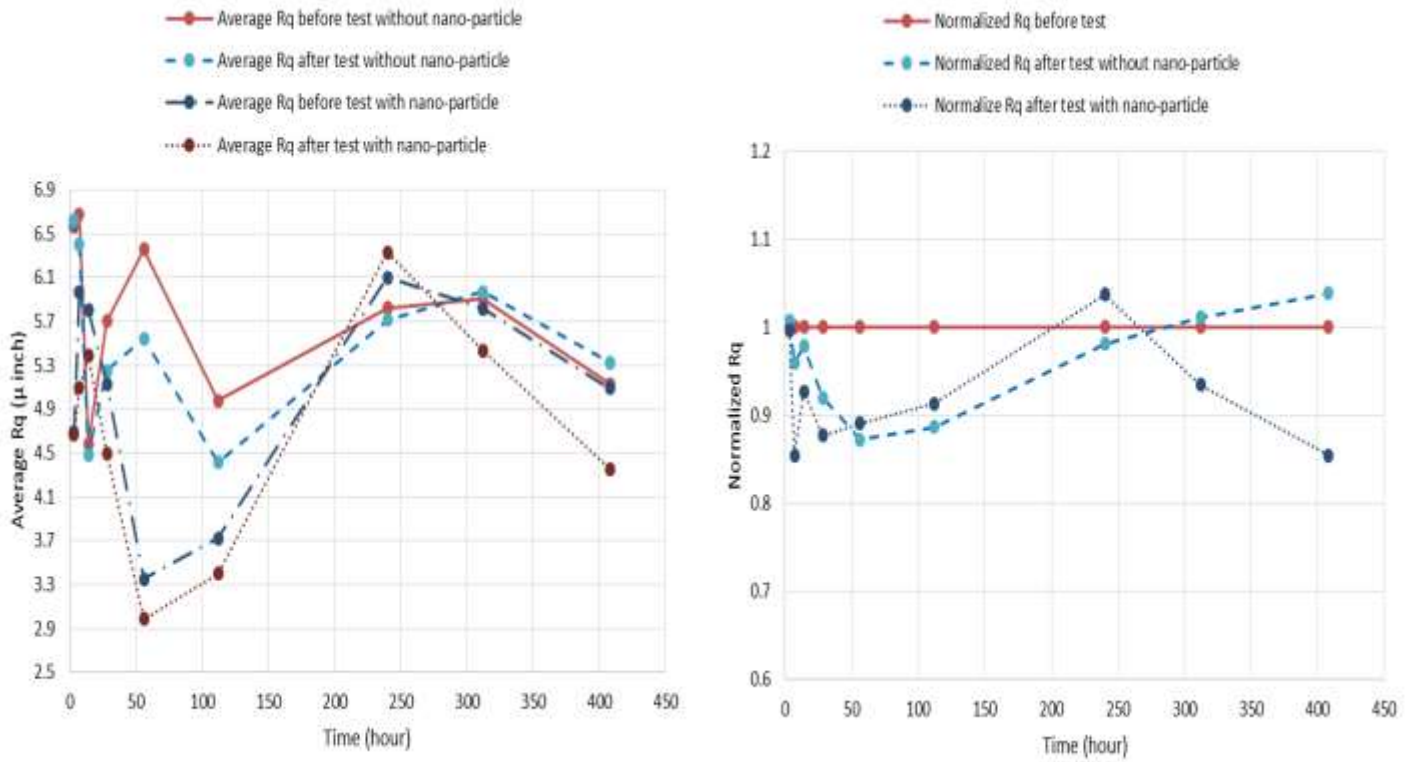


Figure A. 5. Average and normalized Rq roughness for 3003-T3 aluminum before and after 3, 7, 14, 28, 56, 112, 240, 312 and 408 hour-treatments with the reference fluid of 50/50% Ethylene Glycol in water and its 2% alumina nanofluid and jet speed of 3.5 m/s.

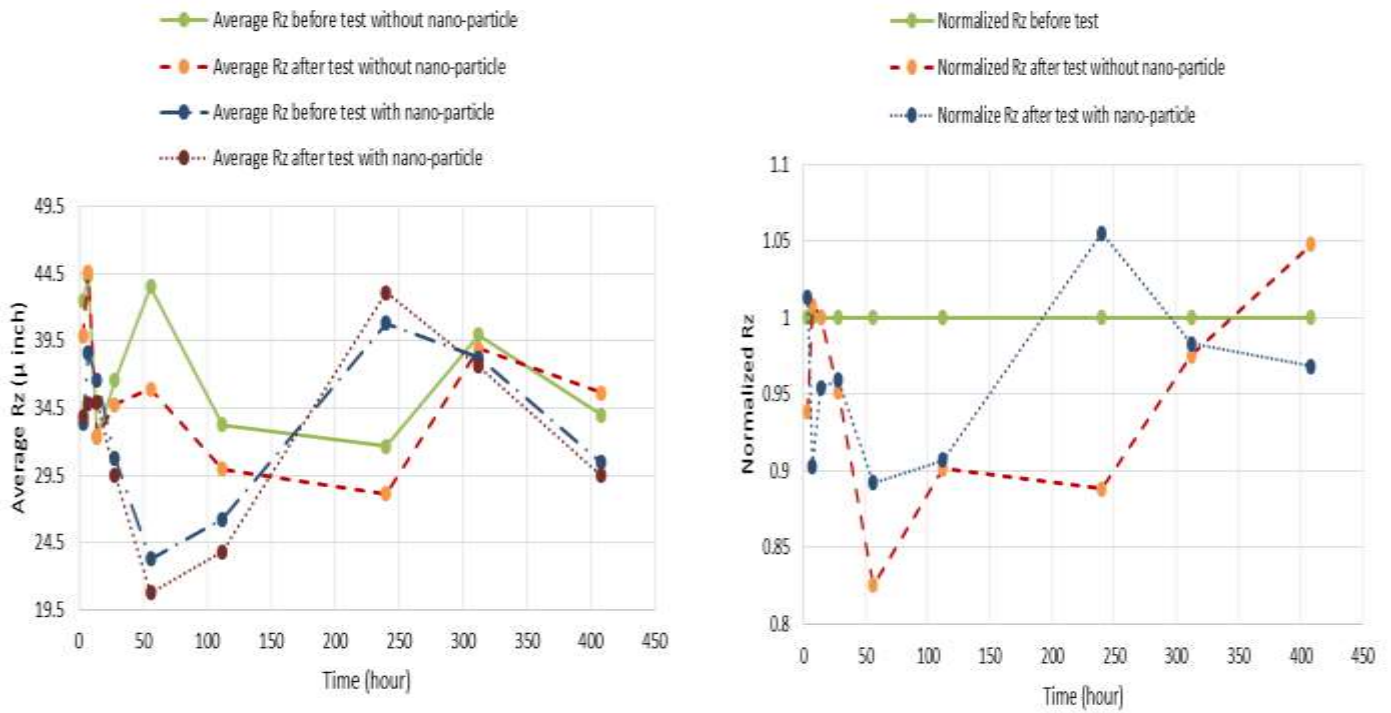


Figure A. 6. Average and normal Rz roughness for 3003-T3 aluminum before and after 3, 7, 14, 28, 56, 112, 240, 312 and 408 hour-treatments with the reference fluid of 50/50% Ethylene Glycol in water and its 2% alumina nanofluid and jet speed of 3.5 m/s.

### A.1.1.4 Test results of 3.5 m/s jet impingement with 50/50% Ethylene Glycol as base fluid and its 2% alumina nanofluid on Copper

Table A. 56. Surface roughness data for copper alloy110 before- and after- 3 hours of tests with a 3.5- m/s jet of reference fluid of 50% Ethylene Glycol in water.

Surface roughness ( $\mu$ inch)	Before test			After test		
	Ra	Rq	Rz	Ra	Rq	Rz
Longitudinal	2	2.92	23.31	2.41	3.14	21.1
	2.96	3.89	24.15	1.94	2.78	20.95
	2.61	3.17	23.91	1.77	2.54	23.52
Transvers	2.55	3.64	29.39	2.11	3.19	26.49
	2.62	3.61	22.19	2.23	2.87	17.06
	2.51	3.65	29.19	3.95	5.49	26.32
Average	2.54	3.48	25.36	2.40	3.34	22.57

Table A. 58. Surface roughness data for copper alloy110 before- and after- 14 hours of tests with a 3.5- m/s jet of reference fluid of 50% Ethylene Glycol in water.

Surface roughness ( $\mu$ inch)	Before test			After test		
	Ra	Rq	Rz	Ra	Rq	Rz
Longitudinal	2.16	2.92	21.78	2.2	3.32	25.98
	3.32	5.21	38.17	1.97	2.91	22.98
	2.24	3	23.16	2.1	3.17	27.64
Transvers	2.17	2.81	22.17	1.88	2.69	21.31
	3.13	5.12	37.17	2.42	4	33.75
	3.11	4.81	37.16	2.58	3.76	30.12
Average	2.69	3.98	29.94	2.20	3.31	26.96

Table A. 60. Surface roughness data for copper alloy110 before- and after- 56 hours of tests with a 3.5- m/s jet of reference fluid of 50% Ethylene Glycol in water.

Surface roughness ( $\mu$ inch)	Before test			After test		
	Ra	Rq	Rz	Ra	Rq	Rz
Longitudinal	2.87	4.07	32.37	2.07	2.83	19.38
	2.42	3.14	20.92	1.65	2.39	22.44
	4.17	6.24	41.78	1.88	2.74	20.11
Transvers	2.69	4.08	31.65	1.7	2.56	22.29
	3.13	4.74	22.12	2.2	3.14	23.39
				2.04	2.93	22.74
Average	3.06	4.45	29.77	1.92	2.77	21.73

Table A. 57. Surface roughness data for copper alloy110 before- and after- 7 hours of tests with a 3.5- m/s jet of reference fluid of 50% Ethylene Glycol in water.

Surface roughness ( $\mu$ inch)	Before test			After test		
	Ra	Rq	Rz	Ra	Rq	Rz
Longitudinal	2.36	3.49	31.52	2.77	3.25	25.78
	2.11	2.95	24.57	2.04	2.84	20.76
	3.93	5.66	46.59	2.84	4.4	36.62
Transvers	3.13	5.12	46.15	2.97	4.33	33.53
	2.19	2.98	24.71	2.56	3.72	27.69
	3.19	4.98	46.51	2.34	3.42	26.56
Average	2.82	4.20	36.68	2.59	3.66	28.49

Table A. 59. Surface roughness data for copper alloy110 before- and after- 28 hours of tests with a 3.5- m/s jet of reference fluid of 50% Ethylene Glycol in water.

Surface roughness ( $\mu$ inch)	Before test			After test		
	Ra	Rq	Rz	Ra	Rq	Rz
Longitudinal	4.87	5.83	33.48	3.22	4.45	33.59
	3.33	4.6	38.08	3.2	4.4	38.04
	3.13	4.15	37.89	2.84	3.9	27.1
Transvers	3.34	4.51	37.19	3.18	5.61	47.7
	3.45	5.78	50.97	2.4	4.01	31.51
	3.33	4.6	38.08	3.2	4.4	38.04
Average	3.63	4.98	39.52	2.97	4.47	35.59

Table A. 61. Surface roughness data for copper alloy110 before- and after- 112 hours of tests with a 3.5- m/s jet of reference fluid of 50% Ethylene Glycol in water.

Surface roughness ( $\mu$ inch)	Before test			After test		
	Ra	Rq	Rz	Ra	Rq	Rz
Longitudinal	5.42	7.4	48.65	3.13	6.57	57.11
	3.2	5.17	43.95	2.01	2.91	23.38
	3.4	5.98	59.16	2.75	4.11	31.7
Transvers	4.76	6.78	40.45	2.9	4.42	40.3
	3.33	5.19	43.59	2.64	3.62	27.71
	4.16	6.18	40.24	2.39	3.65	30.49
Average	4.05	6.12	46.01	2.64	4.21	35.12

Table A. 62. Surface roughness data for copper alloy110 before- and after- 240 hours of tests with a 3.5- m/s jet of reference fluid of 50% Ethylene Glycol in water.

Surface roughness ( $\mu$ inch)	Before test			After test		
	Ra	Rq	Rz	Ra	Rq	Rz
Longitudinal	2.6	3.81	31.05	2.2	3.18	23.87
	4.06	5.78	45.62	1.9	2.65	19.66
	4.17	5.17	44.89	2.64	3.85	31.18
Transvers	3.26	3.17	32.06	3.23	4.69	35.15
	2.05	2.91	23.07	2.06	2.81	21.69
	2.71	3.01	24.16	2.62	3.73	25.01
Average	3.14	3.98	33.48	2.44	3.49	26.09

Table A. 64. Surface roughness data for copper alloy110 before- and after- 408 hours of tests with a 3.5- m/s jet of reference fluid of 50% Ethylene Glycol in water.

Surface roughness ( $\mu$ inch)	Before test			After test		
	Ra	Rq	Rz	Ra	Rq	Rz
Longitudinal	3.41	5.22	38.48	3.49	5.09	41.57
	2.55	3.73	31.82	3.48	4.8	36.1
	2.93	4.11	31.81	3.5	4.9	37.2
Transvers	3.14	5.22	38.46	3.83	5.56	40.69
	3.21	5.11	37.98	3.5	4.48	33.13
	3.41	5.22	38.48	3.15	4.05	27.85
Average	3.05	4.68	35.71	3.49	4.81	36.09

Table A. 66. Surface roughness data for copper alloy110 before- and after- 7 hours of tests with a 3.5- m/s jet of 2% alumina nanofluid of 50% Ethylene Glycol in water.

Surface roughness ( $\mu$ inch)	Before test			After test		
	Ra	Rq	Rz	Ra	Rq	Rz
Longitudinal	4.39	6.66	43.006	2.67	4.35	32.35
	3.3	5.27	44.23	2.48	3.74	28.17
	4.14	6.76	43.13	3.91	4.23	39.17
Transvers	4.24	6.17	43.23	3.87	5.87	43.23
	3.39	5.28	43.98	3.92	4.23	39.17
	4.14	6.76	43.13	2.24	3.71	28.23
Average	3.89	6.03	43.52	3.18	4.36	35.05

Table A. 68. Surface roughness data for copper alloy110 before- and after- 28 hours of tests with a 3.5- m/s jet of 2% alumina nanofluid of 50% Ethylene Glycol in water.

Surface roughness ( $\mu$ inch)	Before test			After test		
	Ra	Rq	Rz	Ra	Rq	Rz
Longitudinal	4.185	6.17	42.75	3.5	5.2	38.44
	3.91	5.53	35.55	2.68	4.24	37.09
	4.87	6.83	45.49	3.43	5.46	42.47
Transvers	3.93	5.56	36.15	3.52	5.22	38.14
	4.81	6.81	44.47	2.87	4.32	38.27
	3.91	5.53	35.55	3.11	5.29	39.17
Average	4.34	6.18	40.88	3.19	4.96	38.93

Table A. 63. Surface roughness data for copper alloy110 before- and after- 312 hours of tests with a 3.5- m/s jet of reference fluid of 50% Ethylene Glycol in water.

Surface roughness ( $\mu$ inch)	Before test			After test		
	Ra	Rq	Rz	Ra	Rq	Rz
Longitudinal	3.27	4.64	41.04	4.73	6.61	45.57
	5.74	7.76	54.52	4.99	6.95	50.22
	3.09	4.17	26.14	4.73	6.61	45.57
Transvers	6.67	9.08	48.96	4.7	6.59	42.8
	5.75	7.78	54.53	4.5	6.43	42.49
	5.15	7.18	53.98	4.7	6.59	42.8
Average	4.95	6.77	46.53	4.73	6.65	45.27

Table A. 65. Surface roughness data for copper alloy110 before- and after- 3 hours of tests with a 3.5- m/s jet of 2% alumina nanofluid of 50% Ethylene Glycol in water.

Surface roughness ( $\mu$ inch)	Before test			After test		
	Ra	Rq	Rz	Ra	Rq	Rz
Longitudinal	2.036	3.25	28.83	3.59	5.82	52.06
	2.05	3.08	25.67	2.88	4.12	39.6
	3.12	3.35	24.44	3.36	5.34	45.86
Transvers	2.91	4.79	43.99	3.34	4.98	45.11
	3.44	5.56	46.25	2.88	4.71	36.75
	3.82	6.45	59.92	3.39	5.15	36.64
Average	2.89	4.41	38.18	3.24	5.02	42.67

Table A. 67. Surface roughness data for copper alloy110 before- and after- 14 hours of tests with a 3.5- m/s jet of 2% alumina nanofluid of 50% Ethylene Glycol in water.

Surface roughness ( $\mu$ inch)	Before test			After test		
	Ra	Rq	Rz	Ra	Rq	Rz
Longitudinal	3.03	4.91	47.38	3.58	5.45	46.96
	4.47	6.05	41.21	3.59	5.85	53.35
	4.75	6.96	43.03	3.47	5.17	37.26
Transvers	3.67	4.98	48.31	3.69	5.23	44.83
	3.17	4.99	48.57	3.65	5.38	43.91
	4.17	6.15	42.01	3.66	5.65	52.66
Average	3.88	5.67	45.09	3.61	5.46	46.50

Table A. 69. Surface roughness data for copper alloy110 before- and after- 56 hours of tests with a 3.5- m/s jet of 2% alumina nanofluid of 50% Ethylene Glycol in water.

Surface roughness ( $\mu$ inch)	Before test			After test		
	Ra	Rq	Rz	Ra	Rq	Rz
Longitudinal	2.44	3.83	32.76	1.39	2.01	14.81
	1.89	2.76	21.22	2.01	2.69	18.06
	2.25	3.19	22.57	2.01	2.99	22.72
Transvers	1.99	2.89	22.11	1.43	2.26	22.63
	2.22	3.12	21.75	1.66	2.64	23.33
	2.41	2.58	33.11	1.59	2.63	21.22
Average	2.2	3.06	25.59	1.68	2.54	20.46

Table A. 70. Surface roughness data for copper alloy110 before- and after- 112 hours of tests with a 3.5- m/s jet of 2% alumina nanofluid of 50% Ethylene Glycol in water.

Surface roughness ( $\mu$ inch)	Before test			After test		
	Ra	Rq	Rz	Ra	Rq	Rz
Longitudinal	2.78	3.67	33.13	1.38	2.01	15.61
	1.87	2.62	21.36	1.79	2.69	16.98
	2.57	3.24	29.43	1.74	2.52	22.04
Transversers	2.1	3.15	24.93	1.94	3.12	31.18
	2.05	3.25	25.39	2.11	3.25	29.11
	2.01	3.12	22.39	2.1	3.22	25.29
Average	2.23	3.18	26.11	1.84	2.80	23.37

Table A. 72. Surface roughness data for copper alloy110 before- and after- 312 hours of tests with a 3.5- m/s jet of 2% alumina nanofluid of 50% Ethylene Glycol in water.

Surface roughness ( $\mu$ inch)	Before test			After test		
	Ra	Rq	Rz	Ra	Rq	Rz
Longitudinal	3.91	5.74	42	3.67	5.26	39.87
	4.25	6.23	50.7	3.64	5.2	39.98
	4.15	6.12	51.17	3.87	6.58	50.51
Transversers	3.87	5.89	42.11	3.71	6.11	42.55
	4.61	6.06	38.28	3.68	5.55	41.26
	4.11	6.13	50.87	3.69	5.34	43.01
Average	4.15	6.03	45.86	3.71	5.67	42.86

Table A. 71. Surface roughness data for copper alloy110 before- and after- 240 hours of tests with a 3.5- m/s jet of 2% alumina nanofluid of 50% Ethylene Glycol in water.

Surface roughness ( $\mu$ inch)	Before test			After test		
	Ra	Rq	Rz	Ra	Rq	Rz
Longitudinal	3.09	4.31	33.03	2.69	3.98	36.25
	2.61	3.5	26.48	2.4	3.36	29.99
	2.85	4.03	35.18	2.5	4.09	43.16
Transversers	2.71	3.55	26.78	2.94	4.32	34.99
	2.78	3.56	26.81	2.94	4.31	37.46
	3.19	4.15	32.71	3.04	4.53	37.56
Average	2.87	3.85	30.17	2.75	4.10	36.57

Table A. 73. Surface roughness data for copper alloy110 before- and after- 408 hours of tests with a 3.5- m/s jet of 2% alumina nanofluid of 50% Ethylene Glycol in water.

Surface roughness ( $\mu$ inch)	Before test			After test		
	Ra	Rq	Rz	Ra	Rq	Rz
Longitudinal	4.51	6.77	60.28	4.3	6.31	47.67
	4.41	7	56.49	4.29	6.11	42.28
	4.27	6.15	43.76	3.34	4.55	30.77
Transversers	4.15	7.11	55.47	3.89	5.64	41.23
	4.51	6.57	42.16	3.99	5.63	42.11
	4.62	6.17	41.76	4.01	6.01	41.33
Average	4.41	6.63	49.99	3.97	5.71	40.89



Following Figures A.7 and A.8 displays plots of average and normalized values of Rq and Rz roughness for copper alloy110 before and after 3, 7, 14, 28, 56, 112, 240, 312 and 408 hour-treatments with the reference fluid of 50/50% Ethylene Glycol in water and its 2% alumina nanofluid with 3.5 m/s jet speed respectively.

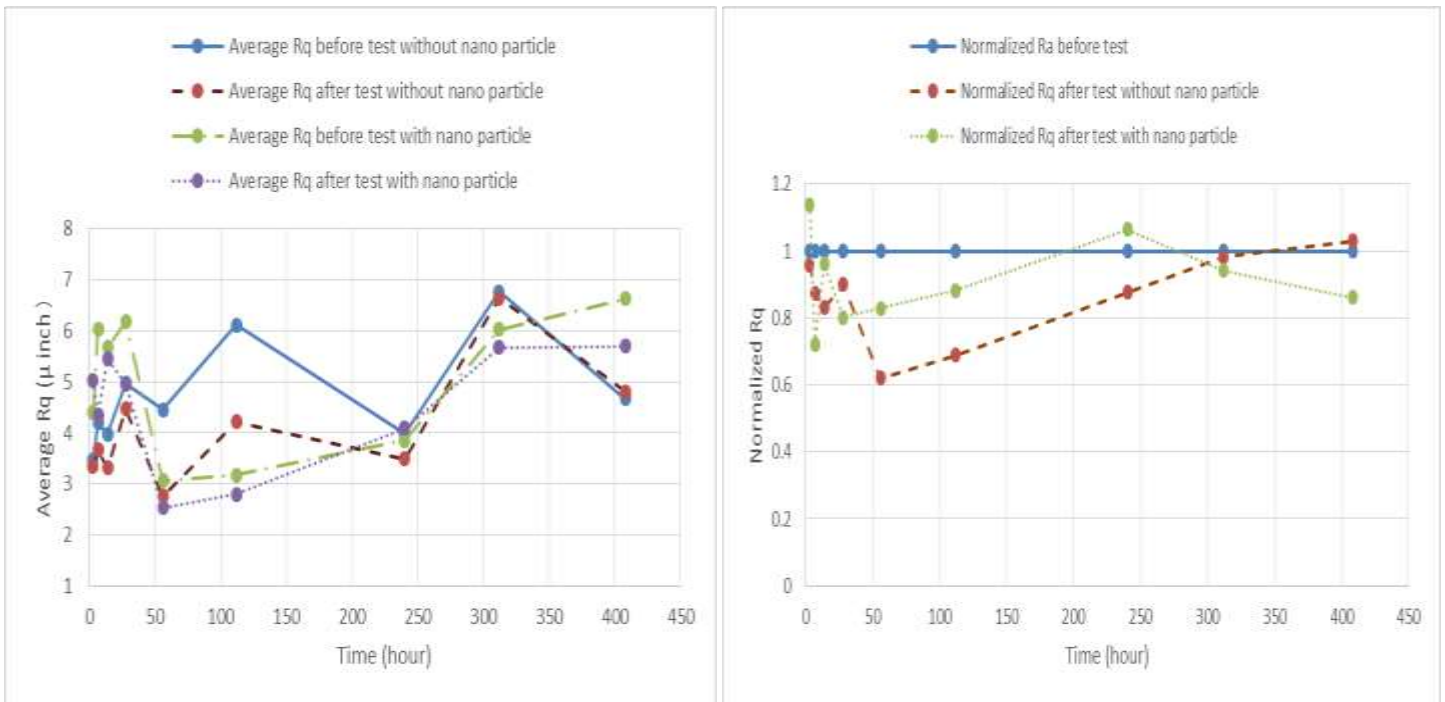


Figure A. 7. Average and normal Rq roughness for copper alloy110 before and after 3, 7, 14, 28, 56, 112, 240, 312 and 408 hour-treatments with the reference fluid of 50/50% Ethylene Glycol in water and its 2% alumina nanofluid and jet speed of 3.5 m/s.

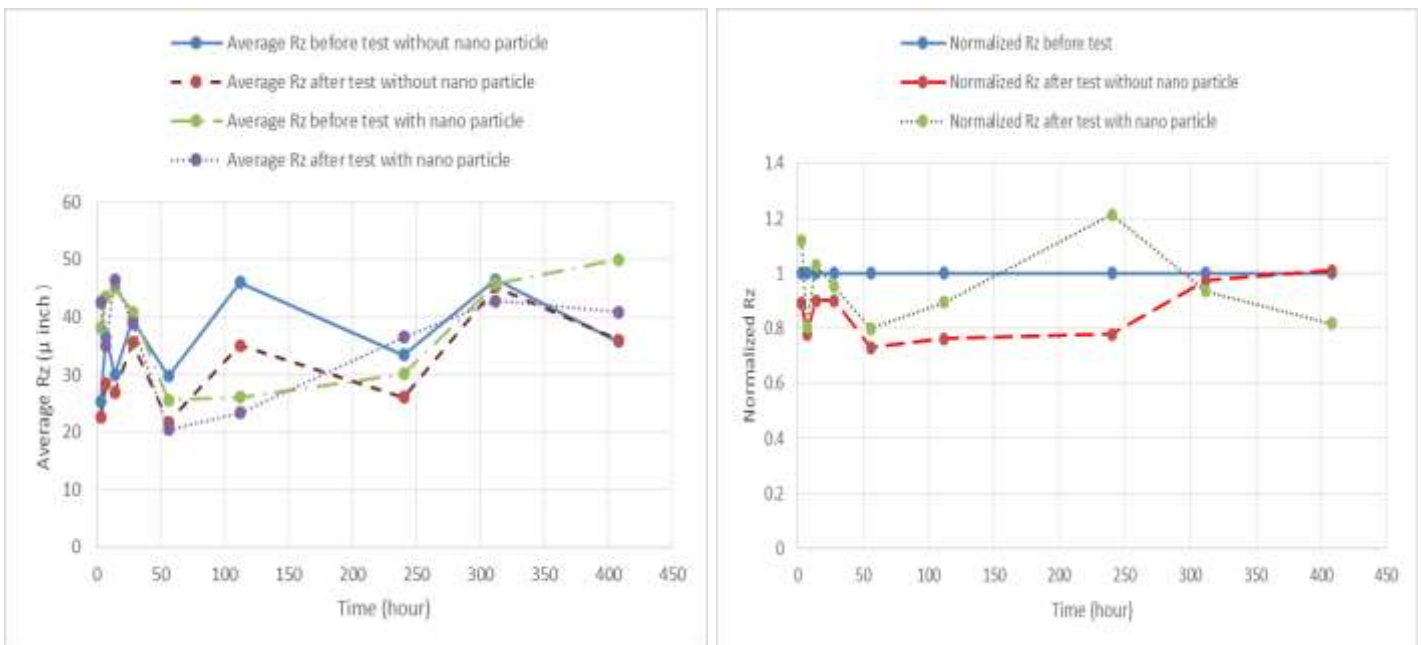


Figure A. 8. Average and normal Rz roughness for copper alloy110 before and after 3, 7, 14, 28, 56, 112, 240, 312 and 408 hour-treatments with the reference fluid of 50/50% Ethylene Glycol in water and its 2% alumina nanofluid and jet speed of 3.5 m/s.

## A.1.2 Test results for 10.7 m/s jet impingement treatments

### A.1.2.1 Test results of 10.7 m/s jet impingement with distilled water as base fluid and its nanofluid on aluminum

Table A. 74. Surface roughness data for 3003-T3 aluminum before- and after- 3 hours of tests with a 3.5- m/s jet of distilled water.

Surface roughness ( $\mu$ inch)	Before test			After test		
	Ra	Rq	Rz	Ra	Rq	Rz
Longitudinal	3.47	3.98	35.41	11.89	12.45	75.68
	4.01	4.28	36.01	12.12	11.75	81.56
	3.24	4.35	33.25	10.72	13.34	88.06
Transvers	4.62	5.9	36.3	9.68	12.05	94.67
	3.61	4.73	33.42	11.27	14.75	112.5
	3.34	4.35	33.25	10.72	14.34	88.06
Average	3.15	4.09	33.35	11.31	12.32	79.81

Table A. 75. Surface roughness data for 3003-T3 aluminum before- and after- 7 hours of tests with a 3.5- m/s jet of distilled water.

Surface roughness ( $\mu$ inch)	Before test			After test		
	Ra	Rq	Rz	Ra	Rq	Rz
Longitudinal	3.54	4.35	33.25	10.72	13.34	98.06
	4.52	5.91	36.34	9.68	14.05	114.67
	4.01	4.28	31.01	12.12	11.75	81.56
Transvers	3.24	4.35	23.25	10.72	13.34	108.06
	3.25	4.73	33.42	11.27	14.75	92.5
	3.14	4.35	33.25	10.72	14.34	88.06
Average	3.65	4.43	32.65	11.56	13.38	101.41

Table A. 76. Surface roughness data for 3003-T3 aluminum before- and after- 14 hours of tests with a 3.5- m/s jet of distilled water.

Surface roughness ( $\mu$ inch)	Before test			After test		
	Ra	Rq	Rz	Ra	Rq	Rz
Longitudinal	4.62	5.9	36.3	9.68	14.05	104.67
	3.71	4.73	33.42	11.27	14.75	102.5
	3.24	4.35	33.25	10.72	14.34	88.06
Transvers	4.62	5.9	36.3	9.68	14.05	104.67
	3.71	4.73	33.42	11.27	14.75	102.5
	3.24	4.35	33.25	10.72	14.34	88.06
Average	3.85	4.99	34.32	10.56	14.38	98.41

Table A. 77. Surface roughness data for 3003-T3 aluminum before- and after- 28 hours of tests with a 3.5- m/s jet of distilled water.

Surface roughness ( $\mu$ inch)	Before test			After test		
	Ra	Rq	Rz	Ra	Rq	Rz
Longitudinal	3.24	4.35	23.25	10.72	13.34	98.06
	3.25	4.73	33.42	11.27	14.75	95.51
	3.24	4.35	33.25	10.72	14.34	88.06
Transvers	4.62	5.9	36.3	9.68	14.05	94.67
	3.71	4.73	33.42	11.27	14.75	112.5
	3.24	4.35	33.25	10.72	14.34	108.06
Average	3.75	4.19	33.36	12.57	16.39	101.41

Table A. 78. Surface roughness data for 3003-T3 aluminum before- and after- 56 hours of tests with a 3.5- m/s jet of distilled water.

Surface roughness ( $\mu$ inch)	Before test			After test		
	Ra	Rq	Rz	Ra	Rq	Rz
Longitudinal	4.75	5.92	35.23	14.69	18.91	110.44
	4.74	6.2	40.75	16.44	20.67	111.18
	3.98	5.11	33.25	17.3	20.75	104.07
Transvers	4.75	5.92	35.23	14.69	18.91	110.44
	4.74	6.2	40.75	16.44	20.67	111.18
	3.98	5.11	33.25	17.3	20.75	104.07
Average	4.49	5.74	36.41	16.14	20.11	108.56

Table A. 79. Surface roughness data for 3003-T3 aluminum before- and after- 112 hours of tests with a 3.5- m/s jet of distilled water.

Surface roughness ( $\mu$ inch)	Before test			After test		
	Ra	Rq	Rz	Ra	Rq	Rz
Longitudinal	3.44	4.52	32.3	17.05	23.79	172.81
	2.4	3.16	23	18.73	26.11	157.03
	3.2	4.08	23.68	17.29	23.77	138.44
Transvers	3.44	4.52	32.3	24.69	18.91	110.44
	2.4	3.16	23	19.44	20.67	111.18
	3.2	4.08	23.68	27.3	20.75	104.07
Average	3.01	3.92	26.32	19.45	24.23	135.37

Table A. 81. Surface roughness data for 3003-T3 aluminum before- and after- 3 hours of tests with a 3.5- m/s jet of 2% nano-alumina nanofluid of distilled water.

Surface roughness ( $\mu$ inch)	Before test			After test		
	Ra	Rq	Rz	Ra	Rq	Rz
Longitudinal	3.54	4.35	33.25	10.72	13.34	98.06
	4.52	5.91	36.34	9.68	14.05	114.67
	4.01	4.28	31.01	12.12	11.75	81.56
Transvers	3.24	4.35	23.25	10.72	13.34	108.06
	3.25	4.73	33.42	11.27	14.75	92.5
	3.14	4.35	33.25	10.72	14.34	88.06
Average	3.65	4.43	32.65	11.56	13.38	101.41

Table A. 83. Surface roughness data for 3003-T3 aluminum before- and after- 14 hours of tests with a 3.5- m/s jet of 2% nano-alumina nanofluid of distilled water.

Surface roughness ( $\mu$ inch)	Before test			After test		
	Ra	Rq	Rz	Ra	Rq	Rz
Longitudinal	4.91	7.28	44.32	14.03	21.3	133.32
	3.26	4.28	31.71	16	25.04	150.33
	4.22	5.46	38.78	17.74	25.56	147.26
Transvers	4.91	7.28	44.32	14.03	21.3	133.32
	3.26	4.28	31.71	16	25.04	150.33
	4.22	5.46	38.78	17.74	25.56	147.26
Average	4.13	5.68	38.27	15.93	23.97	143.64

Table A. 85. Surface roughness data for 3003-T3 aluminum before- and after- 56 hours of tests with a 3.5- m/s jet of 2% nano-alumina nanofluid of distilled water.

Surface roughness ( $\mu$ inch)	Before test			After test		
	Ra	Rq	Rz	Ra	Rq	Rz
Longitudinal	2.66	3.47	21.37	17.05	23.79	172.81
	3.08	4	25.55	18.73	26.11	157.03
	3.24	4.14	26.05	17.29	23.77	138.44
Transvers	2.66	3.47	21.37	17.05	23.79	172.81
	3.08	4	25.55	18.73	26.11	157.03
	3.24	4.14	26.05	17.29	23.77	138.44
Average	2.99	3.87	24.33	17.69	24.56	156.09

Table A. 82. Surface roughness data for 3003-T3 aluminum before- and after- 7 hours of tests with a 3.5- m/s jet of 2% nano-alumina nanofluid of distilled water.

Surface roughness ( $\mu$ inch)	Before test			After test		
	Ra	Rq	Rz	Ra	Rq	Rz
Longitudinal	3.24	4.35	23.25	10.72	13.34	98.06
	3.25	4.73	33.42	11.27	14.75	95.51
	3.24	4.35	33.25	10.72	14.34	88.06
Transvers	4.62	5.9	36.3	9.68	14.05	94.67
	3.71	4.73	33.42	11.27	14.75	112.5
	3.24	4.35	33.25	10.72	14.34	108.06
Average	3.75	4.19	33.36	12.57	16.39	101.41

Table A. 84. Surface roughness data for 3003-T3 aluminum before- and after- 28 hours of tests with a 3.5- m/s jet of 2% nano-alumina nanofluid of distilled water.

Surface roughness ( $\mu$ inch)	Before test			After test		
	Ra	Rq	Rz	Ra	Rq	Rz
Longitudinal	3.47	3.98	35.41	11.89	12.45	75.68
	4.01	4.28	36.01	12.12	11.75	81.56
	3.24	4.35	33.25	10.72	13.34	88.06
Transvers	4.62	5.9	36.3	9.68	12.05	94.67
	3.61	4.73	33.42	11.27	14.75	112.5
	3.34	4.35	33.25	10.72	14.34	88.06
Average	3.15	4.09	33.35	11.31	12.32	79.81

Table A. 86. Surface roughness data for 3003-T3 aluminum before- and after- 112 hours of tests with a 3.5- m/s jet of 2% nano-alumina nanofluid of distilled water.

Surface roughness ( $\mu$ inch)	Before test			After test		
	Ra	Rq	Rz	Ra	Rq	Rz
Longitudinal	3.44	4.52	32.3	37.88	49.56	248.66
	2.4	3.16	23	34.3	44.94	312.08
	3.2	4.08	23.68	28.48	55.05	237.09
Transvers	3.44	4.52	32.3	37.88	49.16	148.66
	2.4	3.16	23	34.3	44.94	212.08
	3.2	4.08	23.68	38.48	45.05	137.09
Average	3.02	3.92	26.33	35.23	49.01	265.13

Following Figures A.9 and A.10 displays plots of average and normalized values of Rq and Rz roughness for 3003-T3 aluminum before and after 3, 7, 14, 28, 56 and 112 hour-treatments with the reference fluid of distilled water and its 2% alumina nanofluid with 10.7 m/s jet speed respectively.

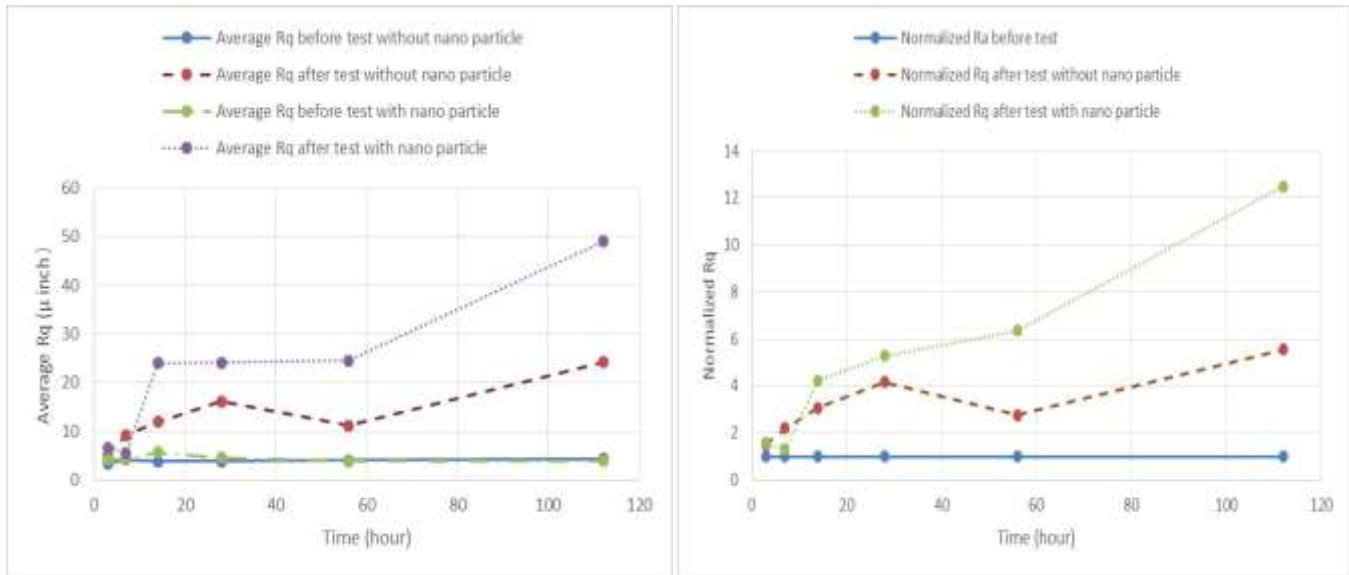


Figure A. 9. Average and normalized Rq roughness for 3003-T3 aluminum before and after 3, 7, 14, 28, 56 and 112 hour-treatments with the reference fluid distilled water, and with nanofluid of 2% nano-alumina in reference fluid and jet speed of 10.7 m/s.

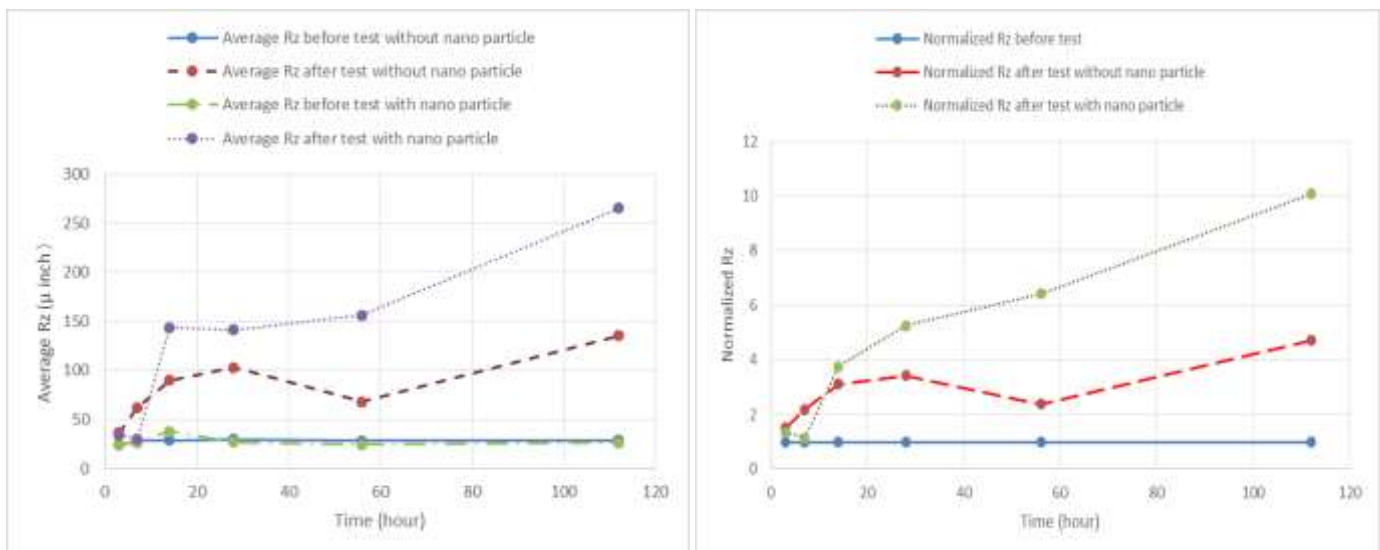


Figure A. 10. Average and normalized Rz roughness for 3003-T3 aluminum before and after 3, 7, 14, 28, 56 and 112 hour-treatments with the reference fluid of distilled water, and with nanofluid of 2% nano-alumina in reference fluid and jet speed of 10.7 m/s.

## A.1.2.2 Test results of 10.7 m/s jet impingement with distilled water as base fluid and its 2

### % nanofluid on copper

Table A. 87. Surface roughness data for copper alloy110 before- and after- 3 hours of tests with a 3.5- m/s jet of distilled water.

Surface roughness ( $\mu$ inch)	Before test			After test		
	Ra	Rq	Rz	Ra	Rq	Rz
Longitudinal	3.89	4.82	42.06	3.25	4.92	42.98
	3.04	5.03	39.8	3.68	4.13	36.15
	3.87	4.17	36.43	3.03	4.7	38.1
Transvers	4.89	4.82	42.06	3.25	4.92	42.98
	3.04	5.03	39.8	4.68	4.12	36.15
	3.87	4.17	36.43	4.03	4.7	38.1
Average	3.94	4.69	39.43	3.88	4.58	38.97

Table A. 89. Surface roughness data for copper alloy110 before- and after- 14 hours of tests with a 3.5- m/s jet of distilled water.

Surface roughness ( $\mu$ inch)	Before test			After test		
	Ra	Rq	Rz	Ra	Rq	Rz
Longitudinal	2.89	4.82	42.06	3.25	4.92	42.98
	3.04	5.03	39.8	2.68	4.13	36.15
	2.87	4.17	36.43	3.03	4.7	38.1
Transvers	2.89	4.82	42.06	3.25	4.92	42.98
	3.04	5.03	39.8	2.68	4.12	36.15
	2.87	4.17	36.43	3.03	4.7	38.1
Average	2.93	4.67	39.43	2.98	4.57	39.07

Table A. 91. Surface roughness data for copper alloy110 before- and after- 56 hours of tests with a 3.5- m/s jet of distilled water.

Surface roughness ( $\mu$ inch)	Before test			After test		
	Ra	Rq	Rz	Ra	Rq	Rz
Longitudinal	6.21	7.91	43.98	7.55	9.72	56.26
	6.19	9.58	57.2	5.74	7.18	37.69
	7.29	7.94	37.51	4.58	6.26	38.69
Transvers	5.93	7.87	46.58	5.28	7.17	46.2
	7.59	6.95	36.11	4.98	5.99	38.18
	7.44	7.65	44.27	5.62	7.264	43.40
Average	7.21	7.91	43.98	7.55	9.72	56.26

Table A. 88. Surface roughness data for copper alloy110 before- and after- 7 hours of tests with a 3.5- m/s jet of distilled water.

Surface roughness ( $\mu$ inch)	Before test			After test		
	Ra	Rq	Rz	Ra	Rq	Rz
Longitudinal	3.15	4.6	36.28	4.92	6.69	41.49
	2.64	3.88	31.17	2.86	4.02	30.73
	3.06	4.36	27.61	5.1	6.75	47.85
Transvers	3.15	4.6	36.28	4.92	6.69	41.49
	2.64	3.88	31.17	2.86	4.02	30.73
	3.06	4.36	27.61	5.1	6.75	47.85
Average	2.95	4.28	31.69	4.29	5.82	40.02

Table A. 90. Surface roughness data for copper alloy110 before- and after- 28 hours of tests with a 3.5- m/s jet of distilled water.

Surface roughness ( $\mu$ inch)	Before test			After test		
	Ra	Rq	Rz	Ra	Rq	Rz
Longitudinal	3.91	5.74	42.01	3.67	5.26	39.87
	4.25	6.23	50.7	3.64	5.2	39.98
	4.15	6.12	51.17	3.87	6.58	50.51
Transvers	3.87	5.89	42.11	3.71	6.11	42.55
	4.61	6.06	38.28	3.68	5.55	41.26
	4.11	6.13	50.87	3.69	5.34	43.01
Average	4.15	6.03	45.86	3.71	5.67	42.86

Table A. 92. Surface roughness data for copper alloy110 before- and after- 112 hours of tests with a 3.5- m/s jet of distilled water.

Surface roughness ( $\mu$ inch)	Before test			After test		
	Ra	Rq	Rz	Ra	Rq	Rz
Longitudinal	4.67	6.9	50.26	3.55	5.56	43.64
	3.3	5.12	39.95	3.69	3.85	29.07
	3.77	4.99	31.34	2.49	3.42	26.62
Transvers	4.67	6.9	50.26	3.55	5.56	43.64
	3.3	5.12	39.95	2.69	3.85	29.07
	3.77	4.99	31.34	3.48	3.42	26.62
Average	3.91	5.67	40.52	3.88	4.28	33.11

Table A. 93. Surface roughness data for copper alloy110 before- and after- 3 hours of tests with a 3.5- m/s jet of 2% alumina nanofluid of distilled water.

Surface roughness ( $\mu$ inch)	Before test			After test		
	Ra	Rq	Rz	Ra	Rq	Rz
Longitudinal	3.69	4.73	29.88	3.12	4.24	36.59
	3.92	5.03	36.2	4.94	6.39	36.73
	3.96	5.11	35.38	3.35	4.29	33.79
Transvers	3.87	5.01	35.77	3.71	11.95	35.77
	3.29	4.87	29.11	3.72	6.81	35.59
	3.57	5.11	34.21	3.82	6.60	35.83
Average	3.71	4.97	33.42	3.78	6.71	35.72

Table A. 95. Surface roughness data for copper alloy110 before- and after- 14 hours of tests with a 3.5- m/s jet of 2% alumina nanofluid of distilled water.

Surface roughness ( $\mu$ inch)	Before test			After test		
	Ra	Rq	Rz	Ra	Rq	Rz
Longitudinal	3.85	5.64	49.99	3.28	4.59	33.81
	2.61	3.84	31.85	3.7	5.29	41.54
	3.61	5.13	34.99	2.91	3.98	26.52
Transvers	3.85	5.64	49.99	3.28	4.59	33.81
	2.61	3.84	31.85	3.7	5.29	41.54
	3.61	5.13	34.99	2.91	3.98	26.52
Average	3.36	4.87	38.94	3.29	4.62	33.96

Table A. 97. Surface roughness data for copper alloy110 before- and after- 56 hours of tests with a 3.5- m/s jet of 2% alumina nanofluid of distilled water.

Surface roughness ( $\mu$ inch)	Before test			After test		
	Ra	Rq	Rz	Ra	Rq	Rz
Longitudinal	1.85	2.91	29.45	2.91	4.05	25.18
	2.4	3.89	28.16	1.98	2.95	23.34
	2.25	3.15	28.11	2.24	3.32	27.85
Transvers	1.85	2.91	29.45	2.91	4.05	25.18
	2.4	3.89	28.16	1.98	2.95	23.34
	2.25	3.15	28.11	2.24	3.32	27.85
Average	2.17	3.32	28.58	2.38	3.44	25.46

Table A. 94. Surface roughness data for copper alloy110 before- and after- 7 hours of tests with a 3.5- m/s jet of 2% alumina nanofluid of distilled water.

Surface roughness ( $\mu$ inch)	Before test			After test		
	Ra	Rq	Rz	Ra	Rq	Rz
Longitudinal	4.62	5.86	38.32	3.58	4.97	38.28
	4.17	5.57	35.11	3.79	5.14	41.3
	3.44	4.43	28.36	3.55	4.63	33.44
Transvers	3.14	4.35	29.12	3.25	4.91	37.89
	4.04	5.25	29.98	3.19	3.92	36.83
	3.57	4.98	31.27	3.58	6.71	35.82
Average	3.83	5.7	32.03	3.54	4.91	37.73

Table A. 96. Surface roughness data for copper alloy110 before- and after- 28 hours of tests with a 3.5- m/s jet of 2% alumina nanofluid of distilled water.

Surface roughness ( $\mu$ inch)	Before test			After test		
	Ra	Rq	Rz	Ra	Rq	Rz
Longitudinal	4.02	5.41	34.35	4.15	5.79	36.84
	3.17	4.17	27.88	4.57	6.73	50.61
	5.92	6.92	41.7	4.4	6.81	45.75
Transvers	5.14	7.09	44.4	3.53	4.72	27.49
	3.04	4.18	26.98	2.45	3.13	20.3
	4.41	6.46	43.93	3.25	4.31	27.57
Average	4.28	5.71	36.54	3.73	5.25	34.76

Table A. 98. Surface roughness data for copper alloy110 before- and after- 112 hours of tests with a 3.5- m/s jet of 2% alumina nanofluid of distilled water.

Surface roughness ( $\mu$ inch)	Before test			After test		
	Ra	Rq	Rz	Ra	Rq	Rz
Longitudinal	4.22	6.14	44.97	3.97	6.36	54.8
	2.38	3.75	31.96	3.34	4.93	37.46
	3.11	4.11	35.66	3.57	5.09	31.93
Transvers	4.43	6.14	44.97	3.97	6.36	54.8
	2.38	3.75	31.96	3.34	4.91	37.46
	3.11	4.11	35.66	3.57	5.09	31.93
Average	3.16	4.67	37.53	3.63	5.45	41.40

Following Figures A.11 and A.12 displays plots of average and normalized values of Rq and Rz roughness for copper alloy110 before and after 3, 7, 14, 28, 56 and 112 hour-treatments with the reference fluid of distilled water and its 2% alumina nanofluid with 10.7 m/s jet speed respectively.

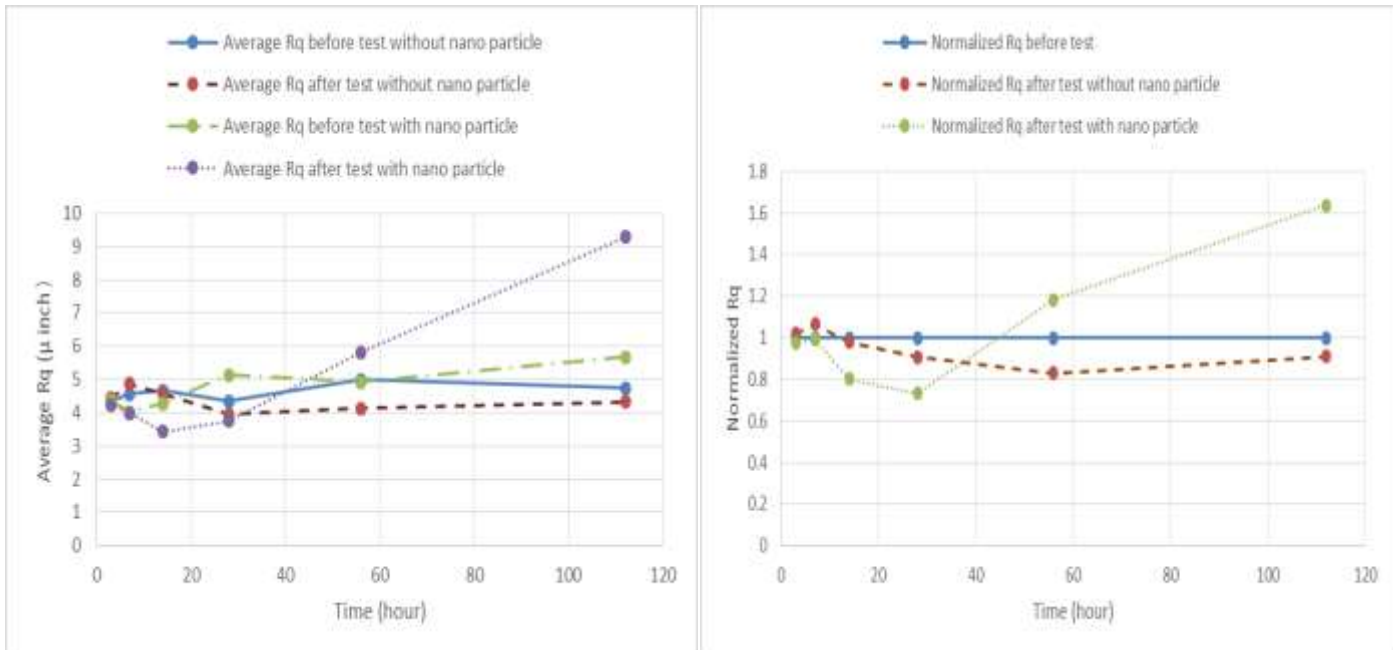


Figure A. 11. Average and normalized Rq roughness for copper alloy110 before and after 3, 7, 14, 28, 56 and 112 hour-treatments with the reference fluid distilled water, and with nanofluid of 2% nano-alumina in reference fluid and jet speed of 10.7 m/s.

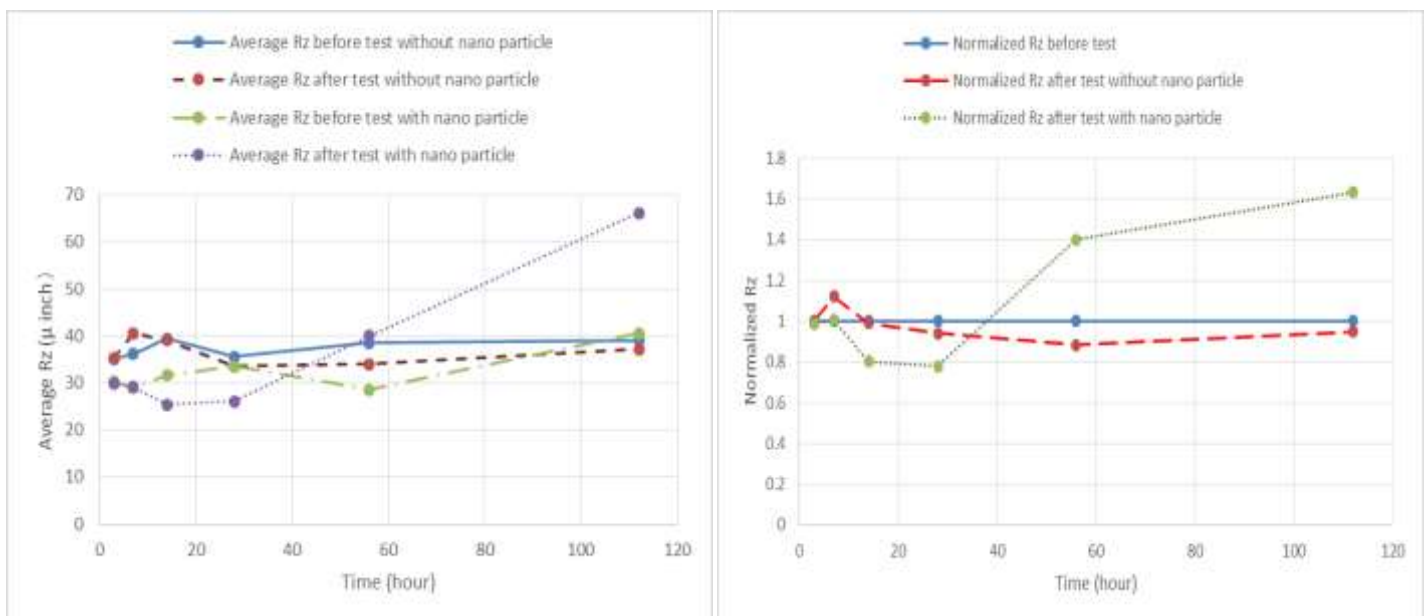


Figure A. 12. Average and normalized Rz roughness for copper alloy110 before and after 3, 7, 14, 28, 56, 112, 240, 312 and 408 hour-treatments with the reference fluid distilled water, and with nanofluid of 2% nano-alumina in reference fluid and jet speed of 10.7 m/s.

### A.1.2.3 Test results of 10.7 m/s jet impingement with 50/50% Ethylene Glycol as base fluid and its 2% alumina nanofluid on aluminum

Table A. 99. Surface roughness data for 3003-T3 aluminum before- and after- 3 hours of tests with a 3.5- m/s jet of 50% Ethylene Glycol in water.

Surface roughness ( $\mu$ inch)	Before test			After test		
	Ra	Rq	Rz	Ra	Rq	Rz
Longitudinal	3.52	4.79	34.82	3.49	4.58	32.93
	3.98	5.49	39	3.4	4.57	32.19
	3.51	4.76	29.97	3.38	4.63	31.71
Transvers	3.96	5.43	37.46	12.72	16.63	87.81
	3.48	4.56	31.37	9.04	11	53.85
Average	3.65	4.98	35.18	6.41	8.28	47.70

Table A. 100. Surface roughness data for 3003-T3 aluminum before- and after- 7 hours of tests with a 3.5- m/s jet of 50% Ethylene Glycol in water.

Surface roughness ( $\mu$ inch)	Before test			After test		
	Ra	Rq	Rz	Ra	Rq	Rz
Longitudinal	2.82	3.5	19.38	3.88	5.01	35.15
	2.3	3	16.31	3.12	3.9	23.18
	2.35	2.94	17.9	3.03	3.92	24.85
Transvers	2.82	3.51	22.14	4.71	7.43	51.64
	2.8	3.57	22.17	7.02	10.28	69.87
	3.02	3.75	21.13	4.54	6.64	52.5
Average	2.69	3.38	19.84	4.38	6.20	42.87

Table A. 101. Surface roughness data for 3003-T3 aluminum before- and after- 14 hours of tests with a 3.5- m/s jet of 50% Ethylene Glycol in water.

Surface roughness ( $\mu$ inch)	Before test			After test		
	Ra	Rq	Rz	Ra	Rq	Rz
Longitudinal	5.97	8.47	65.71	15.3	18.63	87.43
	3.52	4.71	33.82	14.54	18.36	87.99
	2.97	3.85	26.39	18.65	28.06	142.45
Transvers	3.26	4.78	42.41	18.41	24.79	118.7
	2.42	3.14	22.91	13.23	16.16	72.93
	2.71	3.88	30.23	11.65	16.6	85.4
Average	3.48	4.80	36.91	15.30	20.43	99.15

Table A. 102. Surface roughness data for 3003-T3 aluminum before- and after- 28 hours of tests with a 3.5- m/s jet of 50% Ethylene Glycol in water.

Surface roughness ( $\mu$ inch)	Before test			After test		
	Ra	Rq	Rz	Ra	Rq	Rz
Longitudinal	7.98	11.12	59.13	6.9	9.03	59.54
	9.36	12.32	68.41	7.33	9.09	52.66
	6.01	8.07	49.9	7.87	9.97	60.85
Transvers	6.02	7.44	42.99	6.72	8.51	44.21
	5.12	6.26	32.66	7.14	8.86	48.07
	5.36	6.89	41.67	5.37	6.77	48.13
Average	6.64	8.68	49.13	6.89	8.71	52.24

Table A. 103. Surface roughness data for 3003-T3 aluminum before- and after- 56 hours of tests with a 3.5- m/s jet of 50% Ethylene Glycol in water.

Surface roughness ( $\mu$ inch)	Before test			After test		
	Ra	Rq	Rz	Ra	Rq	Rz
Longitudinal	2.00	2.55	18.22	6.36	8.52	56.69
	2.08	2.74	21.56	10.03	12.62	56.99
	1.75	2.36	18.19	14.90	20.14	110.95
Transvers	2.27	2.97	20.97	9.04	13.77	67.25
	2.32	3.06	23.21	10.01	11.78	51.97
	2.43	3.12	20.38	7.40	9.69	48.16
Average	2.14	2.80	20.42	9.62	12.75	65.34

Table A. 104. Surface roughness data for 3003-T3 aluminum before- and after- 112 hours of tests with a 3.5- m/s jet of 50% Ethylene Glycol in water.

Surface roughness ( $\mu$ inch)	Before test			After test		
	Ra	Rq	Rz	Ra	Rq	Rz
Longitudinal	2.52	3.53	28.54	20.1	29.73	164.86
	2.87	3.83	24.16	16.29	23.34	151.97
	2.15	2.82	20.49	29.93	41.91	215.09
Transvers	3.55	4.68	27.89	28.08	36.78	186.01
	3.26	4.17	24.81	37.46	49.08	230.4
	3.41	4.55	36.4	27.47	35.5	180.22
Average	2.96	3.93	27.05	26.55	36.06	188.10



Table A. 105. Surface roughness data for 3003-T3 aluminum before- and after- 3 hours of tests with a 3.5- m/s jet of 2% alumina nanofluid of 50% Ethylene Glycol in water.

Surface roughness ( $\mu$ inch)	Before test			After test		
	Ra	Rq	Rz	Ra	Rq	Rz
Longitudinal	3.64	5.08	41.14	5.04	6.68	42.23
	4.35	6.32	47.52	23.56	35.18	168.78
	5.24	7.37	46.92	7.25	10.18	67.43
Transvers	4.43	5.83	43.74	5.77	8.17	54.06
	4.01	5.52	41.05	14.18	20.55	137.08
	4.09	5.58	36.83	18.98	28.08	153.97
Average	4.30	5.95	42.87	12.47	14.73	103.93

Table A. 107. Surface roughness data for 3003-T3 aluminum before- and after- 14 hours of tests with a 3.5- m/s jet of 2% alumina nanofluid of 50% Ethylene Glycol in water.

Surface roughness ( $\mu$ inch)	Before test			After test		
	Ra	Rq	Rz	Ra	Rq	Rz
Longitudinal	5.26	7.12	45.65	6	7.67	45.33
	5.71	7.5	44.34	6.31	8.31	50.35
	6.28	8.22	53.83	5.72	7.42	50.93
Transvers	6.44	8.92	60.2	5.32	6.81	39.14
	6.4	8.85	58.06	5.7	7.4	40.21
	5.65	7.53	44.55	5.68	7.3	43.9
Average	5.96	8.02	51.11	5.79	7.49	44.98

Table A. 109. Surface roughness data for 3003-T3 aluminum before- and after- 56 hours of tests with a 3.5- m/s jet of 2% alumina nanofluid of 50% Ethylene Glycol in water.

Surface roughness ( $\mu$ inch)	Before test			After test		
	Ra	Rq	Rz	Ra	Rq	Rz
Longitudinal	2.76	3.64	22.31	6.02	10.79	70.47
	2.56	3.5	26.55	16.95	25.98	147.83
	2.43	3.28	22.99	19.19	25.02	121.88
Transvers	2.49	3.22	23.77	5.14	9.09	53.86
	2.46	3.5	26.55	17.41	23.97	127.44
	2.53	3.28	22.99	7.31	9.11	45.83
Average	2.56	3.41	23.91	11.98	17.33	94.55

Table A. 106. Surface roughness data for 3003-T3 aluminum before- and after- 7 hours of tests with a 3.5- m/s jet of 2% alumina nanofluid of 50% Ethylene Glycol in water.

Surface roughness ( $\mu$ inch)	Before test			After test		
	Ra	Rq	Rz	Ra	Rq	Rz
Longitudinal	3.93	5.43	42.38	9.96	13.02	60.99
	4.96	7.07	49.98	5.01	6.86	32.54
	5.23	7.25	53.76	6.92	8.79	42.38
Transvers	6.68	9.07	65.73	30.66	48.38	121.11
	6.55	8.94	68.82	20.55	29.94	133.02
	5.46	7.79	67.78	11.63	15.39	88.68
Average	5.47	7.59	58.08	14.12	20.40	79.79

Table A. 108. Surface roughness data for 3003-T3 aluminum before- and after- 28 hours of tests with a 3.5- m/s jet of 2% alumina nanofluid of 50% Ethylene Glycol in water.

Surface roughness ( $\mu$ inch)	Before test			After test		
	Ra	Rq	Rz	Ra	Rq	Rz
Longitudinal	5.55	6.62	29.66	2.34	3.1	20.65
	2.53	3.21	20.58	2.82	3.62	24.03
	2.96	4.08	29.28	2.98	4.11	33.49
Transvers	2.59	3.28	20.73	2.83	3.79	25.68
	2.67	3.6	28.68	2.77	3.46	21.02
	2.5	3.32	25.46	3.39	4.69	28.78
Average	3.13	4.02	25.74	2.86	3.79	25.61

Table A. 110. Surface roughness data for 3003-T3 aluminum before- and after- 112 hours of tests with a 3.5- m/s jet of 2% alumina nanofluid of 50% Ethylene Glycol in water.

Surface roughness ( $\mu$ inch)	Before test			After test		
	Ra	Rq	Rz	Ra	Rq	Rz
Longitudinal	2.17	2.96	25.92	28.80	36.82	176.01
	2.50	3.79	32.76	22.69	33.64	189.43
	2.17	2.83	20.97	20.36	32.58	195.63
Transvers	2.66	3.50	29.30	25.51	34.89	154.85
	2.32	3.04	22.97	10.87	15.63	79.12
	3.31	5.15	40.87	13.03	17.09	80.81
Average	2.52	3.55	28.80	20.21	28.44	145.98

Following Figures A.13 and A.14 displays plots of average and normalized values of Rq and Rz roughness for 3003-T3 aluminum before and after 3, 7, 14, 28, 56 and 112 hour-treatments with the reference fluid of 50% Ethylene Glycol in water and its 2% alumina nanofluid with 10.7 m/s jet speed respectively.

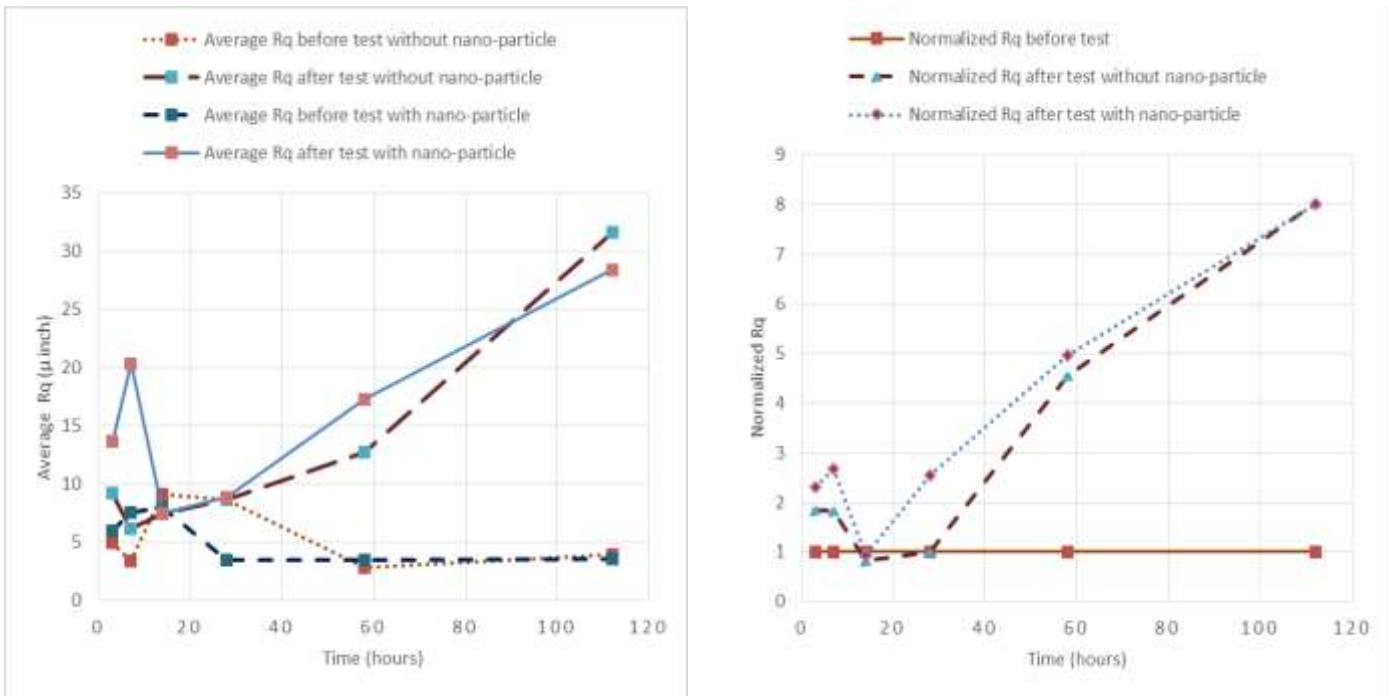


Figure A. 13. Average and normalized Rq roughness for 3003-T3 aluminum before and after 3, 7, 14, 28, 56 and 112 hour-treatments with the reference fluid of 50% Ethylene Glycol in water, and its nanofluid of 2% nano-alumina in reference fluid and jet speed of 10.7 m/s.

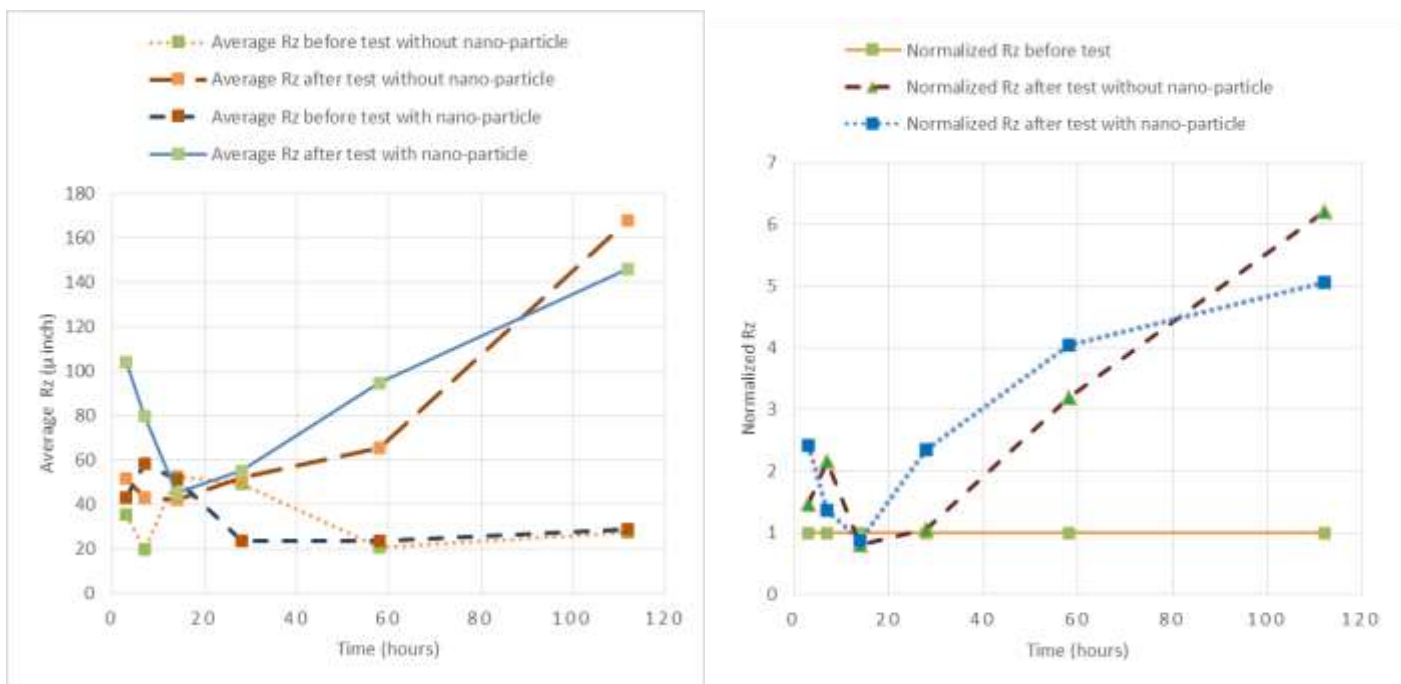


Figure A. 14. Average and normalized Rz roughness for 3003-T3 aluminum before and after 3, 7, 14, 28, 56 and 112 hour-treatments with the reference fluid of 50% Ethylene Glycol in water and its nanofluid of 2% nano-alumina in reference fluid and jet speed of 10.7 m/s.

### A.1.2.4 Test results of 10.7 m/s jet impingement with 50/50% Ethylene Glycol as base fluid and its 2% alumina nanofluid on copper

Table A. 111. Surface roughness data for copper alloy110 before- and after- 3 hours of tests with a 3.5- m/s jet of 50% Ethylene Glycol in water.

Surface roughness ( $\mu$ inch)	Before test			After test		
	Ra	Rq	Rz	Ra	Rq	Rz
Longitudinal	2.2	4.78	16.54	3.33	4.05	21.51
	2.76	3.51	23.37	2.58	3.87	33.19
	2.16	2.83	18.88	2.94	4.12	28.51
Transvers	1.59	2.15	16.98	1.96	2.53	17.63
	3.26	4.1	29.17	3.54	4.74	32.89
	3.17	3.15	28.03	3.07	3.98	25.03
Average	2.52	3.42	22.16	2.90	3.88	26.46

Table A. 113. Surface roughness data for copper alloy110 before- and after- 14 hours of tests with a 3.5- m/s jet of 50% Ethylene Glycol in water.

Surface roughness ( $\mu$ inch)	Before test			After test		
	Ra	Rq	Rz	Ra	Rq	Rz
Longitudinal	2.41	3.19	21.08	2.2	2.78	16.5
	2.22	3.02	22.55	2.76	3.51	23.37
	2.15	3.04	21.34	2.16	2.83	18.88
Transvers	11.4	16.39	79.65	2.44	3.22	25.31
	2.71	3.27	20.07	2.1	2.69	17.95
	2.17	3.05	26.04	2.25	3.16	22.32
Average	3.84	5.33	31.79	2.32	3.03	20.72

Table A. 115. Surface roughness data for copper alloy110 before- and after- 56 hours of tests with a 3.5- m/s jet of 50% Ethylene Glycol in water.

Surface roughness ( $\mu$ inch)	Before test			After test		
	Ra	Rq	Rz	Ra	Rq	Rz
Longitudinal	4.09	6.03	45.6	2.15	3.3	25.35
	4.72	5.85	28.02	2.63	3.99	28.28
	2.5	3.54	32.2	2.59	3.76	23.1
Transvers	2.87	3.49	19.16	3.18	4.51	29.15
	3.38	4.57	29.88	2.16	3.75	25.08
	4.68	5.68	23.5	2.55	3.75	25.75
Average	3.71	4.86	29.73	2.55	3.84	26.11

Table A. 112. Surface roughness data for copper alloy110 before- and after- 7 hours of tests with a 3.5- m/s jet of 50% Ethylene Glycol in water.

Surface roughness ( $\mu$ inch)	Before test			After test		
	Ra	Rq	Rz	Ra	Rq	Rz
Longitudinal	2.28	3.2	18.98	2.26	3.04	19.94
	2.54	3.96	32.37	2.82	4.6	35.41
	2.21	2.9	19.65	2.24	2.85	17.28
Transvers	3.41	5.01	33.78	17.65	23.34	95.01
	2.7	3.94	27.98	2.94	4.32	28.347
	2.04	2.76	19.83	2.76	3.97	29.35
Average	2.53	3.63	25.43	5.11	7.02	37.56

Table A. 114. Surface roughness data for copper alloy110 before- and after- 28 hours of tests with a 3.5- m/s jet of 50% Ethylene Glycol in water.

Surface roughness ( $\mu$ inch)	Before test			After test		
	Ra	Rq	Rz	Ra	Rq	Rz
Longitudinal	2.53	3.4	23.57	2.6	3.24	18.47
	2.55	3.94	27.44	2.8	2.75	16.47
	2.54	3.46	18.82	2.56	3.57	21.07
Transvers	3.16	4.2	30.35	3.06	3.91	24.42
	3.31	4.3	25.7	2.89	3.72	22.34
	3.1	4.08	26.64	2.83	3.64	21.83
Average	2.86	3.90	25.42	2.79	3.47	20.77

Table A. 116. Surface roughness data for copper alloy110 before- and after- 112 hours of tests with a 3.5- m/s jet of 50% Ethylene Glycol in water.

Surface roughness ( $\mu$ inch)	Before test			After test		
	Ra	Rq	Rz	Ra	Rq	Rz
Longitudinal	1.94	2.86	21.72	2.2	2.95	18.74
	1.69	2.2	13.96	1.66	2.51	20.04
	1.5	1.93	12.82	2.53	3.67	23.54
Transvers	2.47	3.33	23.37	2.17	2.92	19.03
	3.02	4.66	35.52	2.49	3.81	31.4
	3.63	4.86	25.44	2.1	2.74	16.32
Average	2.37	3.31	22.14	2.19	3.1	21.51

Table A. 117. Surface roughness data for copper alloy110 before- and after- 3 hours of tests with a 3.5- m/s jet of 2% alumina nanofluid of 50% Ethylene Glycol in water.

Surface roughness ( $\mu$ inch)	Before test			After test		
	Ra	Rq	Rz	Ra	Rq	Rz
Longitudinal	1.9	2.54	13.86	2.98	3.85	20.42
	2.65	3.56	20.22	2.04	2.6	15.93
	2.16	2.91	19.35	1.85	2.6	18.37
Transvers	2.41	3.19	20.59	1.49	1.94	12.67
	2.35	3.32	22.82	1.89	2.88	21.32
	1.63	2.29	14.66	1.39	1.78	10.94
Average	2.18	2.97	18.58	1.94	2.61	16.61

Table A. 119. Surface roughness data for copper alloy110 before- and after- 14 hours of tests with a 3.5- m/s jet of 2% alumina nanofluid of 50% Ethylene Glycol in water.

Surface roughness ( $\mu$ inch)	Before test			After test		
	Ra	Rq	Rz	Ra	Rq	Rz
Longitudinal	6.86	8.63	41.89	2.28	3.17	22.15
	3.33	5.25	40.38	1.89	2.56	18.88
	3.6	4.49	21.73	1.86	2.65	18.95
Transvers	4.43	5.38	24.59	2.18	2.94	17.14
	3.75	4.68	26.18	1.97	2.58	15.64
	4.6	5.65	28.32	3.85	4.72	24.81
Average	4.43	5.68	30.51	2.34	3.10	19.60

Table A. 121. Surface roughness data for copper alloy110 before- and after- 56 hours of tests with a 3.5- m/s jet of 2% alumina nanofluid of 50% Ethylene Glycol in water.

Surface roughness ( $\mu$ inch)	Before test			After test		
	Ra	Rq	Rz	Ra	Rq	Rz
Longitudinal	2.51	3.09	15.97	1.46	1.93	11.91
	2.2	3.02	18.23	1.72	2.27	13.57
	2.58	3.62	19.22	1.81	2.43	17.03
Transvers	3.41	4.6	27.5	2.83	3.66	17.24
	3.75	5.08	25.27	2.51	3.41	17.43
	3.49	6.48	44.15	2.2	3.24	18.21
Average	2.99	4.36	25.06	2.09	2.82	15.90

Table A. 118. Surface roughness data for copper alloy110 before- and after- 7 hours of tests with a 3.5- m/s jet of 2% alumina nanofluid of 50% Ethylene Glycol in water.

Surface roughness ( $\mu$ inch)	Before test			After test		
	Ra	Rq	Rz	Ra	Rq	Rz
Longitudinal	2.23	3.1	20.49	2.42	3.71	21.68
	1.91	2.96	19.39	1.68	2.11	12.13
	2.19	2.57	17.61	1.95	2.49	14.96
Transvers	2.61	3.49	22.89	2.68	3.73	17.13
	2.13	2.77	16.36	1.6	2.01	11.23
	1.93	2.54	15.54	1.77	2.22	12.26
Average	2.17	2.91	18.71	2.02	2.71	14.90

Table A. 120. Surface roughness data for copper alloy110 before- and after- 28 hours of tests with a 3.5- m/s jet of 2% alumina nanofluid of 50% Ethylene Glycol in water.

Surface roughness ( $\mu$ inch)	Before test			After test		
	Ra	Rq	Rz	Ra	Rq	Rz
Longitudinal	3.11	4.04	27.26	2.21	3.08	24.55
	3	3.98	26.33	2.28	3.17	24.89
	2.93	4.02	33.19	2.59	3.44	24.63
Transvers	2.87	3.92	22.16	2.66	3.94	29.96
	2.92	3.92	21	2.75	3.94	29.84
	2.29	3.05	20.9	2.5	3.63	33.09
Average	2.85	3.82	25.14	2.50	3.54	27.83

Table A. 122. Surface roughness data for copper alloy110 before- and after- 112 hours of tests with a 3.5- m/s jet of 2% alumina nanofluid of 50% Ethylene Glycol in water.

Surface roughness ( $\mu$ inch)	Before test			After test		
	Ra	Rq	Rz	Ra	Rq	Rz
Longitudinal	2.33	3.02	18.11	2.59	3.18	15.83
	3.97	5.1	37.79	2.61	3.39	22.14
	2.81	3.54	20.77	2.75	3.57	20.51
Transvers	3.5	4.52	26.43	3.86	5.94	35.6
	2.97	4.02	25.72	2.14	2.74	15.02
	2.3	3.37	25.59	2.63	3.44	25.01
Average	2.98	3.93	25.74	2.76	3.71	22.35

Following Figures A.13 and A.14 displays plots of average and normalized values of Rq and Rz roughness for copper alloy110 before and after 3, 7, 14, 28, 56 and 112 hour-treatments with the reference fluid of 50% Ethylene Glycol in water and its 2% alumina nanofluid with 10.7 m/s jet speed respectively.

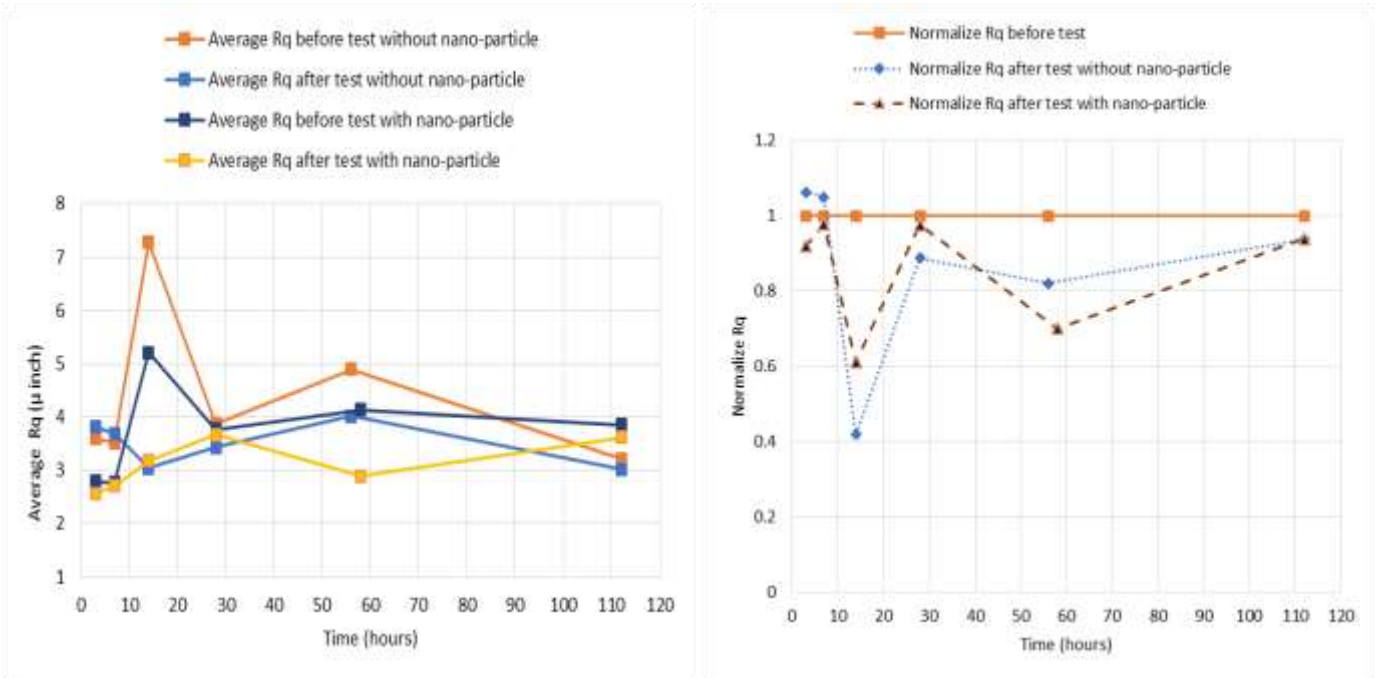


Figure A. 15. Average and normalized Rq roughness for copper alloy110 before and after 3, 7, 14, 28, 56 and 112 hour-treatments with the reference fluid of 50% Ethylene Glycol in water, and with nanofluid of 2% nano-alumina in reference fluid and jet speed of 10.7 m/s.

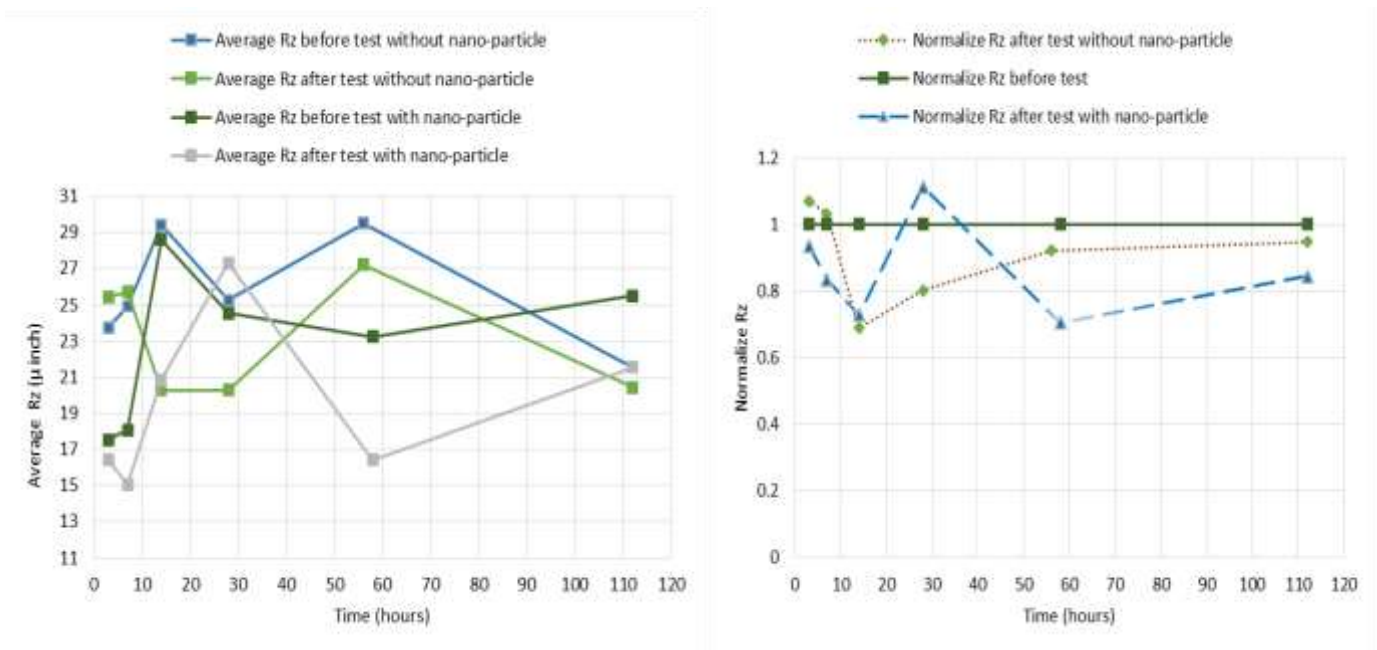


Figure A. 16. Average and normalized Rz roughness for copper alloy110 before and after 3, 7, 14, 28, 56 and 112 hour-treatments with the reference fluid of 50% Ethylene Glycol in water, and with nanofluid of 2% nano-alumina in reference fluid and jet speed of 10.7 m/s.

### A.1.3. Test results for 15.5 m/s jet impingement treatments

#### A.1.3.1. Test results of 15.5 m/s jet impingement with distilled water as base fluid and its 2% alumina nanofluid on aluminum

Table A. 123. Surface roughness data for 3003-T3 aluminum before- and after- 3 hours of tests with a 15.5- m/s jet of distilled water.

Surface roughness ( $\mu$ inch)	Before test			After test		
	Ra	Rq	Rz	Ra	Rq	Rz
Longitudinal	2.43	3.15	21.36	4.05	5.43	37.01
	2.95	3.9	28.07	3.76	5.01	37.77
	2.47	3.29	23.12	3.68	5.04	35.07
Transvers	2.43	3.15	21.36	4.05	5.43	37.01
	2.95	3.9	28.07	3.76	5.01	37.77
	2.47	3.29	23.12	3.68	5.04	35.07
Average	2.62	3.45	24.18	3.83	5.16	36.62

Table A. 125. Surface roughness data for 3003-T3 aluminum before- and after- 14 hours of tests with a 15.5- m/s jet of distilled water.

Surface roughness ( $\mu$ inch)	Before test			After test		
	Ra	Rq	Rz	Ra	Rq	Rz
Longitudinal	2.32	3.2	25.39	8.59	11.51	96.77
	3.18	4.21	31.67	10.07	13.84	94.82
	3.37	4.36	29.48	7.45	10.38	77.5
Transvers	3.28	4.17	28.48	8.59	11.51	96.77
	3.11	4.17	30.33	10.07	13.84	94.82
	2.98	3.11	27.13	7.45	10.38	77.5
Average	3.04	3.87	28.75	8.70	11.91	89.70

Table A. 127. Surface roughness data for 3003-T3 aluminum before- and after- 56 hours of tests with a 15.5- m/s jet of distilled water.

Surface roughness ( $\mu$ inch)	Before test			After test		
	Ra	Rq	Rz	Ra	Rq	Rz
Longitudinal	2.73	3.53	24.19	8.82	11.28	69.89
	2.86	3.72	27.19	8.23	10.91	68.96
	3.5	4.62	30.51	8.75	11.25	65.76
Transvers	3.12	4.21	31.21	8.82	11.28	69.89
	3.21	4.35	28.01	8.24	10.91	68.96
	2.97	3.77	30.12	8.75	11.25	65.76
Average	3.07	4.04	28.54	8.59	11.15	68.20

Table A. 124. Surface roughness data for 3003-T3 aluminum before- and after- 7 hours of tests with a 15.5- m/s jet of distilled water.

Surface roughness ( $\mu$ inch)	Before test			After test		
	Ra	Rq	Rz	Ra	Rq	Rz
Longitudinal	2.74	3.74	29.81	6.87	9.39	68.26
	3.09	4.04	26.62	6.63	8.64	50.12
	3.92	5.16	35.21	6.97	9.77	69.07
Transvers	3.12	4.03	25.89	6.87	9.39	68.26
	3.22	4.23	26.21	6.63	8.64	50.12
	3.07	4.01	26.78	6.97	9.77	69.07
Average	3.19	4.20	28.42	6.82	9.27	62.48

Table A. 126. Surface roughness data for 3003-T3 aluminum before- and after- 28 hours of tests with a 15.5- m/s jet of distilled water.

Surface roughness ( $\mu$ inch)	Before test			After test		
	Ra	Rq	Rz	Ra	Rq	Rz
Longitudinal	2.89	4.37	37.43	12.01	15.18	91.02
	3.02	3.96	26.9	11.18	14.6	95.35
	3.23	4.35	31.58	11.28	14.17	92.12
Transvers	3.13	4.31	31.11	14.74	19.23	126.48
	3.02	3.16	26.19	13.71	16.22	120.48
	3.01	3.11	26.19	15.25	17.22	91.12
Average	3.05	3.88	29.9	13.03	16.10	102.76

Table A. 128. Surface roughness data for 3003-T3 aluminum before- and after- 112 hours of tests with a 15.5- m/s jet of distilled water.

Surface roughness ( $\mu$ inch)	Before test			After test		
	Ra	Rq	Rz	Ra	Rq	Rz
Longitudinal	3.53	4.418	29.69	20.12	25.06	136.27
	3.59	4.58	29.8	18.94	23.79	134.98
	3.3	4.23	29.28	19.42	24.54	136.08
Transvers	3.14	4.11	27.21	20.13	24.98	134.98
	3.22	4.57	28.12	20.01	23.78	134.98
	3.12	4.31	27.98	18.11	23.22	134.91
Average	3.32	4.70	28.68	19.45	24.23	135.37

Table A. 129. Surface roughness data for 3003-T3 aluminum before- and after- 3 hours of tests with a 15.5- m/s jet of 2% nano-alumina nanofluid of distilled water.

Surface roughness ( $\mu$ inch)	Before test			After test		
	Ra	Rq	Rz	Ra	Rq	Rz
Longitudinal	2.93	3.96	33.55	3.89	5.58	48.99
	2.97	4.07	33.74	3.91	5.61	41.39
	2.98	4.05	34.11	3.73	5.39	52.94
Transvers	2.93	3.96	33.55	3.89	5.58	48.99
	2.97	4.07	33.74	3.91	5.61	41.39
	2.98	4.05	34.11	3.73	5.39	52.94
Average	2.96	4.03	33.8	3.84	5.53	47.77

Table A. 131. Surface roughness data for 3003-T3 aluminum before- and after- 14 hours of tests with a 15.5- m/s jet of 2% nano-alumina nanofluid of distilled water.

Surface roughness ( $\mu$ inch)	Before test			After test		
	Ra	Rq	Rz	Ra	Rq	Rz
Longitudinal	2.51	3.28	24.5	7.92	14.07	106.07
	2.54	3.37	24.17	5.74	10.51	85.79
	2.63	3.13	24.24	7.51	12.86	99.49
Transvers	2.71	3.81	24.22	7.92	14.07	106.07
	3.68	4.73	30.76	5.74	10.51	85.79
	3.71	4.88	32.12	7.53	12.86	99.49
Average	2.96	3.87	26.67	7.05	12.48	97.12

Table A. 133. Surface roughness data for 3003-T3 aluminum before- and after- 56 hours of tests with a 15.5- m/s jet of 2% nano-alumina nanofluid of distilled water.

Surface roughness ( $\mu$ inch)	Before test			After test		
	Ra	Rq	Rz	Ra	Rq	Rz
Longitudinal	2.46	3.26	22.34	18.67	25.49	140.28
	2.96	3.08	27.51	21.41	32.14	223.98
	4.13	5.61	36.14	43.71	54.5	247.15
Transvers	3.21	4.33	31.12	18.67	25.49	140.28
	2.99	3.89	28.11	21.41	32.14	223.98
	3.43	4.87	33.11	43.71	54.5	247.15
Average	3.20	4.17	29.72	27.93	37.37	203.80

Table A. 130. Surface roughness data for 3003-T3 aluminum before- and after- 7 hours of tests with a 15.5- m/s jet of 2% nano-alumina nanofluid of distilled water.

Surface roughness ( $\mu$ inch)	Before test			After test		
	Ra	Rq	Rz	Ra	Rq	Rz
Longitudinal	4.09	5.46	39.98	4.74	6.86	54.03
	3.26	4.33	35.5	3.86	6.01	56.03
	4.15	5.44	35.25	4.73	7.73	61.67
Transvers	4.05	5.13	34.98	4.74	6.86	54.03
	3.17	4.23	35.5	3.86	6.01	56.03
	3.26	5.13	35.66	4.73	7.73	61.67
Average	3.66	4.95	36.15	4.44	6.87	57.24

Table A. 132. Surface roughness data for 3003-T3 aluminum before- and after- 28 hours of tests with a 15.5- m/s jet of 2% nano-alumina nanofluid of distilled water.

Surface roughness ( $\mu$ inch)	Before test			After test		
	Ra	Rq	Rz	Ra	Rq	Rz
Longitudinal	3.39	4.85	30.99	8.85	14.41	112.99
	3.74	4.89	31.3	13.97	21.77	139.57
	3.59	4.27	30.22	14.68	22.73	150.87
Transvers	3.85	4.98	31.2	8.85	14.41	112.99
	3.98	5.26	31.66	13.97	21.77	139.57
	3.99	5.67	32.01	14.68	22.73	150.87
Average	3.76	4.98	31.23	12.5	19.64	134.48

Table A. 134. Surface roughness data for 3003-T3 aluminum before- and after- 112 hours of tests with a 15.5- m/s jet of 2% nano-alumina nanofluid of distilled water.

Surface roughness ( $\mu$ inch)	Before test			After test		
	Ra	Rq	Rz	Ra	Rq	Rz
Longitudinal	2.18	2.88	19.98	11.46	16.11	110.87
	2.41	3.36	26.18	59.6	104.82	559.23
	2.85	3.76	26.42	48.39	68.08	341.12
Transvers	2.71	3.61	26.12	47.62	77.65	394.55
	2.52	3.16	26.22	59.6	104.82	559.23
	2.22	3.01	21.11	48.39	68.08	341.12
Average	2.48	3.29	24.34	41.77	66.67	351.44

Following Figures A.17 and A.18 displays plots of average and normalized values of Rq and Rz roughness for 3003-T3 aluminum before and after 3, 7, 14, 28, 56 and 112 hour-treatments with the reference fluid of distilled water and its 2% alumina nanofluid with 15.5 m/s jet speed respectively.

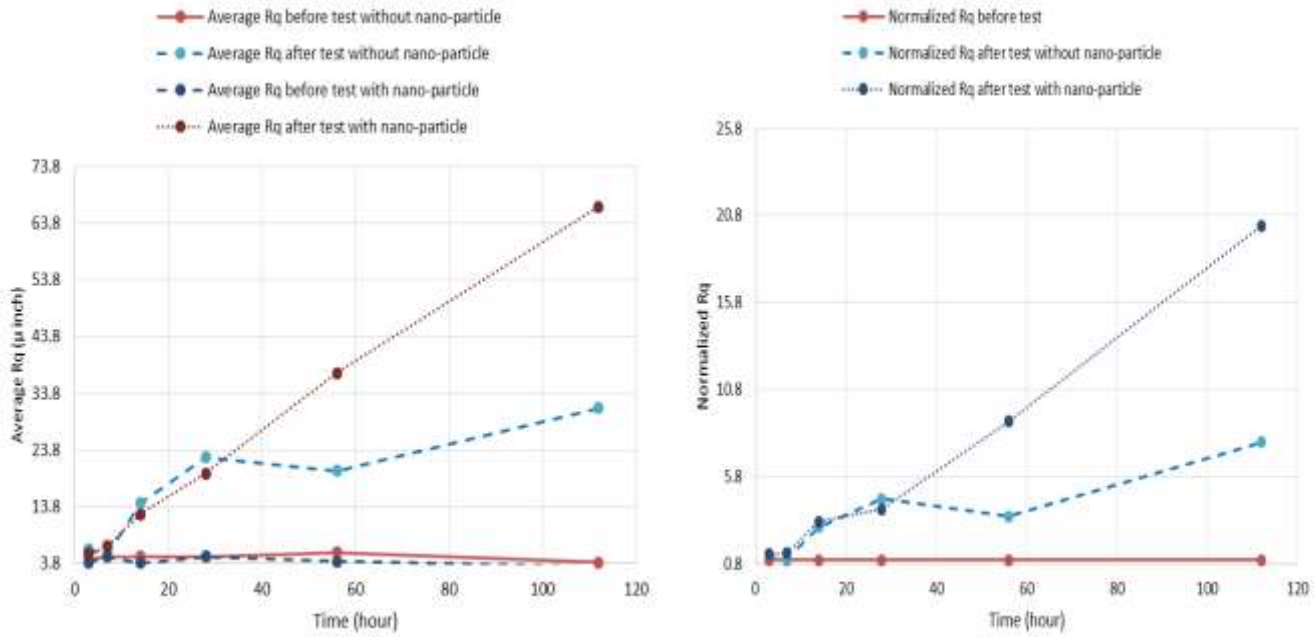


Figure A. 17. Average and normalized Rq roughness for 3003-T3 aluminum before and after 3, 7, 14, 28, 56 and 112 hour-treatments with the reference fluid distilled water, and with nanofluid of 2% nano-alumina in reference fluid and jet speed of 15.5 m/s.

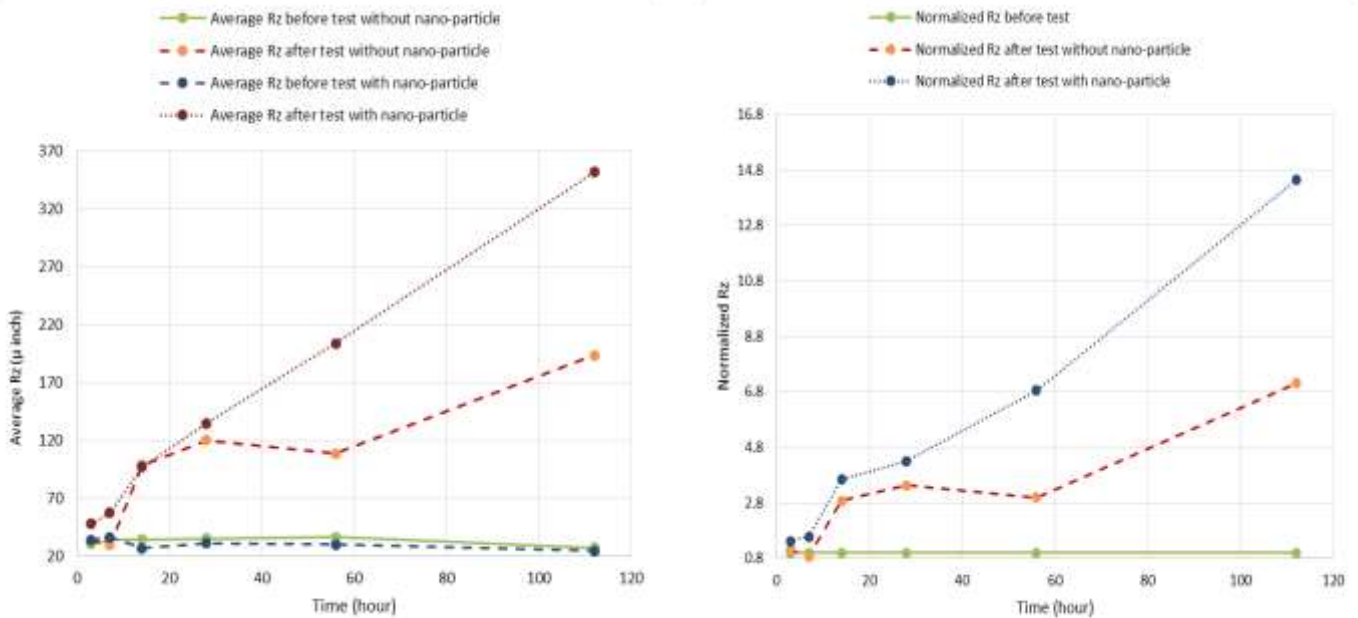


Figure A. 18. Average and normalized Rz roughness for 3003-T3 aluminum before and after 3, 7, 14, 28, 56 and 112 hour-treatments with the reference fluid distilled water, and with nanofluid of 2% nano-alumina in reference fluid and jet speed of 15.5 m/s.



### A.1.3.2. Test results of 15.5 m/s jet impingement with distilled water as base fluid and its 2% alumina nanofluid on copper

Table A. 135. Surface roughness data for copper alloy110 before- and after- 3 hours of tests with a 15.5- m/s jet of distilled water.

Surface roughness ( $\mu$ inch)	Before test			After test		
	Ra	Rq	Rz	Ra	Rq	Rz
Longitudinal	3.55	5.13	41.51	2.8	3.92	30.23
	3.34	4.69	34.28	3.01	4.11	30.22
	4.37	6.57	58.01	2.71	3.75	30.25
Transvers	3.55	5.13	41.51	2.83	3.92	30.23
	3.34	4.69	34.28	3.01	4.11	30.22
	4.37	6.57	58.01	2.71	3.75	30.25
Average	3.75	5.46	44.6	2.84	3.93	30.23

Table A. 137. Surface roughness data for copper alloy110 before- and after- 14 hours of tests with a 15.5- m/s jet of distilled water.

Surface roughness ( $\mu$ inch)	Before test			After test		
	Ra	Rq	Rz	Ra	Rq	Rz
Longitudinal	3.12	4.25	27.33	3.11	4.18	26.32
	3.15	4.12	26.25	3.11	4.22	27.32
	3.31	4.09	29.44	3.21	4.36	28.11
Transvers	3.12	4.25	27.33	3.35	4.18	26.32
	3.15	4.12	26.25	3.11	4.22	27.32
	3.31	4.09	29.44	3.21	4.36	28.11
Average	3.19	4.15	27.67	3.11	4.25	27.25

Table A. 139. Surface roughness data for copper alloy110 before- and after- 56 hours of tests with a 15.5- m/s jet of distilled water.

Surface roughness ( $\mu$ inch)	Before test			After test		
	Ra	Rq	Rz	Ra	Rq	Rz
Longitudinal	3.94	5.51	40.06	2.55	3.52	25.02
	2.66	3.79	29.15	2.87	4.63	37.71
	3.07	4.93	43.39	3.09	4.82	41.99
Transvers	3.94	5.51	40.06	2.55	3.52	25.02
	2.66	3.79	29.15	2.87	4.63	37.71
	3.07	4.93	43.39	3.09	4.82	41.99
Average	3.22	4.74	37.53	2.84	4.32	34.91

Table A. 136. Surface roughness data for copper alloy110 before- and after- 7 hours of tests with a 15.5- m/s jet of distilled water.

Surface roughness ( $\mu$ inch)	Before test			After test		
	Ra	Rq	Rz	Ra	Rq	Rz
Longitudinal	2.21	5.71	40.63	4.23	5.7	41.63
	5.13	5.23	41.26	4.23	5.91	42.23
	6.21	7.11	49.22	5.11	6.11	46.21
Transvers	2.21	5.71	40.63	4.21	5.7	41.63
	5.13	5.23	41.26	4.23	5.91	42.23
	6.21	7.11	49.22	5.11	6.11	46.21
Average	4.52	6.02	43.70	4.51	5.91	43.35

Table A. 138. Surface roughness data for copper alloy110 before- and after- 28 hours of tests with a 15.5- m/s jet of distilled water.

Surface roughness ( $\mu$ inch)	Before test			After test		
	Ra	Rq	Rz	Ra	Rq	Rz
Longitudinal	5.31	6.52	38.26	3.53	4.75	31.44
	3.53	4.96	38.15	4.22	7.19	68.4
	5.96	7.45	40.19	3.51	4.72	31.42
Transvers	5.31	6.52	38.26	3.51	4.75	31.44
	3.53	4.96	38.15	4.22	7.19	68.4
	5.96	7.45	40.19	3.51	4.72	31.42
Average	4.93	6.31	38.87	3.74	5.55	43.75

Table A. 140. Surface roughness data for copper alloy110 before- and after- 112 hours of tests with a 15.5- m/s jet of distilled water.

Surface roughness ( $\mu$ inch)	Before test			After test		
	Ra	Rq	Rz	Ra	Rq	Rz
Longitudinal	2.66	3.22	28.42	4.53	6.21	40.25
	4.39	5.74	33.52	2.71	4.22	37.75
	4.13	6.42	56.12	2.86	4.02	26.76
Transvers	2.66	3.22	28.42	4.53	6.21	40.25
	4.39	5.74	33.52	2.71	4.22	37.75
	4.14	6.42	56.25	2.86	4.02	26.76
Average	3.68	5.13	39.32	3.37	4.82	34.92

Table A. 141. Surface roughness data for copper alloy110 before- and after- 3 hours of tests with a 15.5- m/s jet of 2% alumina nanofluid of distilled water.

Surface roughness ( $\mu$ inch)	Before test			After test		
	Ra	Rq	Rz	Ra	Rq	Rz
Longitudinal	3.26	4.71	39.01	4.87	7.12	49.29
	4.16	6.79	51.24	4.38	6.89	51.23
	3.51	5.42	47.69	4.22	7.35	47.99
Transvers	3.47	5.06	40.61	4.87	7.12	49.29
	3.77	5.01	41.12	4.38	6.89	51.23
	3.19	4.15	33.01	4.22	7.35	47.99
Average	3.56	5.19	42.07	4.49	7.12	49.50

Table A. 143. Surface roughness data for copper alloy110 before- and after- 14 hours of tests with a 15.5- m/s jet of 2% alumina nanofluid of distilled water.

Surface roughness ( $\mu$ inch)	Before test			After test		
	Ra	Rq	Rz	Ra	Rq	Rz
Longitudinal	4.05	5.2	35.27	2.19	3.34	28.7
	3.12	4.49	29.29	2.09	3.27	28.55
	3.49	5.22	33.04	1.66	2.22	17.37
Transvers	3.19	5.22	32.06	2.19	3.34	28.7
	3.22	4.98	28.19	2.09	3.27	28.55
	3.48	5.29	33.41	1.66	2.22	17.37
Average	3.43	5.07	31.87	1.98	2.94	24.87

Table A. 145. Surface roughness data for copper alloy110 before- and after- 56 hours of tests with a 15.5- m/s jet of 2% alumina nanofluid of distilled water.

Surface roughness ( $\mu$ inch)	Before test			After test		
	Ra	Rq	Rz	Ra	Rq	Rz
Longitudinal	1.94	2.88	24.94	4.12	6.28	40.96
	3.03	4.93	51.23	4.57	6.24	38.52
	1.96	3.15	23.15	4.97	6.67	45.12
Transvers	2.51	3.78	33.15	4.12	6.28	40.96
	2.11	3.07	31.15	4.57	6.24	38.52
	3.01	4.13	50.12	4.97	6.67	45.12
Average	2.43	3.66	35.62	4.55	6.40	41.53

Table A. 142. Surface roughness data for copper alloy110 before- and after- 7 hours of tests with a 15.5- m/s jet of 2% alumina nanofluid of distilled water.

Surface roughness ( $\mu$ inch)	Before test			After test		
	Ra	Rq	Rz	Ra	Rq	Rz
Longitudinal	1.67	2.72	29.81	1.64	2.46	23.24
	1.84	2.85	26.45	1.87	2.11	23.49
	2.65	3.41	23.24	1.56	2.78	23.21
Transvers	2.78	3.59	23.49	1.64	2.46	23.24
	1.98	3.01	27.41	1.87	2.11	23.49
	2.01	3.14	24.41	1.56	2.78	23.21
Average	2.16	3.12	25.80	1.69	2.45	23.31

Table A. 144. Surface roughness data for copper alloy110 before- and after- 28 hours of tests with a 15.5- m/s jet of 2% alumina nanofluid of distilled water.

Surface roughness ( $\mu$ inch)	Before test			After test		
	Ra	Rq	Rz	Ra	Rq	Rz
Longitudinal	2.87	4.58	40.39	2.43	3.96	36.67
	2.81	4.12	31.43	2.51	4.09	36.77
	1.93	3.1	26.24	2.72	3.66	26.09
Transvers	2.12	4.02	30.23	2.43	3.96	36.67
	2.25	3.22	25.22	2.51	4.09	36.77
	1.97	3.21	25.24	2.72	3.66	26.09
Average	2.32	3.71	29.79	2.55	3.90	33.18

Table A. 146. Surface roughness data for copper alloy110 before- and after- 112 hours of tests with a 15.5- m/s jet of 2% alumina nanofluid of distilled water.

Surface roughness ( $\mu$ inch)	Before test			After test		
	Ra	Rq	Rz	Ra	Rq	Rz
Longitudinal	3.44	4.82	33.61	13.42	17.29	101.92
	4.27	5.94	41.77	13.32	17.01	103.29
	3.75	5.21	35.36	11.91	16.53	104.9
Transvers	3.15	5.12	36.16	13.12	17.29	101.92
	4.12	5.41	40.71	13.32	17.01	103.29
	3.59	5.22	42.11	11.91	16.53	104.9
Average	3.72	5.29	38.29	12.74	16.94	103.37

Following Figures A.19 and A.20 displays plots of average and normalized values of Rq and Rz roughness for copper alloy110 before and after 3, 7, 14, 28, 56 and 112 hour-treatments with the reference fluid of distilled water and its 2% alumina nanofluid with 15.5 m/s jet speed respectively.

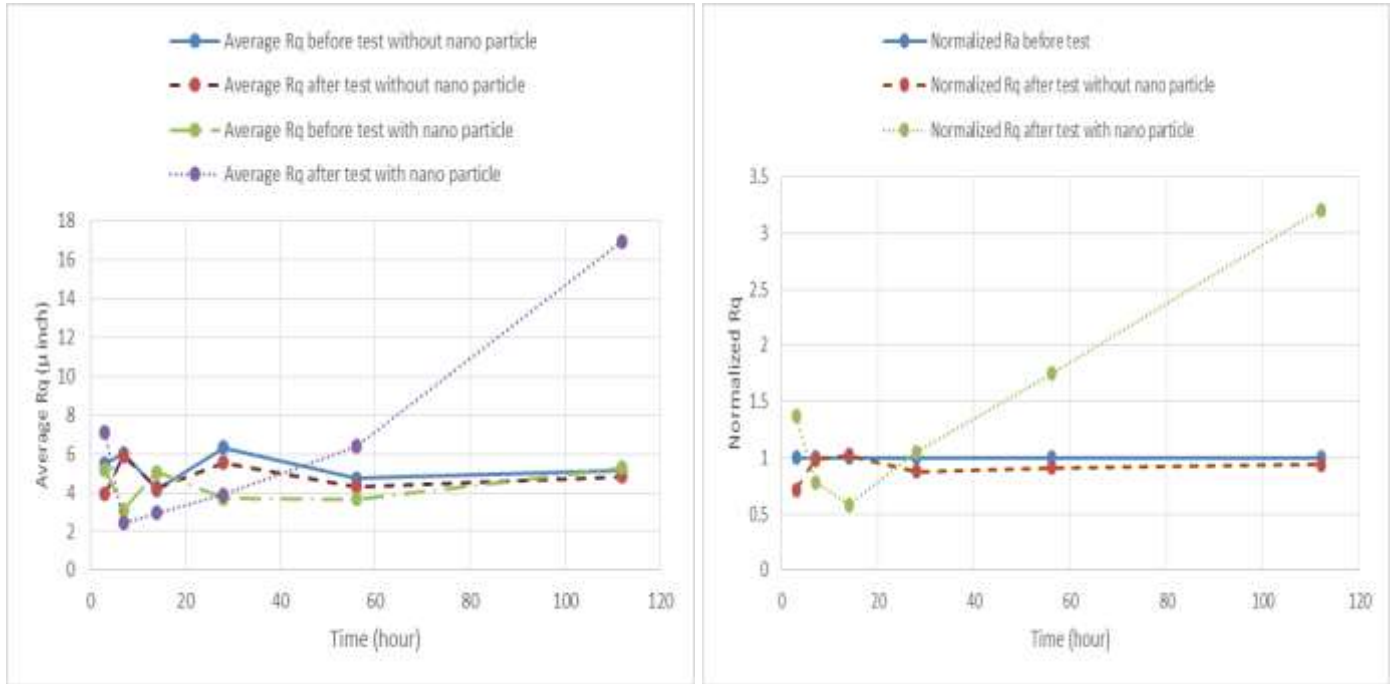


Figure A. 19. Average and normalized Rq roughness for copper alloy110 before and after 3, 7, 14, 28, 56 and 112 hour-treatments with the reference fluid distilled water, and with nanofluid of 2% nano-alumina in reference fluid and jet speed of 15.5 m/s.

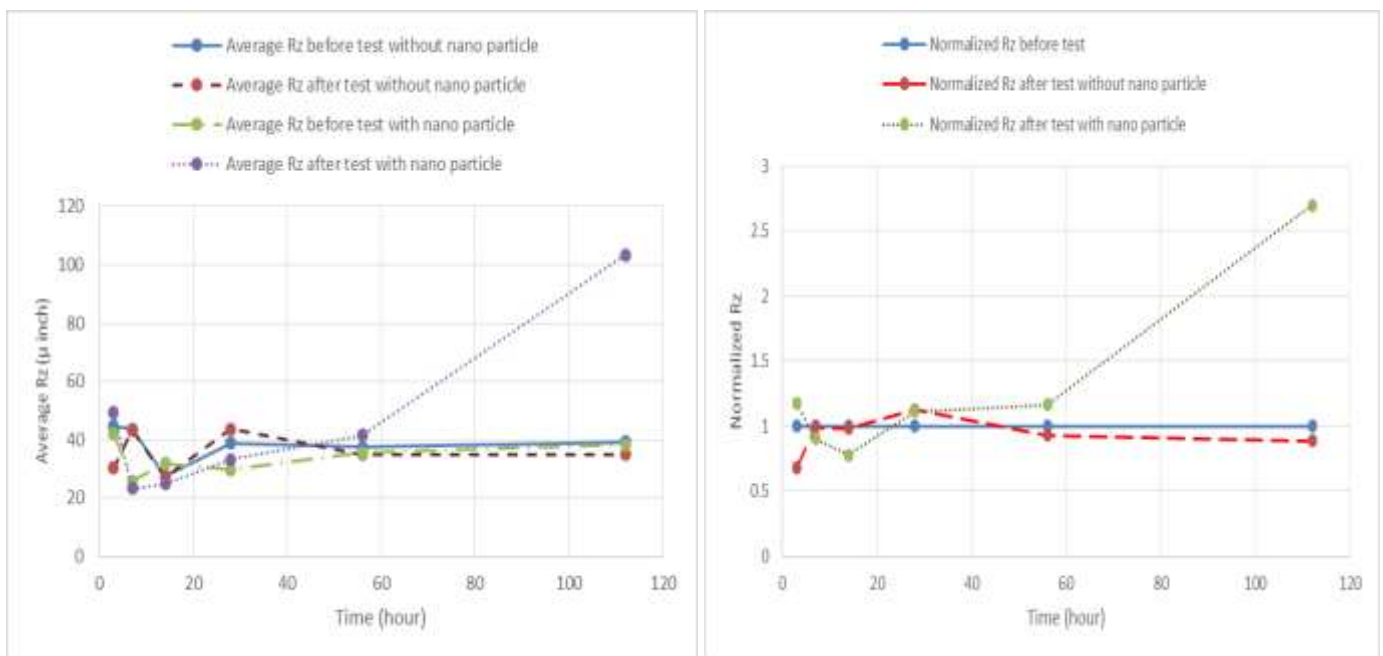


Figure A. 20. Average and normalized Rz roughness for copper alloy110 before and after 3, 7, 14, 28, 56 and 112 hour-treatments with the reference fluid distilled water, and with nanofluid of 2% nano-alumina in reference fluid and jet speed of 15.5 m/s.

## A.2 Test results of 1 m/s parallel flow tests

### A.2.1 Test results of 1 m/s parallel flow with distilled water as base fluid and its 2% alumina nanofluid on aluminum

Table A. 147. Surface roughness data for 3003-T3 aluminum before- and after- 3 hours of tests with 1- m/s parallel flow of distilled water.

Surface roughness ( $\mu$ inch)	Before test			After test		
	Ra	Rq	Rz	Ra	Rq	Rz
Longitudinal	3.18	4.36	27.61	11.12	17.42	104.1
	2.74	3.59	24.28	10.75	25.19	114.2
	3.61	4.67	34.54	10.42	23.81	126.98
Transvers	3.59	4.77	34.58	9.97	15.5	129.42
	2.98	3.78	25.01	12.56	20.81	116.71
	2.95	3.88	24.89	12.89	20.15	126.01
Average	3.19	4.175	28.48	11.96	18.29	123.49

Table A. 148. Surface roughness data for 3003-T3 aluminum before- and after- 7 hours of tests with 1- m/s parallel flow of distilled water.

Surface roughness ( $\mu$ inch)	Before test			After test		
	Ra	Rq	Rz	Ra	Rq	Rz
Longitudinal	2.63	3.04	23.55	8.56	11.34	89.21
	3.15	3.95	24.44	12.81	15.88	106.11
	3.26	3.19	25.51	10.21	18.31	124.68
Transvers	2.31	3.04	23.81	8.61	12.35	95.21
	3.11	3.58	24.45	12.81	14.18	106.23
	3.25	3.78	25.11	11.01	16.31	114.38
Average	2.88	3.53	24.43	10.67	15.92	104.55

Table A. 149. Surface roughness data for 3003-T3 aluminum before- and after- 14 hours of tests with 1- m/s parallel flow of distilled water.

Surface roughness ( $\mu$ inch)	Before test			After test		
	Ra	Rq	Rz	Ra	Rq	Rz
Longitudinal	2.83	3.75	25.53	14.15	20.85	128.58
	2.99	3.09	26.92	15.73	23.84	120.76
	3.21	4.29	26.07	17.26	27.05	155.54
Transvers	3.48	4.55	31.26	15.07	26.83	127.98
	3.24	3.69	24.41	11.86	20.36	129.86
	2.55	3.14	25.51	12.21	18.31	124.68
Average	3.04	3.71	26.17	14.36	21.41	124.75

Table A. 150. Surface roughness data for 3003-T3 aluminum before- and after- 28 hours of tests with 1- m/s parallel flow of distilled water.

Surface roughness ( $\mu$ inch)	Before test			After test		
	Ra	Rq	Rz	Ra	Rq	Rz
Longitudinal	3.36	4.11	26.33	15.97	22.02	175.8
	3.34	4.32	31.01	21.84	22.15	116.26
	2.67	3.4	22.57	20.51	29.9	128.7
Transvers	3.16	3.11	36.33	21.97	32.02	165.8
	2.35	4.92	21.01	25.84	31.15	116.26
	3.57	2.98	25.57	18.51	29.9	118.7
Average	2.95	3.95	26.64	21.03	26.04	129.09

Table A. 151. Surface roughness data for 3003-T3 aluminum before- and after- 56 hours of tests with 1- m/s parallel flow of distilled water.

Surface roughness ( $\mu$ inch)	Before test			After test		
	Ra	Rq	Rz	Ra	Rq	Rz
Longitudinal	3.33	4.34	27.38	23.19	32.63	157.77
	4.74	6.09	36.14	25.07	36.83	157.98
	3.48	4.55	31.26	29.86	32.36	189.86
Transvers	3.24	3.69	24.41	32.88	38.78	136.21
	2.35	3.14	25.51	22.71	38.3	124.78
	3.24	3.95	24.43	31.05	36.14	142.06
Average	3.88	4.99	31.59	29.35	36.73	152.36

Table A. 152. Surface roughness data for 3003-T3 aluminum before- and after- 112 hours of tests with 1- m/s parallel flow of distilled water.

Surface roughness ( $\mu$ inch)	Before test			After test		
	Ra	Rq	Rz	Ra	Rq	Rz
Longitudinal	2.95	3.88	27.99	33.22	38.56	197.26
	3.15	4.08	26.71	30.85	41.64	242.45
	3.12	4.06	26.17	35.17	41.95	242.78
Transvers	2.91	3.87	26.92	38.21	42.13	144.12
	3.54	4.79	33.75	32.16	34.01	256.24
	3.24	4.29	32.98	32.99	34.25	156.13
Average	3.12	4.16	29.08	33.65	41.22	172.35

Table A. 153. Surface roughness data for 3003-T3 aluminum before- and after- 3 hours of tests with 1- m/s parallel flow of 2% alumina nanofluid of distilled water.

Surface roughness ( $\mu$ inch)	Before test			After test		
	Ra	Rq	Rz	Ra	Rq	Rz
Longitudinal	2.13	3.04	23.5	17.66	21.34	145.23
	3.15	3.96	24.4	10.85	18.78	106.21
	3.21	3.59	25.41	12.71	18.37	124.78
Transvers	3.15	3.95	24.44	11.81	18.88	106.11
	3.16	3.19	25.51	10.21	18.31	124.68
	2.31	3.04	23.81	16.61	21.35	135.21
Average	2.78	3.53	24.43	12.35	19.02	125.47

Table A. 155. Surface roughness data for 3003-T3 aluminum before- and after- 14 hours of tests with 1- m/s parallel flow of 2% alumina nanofluid of distilled water.

Surface roughness ( $\mu$ inch)	Before test			After test		
	Ra	Rq	Rz	Ra	Rq	Rz
Longitudinal	2.73	3.65	25.83	13.75	20.85	122.58
	2.69	3.29	26.92	12.73	23.84	120.76
	3.21	4.29	26.07	13.26	27.05	135.54
Transvers	3.58	4.55	31.26	15.07	16.83	127.98
	3.24	3.69	24.41	11.86	20.36	129.86
	2.75	3.74	25.51	12.21	18.31	114.68
Average	3.04	3.71	26.17	13.25	21.45	125.36

Table A. 157. Surface roughness data for 3003-T3 aluminum before- and after- 56 hours of tests with 1- m/s parallel flow of 2% alumina nanofluid of distilled water.

Surface roughness ( $\mu$ inch)	Before test			After test		
	Ra	Rq	Rz	Ra	Rq	Rz
Longitudinal	2.36	3.16	22.35	28.47	25.79	130.48
	2.76	3.08	27.51	21.41	32.14	223.98
	4.23	5.61	36.14	43.71	54.5	247.15
Transvers	3.28	4.33	31.12	18.67	25.49	140.28
	2.79	3.89	28.11	21.41	32.14	223.98
	3.43	4.87	33.11	43.71	54.5	247.15
Average	3.20	4.17	29.72	28.69	37.60	153.01

Table A. 154. Surface roughness data for 3003-T3 aluminum before- and after- 7 hours of tests with 1- m/s parallel flow of 2% alumina nanofluid of distilled water.

Surface roughness ( $\mu$ inch)	Before test			After test		
	Ra	Rq	Rz	Ra	Rq	Rz
Longitudinal	3.28	4.46	27.71	11.22	17.32	114.1
	2.64	3.59	24.28	10.75	15.19	94.2
	3.71	4.67	34.54	10.42	21.81	96.98
Transvers	3.69	4.77	34.58	9.97	15.5	129.42
	2.88	3.78	25.01	12.56	20.81	106.71
	2.98	3.88	24.89	12.89	15.15	116.01
Average	3.29	4.21	29.38	11.35	15.98	103.98

Table A. 156. Surface roughness data for 3003-T3 aluminum before- and after- 28 hours of tests with 1- m/s parallel flow of 2% alumina nanofluid of distilled water.

Surface roughness ( $\mu$ inch)	Before test			After test		
	Ra	Rq	Rz	Ra	Rq	Rz
Longitudinal	3.43	4.41	29.59	20.22	25.16	126.27
	3.59	4.58	29.85	28.94	33.79	134.98
	3.35	4.23	29.28	29.42	24.54	136.08
Transvers	3.14	4.11	27.21	20.13	24.98	124.98
	3.22	4.57	28.12	20.01	23.78	134.98
	3.22	4.31	27.98	28.11	23.22	124.91
Average	3.32	4.70	28.68	25.68	27.02	130.12

Table A. 158. Surface roughness data for 3003-T3 aluminum before- and after- 112 hours of tests with 1- m/s parallel flow of 2% alumina nanofluid of distilled water.

Surface roughness ( $\mu$ inch)	Before test			After test		
	Ra	Rq	Rz	Ra	Rq	Rz
Longitudinal	2.26	4.32	34.12	31.28	46.77	104.24
	3.27	4.92	34.22	42.84	55.02	163.01
	3.45	4.36	27.38	38.77	51.39	280.52
Transvers	2.25	4.44	35.21	36.31	46.94	248.83
	2.29	2.98	21.47	37.13	59.75	274.36
	3.13	2.87	20.98	37.24	49.68	174.01
Average	2.76	3.99	28.88	39.98	55.23	183.15

Following Figures A.21 and A.22 displays plots of average and normalized values of Rq and Rz roughness for 3003-T3 aluminum before and after 3, 7, 14, 28, 56 and 112 hour-treatments with the reference fluid of distilled water and its 2% alumina nanofluid with 1 m/s parallel flow tests.

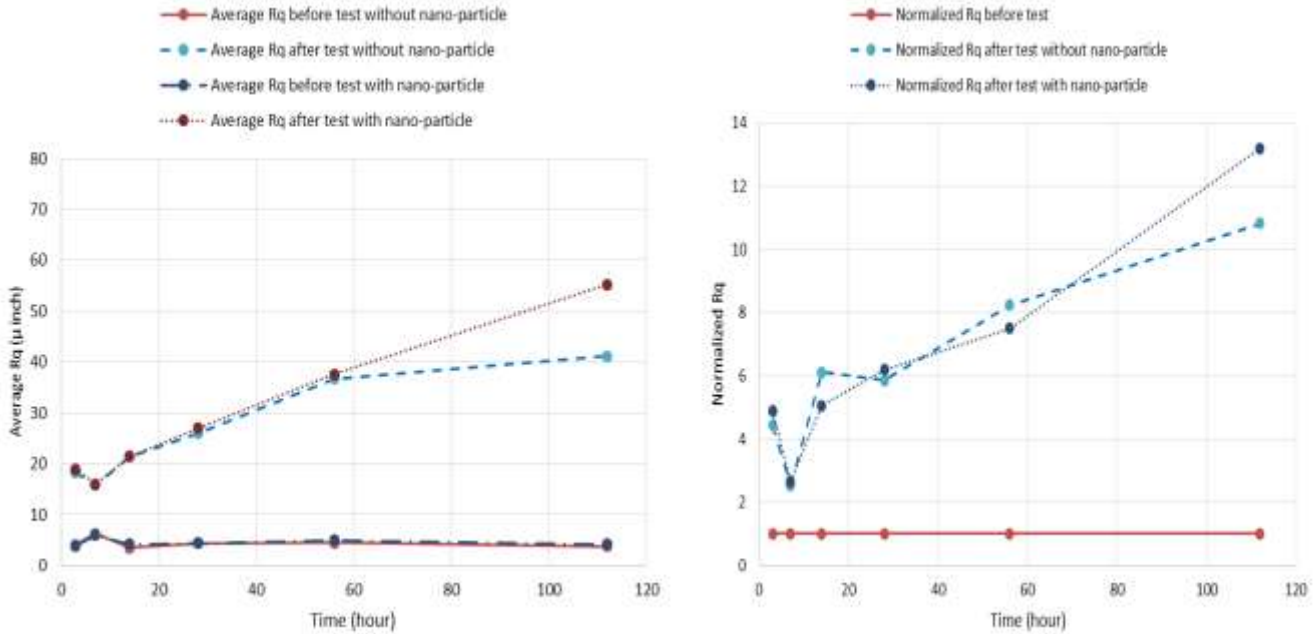


Figure A. 21. Average and normalized Rq roughness for 3003-T3 aluminum before and after 3, 7, 14, 28, 56 and 112 hour-treatments with the reference fluid distilled water, and with nanofluid of 2% nano-alumina in reference fluid and parallel flow speed of 1 m/s.

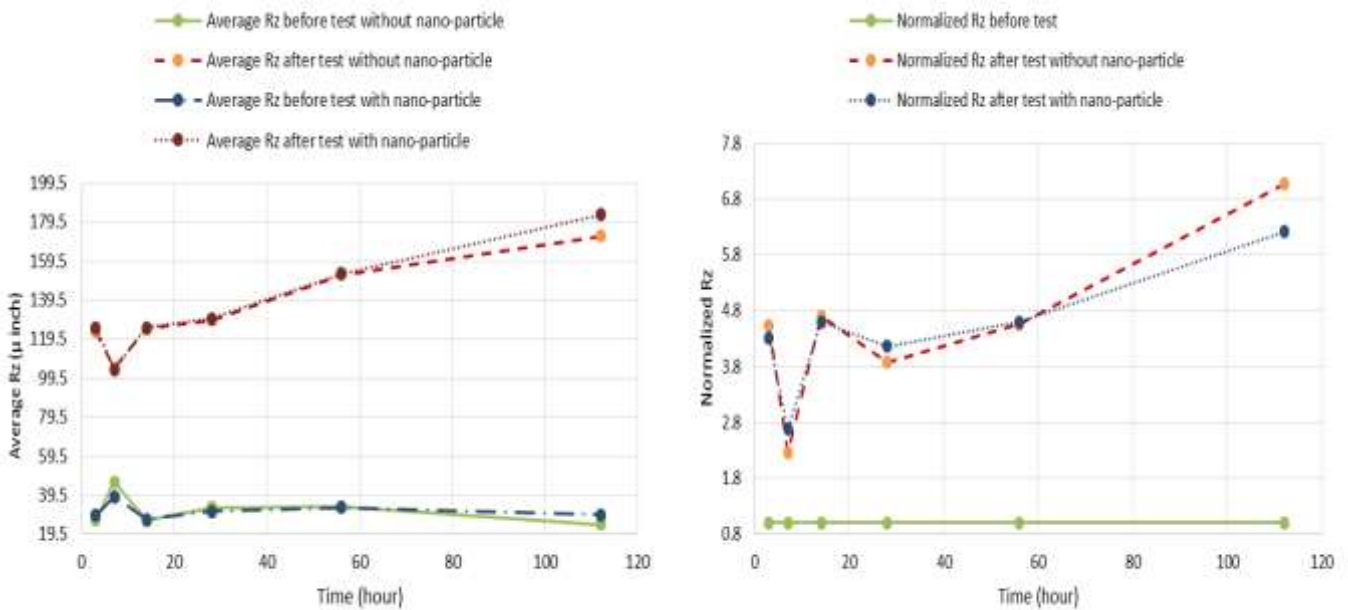


Figure A. 22. Average and normalized Rz roughness for 3003-T3 aluminum before and after 3, 7, 14, 28, 56 and 112 hour-treatments with the reference fluid distilled water, and with nanofluid of 2% nano-alumina in reference fluid and parallel flow speed of 1 m/s.

## A.2.1 Test results of 1 m/s parallel flow with distilled water as base fluid and its 2% alumina nanofluid on copper

Table A. 159. Surface roughness data for copper alloy110 before- and after- 3 hours of tests with 1- m/s parallel flow of distilled water.

Surface roughness ( $\mu$ inch)	Before test			After test		
	Ra	Rq	Rz	Ra	Rq	Rz
Longitudinal	1.19	2.44	13.46	2.58	3.75	30.32
	2.55	3.56	20.22	2.04	2.61	35.93
	2.16	2.91	19.35	2.85	3.6	38.37
Transvers	2.31	3.19	20.59	2.49	3.94	32.67
	2.35	3.32	22.82	2.89	2.88	21.32
	1.53	2.29	14.66	2.39	3.78	30.94
Average	2.28	2.87	18.68	2.41	3.81	32.71

Table A. 160. Surface roughness data for copper alloy110 before- and after- 7 hours of tests with 1- m/s parallel flow of distilled water.

Surface roughness ( $\mu$ inch)	Before test			After test		
	Ra	Rq	Rz	Ra	Rq	Rz
Longitudinal	2.33	3.12	20.39	2.32	3.51	31.58
	1.81	2.96	19.39	1.68	2.11	32.13
	2.29	2.57	17.61	1.95	2.49	24.96
Transvers	2.61	3.49	22.89	2.68	3.73	37.13
	2.23	2.77	16.36	2.61	2.01	21.23
	1.83	2.54	15.54	2.77	2.22	22.26
Average	2.27	2.71	18.51	2.22	3.62	28.55

Table A. 161. Surface roughness data for copper alloy110 before- and after- 14 hours of tests with 1- m/s parallel flow of distilled water.

Surface roughness ( $\mu$ inch)	Before test			After test		
	Ra	Rq	Rz	Ra	Rq	Rz
Longitudinal	6.76	8.73	41.69	2.38	3.27	22.35
	3.23	5.25	40.38	3.89	5.56	38.88
	3.62	4.49	21.73	2.86	4.65	28.95
Transvers	4.53	5.38	24.59	2.18	2.94	17.14
	3.65	4.68	26.18	1.97	2.58	15.64
	4.61	5.65	28.32	3.85	4.72	24.81
Average	4.33	5.58	30.31	2.46	3.42	24.79

Table A. 162. Surface roughness data for copper alloy110 before- and after- 28 hours of tests with 1- m/s parallel flow of distilled water.

Surface roughness ( $\mu$ inch)	Before test			After test		
	Ra	Rq	Rz	Ra	Rq	Rz
Longitudinal	3.21	4.24	27.36	2.41	3.38	24.45
	3.23	3.98	26.33	2.28	3.17	24.89
	2.63	4.02	33.19	2.59	3.44	24.63
Transvers	2.77	3.92	22.16	2.66	3.94	29.96
	2.92	3.92	21	2.75	3.94	29.84
	2.39	3.05	20.9	3.55	5.63	23.09
Average	2.86	3.72	25.24	2.49	3.53	25.70

Table A. 163. Surface roughness data for copper alloy110 before- and after- 56 hours of tests with 1- m/s parallel flow of distilled water.

Surface roughness ( $\mu$ inch)	Before test			After test		
	Ra	Rq	Rz	Ra	Rq	Rz
Longitudinal	2.41	3.19	15.77	2.36	4.83	28.61
	2.22	3.02	18.23	2.72	4.27	23.57
	2.48	3.62	19.22	1.81	2.43	17.03
Transvers	3.31	4.6	27.5	2.83	3.66	17.24
	3.55	5.08	25.27	2.51	3.41	17.43
	3.69	6.48	44.15	2.2	3.24	18.21
Average	2.79	4.66	25.36	2.46	3.44	24.39

Table A. 164. Surface roughness data for copper alloy110 before- and after- 112 hours of tests with 1- m/s parallel flow of distilled water.

Surface roughness ( $\mu$ inch)	Before test			After test		
	Ra	Rq	Rz	Ra	Rq	Rz
Longitudinal	2.43	3.52	18.21	4.49	5.28	35.73
	3.37	5.15	37.79	2.61	3.39	22.14
	2.71	3.54	20.77	5.75	6.57	30.51
Transvers	3.56	4.52	26.43	3.86	5.94	35.6
	2.67	4.02	25.72	3.14	4.74	35.02
	2.31	3.37	25.59	2.63	3.44	25.01
Average	2.68	3.43	25.54	3.18	4.37	30.22

Table A. 165. Surface roughness data for copper alloy110 before- and after- xxx hours of tests with 1- m/s parallel flow of 2% alumina nanofluid of distilled water.

Surface roughness ( $\mu$ inch)	Before test			After test		
	Ra	Rq	Rz	Ra	Rq	Rz
Longitudinal	3.15	5.23	41.61	2.85	3.72	39.23
	3.44	4.59	34.28	3.01	4.11	30.22
	4.27	6.67	58.01	2.71	3.75	35.25

Table A. 166. Surface roughness data for copper alloy110 before- and after- xxx hours of tests with 1- m/s parallel flow of 2% alumina nanofluid of distilled water.

Surface roughness ( $\mu$ inch)	Before test			After test		
	Ra	Rq	Rz	Ra	Rq	Rz
Longitudinal	2.11	5.81	40.73	2.33	3.75	21.73
	5213	5.23	41.26	2.23	3.91	22.23
	6321	7.11	49.22	2.11	4.11	26.21

Transvers	3.65	5.23	41.51	2.83	3.92	30.23
	3.44	4.39	34.28	3.01	4.11	36.22
	4.47	6.47	58.01	2.71	3.75	33.25
Average	3.65	5.56	44.16	2.87	3.75	33.16

Table A. 167. Surface roughness data for copper alloy110 before- and after- xxx hours of tests with 1- m/s parallel flow of 2% alumina nanofluid of distilled water.

Surface roughness ( $\mu$ inch)	Before test			After test		
	Ra	Rq	Rz	Ra	Rq	Rz
Longitudinal	3.22	4.35	27.43	3.21	4.38	26.42
	3.25	4.12	26.25	3.11	4.22	27.32
	3.31	4.09	29.44	3.21	4.36	28.11
Transvers	3.32	4.25	27.33	3.35	4.18	26.32
	3.15	4.12	26.25	3.11	4.22	27.32
	3.51	4.09	29.44	3.21	4.36	28.11
Average	3.29	4.25	27.57	3.35	4.92	28.89

Table A. 169. Surface roughness data for copper alloy110 before- and after- xxx hours of tests with 1- m/s parallel flow of 2% alumina nanofluid of distilled water.

Surface roughness ( $\mu$ inch)	Before test			After test		
	Ra	Rq	Rz	Ra	Rq	Rz
Longitudinal	3.74	5.61	40.16	2.45	5.32	45.12
	2.66	3.79	29.15	2.87	7.63	57.71
	3.17	4.93	43.39	3.09	4.82	41.99
Transvers	3.94	5.51	40.06	2.55	6.52	45.02
	2.56	3.79	29.15	2.87	4.63	37.71
	3.17	4.93	43.39	3.09	7.82	49.99
Average	3.32	4.84	36.43	3.92	6.99	43.60

Transvers	2.41	5.71	40.63	4.21	5.7	41.63
	5.23	5.23	41.26	2.23	3.91	22.23
	6.31	7.11	49.22	2.11	3.11	26.21
Average	4.52	6.02	43.70	2.35	3.51	24.16

Table A. 168. Surface roughness data for copper alloy110 before- and after- xxx hours of tests with 1- m/s parallel flow of 2% alumina nanofluid of distilled water.

Surface roughness ( $\mu$ inch)	Before test			After test		
	Ra	Rq	Rz	Ra	Rq	Rz
Longitudinal	5.11	6.22	38.16	3.33	3.55	21.14
	3.13	4.96	38.15	2.22	3.19	28.45
	5.36	7.45	40.19	3.51	4.72	31.42
Transvers	5.11	6.52	38.26	3.51	4.75	31.44
	3.23	4.96	38.15	4.22	7.19	28.42
	5.76	7.45	40.19	3.51	4.72	21.42
Average	4.53	6.21	38.77	4.68	4.68	28.66

Table A. 170. Surface roughness data for copper alloy110 before- and after- xxx hours of tests with 1- m/s parallel flow of 2% alumina nanofluid of distilled water.

Surface roughness ( $\mu$ inch)	Before test			After test		
	Ra	Rq	Rz	Ra	Rq	Rz
Longitudinal	2.46	3.32	28.22	4.33	6.11	40.15
	4.19	5.74	33.52	5.71	6.22	47.75
	4.33	6.42	56.12	5.86	9.02	46.76
Transvers	2.36	3.22	28.42	4.53	6.21	60.25
	4.19	5.74	33.52	5.71	9.22	67.75
	4.24	6.42	56.25	5.86	9.02	66.76
Average	3.48	5.23	39.52	5.96	8.21	53.18



Following Figures A.23 and A.24 displays plots of average and normalized values of Rq and Rz roughness for copper alloy110 before and after 3, 7, 14, 28, 56 and 112 hour-treatments with the reference fluid of distilled water and its 2% alumina nanofluid with 1 m/s parallel flow tests.

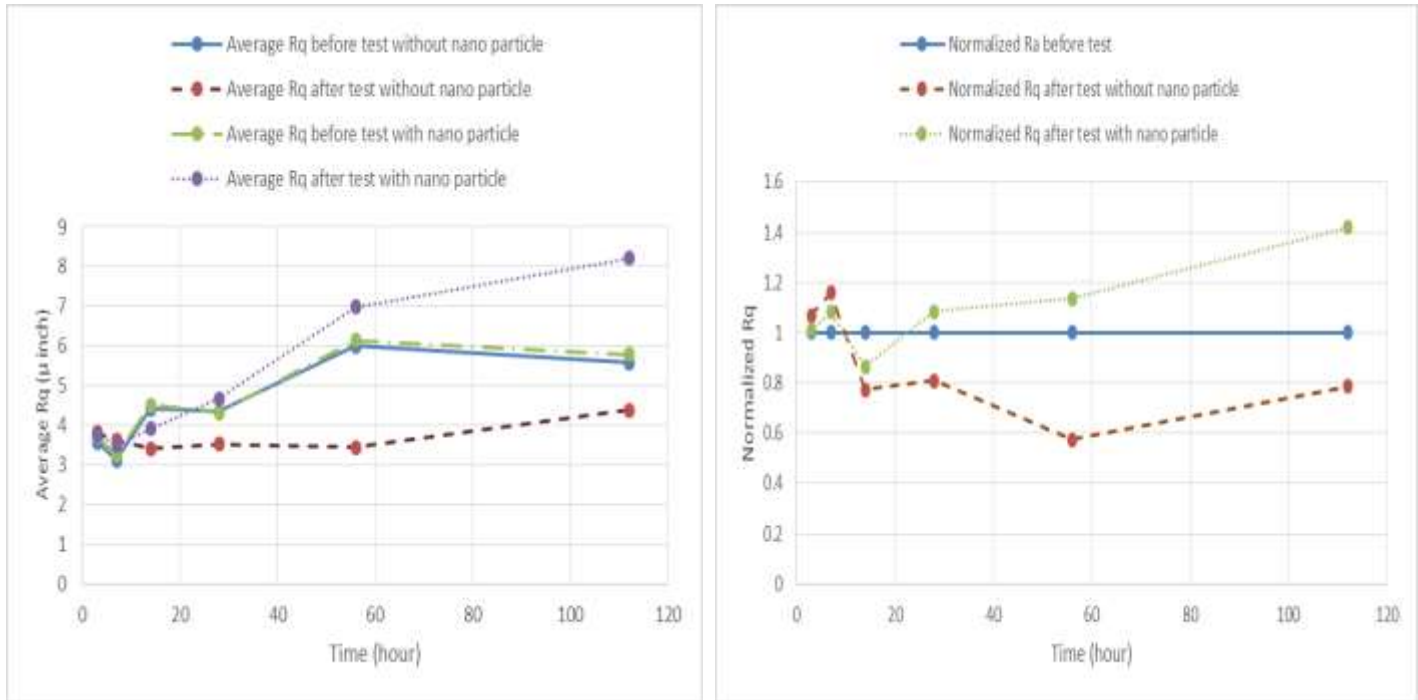


Figure A. 23. Average and normalized Rq roughness for copper alloy110 before and after 3, 7, 14, 28, 56 and 112 hour-treatments with the reference fluid distilled water, and with nanofluid of 2% nano-alumina in reference fluid and parallel flow speed of 1 m/s.

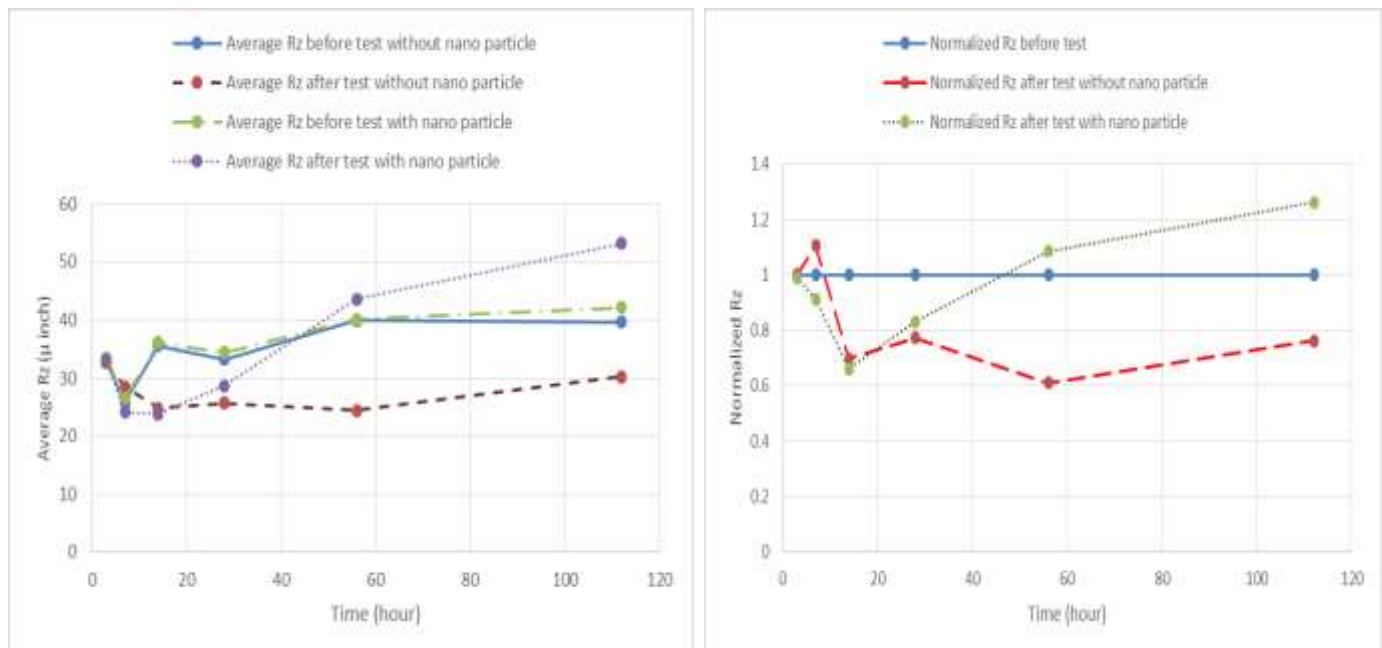






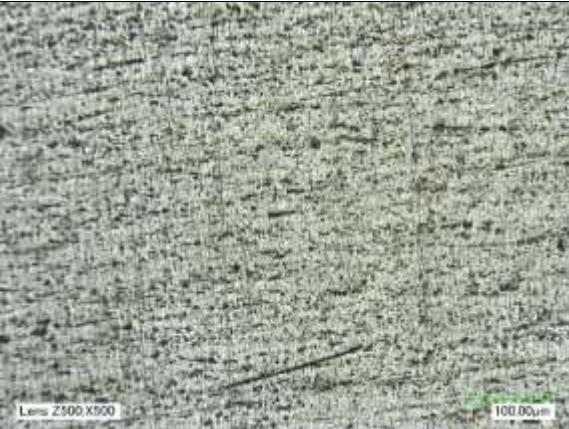

Figure A. 24. Average and normalized Rz roughness for copper alloy110 before and after 3, 7, 14, 28, 56 and 112 hour-treatments with the reference fluid distilled water, and with nanofluid of 2% nano-alumina in reference fluid and parallel flow speed of 1 m/s.

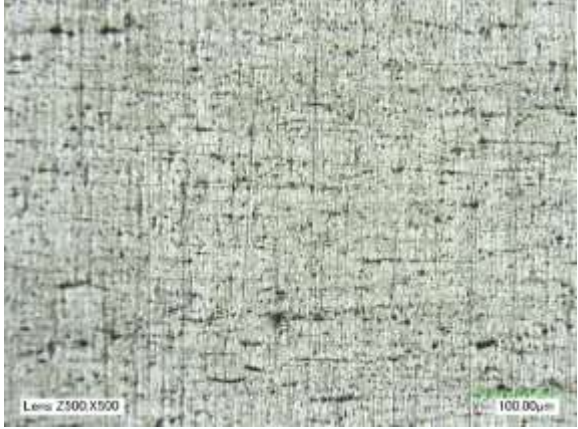

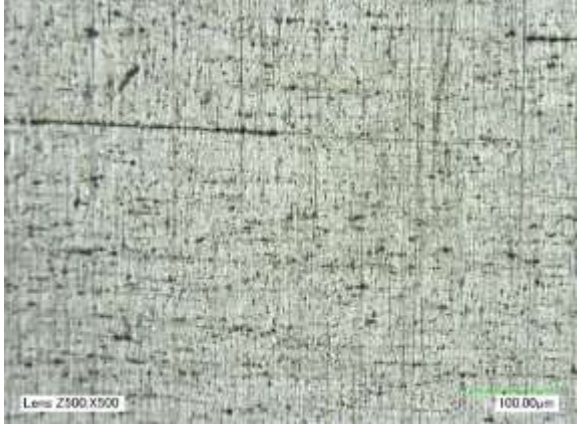
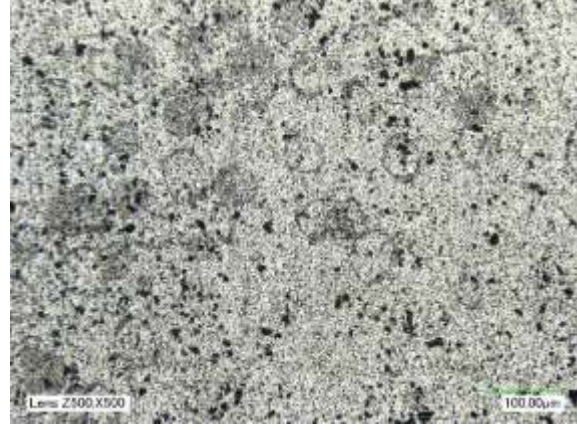


## **APPENDIX B**

### **OPTICAL MICROSCOPY IMAGES**

This Appendix includes all the microscopy images analysis carried out as part of the research work of this thesis. Optical microscopy observations were carried out for the impacted material surfaces (of aluminum and copper specimens) before and after the jet-impingement and the parallel-flow tests, to assess surface modifications and to help elucidate the mechanisms of surface change. A Keyence VHX 1000 Digital Microscope of 54 Megapixel resolution was used. Surface images were captured by a high resolution zoom lens VH-Z500R/W for magnifications of 500x to 5000x (in the sequence 500x, 1000x, 2000x, 3000x, and 5000 x). A lower resolution lens (VH-Z20R) also was used at magnifications of 20x to 200x (in the sequence 20x, 30x, 50x, 100x, 150x and 200x). A VH-Z20R lens was employed for capturing images by three other lens angles (15°, 45°, and 90°).

Figure B. 1. Optical microscopy images (Magnification: 500X) of 3003-T3 aluminum before and after 3, 7, 14, 28, 56, 112, 240, 312 and 408 hour-treatments with the reference fluid of distilled water and jet speed of 3.5 m/s.

Hours	Before test	After test
3		
7		
14		

28	 <p>Lens Z500.X500 100.00µm</p>	 <p>Lens Z500.X500 100.00µm</p>
56	 <p>Lens Z500.X500 100.00µm</p>	 <p>Lens Z500.X500 100.00µm</p>
112	 <p>Lens Z500.X500 100.00µm</p>	 <p>Lens Z500.X500 100.00µm</p>


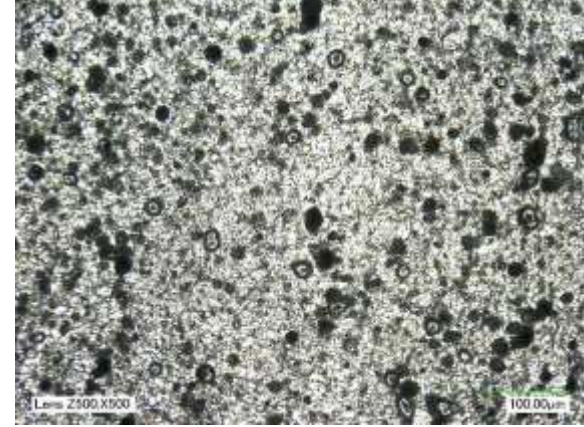

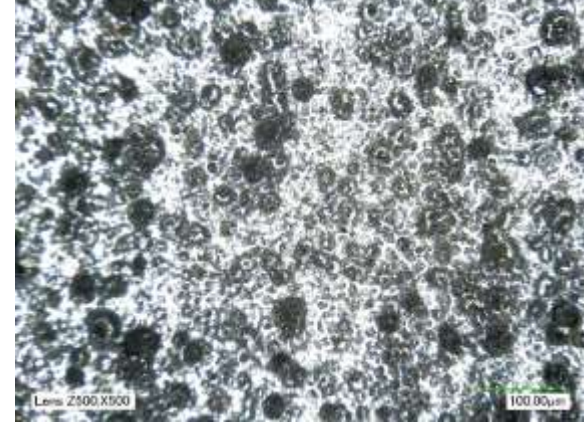

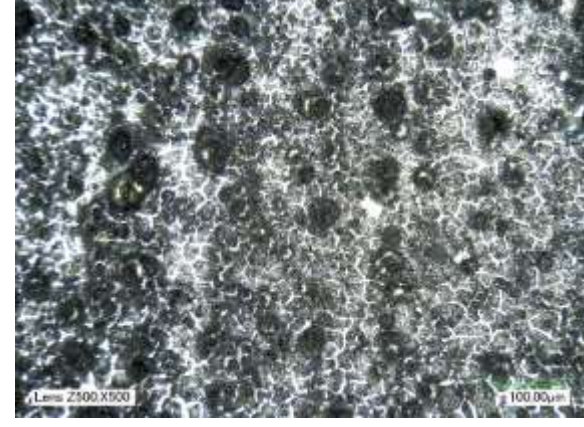




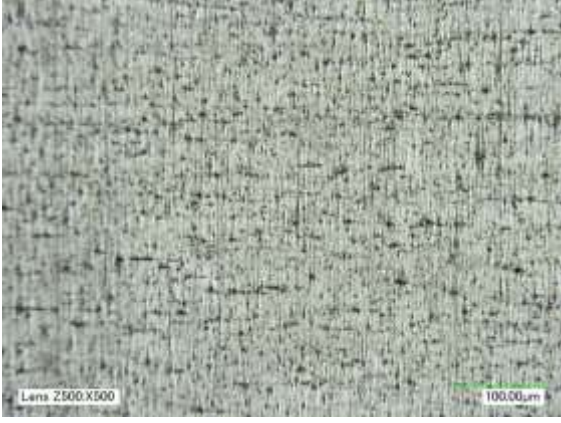

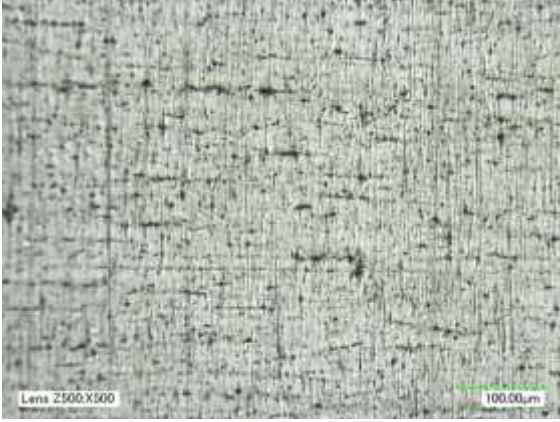
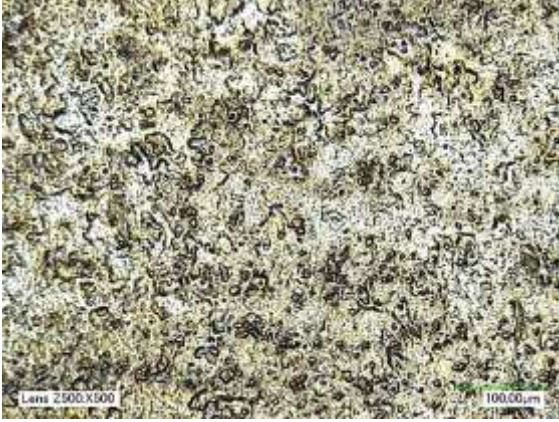
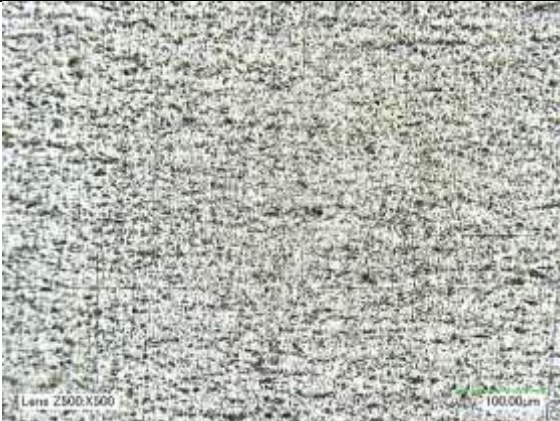
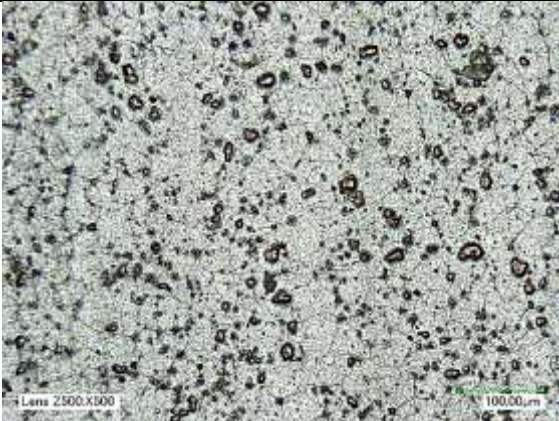

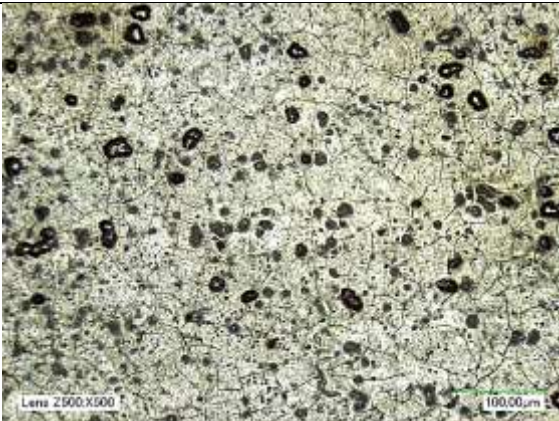
240		
312		
408		

Figure B. 2. Optical microscopy images (Magnification: 500X) of 3003-T3 aluminum before and after 3, 7, 14, 28, 56, 112, 240, 312 and 408 hour-treatments with the 2% alumina nanofluid of distilled water and jet speed of 3.5 m/s.

Hours	Before test	After test
3		
7		
14		

28	 <p>Lens 2500.X500 100.00um</p>	 <p>Lens 2500.X500 100.00um</p>
56	 <p>Lens 2500.X500 100.00um</p>	 <p>Lens 2500.X500 100.00um</p>
112	 <p>Lens 2500.X500 100.00um</p>	 <p>Lens 2500.X500 100.00um</p>


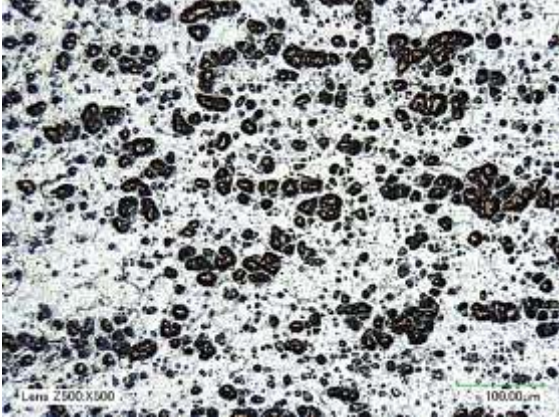
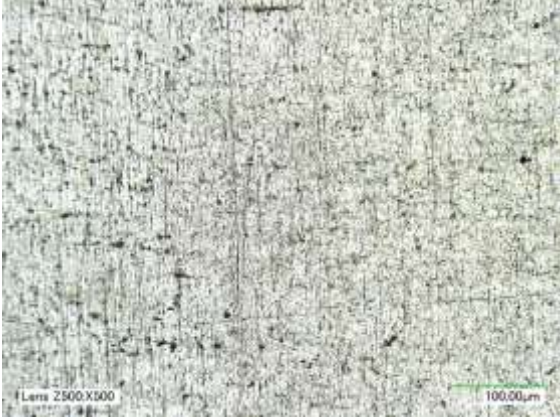
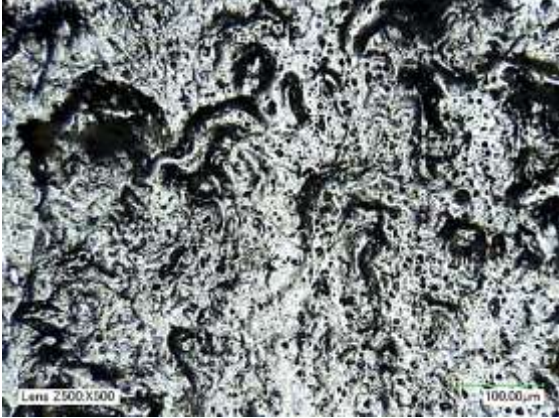
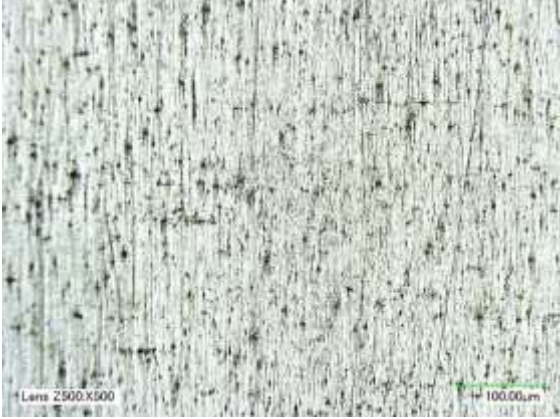
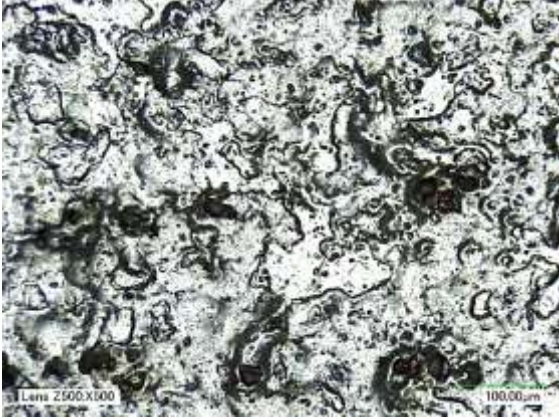
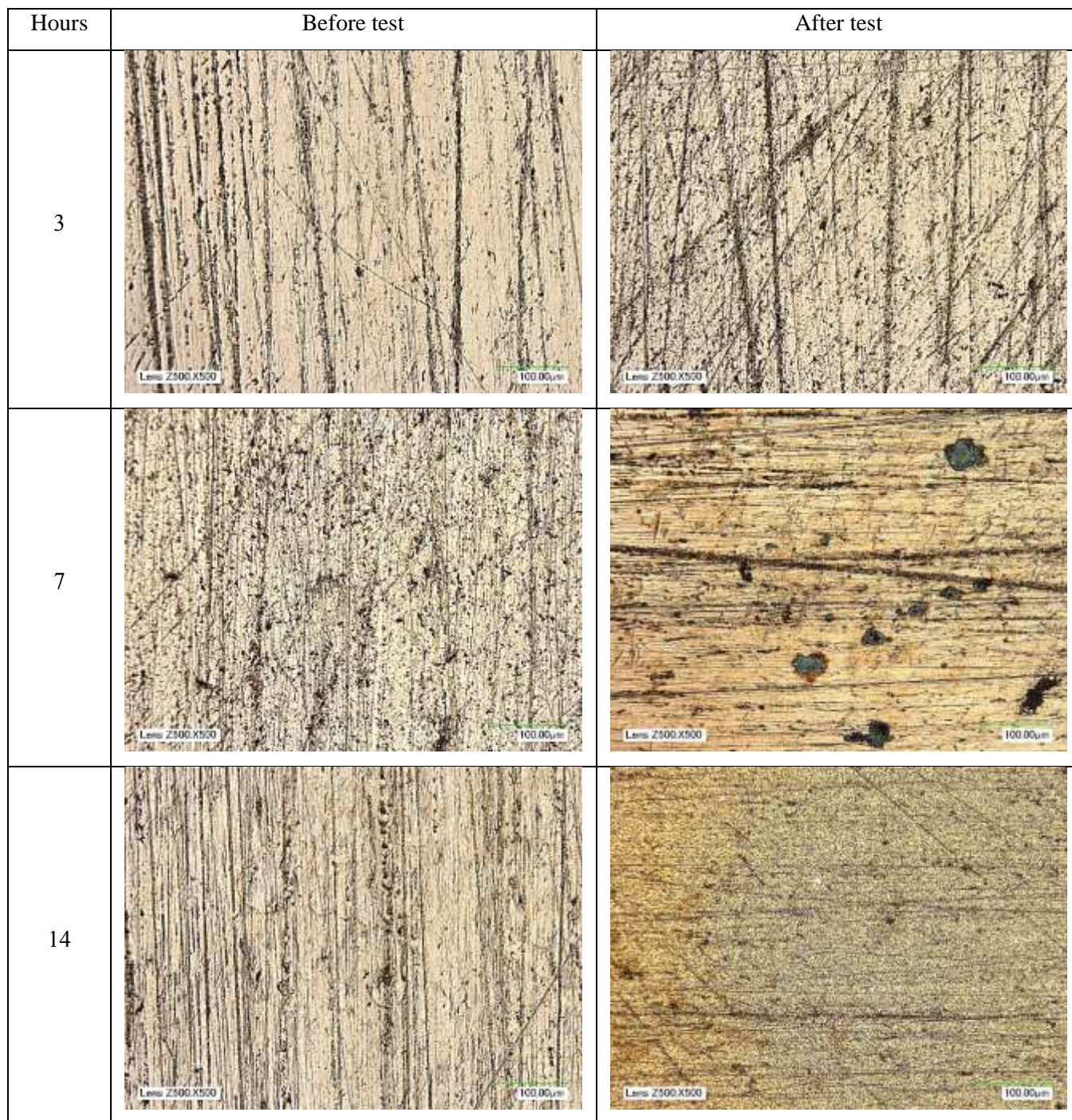
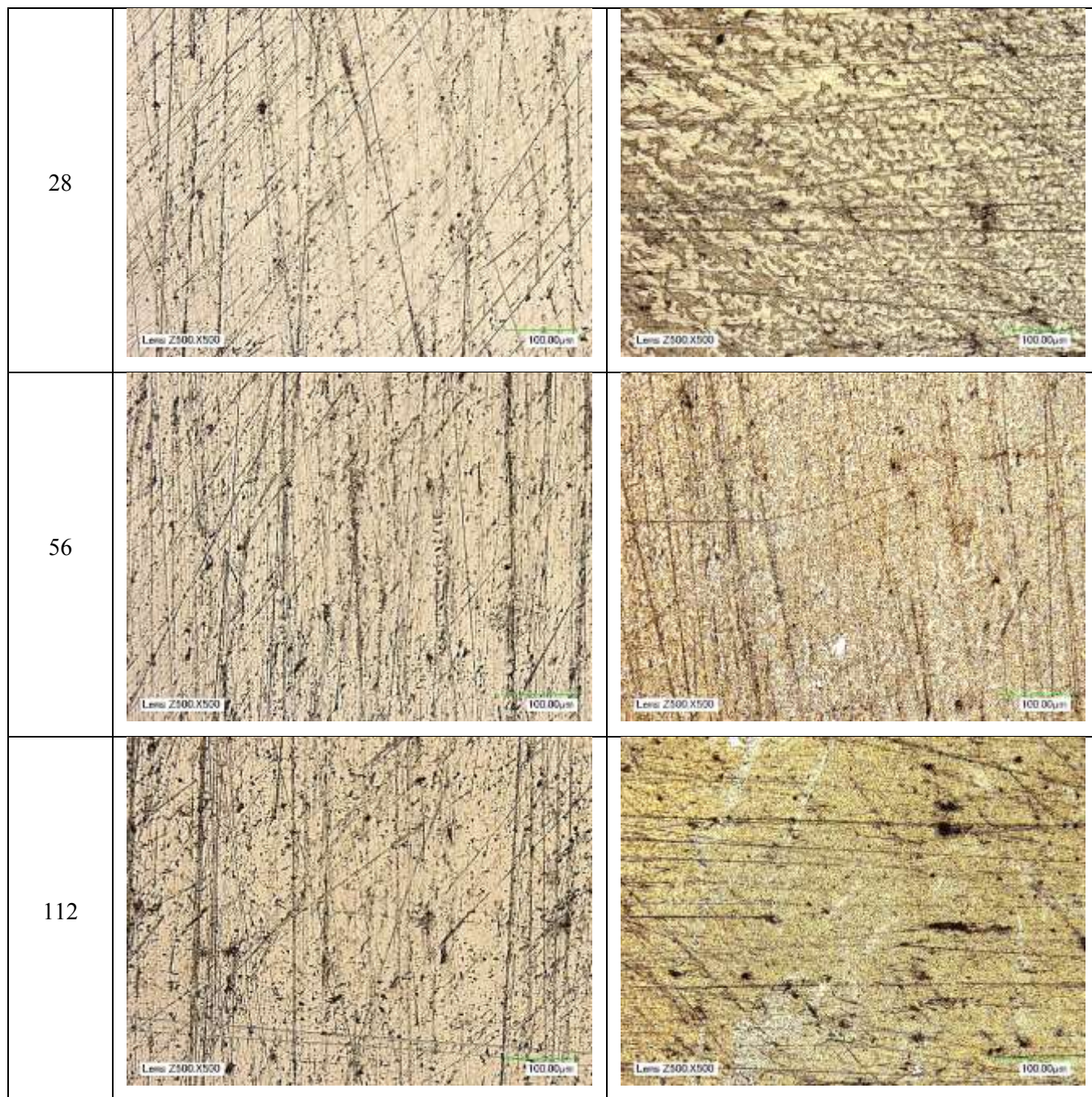
240	 <p>Lens 2500.X500 100.00µm</p>	 <p>Lens 2500.X500 100.00µm</p>
312	 <p>Lens 2500.X500 100.00µm</p>	 <p>Lens 2500.X500 100.00µm</p>
408	 <p>Lens 2500.X500 100.00µm</p>	 <p>Lens 2500.X500 100.00µm</p>



Figure B. 3. Optical microscopy images (Magnification: 500X) of alloy 110 copper before and after 3, 7, 14, 28, 56, 112, 240, 312 and 408 hour-treatments with the reference fluid of distilled water and jet speed of 3.5 m/s.





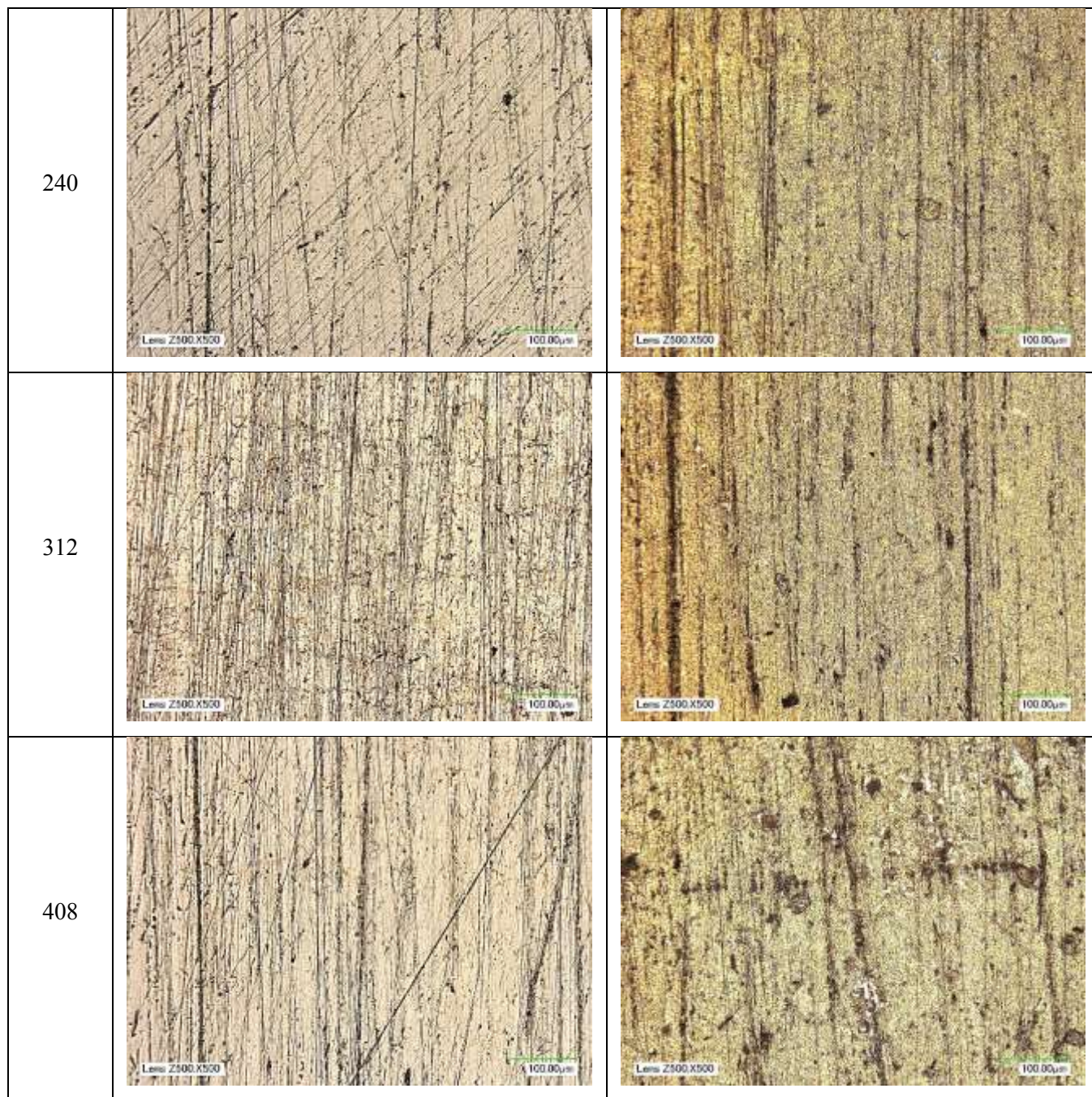

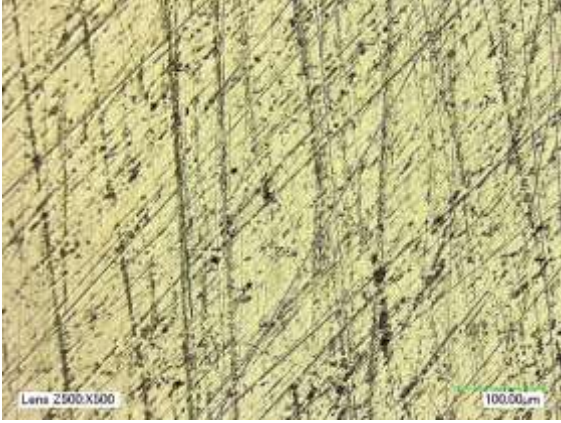

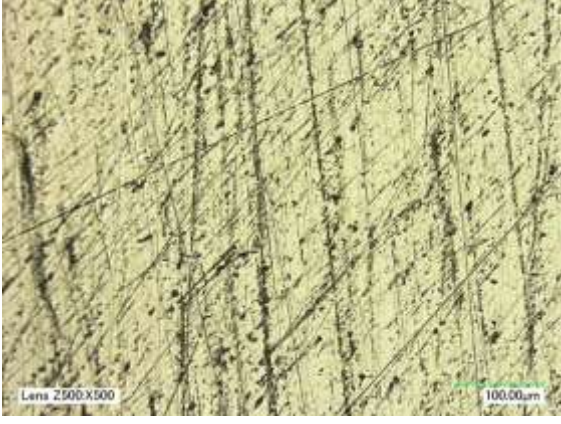
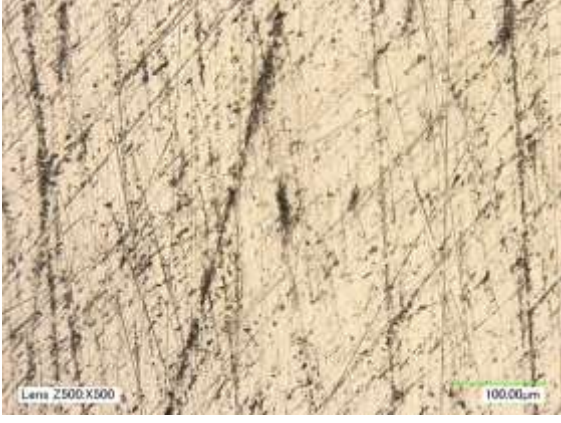
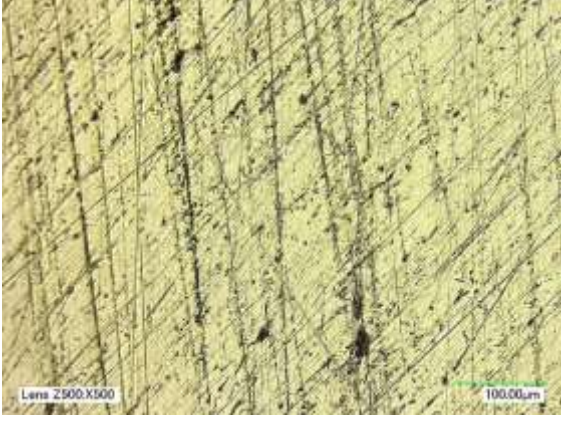
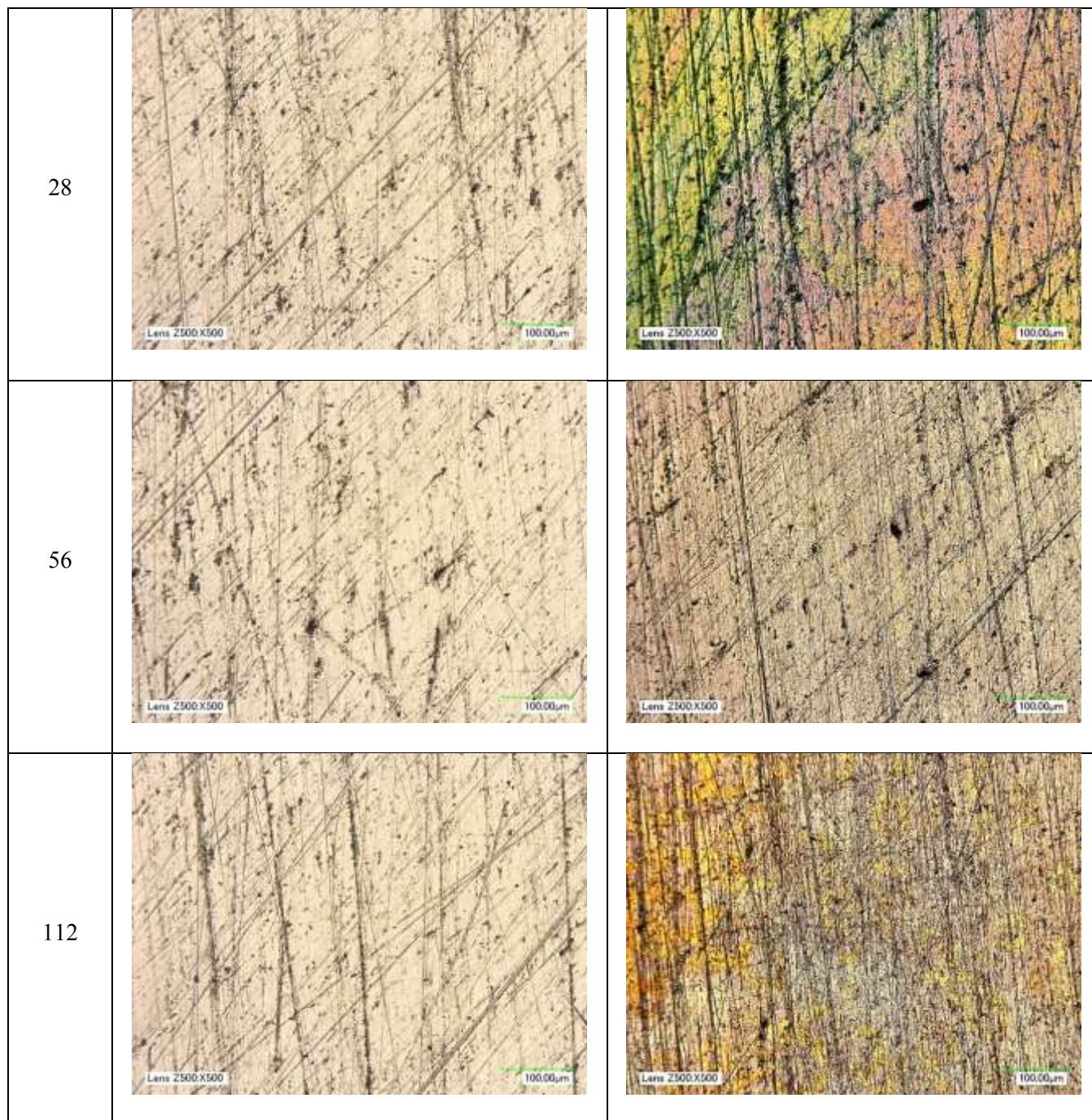


Figure B. 4. Optical microscopy images (Magnification: 500X) of alloy 110 copper before and after 3, 7, 14, 28, 56, 112, 240, 312 and 408 hour-treatments with the 2% alumina nanofluid of distilled water and jet speed of 3.5 m/s.

Hours	Before test	After test
3		
7		
14		




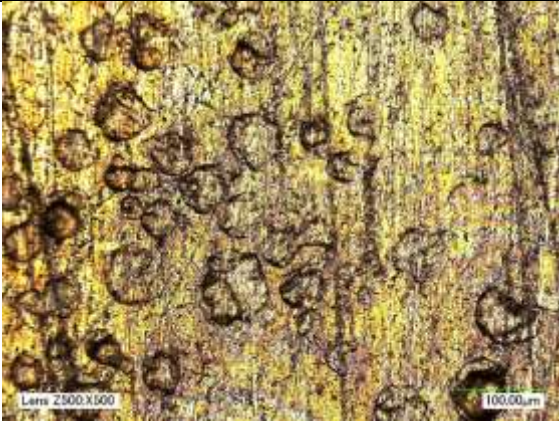
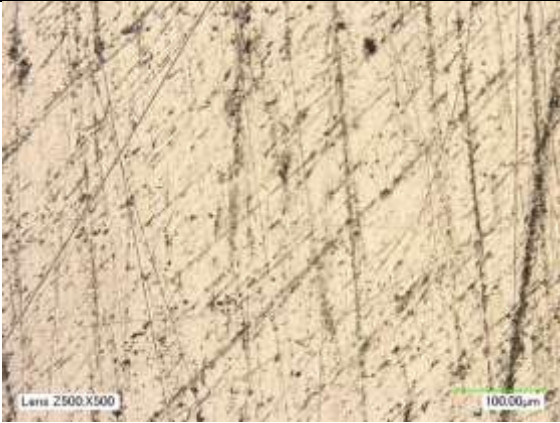
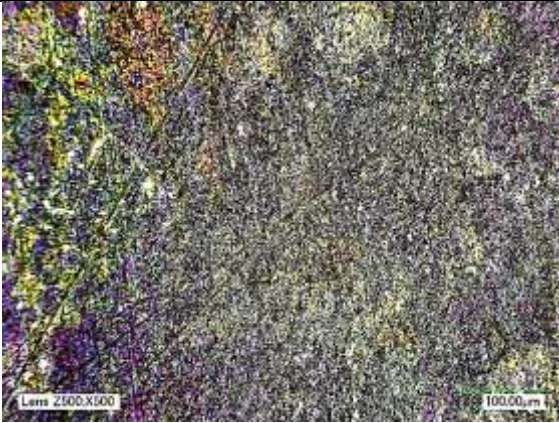


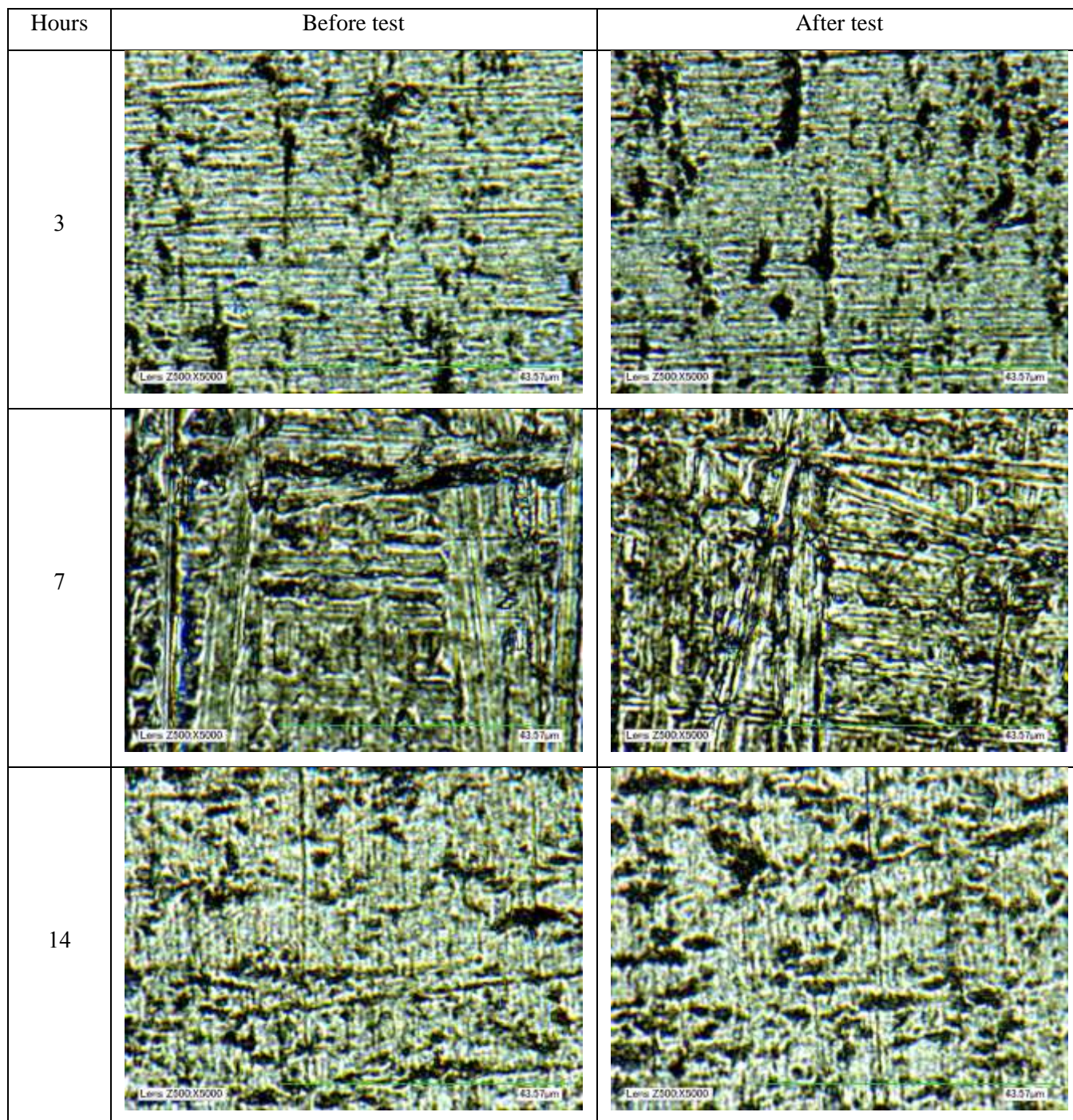
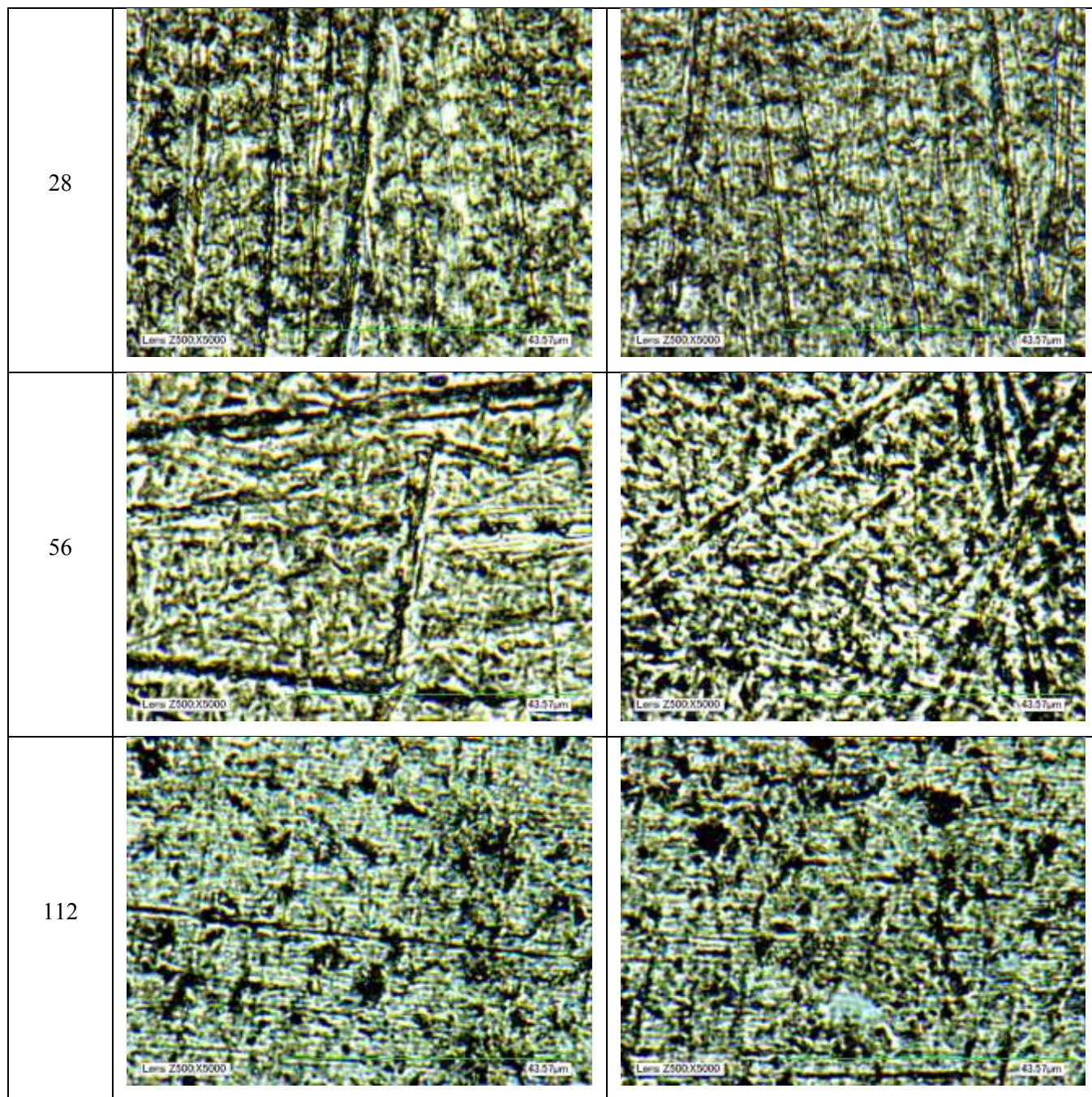
240		
312		
408		

Figure B: 5. Optical microscopy images (Magnification: 5000X) of 3003-T3 aluminum before and after 3, 7, 14, 28, 56, 112, 240, 312 and 408 hour-treatments with the reference fluid of 50/50% Ethylene Glycol in water, and jet speed of 3.5 m/s.







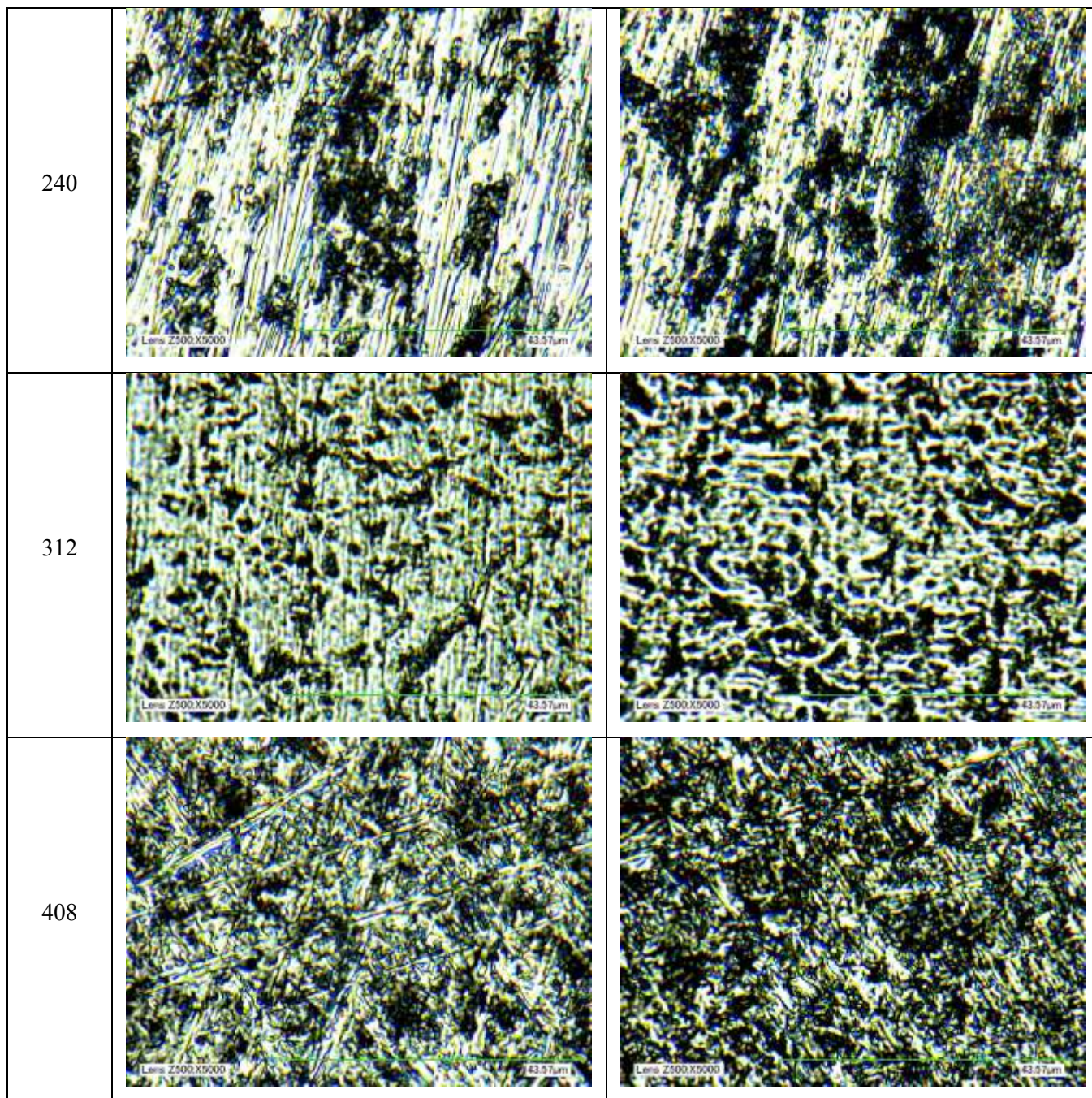
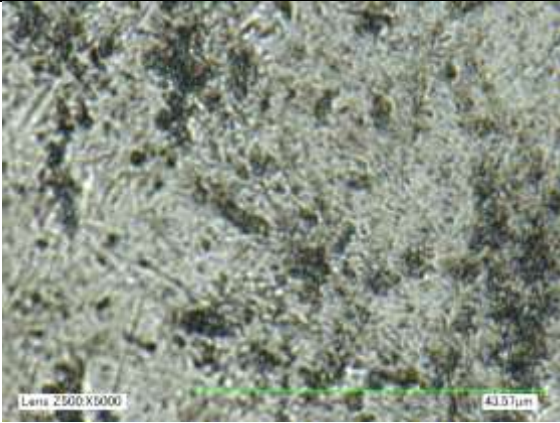
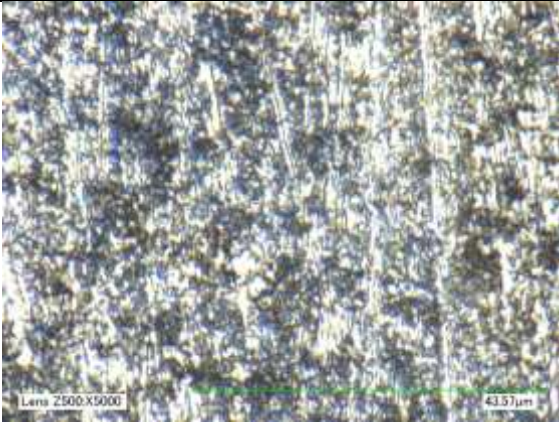
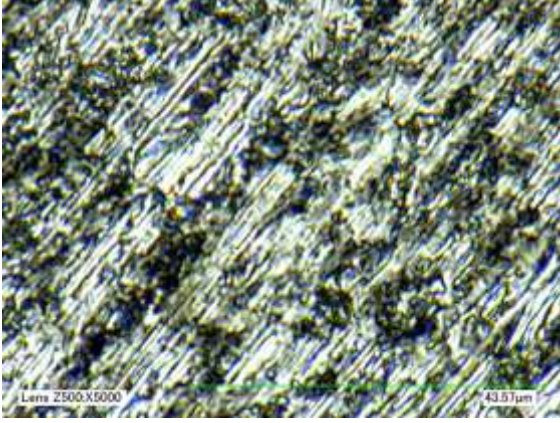
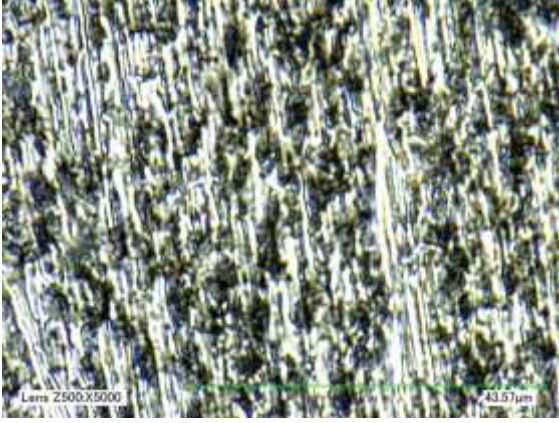
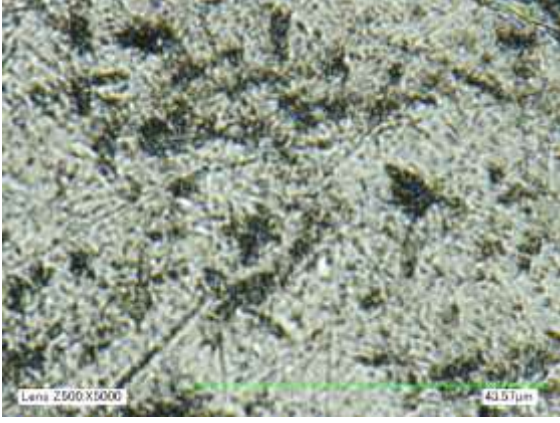
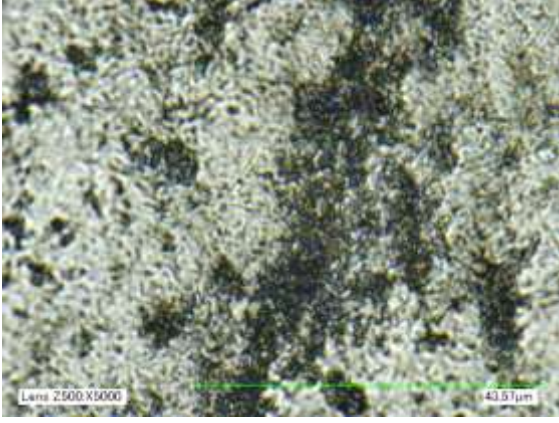
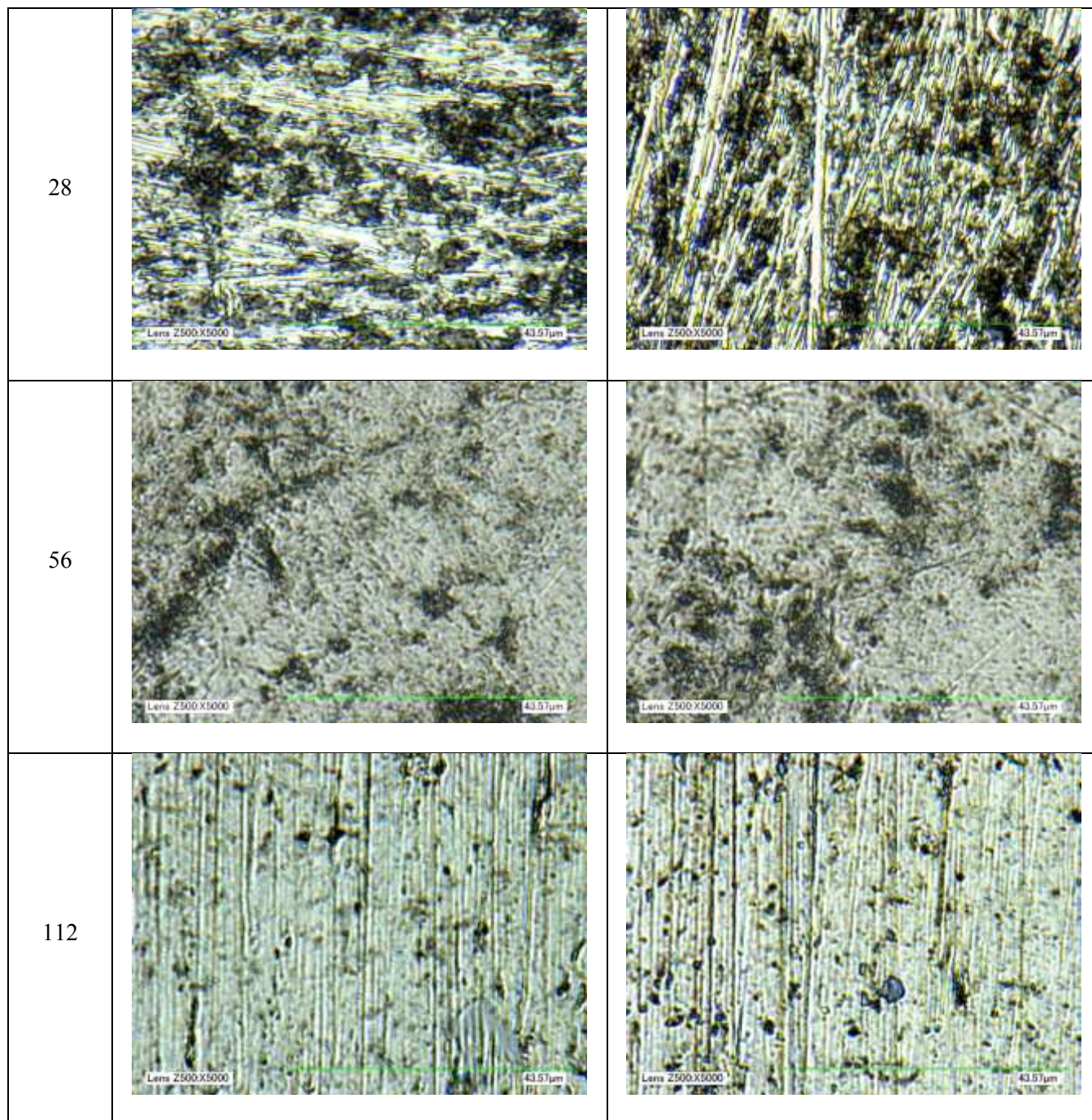


Figure B. 6. Optical microscopy images (Magnification: 5000X) of 3003-T3 aluminum before and after 3, 7, 14, 28, 56, 112, 240, 312 and 408 hour-treatments with the nanofluid of 2% nano-alumina in 50/50% Ethylene Glycol/water, and jet speed of 3.5 m/s.

Hours	Before test	After test
3		
7		
14		



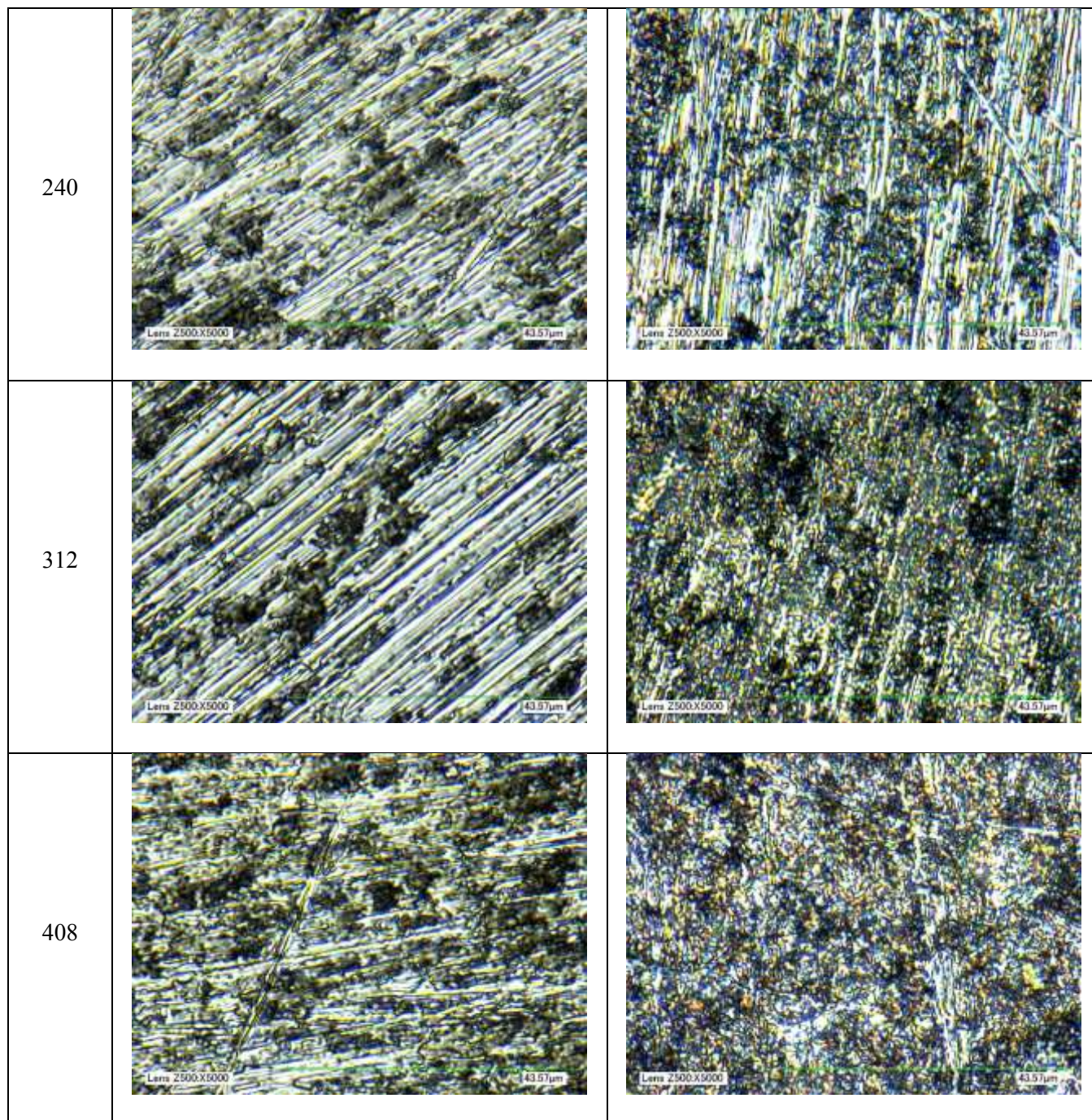
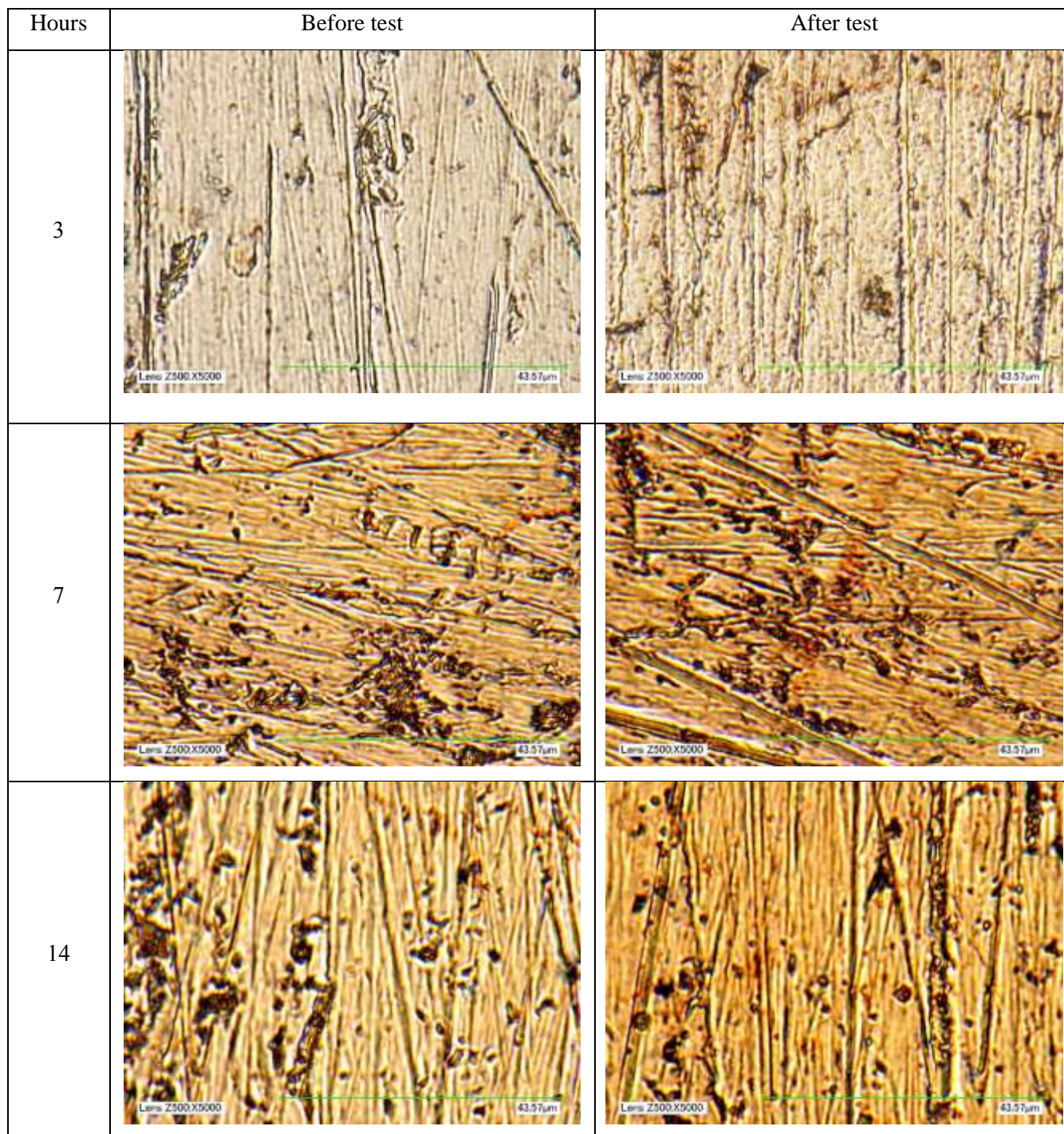

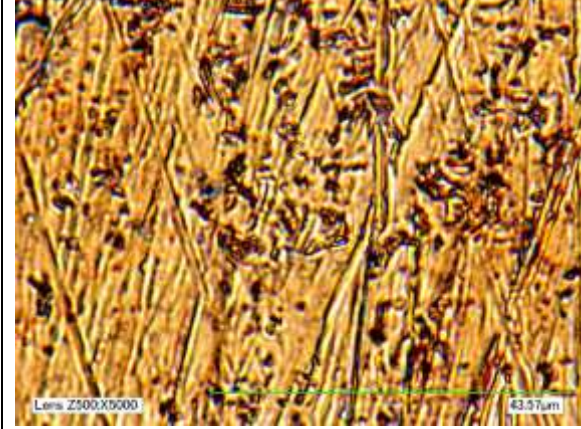
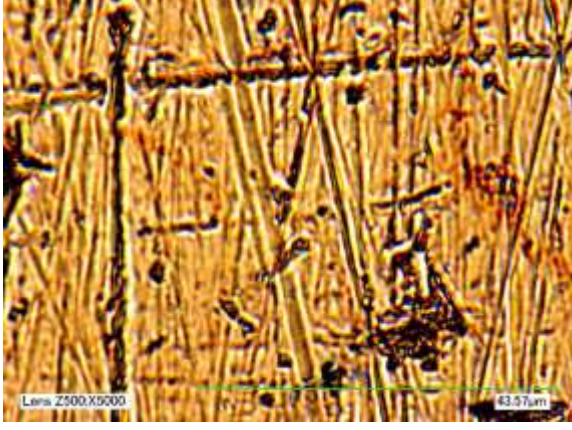
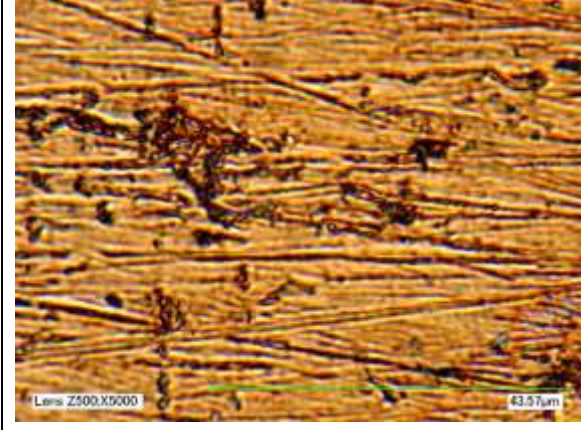
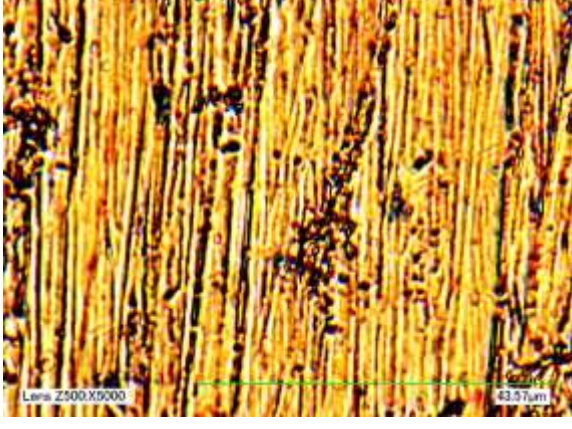



Figure B. 7. Optical microscopy images (Magnification: 5000X) of copper alloy 110 before and after 3, 7, 14, 28, 56, 112, 240, 312 and 408 hour-treatments with the reference fluid of 50/50% Ethylene Glycol in water, and jet speed of 3.5 m/s.



28	 <p>Lens Z500.X5000 43.57µm</p>	 <p>Lens Z500.X5000 43.57µm</p>
56	 <p>Lens Z500.X5000 43.57µm</p>	 <p>Lens Z500.X5000 43.57µm</p>
112	 <p>Lens Z500.X5000 43.57µm</p>	 <p>Lens Z500.X5000 43.57µm</p>

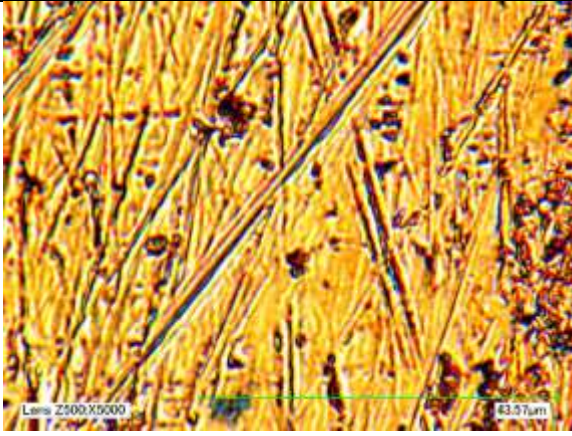
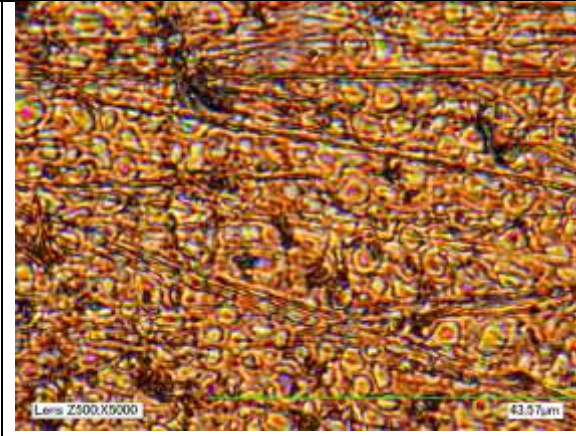
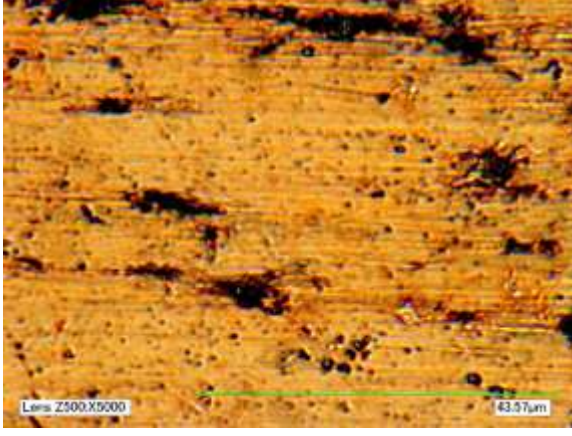
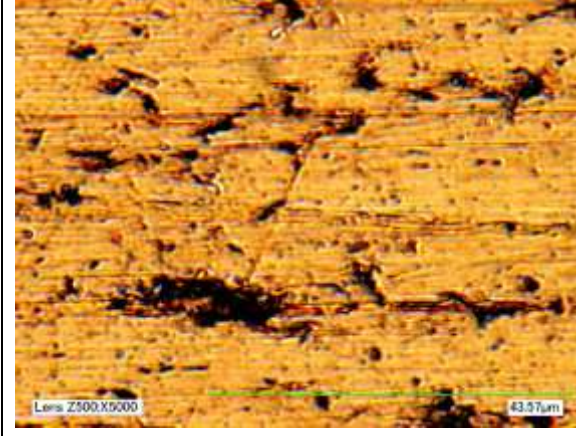
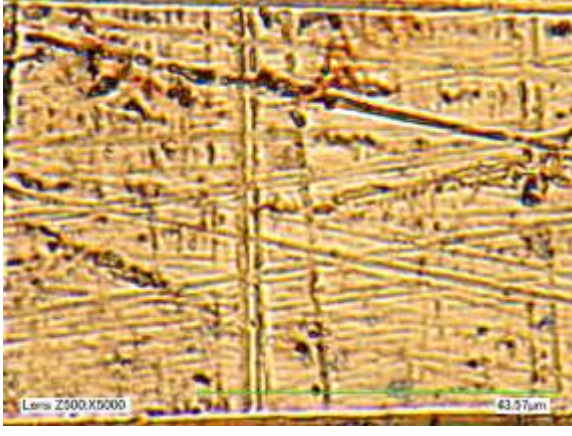
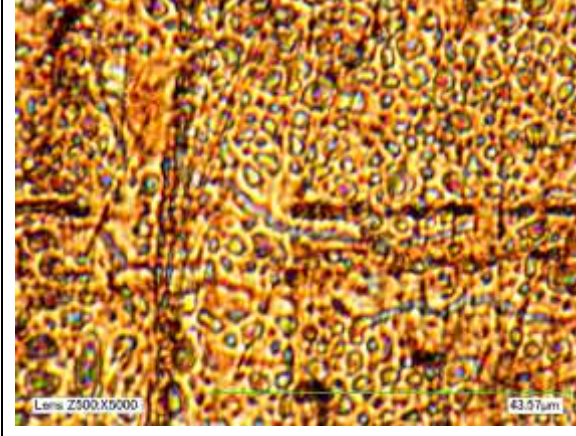
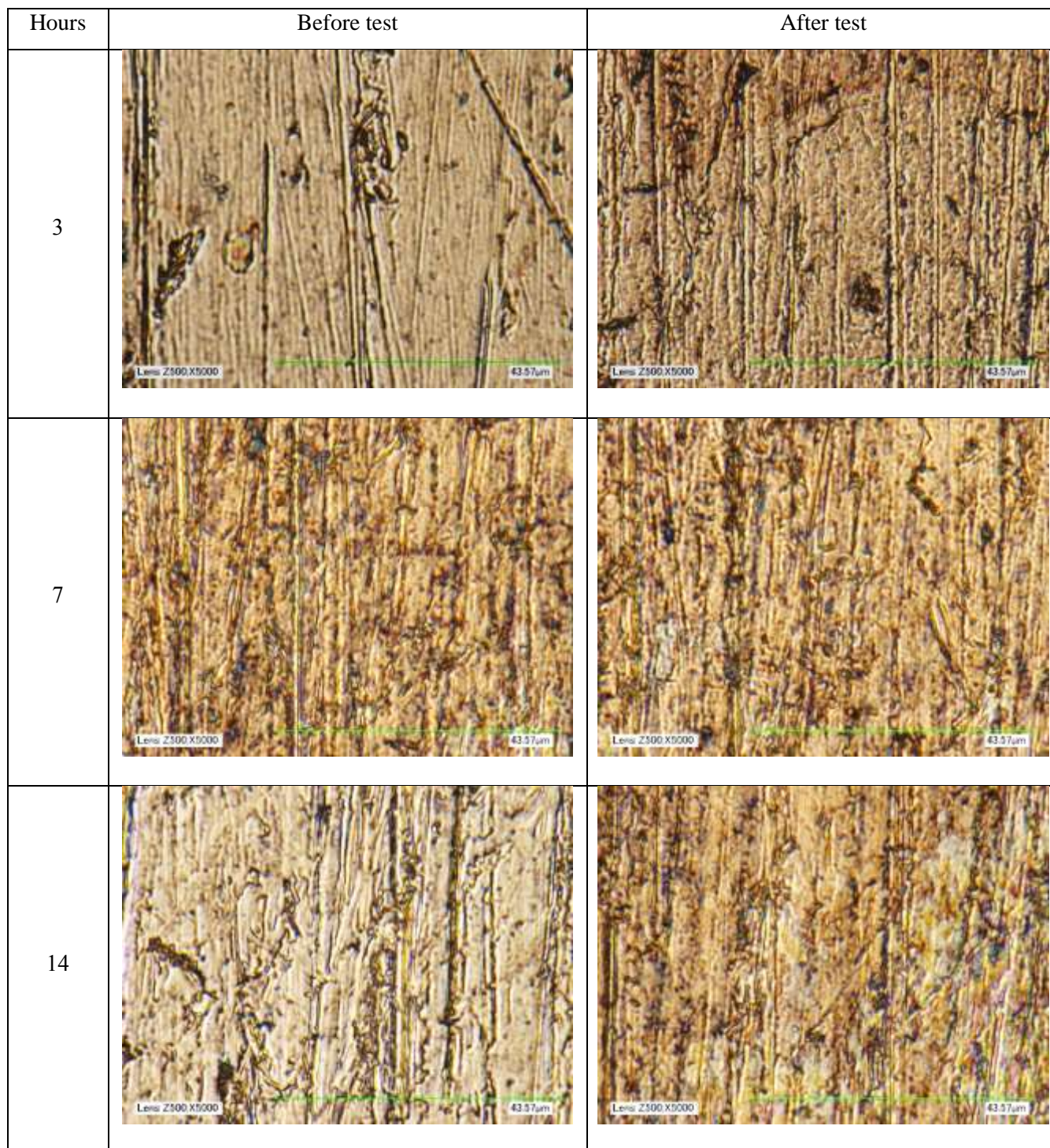
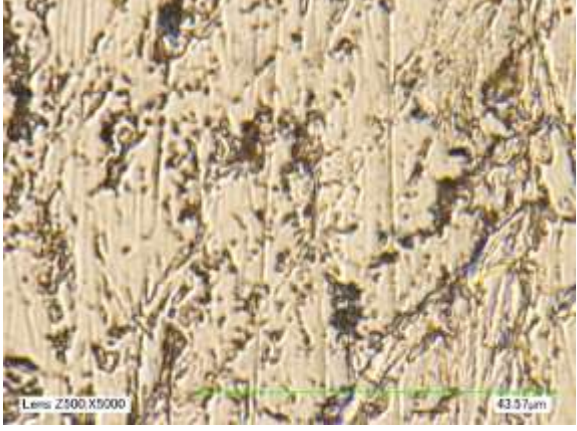
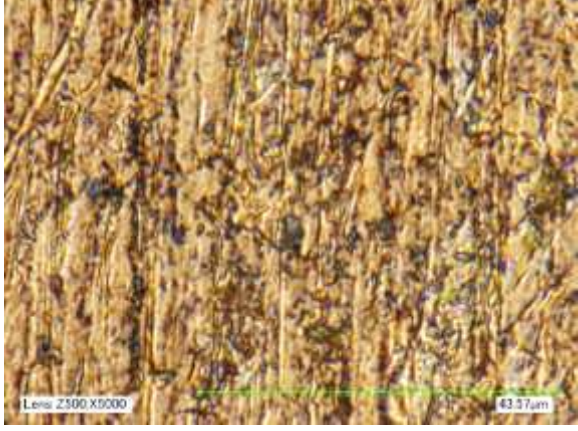
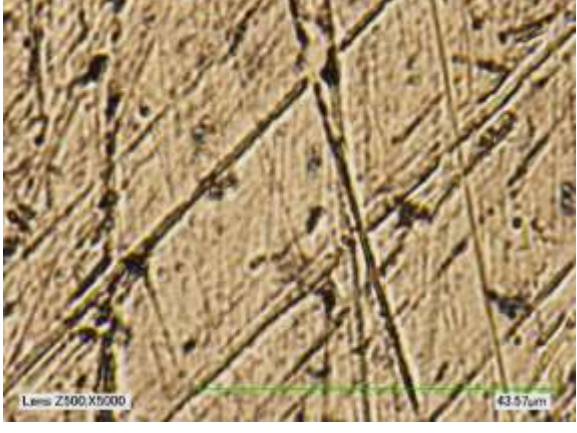



240	 <p>Lens Z500.X5000 43.57µm</p>	 <p>Lens Z500.X5000 43.57µm</p>
312	 <p>Lens Z500.X5000 43.57µm</p>	 <p>Lens Z500.X5000 43.57µm</p>
408	 <p>Lens Z500.X5000 43.57µm</p>	 <p>Lens Z500.X5000 43.57µm</p>

Figure B. 8. Optical microscopy images (Magnification: 5000X) of copper alloy 110 before and after 3, 7, 14, 28, 56, 112, 240, 312 and 408 hour-treatments with the nanofluid of 2% nano-alumina in 50/50% Ethylene Glycol/water and jet speed of 3.5 m/s.





28		
56		
112		

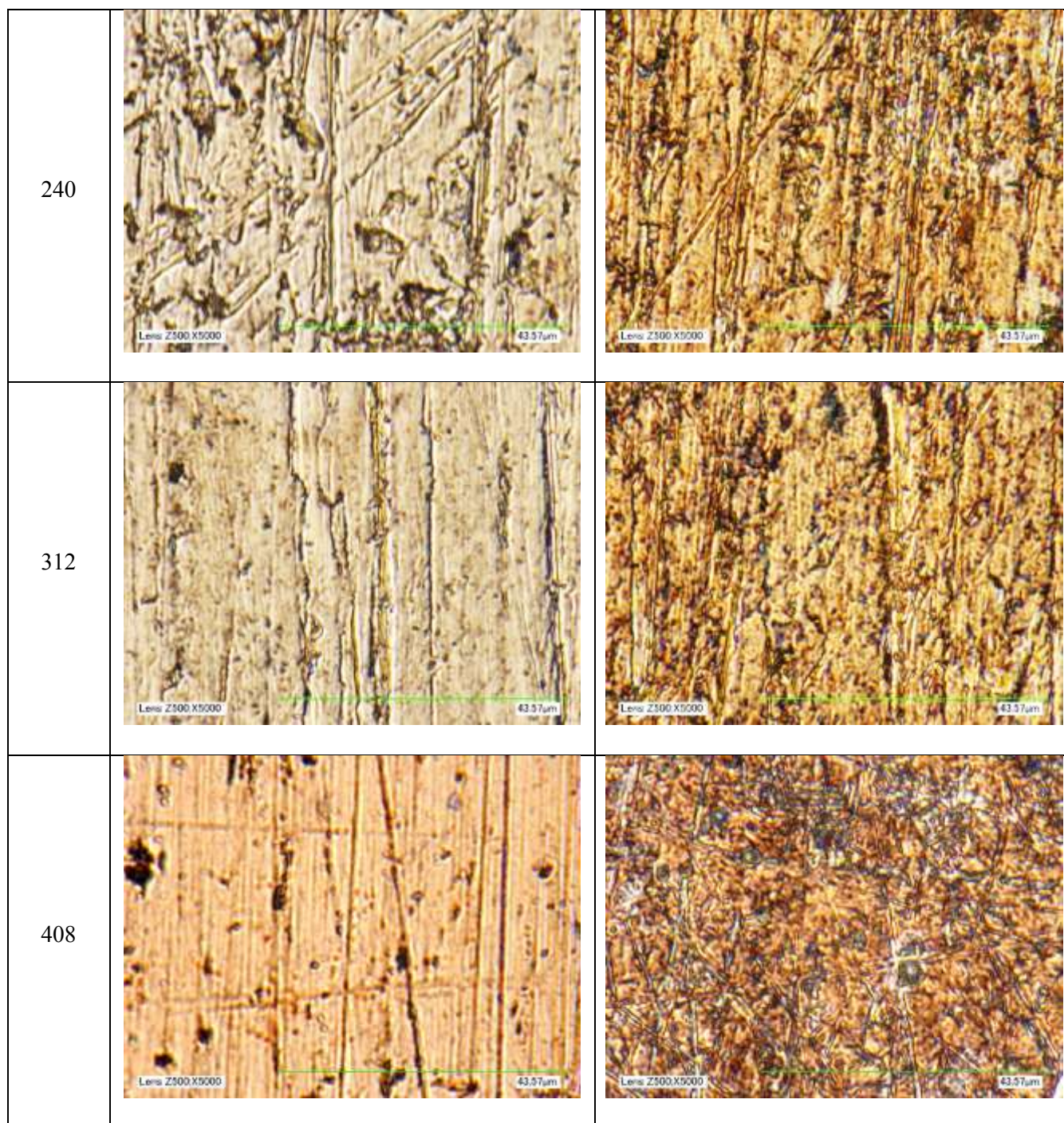
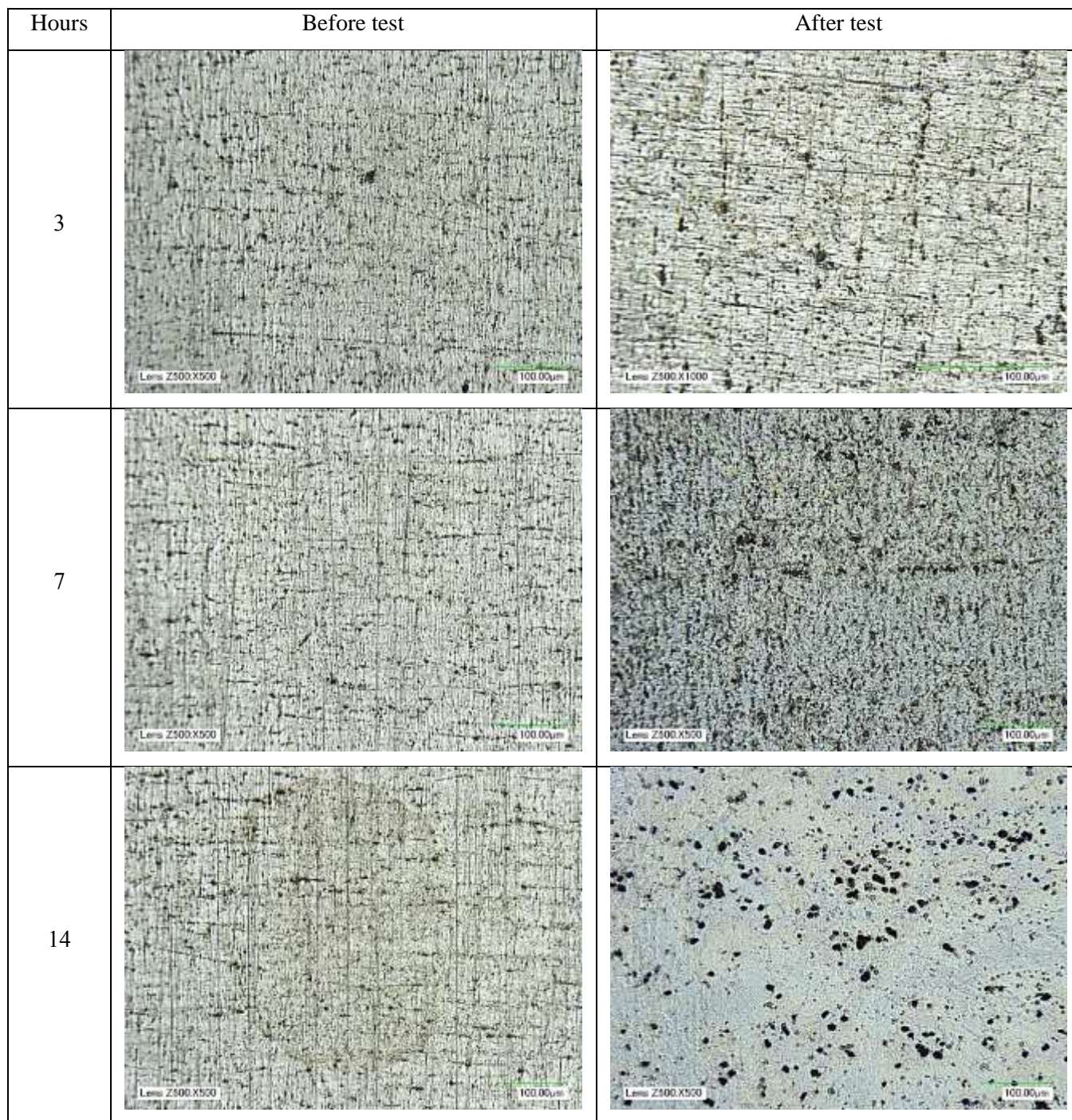


Figure B. 9. Optical microscopy images (Magnification: 500X) of 3003-T3 aluminum before and after 3, 7, 14, 28, 56 and 112 hour-treatments with the reference fluid of distilled water and jet speed of 10.7 m/s.



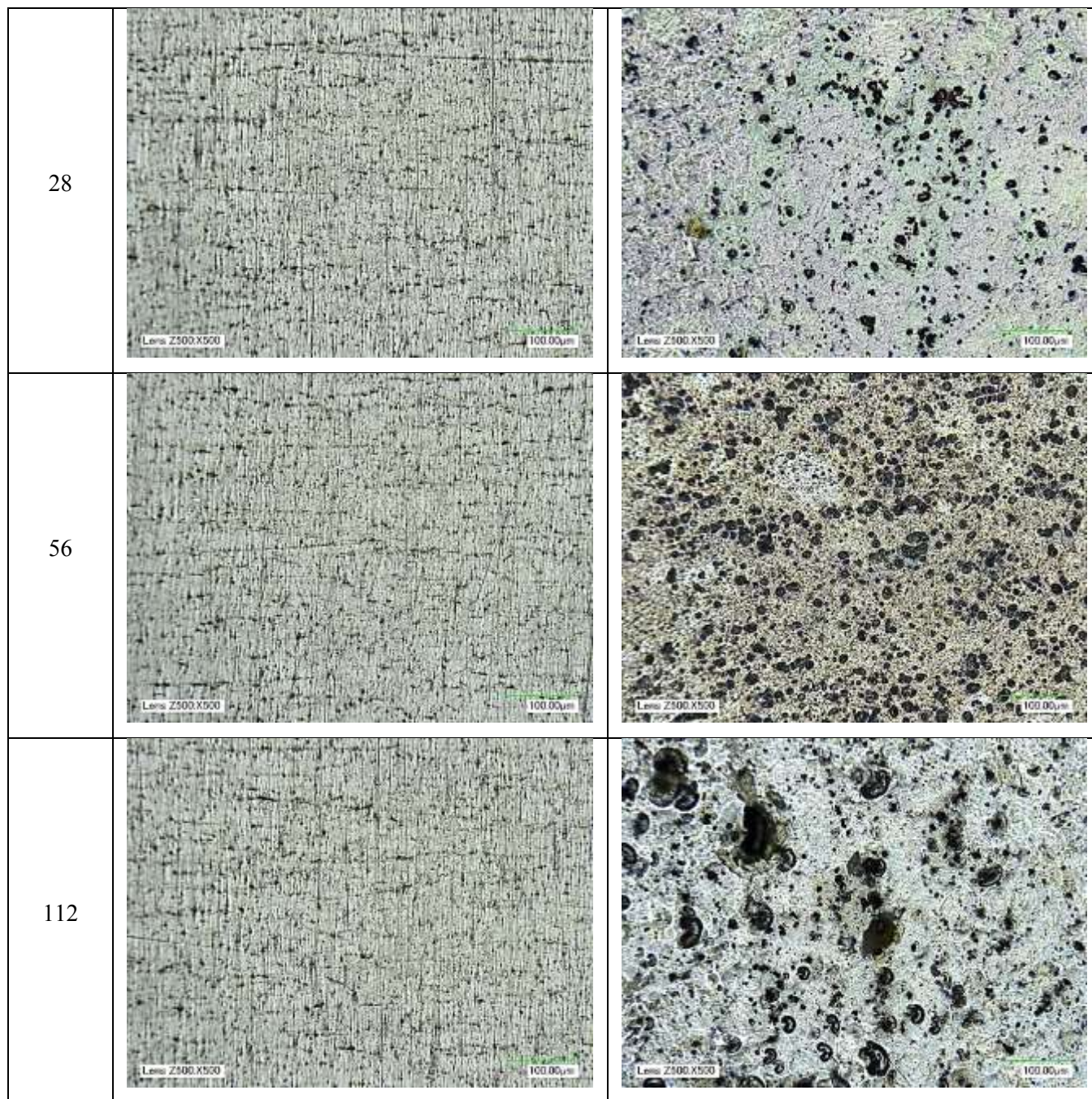
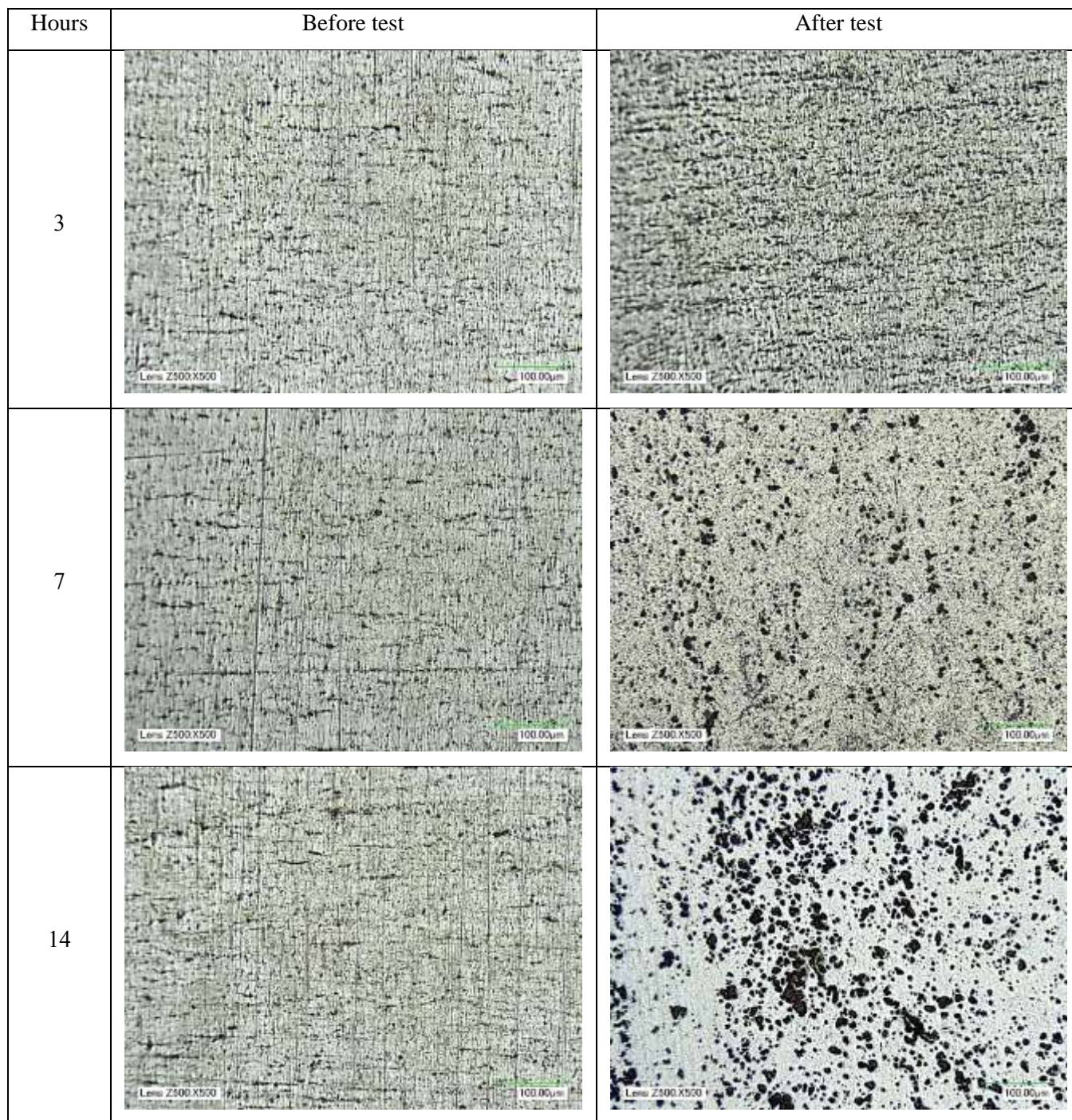


Figure B. 10. Optical microscopy images (Magnification: 500X) of 3003-T3 aluminum before and after 3, 7, 14, 28, 56 and 112 hour-treatments with the 2% alumina nanofluid of distilled water and jet speed of 10.7 m/s.



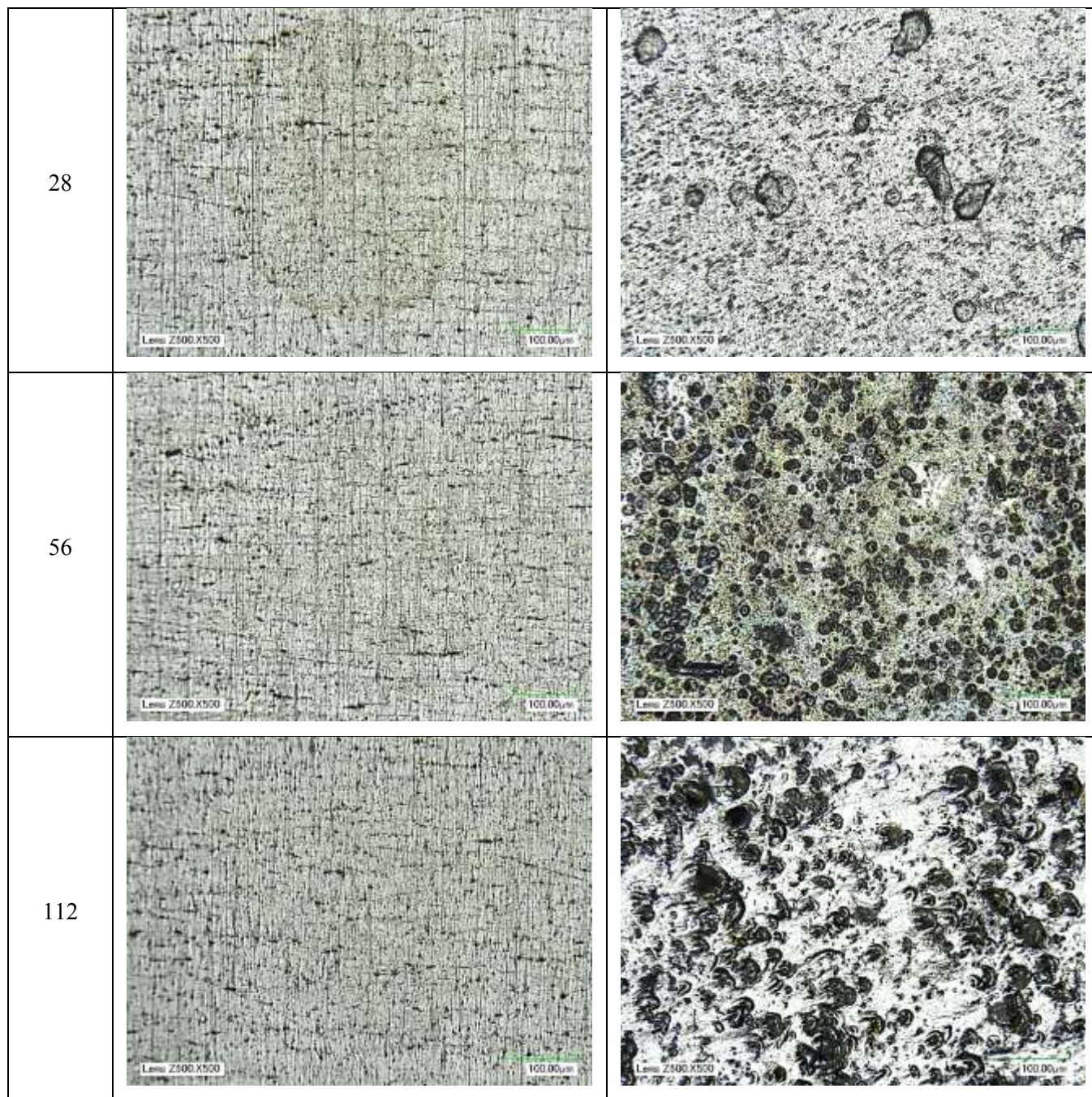
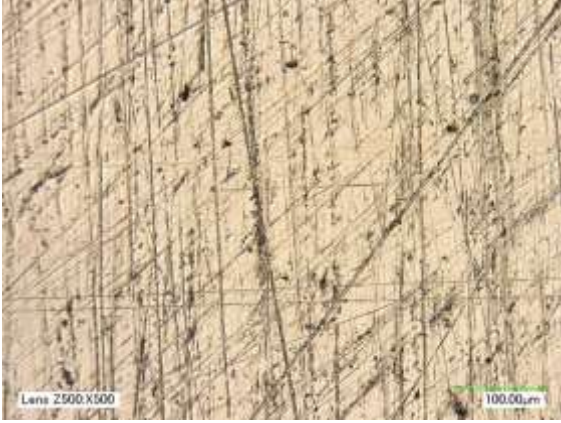
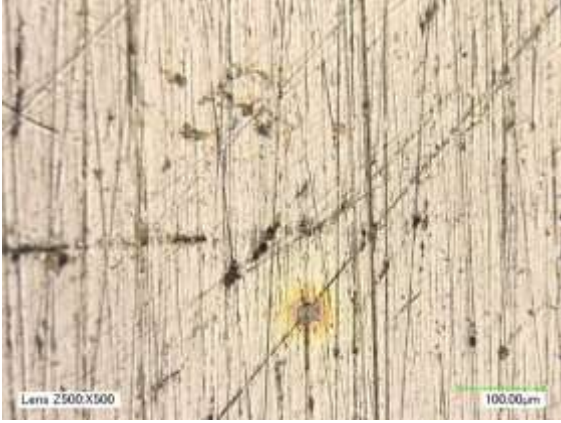

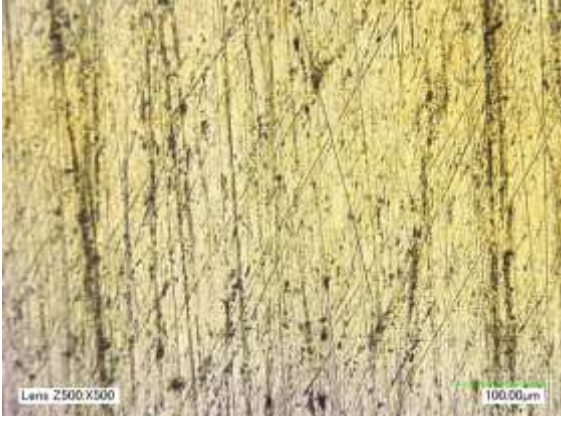
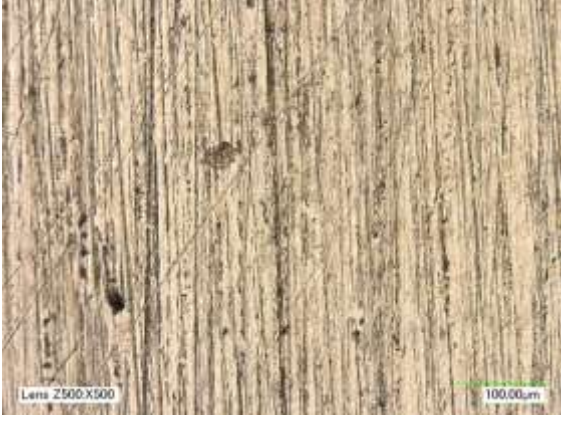
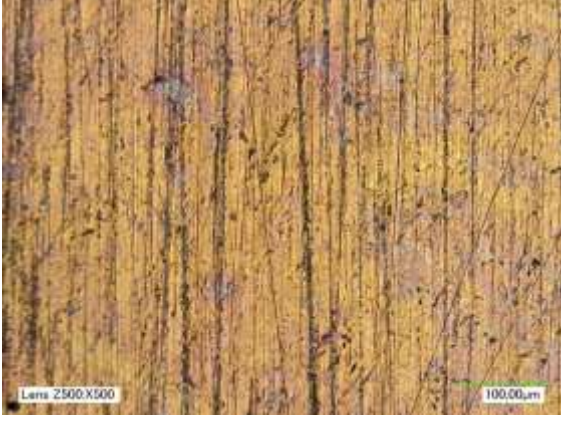


Figure B. 11. Optical microscopy images (Magnification: 500X) of alloy 110 copper before and after 3, 7, 14, 28, 56 and 112 hour-treatments with the reference fluid of distilled water and jet speed of 10.7 m/s.

Hours	Before test	After test
3		
7		
14		

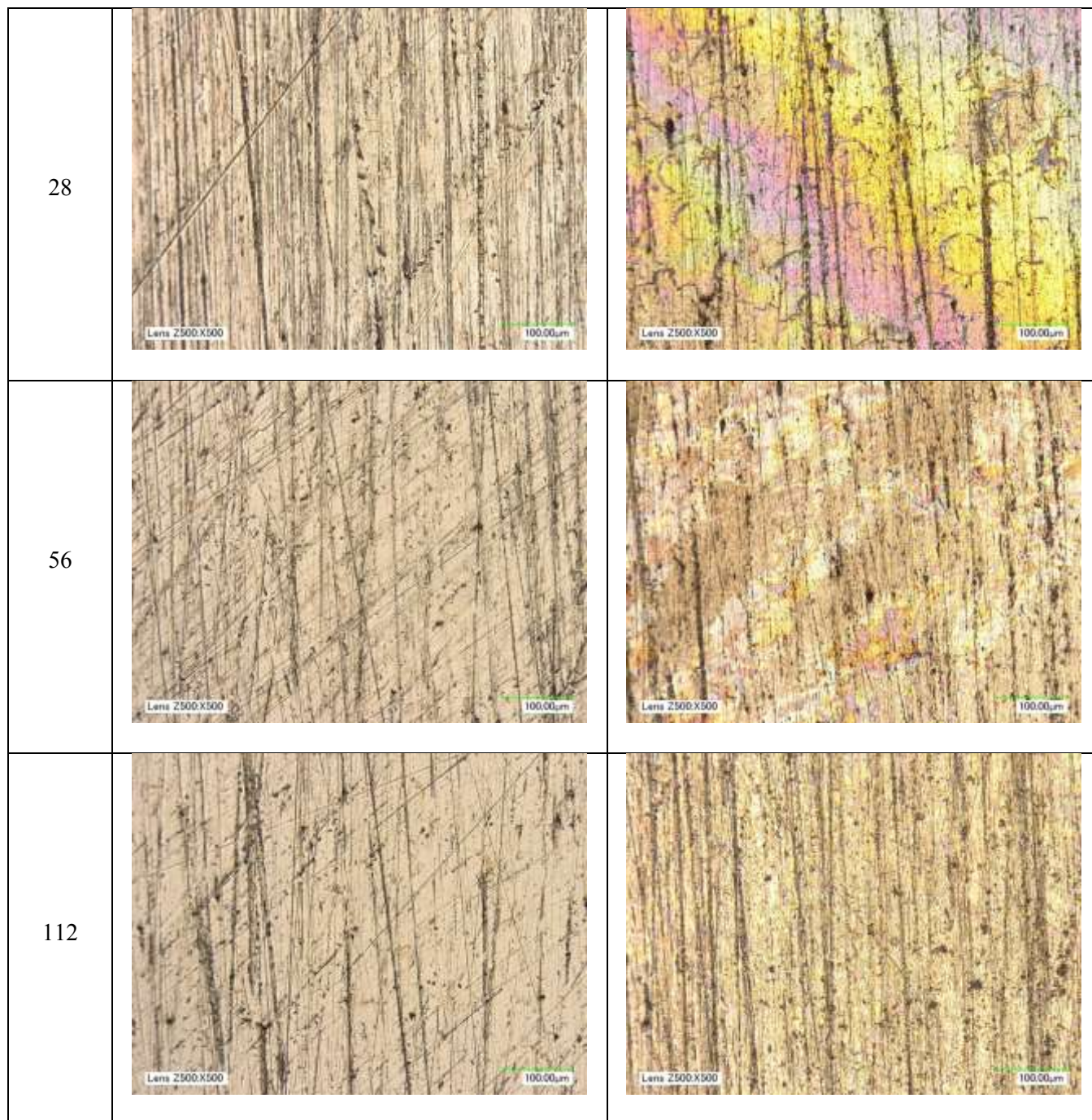





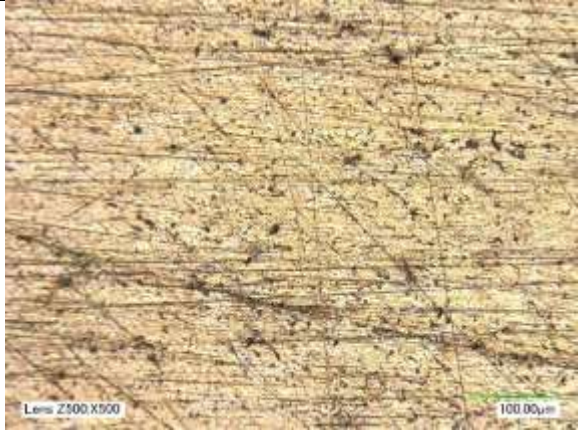




Figure B. 12. Optical microscopy images (Magnification: 500X) of alloy 110 copper before and after 3, 7, 14, 28, 56 and 112 hour-treatments with the 2% alumina nanofluid of distilled water and jet speed of 10.7 m/s.

Hours	Before test	After test
3		
7		
14		

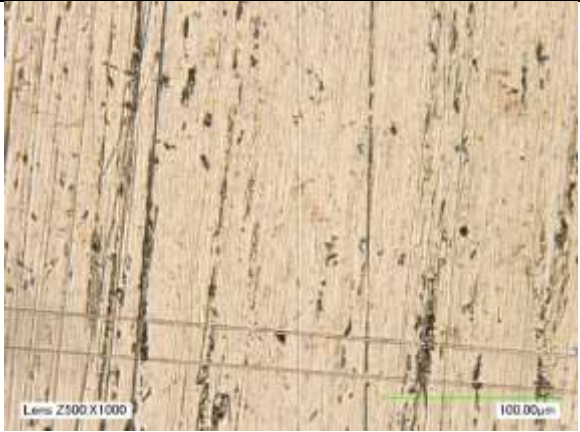

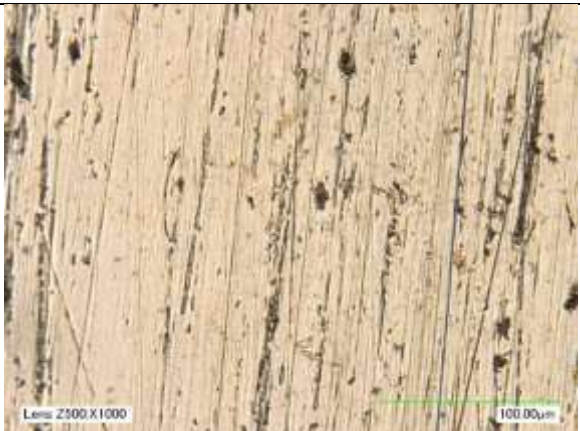
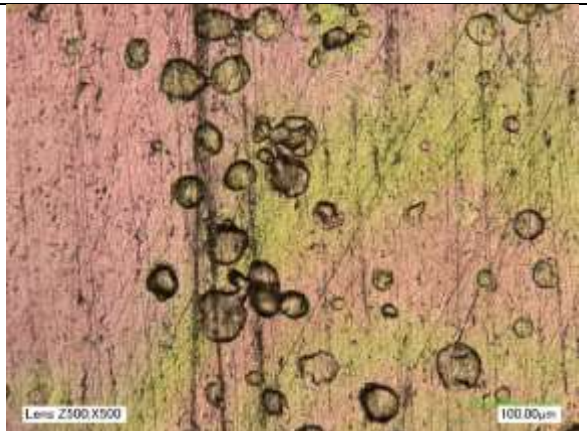
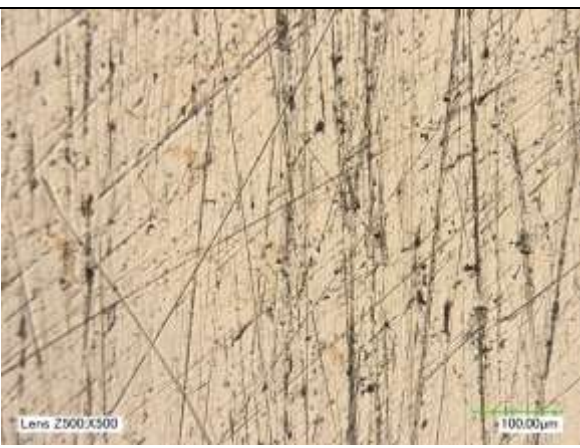
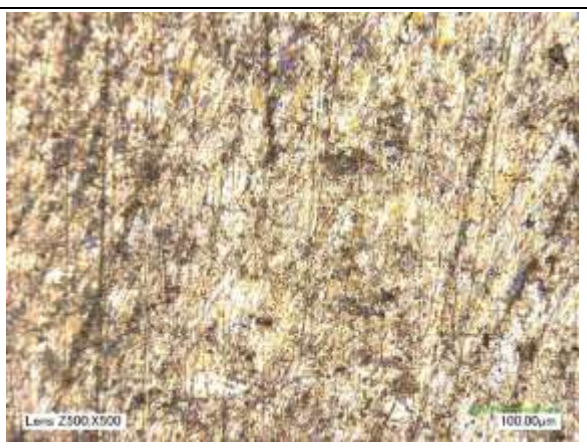


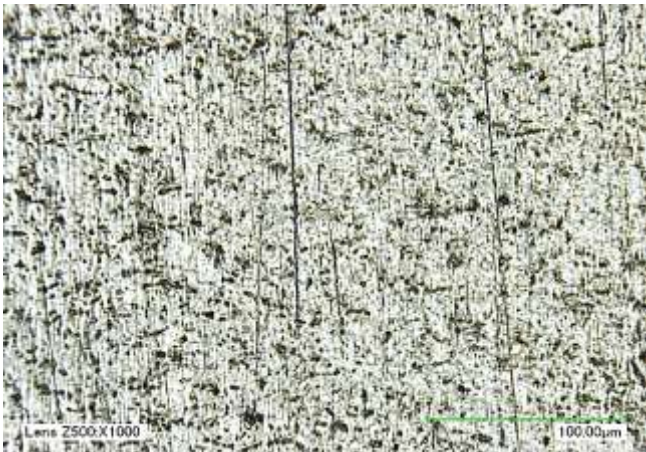



28	 <p>Lens Z500.X1000 100.00µm</p>	 <p>Lens Z500.X500 100.00µm</p>
56	 <p>Lens Z500.X1000 100.00µm</p>	 <p>Lens Z500.X500 100.00µm</p>
112	 <p>Lens Z500.X500 100.00µm</p>	 <p>Lens Z500.X500 100.00µm</p>

Figure B. 13. Optical microscopy images (Magnification: 500X) of 3003-T3 aluminum before and after 3, 7, 14, 28, 56 and 112 hour-treatments with the reference fluid of distilled water and jet speed of 15.5 m/s.

Hours	Before test	After test
3		
7		
14		

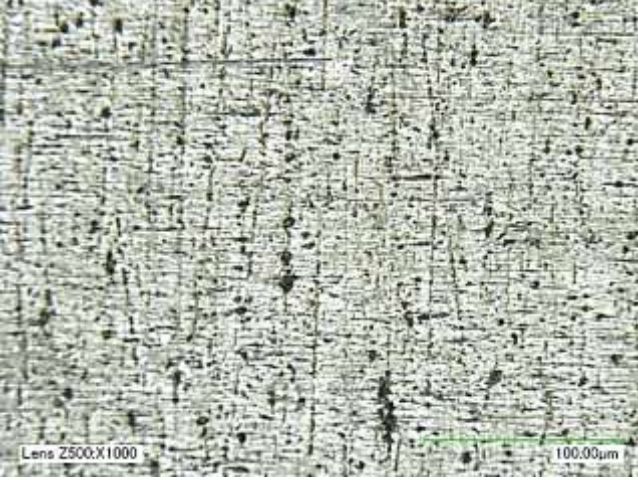




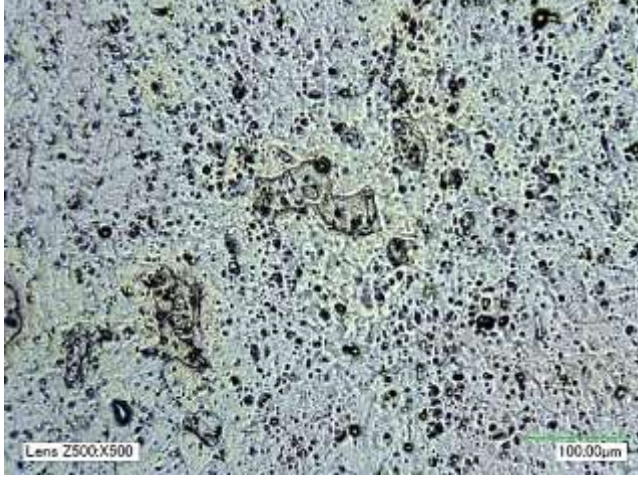

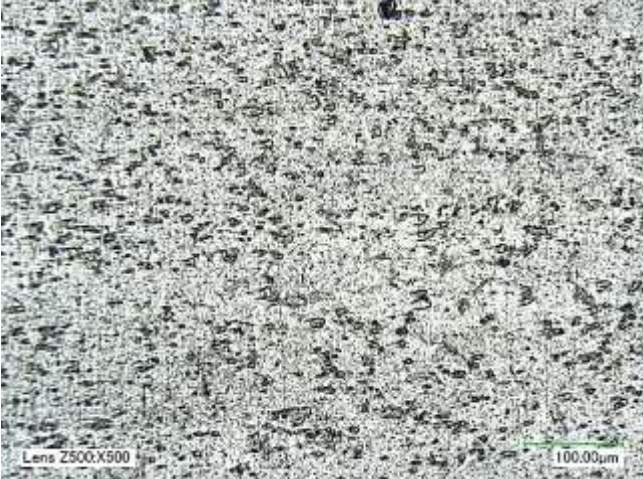


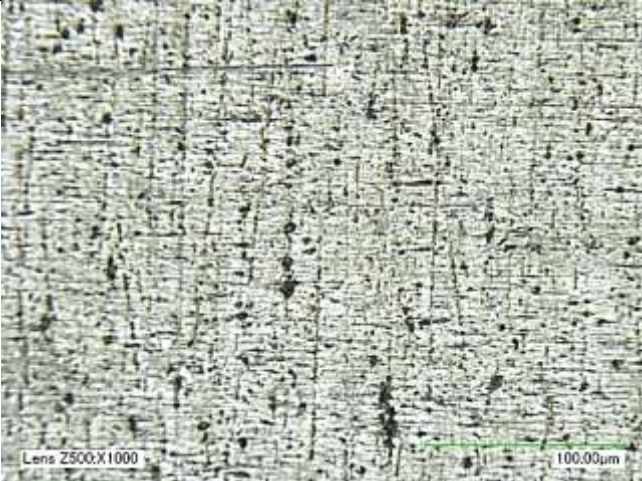

28	 <p>Lens Z500:X1000 100.00µm</p>	 <p>Lens Z500:X500 100.00µm</p>
56	 <p>Lens Z500:X1000 100.00µm</p>	 <p>Lens Z500:X500 100.00µm</p>
112	 <p>Lens Z500:X500 100.00µm</p>	 <p>Lens Z500:X500 100.00µm</p>

Figure B. 14. Optical microscopy images (Magnification: 500X) of 3003-T3 aluminum before and after 3, 7, 14, 28, 56 and 112 hour-treatments with the 2% alumina nanofluid of distilled water and jet speed of 15.5 m/s.

Hours	Before test	After test
3		
7		
14		





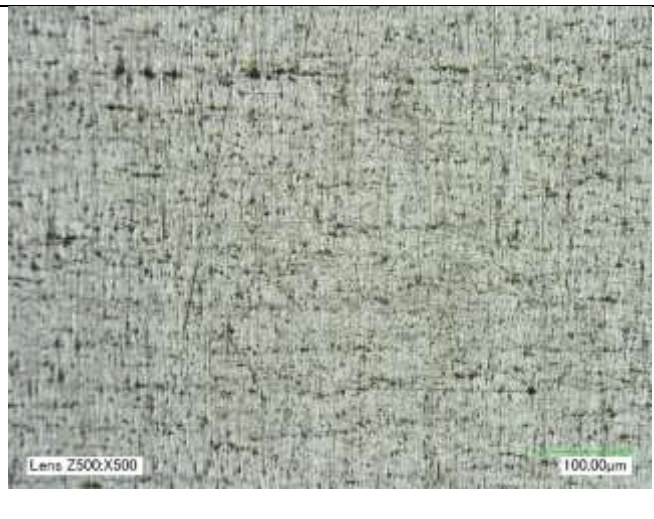

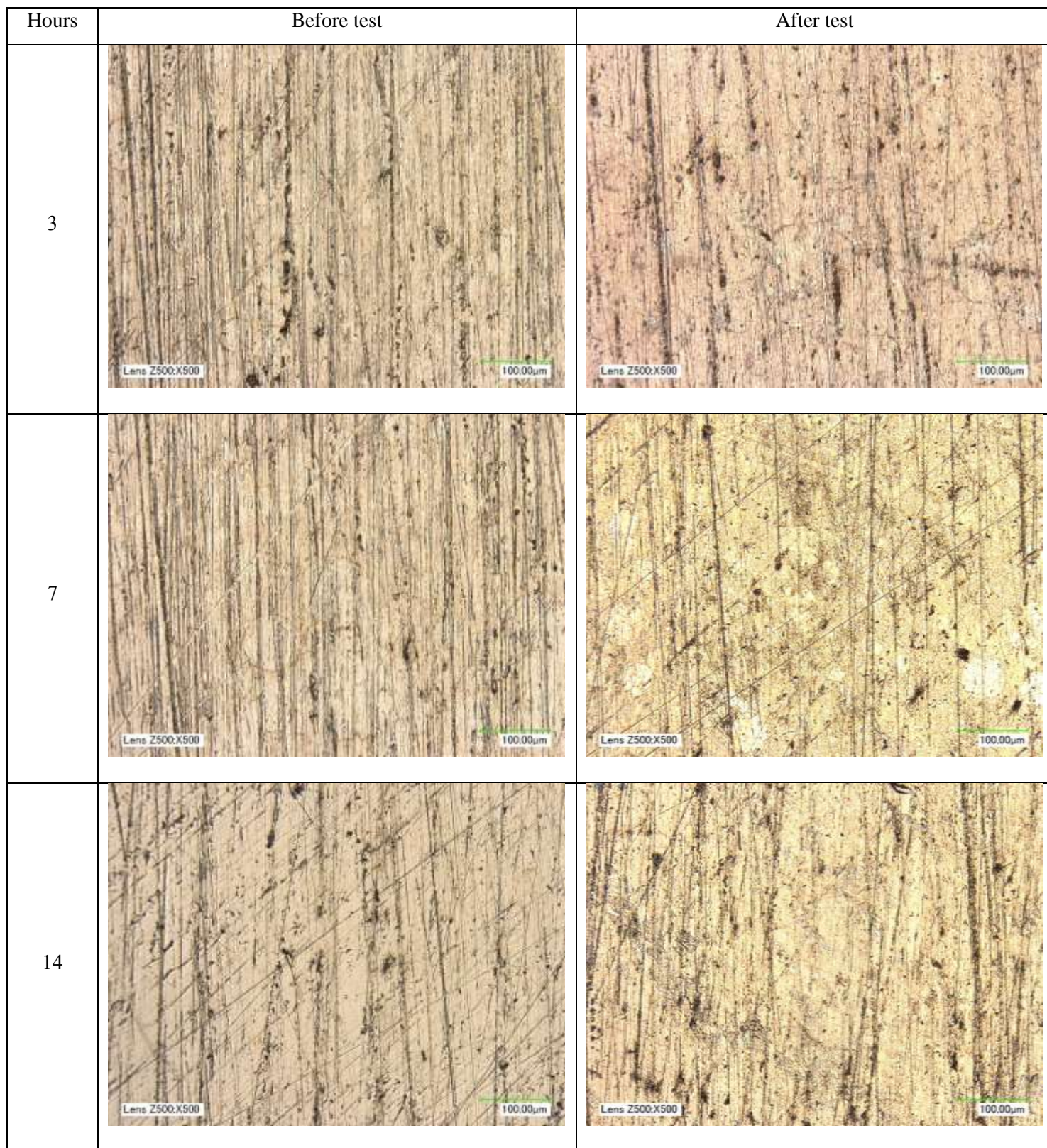
28		
56		
112		

Figure B. 15. Optical microscopy images (Magnification: 500X) of alloy 110 copper before and after 3, 7, 14, 28, 56 and 112 hour-treatments with the reference fluid of distilled water and jet speed of 15.5 m/s.



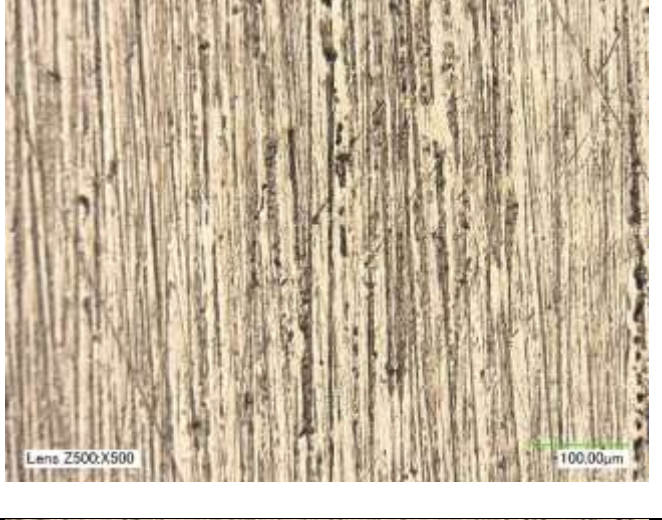

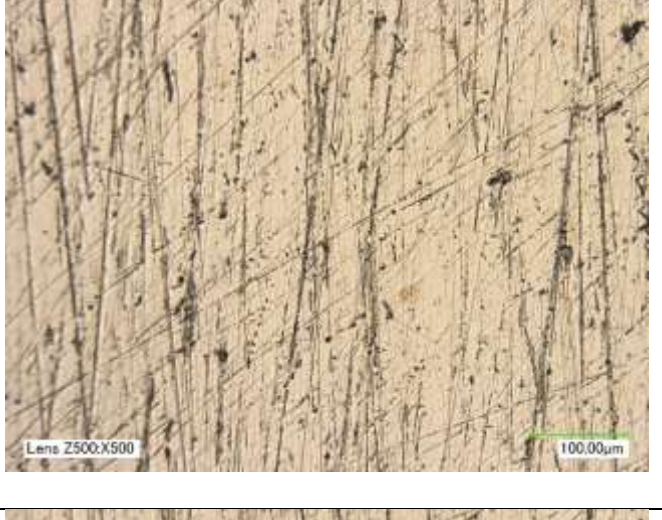


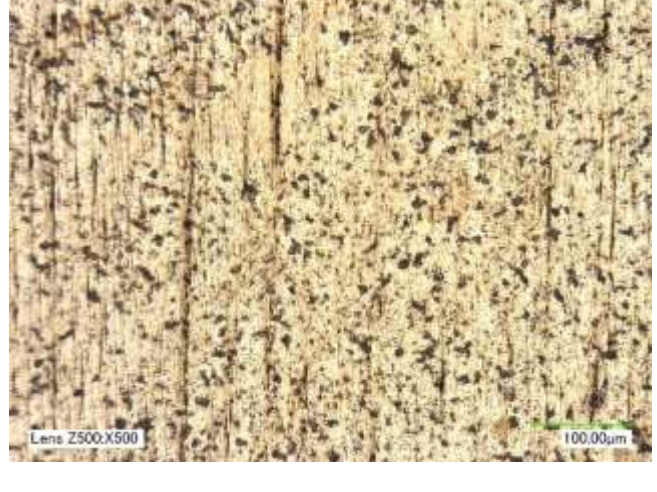
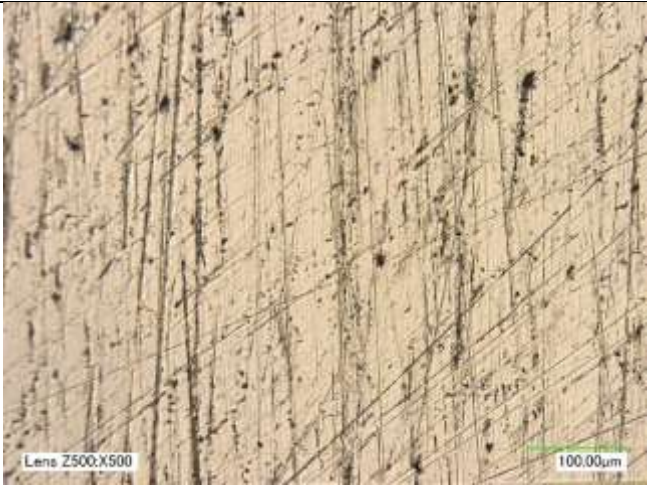
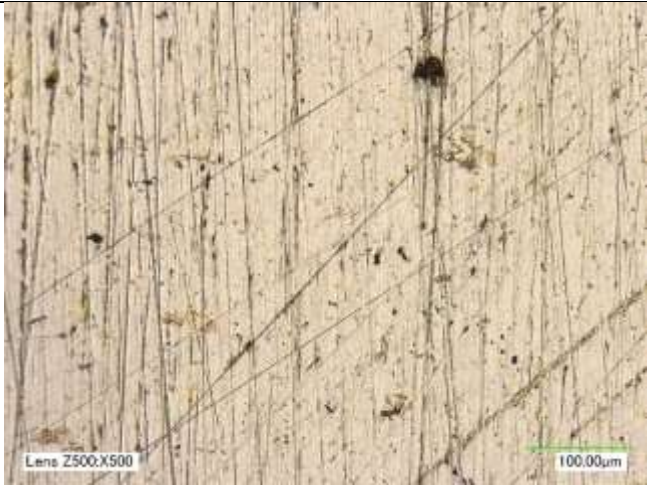
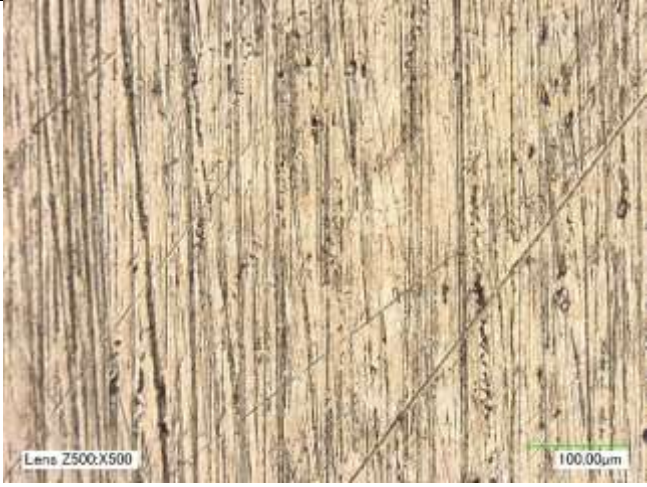

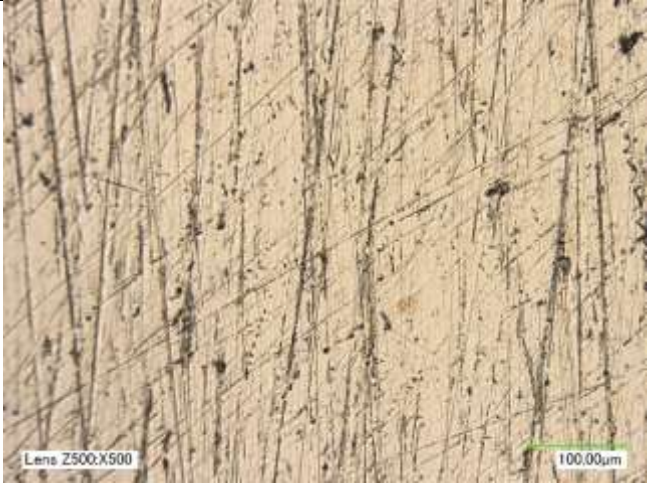
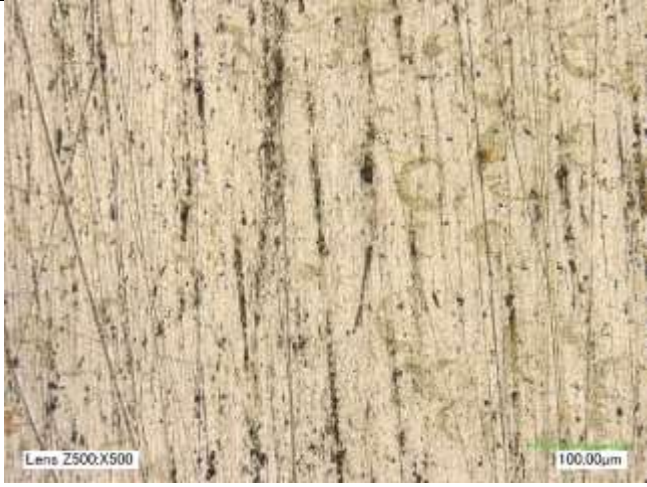
28		
56		
112		



Figure B. 16. Optical microscopy images (Magnification: 500X) of alloy 110 copper before and after 3, 7, 14, 28, 56 and 112 hour-treatments with the 2% alumina nanofluid of distilled water and jet speed of 15.5 m/s.

Hours	Before test	After test
3		
7		
14		


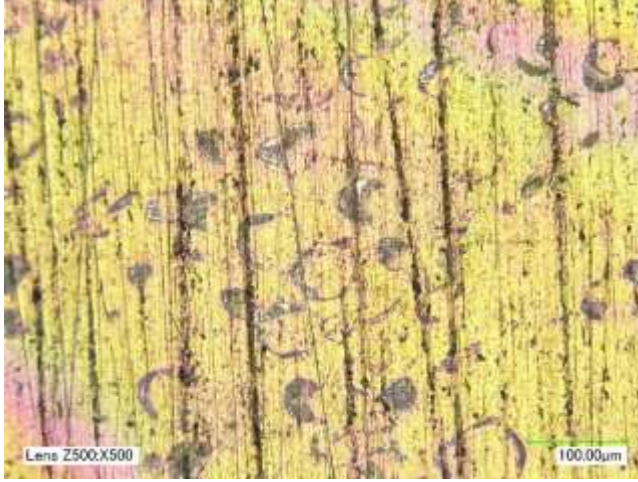
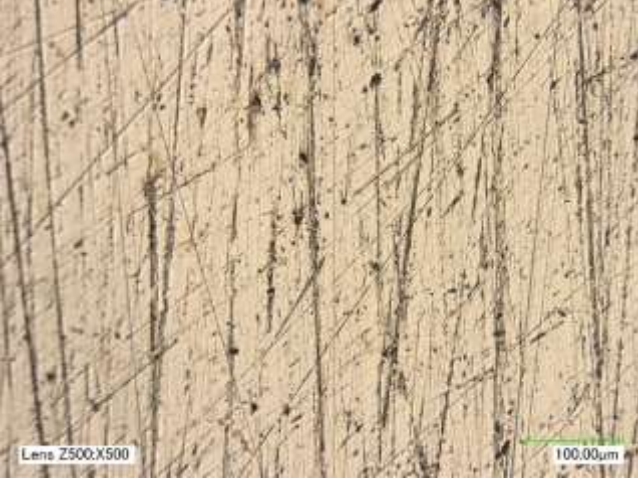

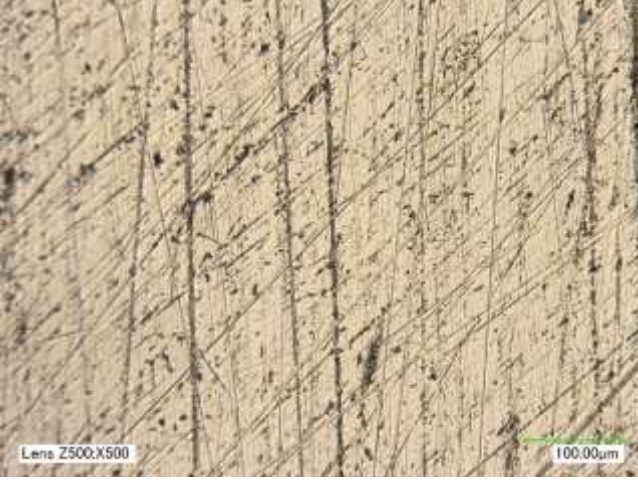
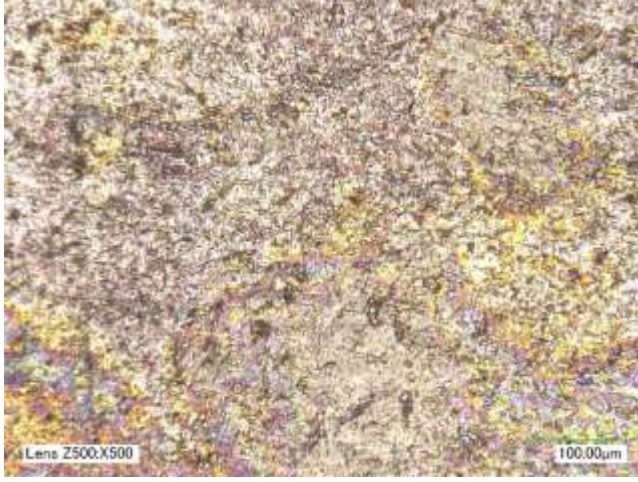
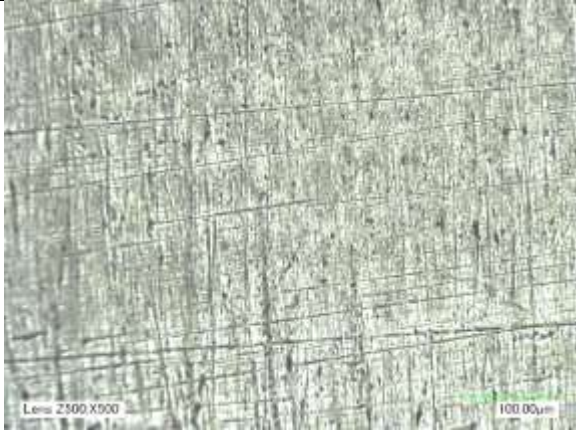


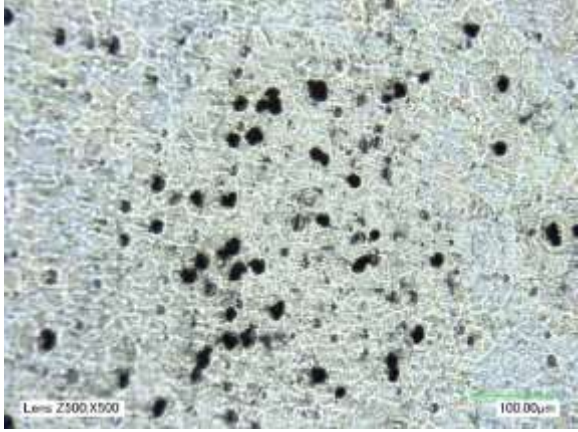

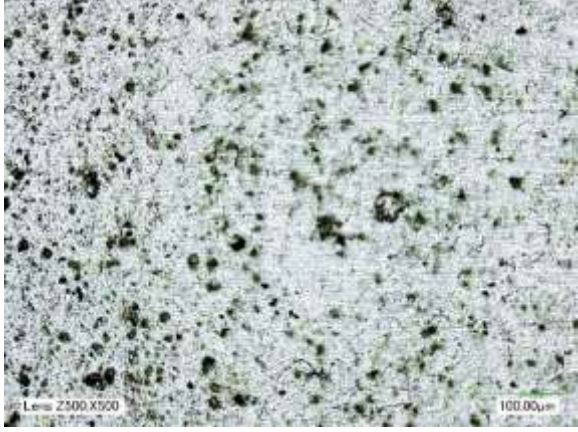
28	 <p>Lens Z500:X500 100.00µm</p>	 <p>Lens Z500:X500 100.00µm</p>
56	 <p>Lens Z500:X500 100.00µm</p>	 <p>Lens Z500:X500 100.00µm</p>
112	 <p>Lens Z500:X500 100.00µm</p>	 <p>Lens Z500:X500 100.00µm</p>

Figure B. 17. Optical microscopy images (Magnification: 500X) of 3003-T3 aluminum before and after 3, 7, 14, 28, 56 and 112 hour-treatments with the reference fluid of distilled water and 1 m/s parallel flow.

Hours	Before test	After test
3		
7		
14		




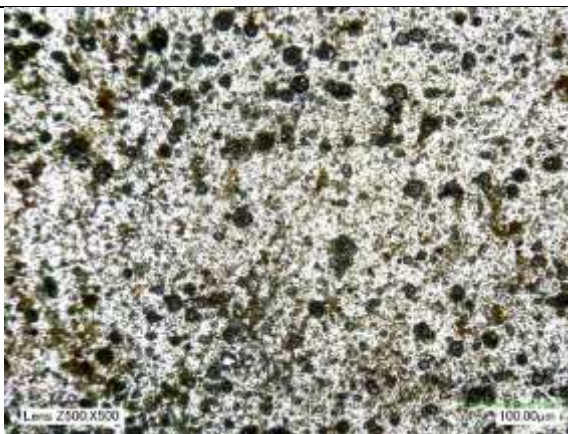

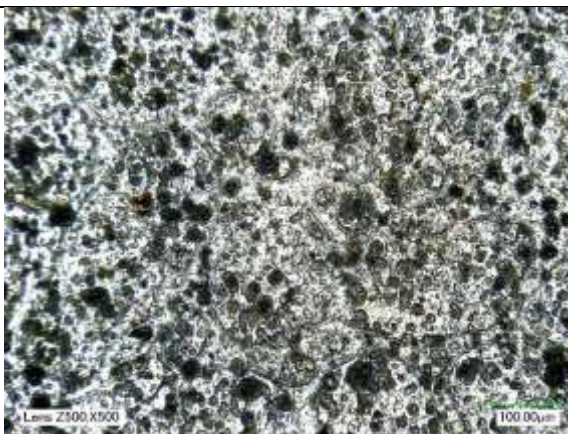
28	 <p>Micrograph showing longitudinal structure of plant tissue at 28 days. The image displays a dense, fibrous texture with vertical striations. A scale bar in the bottom right corner indicates 100.00µm. The text 'Lens Z500.X500' is visible in the bottom left corner.</p>	 <p>Micrograph showing transverse structure of plant tissue at 28 days. The image displays a cellular structure with distinct cell walls and internal organelles. A scale bar in the bottom right corner indicates 100.00µm. The text 'Lens Z500.X500' is visible in the bottom left corner.</p>
56	 <p>Micrograph showing longitudinal structure of plant tissue at 56 days. The image displays a dense, fibrous texture with vertical striations. A scale bar in the bottom right corner indicates 100.00µm. The text 'Lens Z500.X500' is visible in the bottom left corner.</p>	 <p>Micrograph showing transverse structure of plant tissue at 56 days. The image displays a cellular structure with distinct cell walls and internal organelles. A scale bar in the bottom right corner indicates 100.00µm. The text 'Lens Z500.X500' is visible in the bottom left corner.</p>
112	 <p>Micrograph showing longitudinal structure of plant tissue at 112 days. The image displays a dense, fibrous texture with vertical striations. A scale bar in the bottom right corner indicates 100.00µm. The text 'Lens Z500.X500' is visible in the bottom left corner.</p>	 <p>Micrograph showing transverse structure of plant tissue at 112 days. The image displays a cellular structure with distinct cell walls and internal organelles. A scale bar in the bottom right corner indicates 100.00µm. The text 'Lens Z500.X500' is visible in the bottom left corner.</p>

Figure B. 18. Optical microscopy images (Magnification: 500X) of alloy 110 copper before and after 3, 7, 14, 28, 56 and 112 hour-treatments with the reference fluid of distilled water and 1 m/s parallel flow.

